Université de Montréal

Cannabidiol: Exploring New Synthetic Pathways for Late-Stage Functionalization

By

Sophie Rigaut

Département de chimie, Université de Montréal

Faculté des Arts et Sciences

Mémoire présenté en vue de l'obtention du grade de maîtrise ès sciences (M.Sc.) en chimie

Août 2021

Université de Montréal
Département de Chimie, Faculté des Arts et Sciences

Ce mémoire intitulé

Cannabidiol: Exploring New Synthetic Pathways for Late-Stage Functionalization

Présenté par
Sophie Rigaut

A été évalué(e) par un jury composé des personnes suivantes

André Charette
Directeur de recherche

Stephen Hanessian
Membre du jury

Shawn Collins
Membre du jury

Résumé

L'intérêt grandissant suscité par les propriétés thérapeutiques exhibées par les cannabinoïdes a motivé la naissance du projet décrit dans ce mémoire de maîtrise. La synthèse efficace de différents cannabinoïdes est devenue essentielle afin de pouvoir mieux comprendre les mécanismes régulant les propriétés médicales de ces composés ainsi que pour promouvoir le développement de nouveaux traitements médicamenteux. Le cannabidiol est d'intérêt particulier en raison des propriétés anti-inflammatoires, et anticancéreuses exhibées par cette molécule. Ce projet vise à explorer différentes routes permettant la fonctionnalisation du cannabidiol en phase avancée dans le but de faciliter l'accès aux dérivés de ce produit naturel.

La première partie de ce mémoire se concentre sur le développement d'une voie de synthèse permettant la fonctionnalisation d'un précurseur du cannabidiol en utilisant le 1,3-diméthoxybenzène, un produit de départ abordable et commercialement disponible. L'approche proposée comporte six étapes et s'appuie sur une réaction de Diels-Alder pour générer l'adduit bicyclique du cannabidiol. Plusieurs routes ont été explorées pour obtenir la fonctionnalisation de ce précurseur, à savoir une borylation de Hartwig-Miyaura et une bromination du cycle aromatique.

La deuxième partie de ce projet se concentre sur la fonctionnalisation du cannabidiol en phase avancée en s'appuyant sur la fonctionnalité de l'amide de Weinreb. Ces travaux ont abouti au développement d'une voie de synthèse efficace et durable pour la production de l'olivetol, un fragment clé pour la production à grande échelle de cannabidiol dans l'industrie pharmaceutique. Cette méthode se base sur une approche en quatre étapes s'appuyant sur un amide de Weinreb en utilisant un produit de départ abordable, l'acide 3,5-dimethoxy benzoïque. La synthèse de l'amide de Weinreb puis de la cétone correspondante, suivie d'une réduction de Wolff-Kishner, et enfin la démethylation du substrat ont permis d'obtenir le produit désiré. La versatilité de cette approche tolère une fonctionnalisation variée de la molécule, permettant la synthèse potentielle de divers dérivés de l'olivetol.

Mots-clés : Cannabidiol, dérivés, Diels-Alder, post-fonctionnalisation, amide de Weinreb, olivetol

Abstract

The increasing interest around the therapeutic possibilities offered by cannabinoids was the motivation for the project described in this Master's thesis. The efficient synthesis of various CBs has become critical to deepen the understanding of the mechanisms behind the medical properties of cannabinoids as well as for the development of novel drug treatments. Cannabidiol is of particular interest as the molecule exhibits anti-inflammatory, and anticarcinogenic properties. This work aims to explore different routes to enable the late-stage functionalization of cannabidiol in order to easily access derivatives of the natural compound.

The first part of this work focuses on developing a route enabling the functionalization of the cannabidiol precursor utilizing the affordable and commercially available starting material 1,3-Dimethoxybenzene. The proposed six-step approach relies on a Diels-Alder reaction to generate the bicyclic adduct of cannabidiol. Several routes were then explored to obtain the functionalization of the precursor namely a Hartwig-Miyaura borylation and a bromination of the aromatic ring.

The second part of this project focuses on the functionalization of cannabidiol relying on the Weinreb amide functionality. This work led to the development of an efficient and sustainable route for the synthesis of olivetol, a key fragment for the large-scale production of cannabidiol within the pharmaceutical industry. The method relies on a four-step approach relying on a Weinreb amide synthesized using the affordable 3,5-Dimethoxybenzoic acid. The synthesis of the Weinreb amide followed by the formation of the corresponding ketone, subsequent Wolff-Kishner reduction, and finally demethylation of the substrate allowed to generate the desired product. The versatility of the approach allows for variations in functionalization, enabling potential formation of various olivetol derivatives.

Keywords: Cannabidiol, derivatives, Diels-Alder, post-functionalization, Weinreb amide, olivetol

Table of Contents

List of Figures

List of Schemes

List of Tables

List of Abbreviations

°C	degree Celcius
% w/v	percent weight/volume
^{13}C NMR	nuclear magnetic resonance of carbon 13
^{1}H NMR	nuclear magnetic resonance of proton
2-AG	2-arachidonoylglycerol
AEA	anandamide
acac	acetylacetone
APIs	active pharmaceutical ingredients
AIDS	Acquired immunodeficiency syndrome
aq	aqueous
Ar	aromatic
Bn	benzyl
Boc	*tert*-butyloxycarbonyl
Bpin	bispinacol boron
br	broad
Cat.	catalytic
CB	cannabinoid
CBCA	cannabichromenic acid
CBD	cannabidiol
CBDA	cannabidiolic acid
CBDD	cannabidiol dimethyl ether
CBGA	cannabigerolic acid
CNS	central nervous system
COD	cyclooctadiene
d	doublet
dd	doublet of doublets
DEA	Drug Enforcement Administration
DMAP	4-dimethylaminopyridine
DMG	direct metalation group

DMHA	*N,O*-dimethylhydroxylamine
DMSO	dimethyl sulfoxide
dtbpy	di-tert-butyl dicarbonate
eCB	endocannabinoid
ECS	endocannabinoid system
EDC	1-Ethyl-3-(3-dimethylaminopropyl)carbodiimide
equiv	equivalents
Et	ethyl
et al.	and others
FDA	Food and Drug admninstration
FTIR	Fourier-transform infrared spectroscopy
h	hour
HBTU	2-(1H-Benzotriazole-1-yl)-1,1,3,3-tetramethyluronium hexafluorophosphate
HRMS	high-resolution mass spectrometry
HMTA	hexamethylenetetramine
Hz	Hertz
IBC	isobutyl chloroformate
in situ	in the reaction mixture
J	Joules
LDA	lithium diisopropylamide
LED	light-emitting diode
m	multiplet
m-CPBA	meta-Chloroperoxybenzoic acid
Me	methyl
mg	milligrams
min	minutes
mL	milliliter
mmol	millimole
mol%	mole percent
mp	melting point
NBS	*N*-bromosuccimide

NMR	nuclear magnetic resonance
o	ortho
p	para
PG	protecting group
Ph	phenyl
Piv	pivaloyl
pKa	acid dissociation constant
PNS	peripheral nervous system
ppm	parts per million
R_f	retention factor
rt	room temperature
s	singlet
sat	saturated
S_N2	nucleophilic substitution
t	triplet
t-Bu	*tert*-butyl
Tf	trifluoromethysulfoyl
TFA	trifluoroacetic acid
THC	tetrahydrocannabinol
THCA	tetryhydrocannabinolic acid
THF	tetrahydrofuran
TMEDA	tetramethylethylenediamine
TMP	tetramethylpiperide
Ts	tosylate
UV	ultraviolet
WA	Weinreb amide
δ	chemical shift
μg	microgram
μL	microliter
μmol	micromoles

Acknowledgements

I would like to thank Pr. Charette and the University of Montreal for giving me the opportunity to earn my Master's in chemistry. Thank you for cultivating an environment that promotes intellectual freedom and growth. I would like to thank all of the Charette group members who helped guide me during these two years by passing on their knowledge about the lab as well as for encouraging me to always ask questions.

I would like to thank Yousra and Saher for helping me navigate through the lab and teaching me all the tips and tricks. Your work ethic and dedication to your craft were inspiring and I could not have done this without your support.

I would also like to thank my family who even from all the way across the ocean always found ways to be present and supportive, with a special mention for the best care packages in the game.

Finally, I would like to thank my girls Alex and Joel whose apartment became my safe space and who managed to keep me sane during the craziness of 2020. I would also like to thank my best friend Lauren, who even though she was miles away also found the words to keep me going when times were rough.

1. Introduction

1.1. *Medical use of Marijuana throughout History*

1.1.1. Uses in Ancient Civilization

Cannabis sativa (*C. sativa*) has been used for its medical properties in different ancient traditional medicine practices for several centuries. The first written reports of the use of medicinal cannabis are found in ancient Chinese records compiling traditional healing techniques[1] dating back to 4000 BCE. Further reports of the use of medical marijuana were found in Ayurvedic medicine and throughout Eastern Asia. The plant was used for its fibers in materials like paper or textiles but was also embedded in medicinal and spiritual rituals.[2] The long list of medical properties attributed to different parts of the plant comprises analgesic, antiparasitic, anti-inflammatory, antispastic, aphrodisiac, and diuretic properties as well as appetite stimulation. [4,5,6] Additional uses of the plant include the treatment of blood clots, insomnia, gastrointestinal issues, and gynecological disorders.[3] The euphoric and psychoactive properties of *C. sativa* were recognized and valued in religious rituals. [5]

The use of the plant was progressively exported to Europe and the Middle East. In ancient Egypt, *C. sativa* was tightly linked to both spiritual beliefs and medical uses.[7,8] The use of cannabis was also popular throughout the Middle East where the benefits of the plant were extended to treating headaches when administered in alcoholic solutions. [9,10] In Europe, the plant was mostly used for its fibers at first. Eventually its medical virtues were recognized, though doctors warned against abuse of the substance.[6,11] In the following centuries, the use of medical marijuana was progressively abandoned in western medicine due to misconceptions and lack of knowledge surrounding its benefits.[12] Later, it was slowly rehabilitated through the efforts of scientists and psychiatrists documenting the medical properties of *C. sativa.*

1.1.2. Introduction to Western Medicine

The use of marijuana has been reported in many traditional medicines across the globe, though its use in western medicine was not popular. The first scientific records of the benefits of *C. sativa* date back to 1839 when William O'Shaughnessy introduced the idea of medicinal

marijuana through his reports on the various uses of therapeutical cannabis throughout Asia.[6] Using a western scientific approach he officially recorded the virtues of the sacred plant to document the several benefits reported by traditional healers over the centuries. His experiments, first on animals and then on patients, gave the necessary evidence that hemp seed oil can be efficiently used to prevent vomiting and diarrhea in cholera patients. Additionally, he reported the analgesic, orexigenic, anesthesiologic, and antiepileptic properties of the plant, as well as anxiety and sleep disorder relief.[6] The translation of Arabic descriptions of the uses of the plant contributed to the popularization of *C. sativa* in Europe.[13] As the therapeutic possibilities offered by cannabis were gaining exposure, the psychoactive effects, the calming effects, and appetite inducing effects of the plant were examined as well.[13] The medical properties of marijuana were widely studied until 1937, when legal restriction over the consumption of marijuana restricted research activities tremendously.[2]

1.1.3. Identification and Isolation of Cannabidiol

Many chemists and pharmacists attempted to isolate the active ingredients of cannabis over the years. The restrictions on the uses of *C. sativa* became more important as its use for recreational purposes grew and was accompanied by misunderstanding and fear surrounding its psychoactive effects.[2,14] Due to these laws research on the active ingredients of marijuana for potential medical treatment became difficult.

Cannabidiol (CBD) was isolated for the first time by Adams *et al.* in 1942.[15a] They were able to establish the formula of the compound, however they were uncertain about the position of the double bond on the cyclohexyl (see Figure 1). To be able to study the molecule, CBD was isolated from *C. sativa* oil through a lengthy distillation process. [15b]

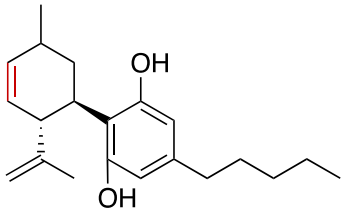

1

Figure 1: Initial Proposal for the Structure of CBD, Adams *et al.*, 1940

The final structure of CBD **2** was established in 1963 through an extensive UV spectral analysis and NMR analysis of the molecule.[16] Through the introduction of an epoxide ring, Mechoulam *et al.* were able to confirm the position of the double bond in the six-membered ring (see Figure 2). Their work continued with the isolation of Δ^9-tetrahydrocannabinol (THC) **4** [16] as well as an inactive cannabinol, another cannabinoid (CB) found in marijuana. The active ingredients were identified by first submitting a hashish extract to flash chromatography followed by recrystallization. The products obtained were subjected to Fourier transform infrared (FTIR) and nuclear magnetic resonance (NMR) analysis, leading to the identification of one aliphatic methyl group and three other methyl groups that would be found at the a position to an oxygen or olefinic.[16] The final chemical structure was confirmed through further analysis of the chemical shifts in comparison to the structure of CBD and supported by partial synthesis of the molecule (see Figure 2).[16]

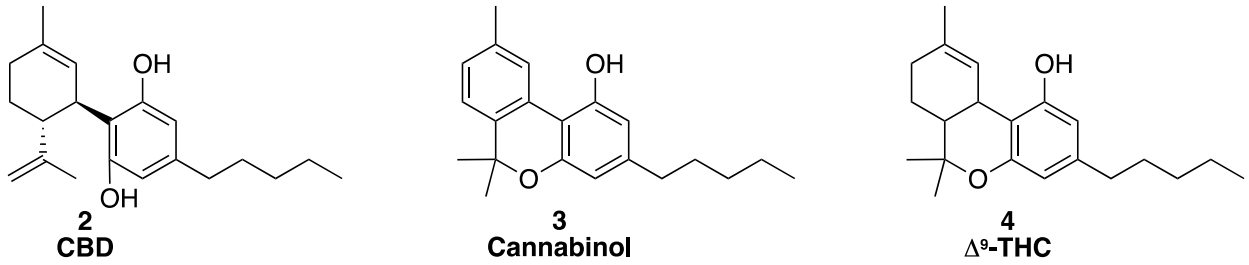

Figure 2: Δ^9-THC, Cannabinol, and CBD, Mechoulam *et al.*, 1965

Following their discovery, Mechoulam *et al*. [17] explored the synthesis of THC leading to a procedure enabling the synthesis of both THC and CBD. The method consisted of the reaction of a citral **6** with a lithium derivative of olivetol dimethyl ether **5** which generated CBD (see Scheme 1). An additional step allowed to obtain the pyran ring characteristic of THC.

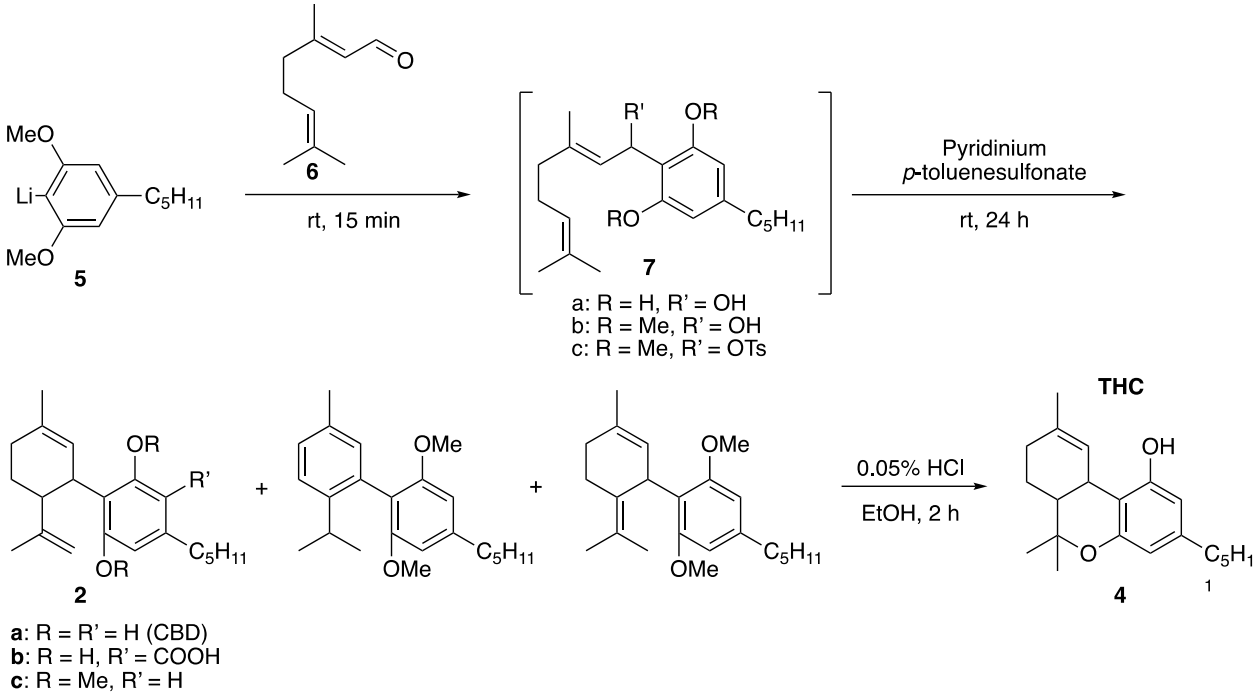

Scheme 1: Synthesis of CBD and THC, Mechoulam *et al.*, 1965

Establishing the structure of CBD and proposing a synthetic pathway to both CBD and THC facilitated the research to understand how the active ingredients can affect different bodily functions and how to best use them for their therapeutical values. The study of cannabis and its biological responses led to the uncovering of the endocannabinoid system (ECS) and unlocked a lot of potential for future treatments, which will be discussed in the following section.

1.2. *Biological Function*

1.2.1. The Endocannabinoid System

In order to understand the importance of CBD based drugs, it is essential to understand their biological interactions. As the legislations around the uses of medical marijuana were softened, it became possible to explore the properties of *C. sativa* and how it affects the endocannabinoid system (ECS). Though the use of medical marijuana had been reported for centuries, its mechanism of action was unknown up until the early 1990s when CB_1 and CB_2 receptors were discovered.[18] These receptors are essential to the ECS. They are located in different parts of the brain, as well as in the peripheral nervous system (PNS), and peripheral organs. The role of the ECS is to regulate synaptic transition through G-coupled proteins that can adjust the activity of different enzymes

responsible for olfaction, sugar and lipid metabolism, cell growth, osmotic stress, heat shock, and inflammation.[18]

The ECS is responsive to endogenous retrograde neurotransmitters called endocannabinoids (eCBs) that can bind to the cannabinoid receptors. The CB_1 and CB_2 receptors have distinct roles in the body. CB_1 receptors are mostly found in the central nervous system (CNS), in the brain and in a less significant amount in the PNS.[18] The activation of CB_1 receptors results in the inhibition of Ca^{2+} channels and the stimulation of K^+ channels, maintaining a regular neuronal activity by controlling the activity of neurotransmitters.[18,19] CB_1 receptors are associated with synaptic plasticity due to their ability to modulate neurotransmission. The ability to modulate neurotransmission has been linked to the regulation of cognitive functions and emotions, movement and posture modulation, and pain perception.[18] Several other essential functions like the cardiovascular, gastrointestinal, and respiratory systems as well as food intake and reproduction also fall under the influence of CB_1 receptors.[18] CB_2 receptors are found in blood cells and immune tissues. The activity of CB_2 receptors has been linked to the regulation of the immune system influencing perception of inflammation and chronic pain and the cell life cycle, though the mechanisms of those processes remain unknown.[20]

1.2.2. Endocannabinoids

There are several endocannabinoids (eCBs) involved in the activation of the ECS. The eCBs are neuroprotective agents whose main function is to adjust and regulate neurotransmitter release to maintain a healthy neuronal activity. Anandamide (AEA) **8** and 2-arachidonoylglycerol (2-AG) **9** are both generated by biological derivatives of linoleic acid, a polyunsaturated fatty acid found in the everyday diet (see Figure 3).[19]

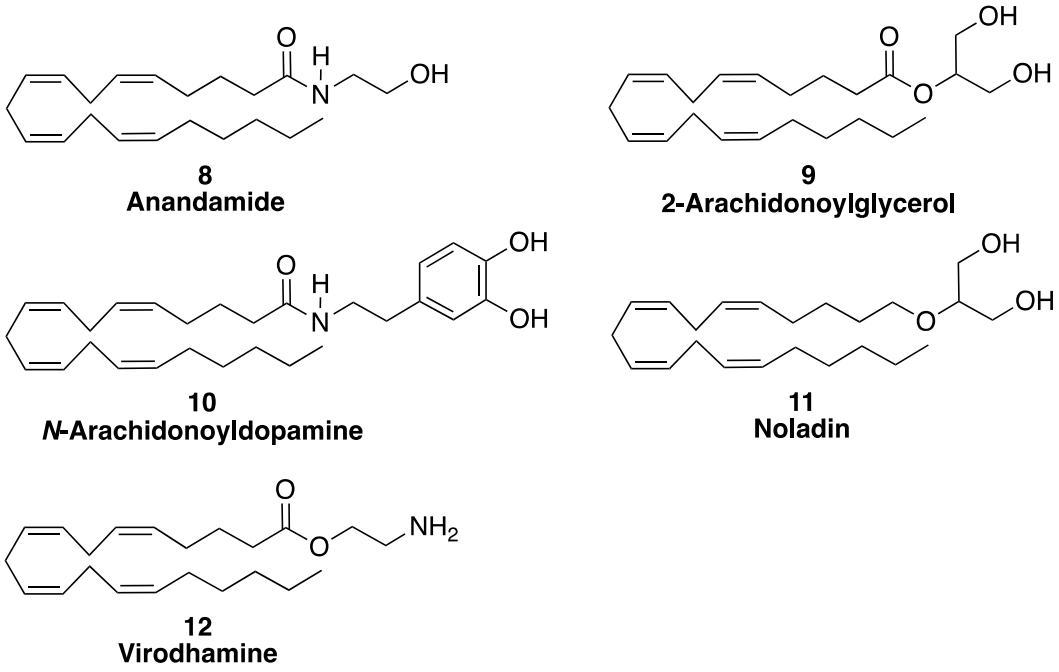

Figure 3: Endocannabinoids

AEA and 2-AG bind to both receptors with different affinities and are found in the body at different concentrations.[18,20,21] eCBs are essential for the proper functioning of the body as the ECS is responsible for the regulation of many bodily functions. Usually, eCB levels are regulated by the body to accommodate disturbances caused by pathologies. However, in case of chronic disease the regulatory process can be permanently affected.[22] Indeed, its deterioration has been linked to the development of several diseases including neurodegenerative diseases, cancers, epilepsy, and strokes.[23] The purpose of eCBs is to regulate the ECS to prevent a pathology from developing. The progressive aspect of diseases like Alzheimer or Parkinson's usually culminates in the overstimulation of the ECS.[18] The overstimulation results in the advancement of the disease and a deteriorating quality of life for patients due to loss of motor function and memory, which are functions closely linked to CB_1 receptors. The increased activity of eCBs also results in inflammation expressed by an increased amount of CB_2 receptors.[18] The observation was interpreted as an adaptation of the ECS developing additional CB_2 receptors to manage the damage cause by the disorder.[18] The eCBs and CB receptors level have also been linked to eating disorders in which case the administration of CB_1 antagonists to animals suffering from obesity led to the amelioration of their condition. [18]

It has been established that CB uses can have a protective effect on an irregular ECS, but it is important to note that the exposure to CBs in young children and teenagers can lead to abnormal eCB signaling leading to both psychological and psychomotor disfunctions.[19] The impact of the development of irregularities in the ECS is such that it has driven scientists to explore the possibility of regulating the ECS using phytocannabinoids to supplant the eCBs deficiencies. The CBs found in *C. sativa*, THC and CBD are compatible with the ECS.[23] THC can bind the CB_1 receptors found in high concentration in the brain. The location of the receptors in areas of the brain responsible for cognition, memory, motor co-ordination, etc., is linked to the psychoactive effects caused by THC.[24] However, CBD does not have a high affinity for either receptor. It acts as an inverse agonist of CB_2 receptors, which can trigger a biological response resulting in anti-inflammatory effects, hence the growing interest surrounding CBD.[19]

1.2.3. Anti-Carcinogenic Properties

Besides the regulation of the ECS, CBD has been studied for its anti-carcinogenic properties. Several eCBs inhibit the growth of different types of cancerous cells ensuing complex processes.[22] When used appropriately, eCBs will stimulate CB receptors and trigger the inhibition of cancer cell invasion, adhesion, and migration, metastasis formation and angiogenesis, as well as the control of signaling pathways.[22] It is important to note that the effectiveness of the use of CBs to inhibit the progression of cancer highly depends on the concentration of CBs. At low concentration, the use of CBs could have the opposite effect specifically the proliferation of cancer cells instead of its inhibition.[22] The phenomenon is due to the relative levels of CB receptor expression of the tumor, and renders this approach very efficient for tumors with high level of CB receptors but counter-productive for tumors with low levels of CB receptors.[22] When CBs levels are much higher in the immune cells than in the tumor cells, using CBs to cause the inhibition or apoptosis of the cell leading to the suppression of the immune cells and therefore, resulting in the growth of the tumor.[22] The use of CBD as cancer treatment has been successfully experimented to slow down the development of breast cancer.[22] Further experiments showed promising results for a cancer treatment when combining the use of CBs agonist and cytotoxic agents.[22]

1.2.4. Available Drugs

As discussed previously, the exploration of the benefits of *C. sativa* in western medicine was slow. The mechanisms of action of THC were elucidated in the 1990s however, due to its psychoactive effects the compound is not suited to be incorporated in drug treatments. Many other CBs are available in marijuana, most of which do not have any psychoactive effect, however their effects on the ECS are still unclear. Nevertheless, CBD and its analogs have a great potential as drug treatment options.

Recently, the debate around the use of marijuana for medical purposes has returned to center stage. The legalization of marijuana for medical uses in several countries during the past decade led to the development of a few drug treatments. In 1986, the first DEA approved drug *Marinol* containing dronabinol **13** was developed.[25] Dronabinol is a synthetic form of (-)-trans-D^9-THC (see Figure 4). The drug is designed to be an appetite stimulant designed for AIDS patients and patients suffering from anorexia as well as to help treat nauseas experienced by cancer patients undergoing chemotherapy.[25] *Syndros* is another FDA approved drug containing the same active ingredient with the same purpose.[25] *Cesamet* is another drug containing a cannabis related compound.[26] The drug contains nabilone **14**, a racemic mixture of a THC derivative bearing a dimethylated alkyl chain (see Figure 4). It is designed for patients suffering from nauseas and vomiting due to cancer drug treatment.[26]

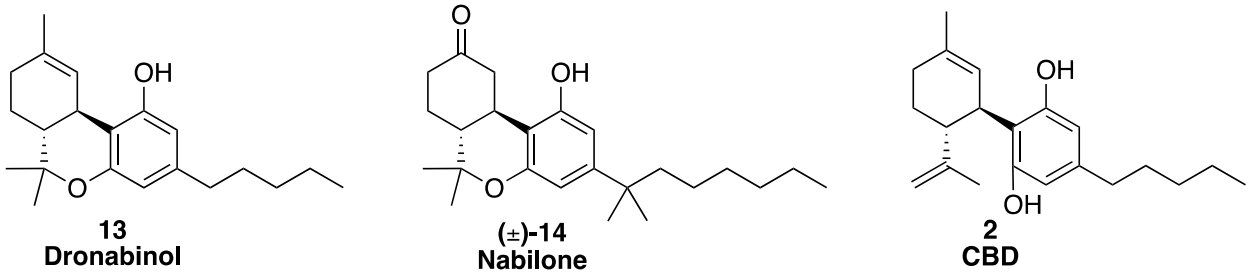

Figure 4: Dronabinol, Nabilone, and CBD

The only CBD-based drug currently available on the market is *Epidiolex* (NDC Code(s): 70127-100-01, 70127-100-10). The drug is a clear solution containing CBD directly extracted from the plant at a 100mg/mL concentration.[27] The extraction of the molecule from the plant is obtained through a standard carbon dioxide extraction. Inactive ingredients include dehydrated alcohol (7.9% w/v), sesame seed oil, strawberry flavor, and sucralose. It was approved by the FDA in 2018

to treat patients suffering from seizures linked to the Dravet syndrome, the Lennox-Gastraut syndrome or tuberous sclerosis complex in children as young as two years old.[28] As of August 2020, the use of *Epidiolex* has been expanded to treating patients suffering from seizures associated with Tuberous Sclerosis complex.[28] The CBD-based drug is made with an active ingredient directly extracted from the plant to ensure its high purity, higher than the one of synthetically produced CBD, making it adequate to be used for young patients. The exact mechanism of action of this seizure preventing drug remains unknown.

Considering the variety of CBs found in the plant and the possibilities offered by synthetic CBs, the potential for new drug treatments is broad provided that the mechanisms of action of CBs becomes better understood.

1.2.5. Bioavailability

It has been established that CBs present some great advantages for the future of medicine. Several drug treatments have been developed; however, the low bioavailability of CBD remains a common obstacle. CBD is a lipophilic molecule due to the presence of an alkyl chain substituent on its aromatic ring. Research reports that the lipophilic nature of the molecule is responsible for its accumulation in fatty tissues, correlating with a poor dissolution in gastrointestinal fluids ultimately resulting in poor absorption.[29] Since they are not water soluble, the bioavailability of CBs such as THC and CBD lies around 9% when orally administrated, meaning that a great majority of the molecules passes through the body.[30] So far, the research and innovation aiming to increase the bioavailability of CBD has relied on new technologies for the administration of the drug, such as nasal sprays, transdermal administration, and self-emulsifying systems rather than oral administration.[30]

Though the development of new drug delivery technologies creates solutions to the solubility limitations of CBD, the synthesis of CB derivatives could also present interesting results for a better assimilation of the drugs. Increasing the bioavailability of CBD can be done by through the introduction of substituents decreasing the lipophilic character of the natural compound. The types of modifications usually explored to increase bioavailability are the introduction of a shorter alkyl chain (see Figure 5) or of a cyclopropane (see Figure 6). The modifications would allow to improve the bioavailability of the molecule while retaining the biological properties of CBD.[31] It

is worth noting that the dimethylated and monomethylated CBD derivatives both exhibited enhanced activity towards certain inhibitors.[31]

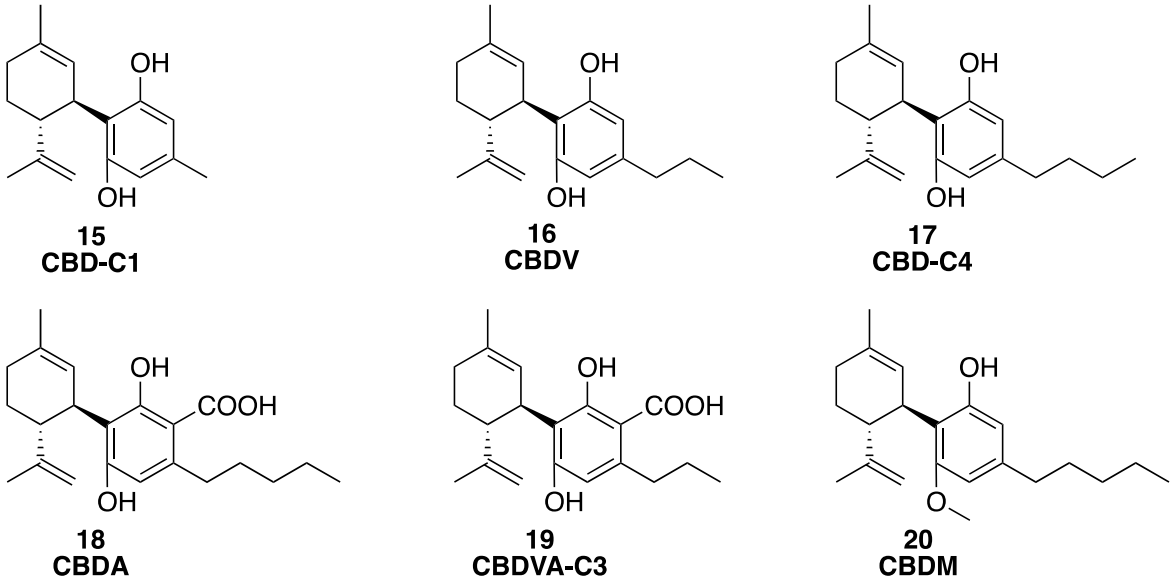

Figure 5: Potential CBD Derivatives

Cyclopropanated compounds are molecules of great interest for the development of new drug treatments due to their versatility and their biological properties.[32] Research has shown that the introduction of a cyclopropane in compound **21** (see Figure 6) led to an increased affinity to the CB_1 receptor[33], encouraging the synthesis of cyclopropanated CBD derivatives.

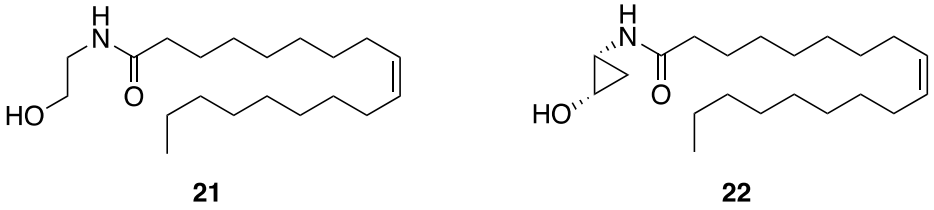

Figure 6: Oleothylethanolamide and Cyclopropanated Derivative

The potential presented by CBD and its derivatives for the development of new drug treatments has been clearly established. The following chapter will discuss the various pathways proposed to synthesize CBD throughout the years.

1.3. *Synthesis of Cannabinoids*

1.3.1. Biosynthesis

Cannabinoids (CBs) obtained from the extraction of the marijuana plant are biosynthesized in the marijuana buds of the female plants. Though the complete biosynthetic process of CBs is still only partially understood it has been established that CBs are generated through the biosynthesis of a shared precursor cannabigerolic acid (CBDGA) **28**. CBDGA is obtained from hexanoyl-coenzyme A (**23**), which is then transformed into different CBs via the appropriate enzymatic reaction (see Scheme 2).[34]

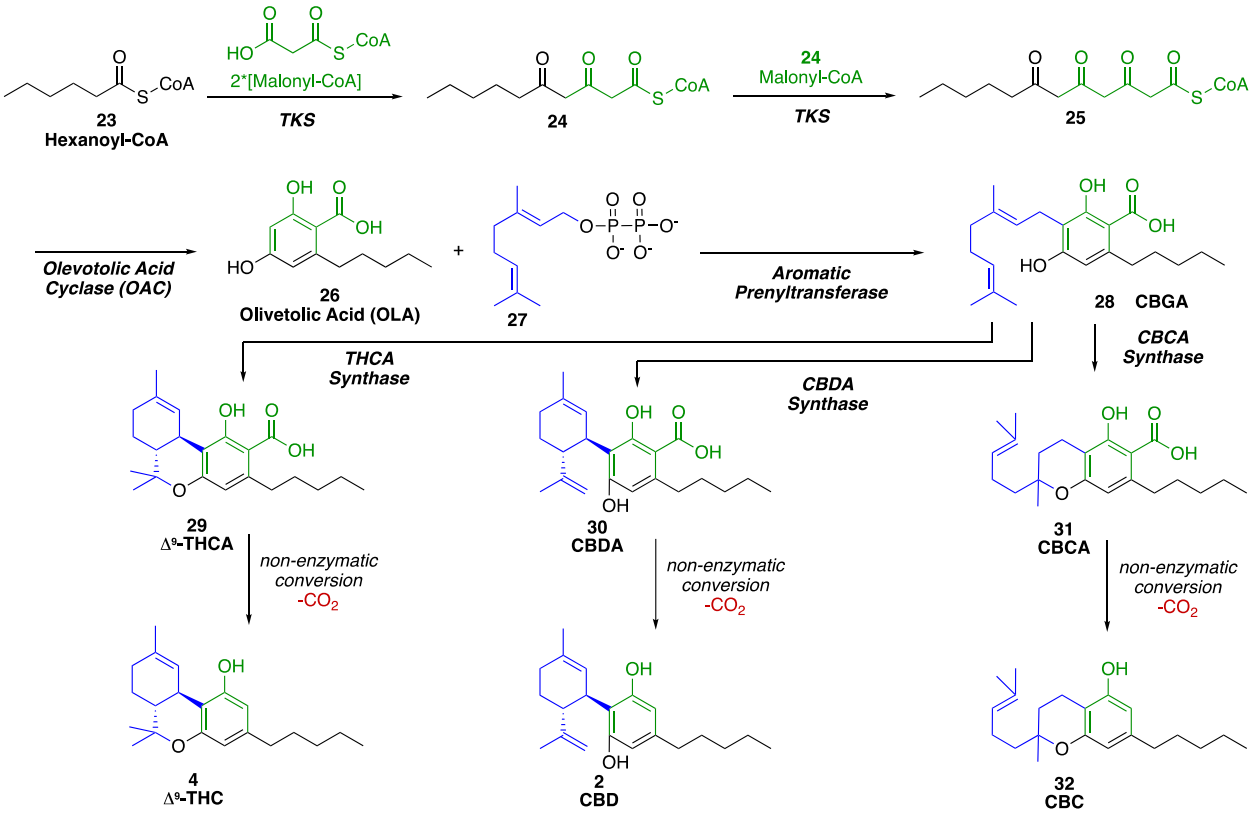

Scheme 2: Biosynthesis of Cannabinoids

Δ^9-Tetrahydrocannabinolic acid (Δ^9-THCA) **29**, cannabidiolic acid (CBDA) **30** and cannabichromenic acid (CBCA) **31** undergo chemical transformations when subjected to heat or light, leading to the loss of carbon dioxide (CO_2) and resulting in the formation of Δ^9-THC, CBD, and CBC respectively.[34] The loss of carbon dioxide demands further research in order to understand the exact mechanisms of decarboxylation and the production of the remaining hundreds of CBs present in the marijuana plant.[34]

1.3.2. Cannabinoid Extraction

CBD can be extracted from the marijuana or the hemp plant and allow to obtain a highly pure product, though the extraction process is not best suited for the future use of CBD and its analogs in the pharmaceutical industry. The extraction of CBD is done by macerating the plant in an organic solvent, followed by the concentration of the desired product. The conditions for solvent extraction can lead to chemical changes of the molecule, namely the loss of the carboxylic acid substituent (see Scheme 2).[35] Additionally, CBD represents only a small fraction of the CBs present in the *C. sativa.* CBD can also be obtained through supercritical fluid extraction, a process that allows to separate components using the supercritical fluid CO_2. However, supercritical fluid extraction may be encountered with solubility issues.[36]

CBD extraction affords a clean product, but it requires large quantities of organic solvents. It requires expensive equipment for the extraction of a molecule that is not present in great quantities in the plant. To increase the potential of CBD for the development of new drug treatments, synthetic production presents a better option. Chemically obtained CBD can be purified using established active pharmaceutical ingredients (APIs) purification methods to ensure the purity of the product.[36] Furthermore, using a chemically produced CBD would facilitate the synthesis of derivatives that are not naturally present in the plant with potential further medical applications (see Figure 7).[36]

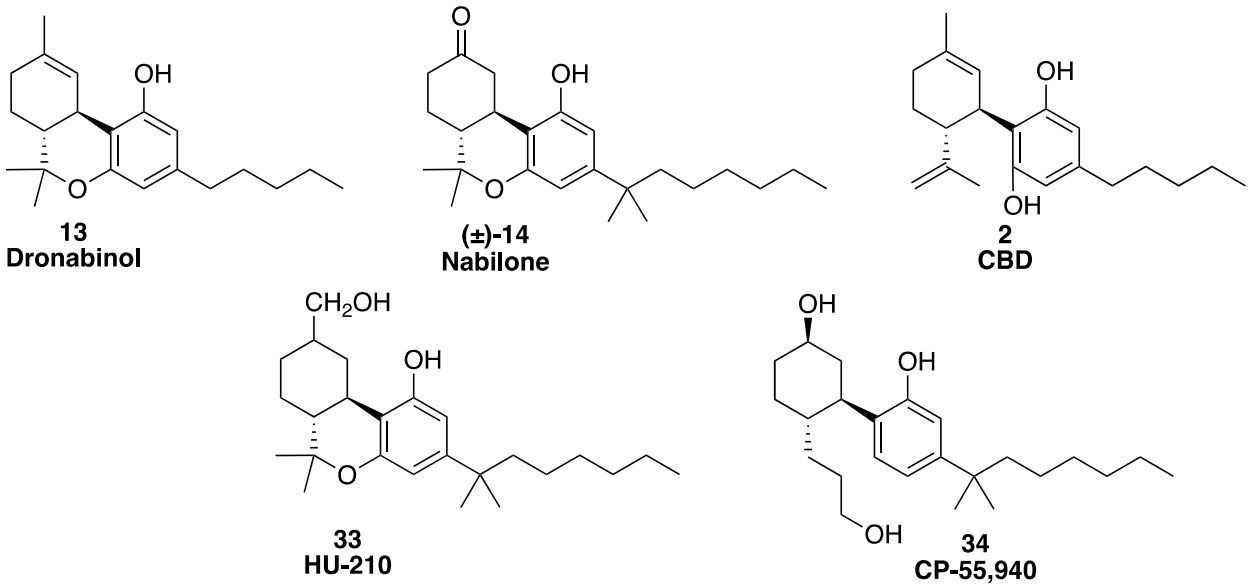

Figure 7: Synthetic Cannabinoids

Since the structure of CBD was first established and synthesized,[17] several chemists have developed different approaches for its synthesis, all of which present some advantages and some limitations. The more challenging aspects of synthesis of CBD are to control the stereochemistry of the terpene ring and the final demethylation.

Generally, the synthetic route to CBD involves a reaction between an olivetol derivative and a terpene obtained from natural products like limonene leading to the bicyclic structure of CBD. An alternative pathway to the precursor of CBD involves a Diels-Alder reaction allowing to build the bicyclic adduct using an olivetol or resorcinol derivative. Recently, a strong focus has been put on adapting those synthetic approaches to flow chemistry in order to be able to efficiently produce large quantities of CBD for the pharmaceutical industry. These synthetic pathways will be discussed in the following sections.

1.3.3. Synthesis of Cannabinoids using Terpenes

As mentioned previously, the first synthetic route to CBD was developed by Mechoulam *et al*.[17] They proposed a method in which citral **6** was used in combination with a lithium derivative of olivetol dimethyl ether **5** to generate CBD (**2**) (see Scheme 1).[17] The reaction of olivetol lithium derivative **5** with citral **6** afforded a mixture of CBs with an overall yield of 2% .[17] *dl*-CBD **2a** was further transformed into *dl*-Δ-3,4-*trans*-THC when treated with a hydrochloric acid to trigger the deprotection and the formation of the pyran. Though the yield afforded by this route is not sufficient to be applicable to large scale production this approach to the synthesis of CBD set the groundwork for later synthetic proposals. Additionally, the synthetic route proposed by Mechoulam *et al.* does not lead to the (-)-CBD diastereomer but to a racemic mixture of (±)-CBD.

In 1992, Vaillancourt *et al.* proposed an alternative route to the synthesis of CBD using fragmentation reactions on 9-bromocamphor **35** (see Scheme 3).[37] The starting material **35** undergoes selective alkylation using a lithium derivative of olivetol **36** and a copper reagent to generate the corresponding α-aryl ketone **37**. The α-aryl ketone **37** is then subjected to a fragmentation via sodium naphthalenide, followed by trapping of the enolate to generate an enol phosphate **38**. [37] The enol phosphate **38** is treated with *tert*-butanol on lithium foil to obtain a reductive cleavage as well as a mono- and bis-deprotection generating both (-)-CBD **2** and (-)-CBD methyl ether **2'** with respective overall yields of 22% and 27%. The stereoselectivity of the method

is ensured by the steric hindrance of the organolithium and the cuprate.[37] Vaillancourt *et al'*s method offers a significant improvement of the overall yield of CBD however, the major product is mono-deprotected CBD. Furthermore, the synthesis utilizes the expensive starting material bromocamphor **35** which is not ideal for large-scale industrial production.

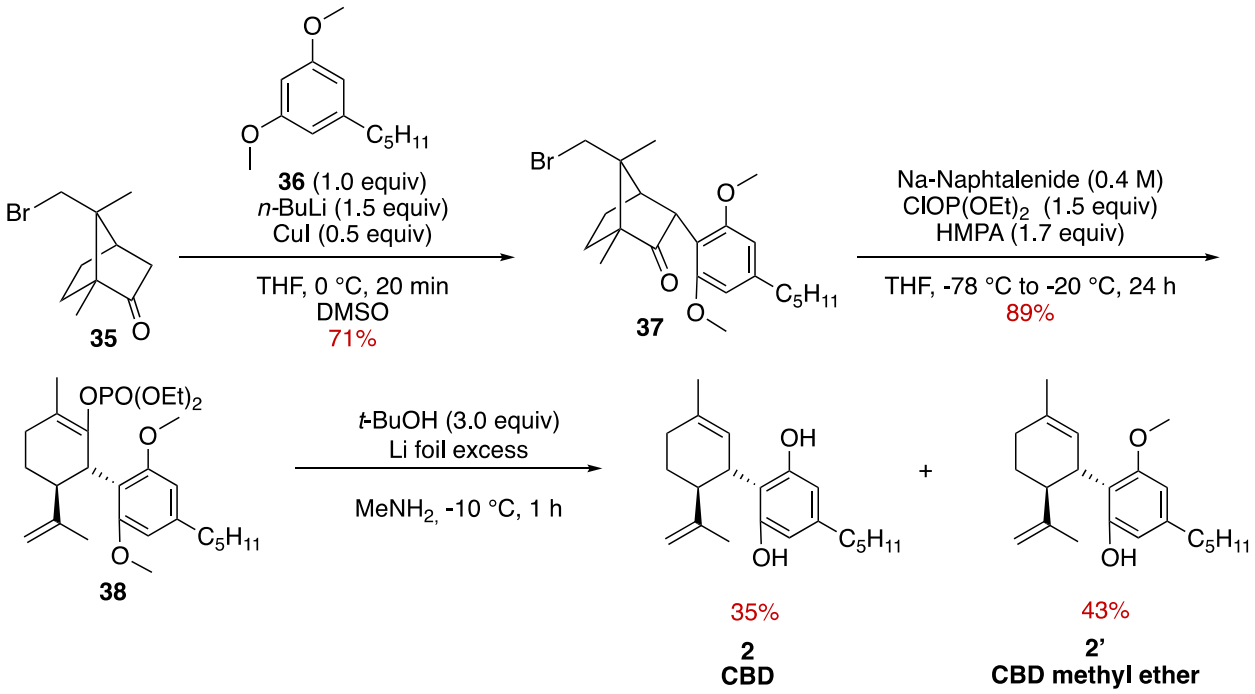

Scheme 3: Synthesis of CBD, Vaillancourt *et al.*, 1992

In 2006, Kobayashi *et al.*[38] proposed an alternate regioselective synthetic pathway to CBs resembling the approach given by Mechoulam *et al.*[17] (see Scheme 1 and 4). The synthesis uses the starting material cyclohexenediol monoacetate **39** subjected to alkenylation with a nickel catalyst followed by a Grignard reaction to generate the corresponding isopropenyl phenol **40**. The phenol then undergoes a Jones oxidation as well as an iodination to generate the iodoenone **41**. A cyanocuprate obtained from olivetol derivative **36** is then added to **41** via a Meinwald rearrangement and nucleophilic substitution to generate the corresponding α-iodoketone **42**.[38] The product is then subjected to three successive Grignard reaction in order to obtain the enol phosphate **43**, then cannabidiol dimethyl ether (CBDD) **2c**, and finally the desired product CBD **2** with an overall yield lower than 10%.[38] Despite being a viable route for the synthesis of CBD, this pathway is unlikely to be retained for the large-scale production of CBD as it results a low yield of the desired product. The starting material is commercially available, though uncommon and expensive

(122k USD/mol); it can be synthesized from cyclohexene which would add three steps to the synthesis and further diminish the overall yield.

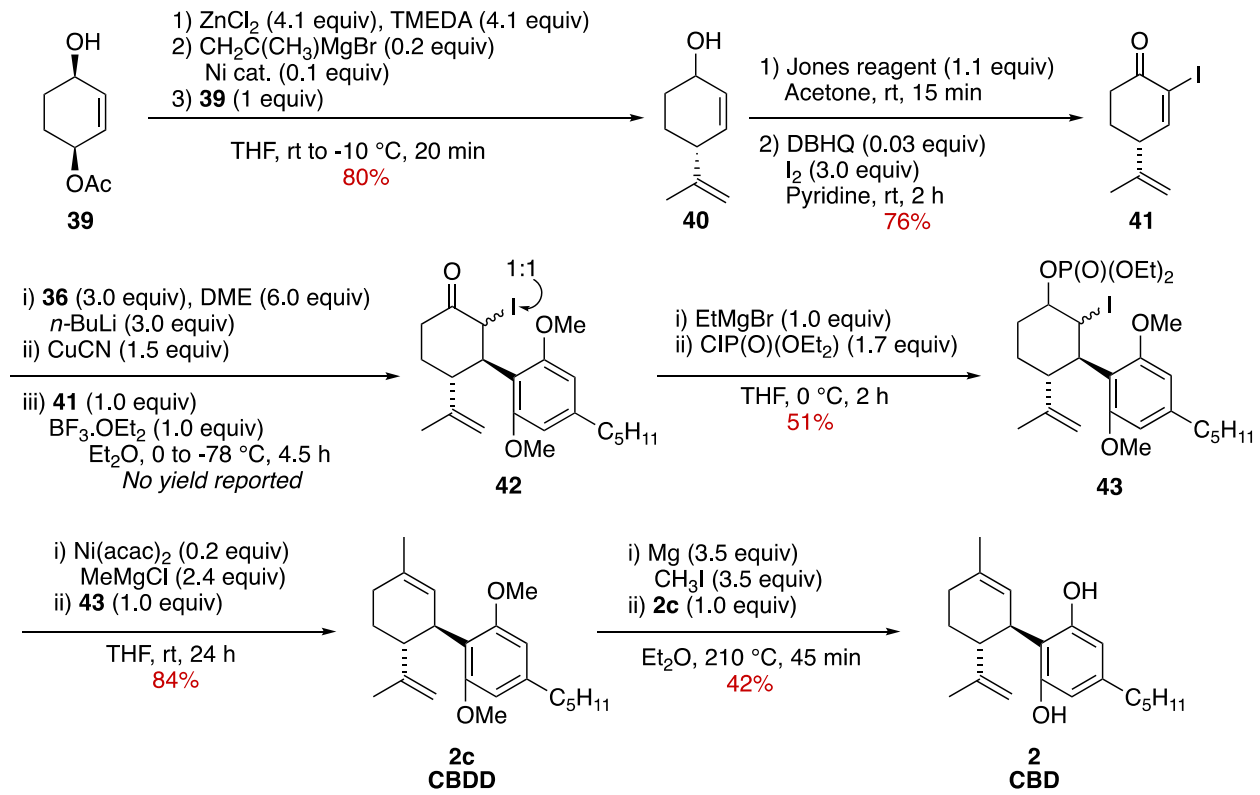

Scheme 4: Synthesis of CBD, Kobayashi *et al.*, 2006

1.3.4. Diels-Alder Syntheses

Using a coupling reaction between a terpene and an olivetol derivative to generate CBD presents conveniences, but the main disadvantage are the expensive starting materials as well as reaction conditions that may not be suitable for mass production in the pharmaceutical industry. Accessing CBD through these procedures also increases the chances of CBD undergoing a cyclization when coupling the terpene and the arene under mild or strong acidic conditions, leading respectively to the formation of Δ^9- THC and Δ^8- THC.[39] A synthetic pathway using a Diels-Alder reaction as the key reaction to generate the bicyclic structure of CBD presents a solution to these limitations.

In 1966, Korte *et al.* presented a synthesis of CBD using the olivetol derivative (*E*)-4-(2,6-dimethoxy-4-pentylphenyl)but-3-en-2-one **44** (see Scheme 5).[40] The ketone **44** was first treated with methyltriphenylphosphonium bromide in a Wittig olefination, and then subjected to a Diels-

Alder reaction with 3-buten-2-one to obtain a bicyclic ketone **46**. The adduct underwent a second Wittig olefination yielding dimethyl ether CBDD **2c***. The final product *cis*+*trans*-*dl*-CBD **2*** was obtained through a Grignard reaction with an overall 13% yield, and 9.5% overall yield for *trans*-CBD.[40] The drawback of Korte *et al.*'s pathway is its lack of stereoselectivity. The stereoselectivity of the Diels-Alder reaction is heavily dependent on the temperature at which it is performed.[40] Indeed, the crude product of this step contains both the *cis* and the *trans* product with a *cis:trans* ratio of 2:1 at 130 °C to 1:6 at 200 °C.[40] *trans*-CBD was able to be isolated using column chromatography, however the *cis* isomer was never isolated.[40] The deprotection of *dl*-CBDD **2c*** poses an issue as well, as a lot of the product is lost in that step, yielding both CBD monomethyl ether and olivetol as byproducts.[40]

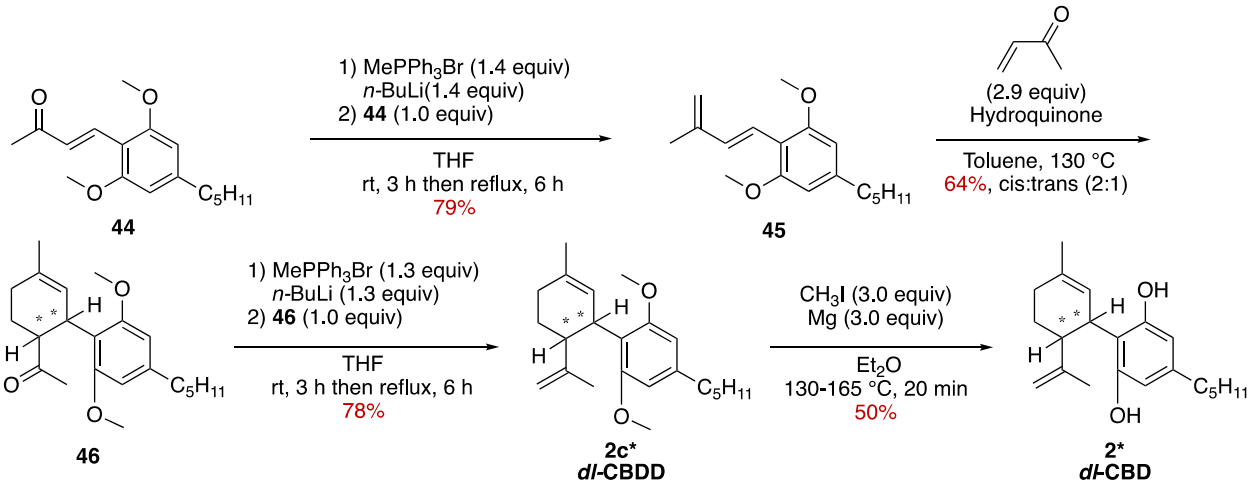

Scheme 5: Synthesis of CBD, Korte *et al.,* 1966

In 2009, Ballerini *et al.* developed a high-pressure Diels-Alder approach under mild conditions that does not require any metal catalysts or high temperatures (see Scheme 6).[41] The method is an optimization of a Diels-Alder reaction on coumarins using isoprene as the diene and 3-cyano-5-hydroxy-7-pentylcoumarin **47** as the dienophile to generate the corresponding cycloadduct.[41] The cycloadduct **47** was subjected to decyanation using sodium bicarbonate to generate benzochromenone **48** before decyanation, methylation, and dehydration to produce *cis*-CBD **2**** with an overall yield of 45%.[41] In the continuity of their work, Ballerini *et al.* developed a procedure using (*E*)-benzylideneacetones **52** to generate the dienophile necessary to the Diels-Alder reaction with the desired dienophile, yielding both the *cis* and *trans* diastereoisomers **54** (see Scheme 7).[42] The formylated resorcinol **51** was first subjected to an aldol condensation using

sodium hydroxide (NaOH) in an aqueous environment, followed by a Wittig olefination to obtain the desired diene **53**. The key Diels-Alder reaction afforded the bicyclic adduct **54** with a 6:1 *cis:trans* ratio with the possibility to isolate 74% yield of pure *cis* product using separation by chromatography.[42] The procedure was then applied to efficiently synthesize Δ^8-THCs **4*a-f**. [42]

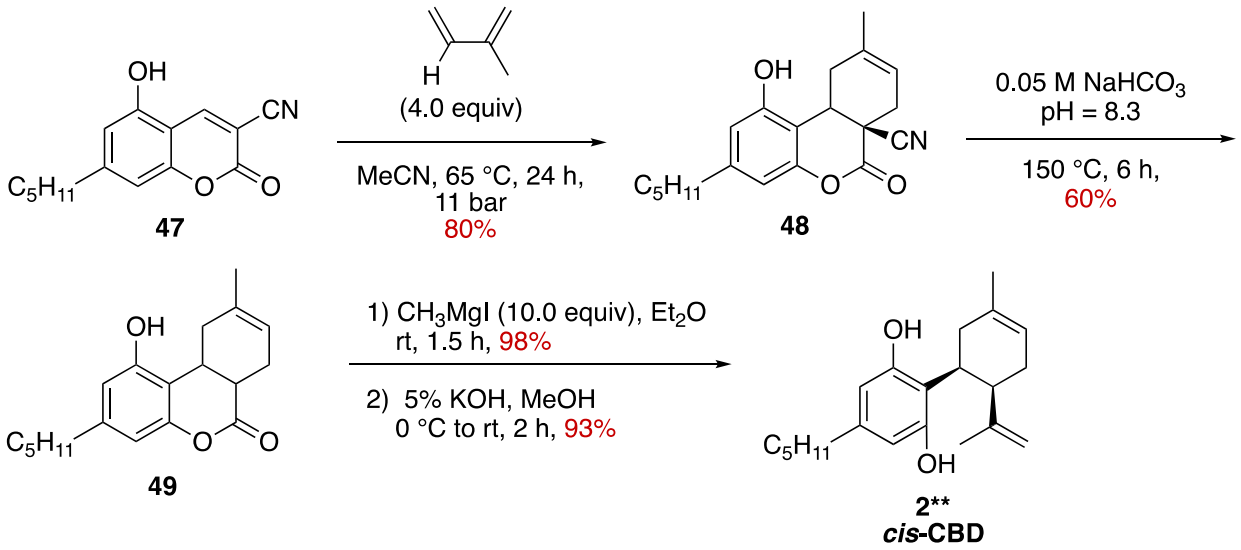

Scheme 6: Synthesis of *cis*-CBD, Ballerini *et al.*, 2009

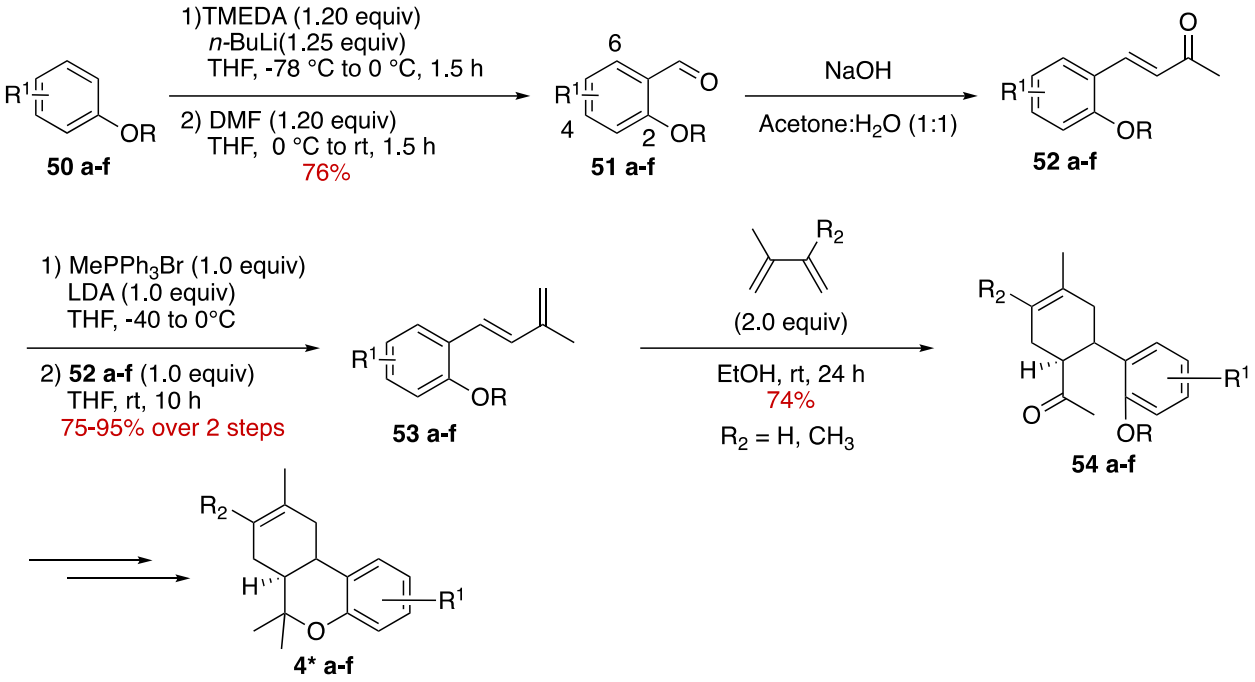

a: R = CH_3; R_1 = H; b: R = CH_3; R_1 = 4'-OCH_3; c: R = CH_3; R_1 = 6'-OCH_3; d: R = CH_2OCH_3; R_1 = 6'-OCH_2OCH_3; e: R = CH_3; R_1 = 4'-C_5H_{11}, 6'-OCH_3; f: R = CH_2OCH_3; R_1= 4'-C_5H_{11}, 6'-OCH_3

Scheme 7: Synthesis of CBD, Ballerini *et al.*, 2011

The use of the Diels-Alder approach enables the functionalization of the terpene and gives access to another category of CBD derivatives. As demonstrated by Ballerini *et al.*, the use of different dienophiles generates different terpene fragment.[41,42] The access to a variety of derivatives enabled through the Diels-Alder approach encouraged us to focus on the Diels-Alder method for the synthesis of the CBD precursor.

1.3.5. Adaptation of the Cannabidiol Synthesis to Flow Chemistry

New synthetic pathways towards CBD have been well explored as it has gained more popularity for the treatment of various illnesses as well as management of different symptoms. The necessity for efficient large-scale production of the molecule is becoming increasingly crucial in order to satisfy the demand for CBD and to support the research aiming to develop novel drug treatments. Therefore, the adaptation of the synthesis of CBD to continuous flow processes is essential.

Continuous flow chemistry has been developed in an effort to provide a solution to the obstacles often encountered with the large-scale production of pharmaceutical targets.[43] Reactions take place

in small tubes and reactors instead of a round bottom flask. The adaptation of batch processes to continuous flow chemistry requires an adaptation of the synthesis to minimize or eliminate quenching, extraction, and purification processes as well as providing alternatives for procedure requiring pyrophoric reagents.[43] A major advantage of continuous flow chemistry lies in the control of the reaction conditions. The temperature of the reaction mixture and the amount of time the reaction is ran for can be strictly regulated, therefore increasing the reproducibility and the turnover numbers of the reactions. Continuous flow chemistry also provides a safer work environment and is nowadays preferred for the production of a significant number of APIs.[43]

In 2021, Bloemendal *et al.* published their work on the development of a synthesis of Δ^9-THC **4**, Δ^8-THC**4***, and CBD **2** under continuous flow chemistry conditions (see Scheme 8).[44] Their approach relies on the use of homogeneous and heterogeneous Lewis acids for the Friedel-Craft alkylation with (-)-verbenol and olivetol ultimately leading to the formation of enantiopure Δ^8-THC.[44] Encouraged by their preliminary results the group explored the possibility of using heterogeneous Lewis acids for the coupling of terpenes and arenes, as those reagents tend to be preferred due to their higher turnover number and their ease of recycling.[44] They were able to use silica-supported boron trifluoride (Si-BF_3) to obtain Δ^9-THC with a 39% yield and no traces of byproduct.[44] Based on preliminary results they were able to adapt the method to the coupling of *p*-mentha-2,8-dien-1-ol **55** and olivetol **56** to generate a mixture of products **2**, **4**, and **4***. Bloemendal *et al.* are currently working towards developing a more efficient synthesis of CBD under continuous flow chemistry conditions.

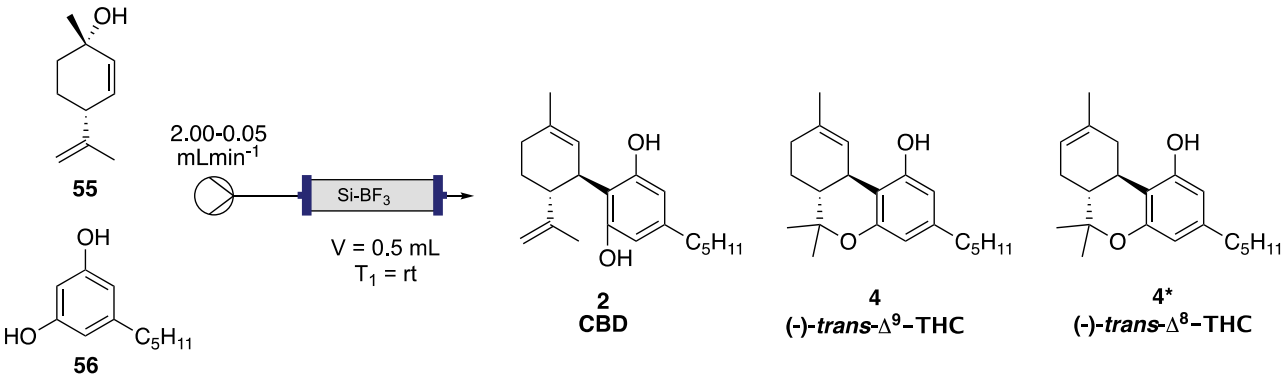

Scheme 8: Continuous Flow Synthesis of CBD and THCs, Bloemendal *et al.,* 2021

1.4. *Late-Stage Functionalization*

The development of synthetic pathway allowing the synthesis of CBD derivatives is of great interest to provide solutions to the bioavailability limitations of CBD. As mentioned previously, introducing modifications in the lipophilic chain substituted on the aromatic ring helps increasing the bioavailability of the molecule and therefore, its therapeutic potential. Different possibilities of late-stage functionalization were examined.

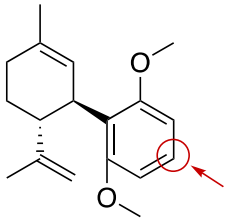

2c

Figure 8: CBD Precursor for Late-Stage Functionalization

1.4.1. Borylation of Substituted Arenes

The synthesis of a CBD precursor leading to various derivatives requires the functionalization of the aromatic portion of the compound. The activation of aromatic rings using transition metal complexes described by Hartwig-Miyaura presents a regioselective activation of substituted aromatic rings.[45] Miyaura *et al.* proposed a C-H activation method via iridium catalyzed borylation for the functionalization of arenes and heteroarenes.[45] The regioselectivity study conducted by Miyaura *et al.* reports the C-H activation at the *meta* position of disubstituted aromatic rings yielding isomerically pure products.[45,46]

Hartwig *et al.* reported the alkylation of borylated arenes via an arylboronate ester intermediate using a Pd and Ni-catalyzed coupling (see Scheme 9).[46] They were able to develop a method for the alkylation of substituted arenes **57** with unactivated alkyl electrophiles.[46] Their work provides an alternative to the traditional Fe-catalyzed, Cu-catalyzed, and Ni-catalyzed Suzuki couplings that present limitations in terms of the functional group tolerance, yields, and substrate tolerance respectively on top of the overall complexity of those reactions.[46]

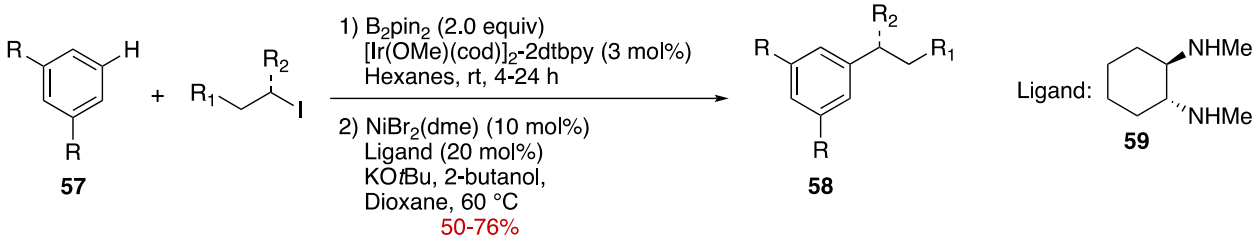

Scheme 9: Scope of Substituted Arene Alkylation, Hartwig *et al.*, 2013

The scope for Hartwig *et al.*'s approach indicates that the method could be a strong candidate for the late-stage functionalization of CBD. However, it is important to consider that the ligand required for this reaction is expensive, which led us to explore alternate options for the synthesis of CBD analogs and the adaptation of the synthesis to an industrial scale.

1.4.2. Suzuki Cross-Coupling

The functionalization of the aromatic portion of CBD derivatives can be obtained using a halogenated arene subjected to a Suzuki cross-coupling. In combination with a Friedel-Crafts activation, the approach can lead to the formation of CBD derivatives. The use of a Friedel-Crafts activation may be met with limitations due to regioselectivity issues caused by the functional groups present on the molecule.[46,47] However, Suzuki cross-coupling has been successfully applied to the synthesis of CBs.

Dethe *et al.*[48] used a Suzuki cross-coupling to generate both enantiomers of machaeriol-D (see Scheme 10) via a new Friedel-Crafts method without the need of protecting groups (PG) and more efficiently than the previous 18-step synthesis [49] The aromatic fragment was generated through Suzuki coupling of the halogenated arene **60** with benzofuran boronic acid **61**, followed by demethylation. The terpene **65** necessary to the Friedel Crafts reaction was synthesized from limonene via allylic oxidation. The bicyclic adduct was obtained after Lewis acid catalyzed coupling. Different reaction conditions allowed the synthesis of (+)-machaeriol-D **64**, (+)-epi-machaeriol-D **67**, and (-)-machaeriol-D **68.**[48] The procedure relies on the functionalization of the aromatic fragment via Suzuki coupling which will be explored for the late-stage functionalization of CBD in this project. The use of a Friedel-Crafts coupling then enabled the synthesis of several THC analogs and could potentially be applied to the synthesis of CBD analogs.

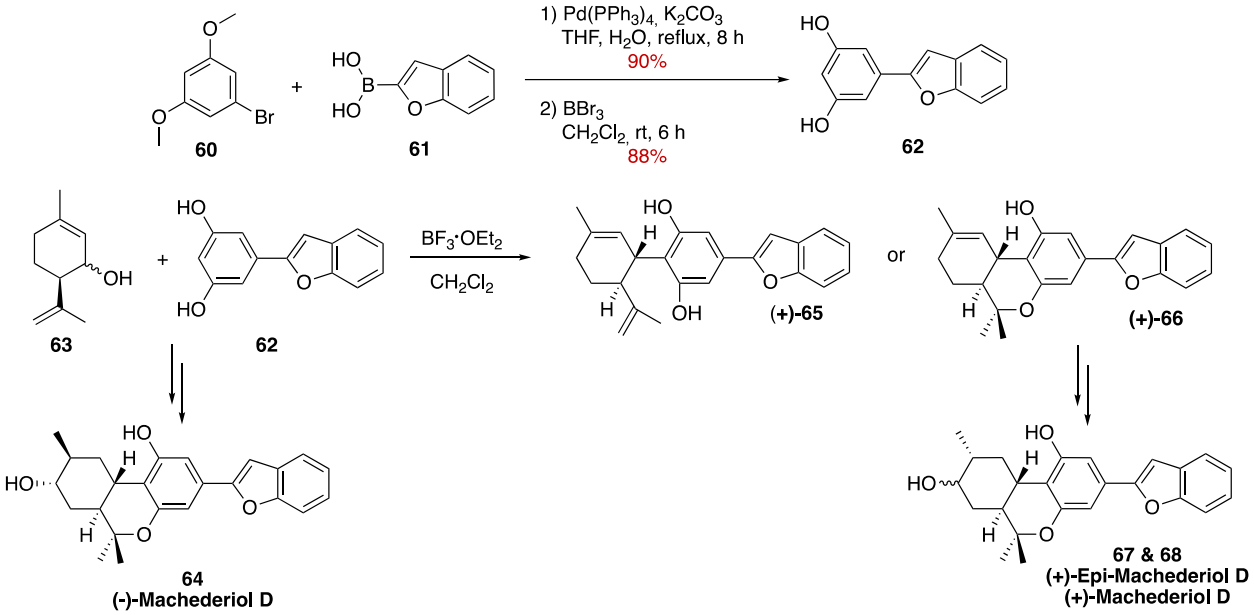

Scheme 10: Synthesis of THC Derivatives via Friedel-Crafts Alkylation, Dethe *et al.*, 2015

In 2009, Von Wangelin *et al.* optimized a cross-coupling method aiming to avoid the use of transition-metal catalysts (see Scheme 11).[50] The method allows the coupling of organohalides **69** through "domino effect catalysis".[50] The one pot reaction proceeds through the formation of a [Fe(MgBr)$_n$] complex, while the presence of TMEDA prevents the homocoupling reaction.[50]

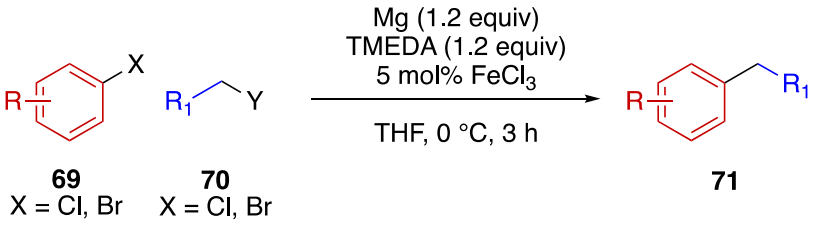

Scheme 11: Domino Fe-cat. Cross-Coupling, Von Wangelin *et al.,* 2009

Though the domino cross-coupling would need some further optimization to be adapted to the substrate, the use of a more sustainable and more affordable iron pre-catalyst in a cross-coupling reaction presents an attractive alternative for the post-functionalization of CBD.

1.4.3. Negishi Cross-Coupling

The goal of the proposed project is to provide a late-stage functionalization option for the synthesis of CBD and its analogs. Cross-coupling reactions are a widely developed tool applied to

sp^3-sp^3 or sp^2-sp^2 coupling via methods developed by Suzuki *et al.*[51], Sonogoshira *et al.*[52], or Kumada *et al.*[53] respectively. The project requires a versatile method that would enable a sp^2-sp^3 cross-coupling between the aryl substrate and the alkyl chain needed to generate the target molecule CBD and its derivatives.

Gong *et al.* developed a synthetic approach enabling the late functionalization of CBD in order to facilitate the synthesis of CBD analogs (see Scheme 12).[54] Gong *et al.'s* method was published in 2020, after the project for the late-stage functionalization of CBD had already been started. Their novel approach offers an efficient post-functionalization pathway to CBD analogs via Friedel-Crafts alkylation. CBD analogs were synthesized through the coupling of *p*-mentha-2,8-dien-1-ol **55** and phloroglucinol **72**. The regioselective triflation of the hydroxy group at the C5 position of arene **72** was possible due to the steric hindrance around the other two hydroxy groups found on the molecule. The two hydroxy groups were protected using a pivalate (Piv) protecting group (PG) before functionalization via Negishi cross-coupling of the C5 position. The final deprotection generated CBD with an overall yield of 52%. Gong *et al.'s* approach enabled the synthesis of several CBD derivatives (see Scheme 13).[54]

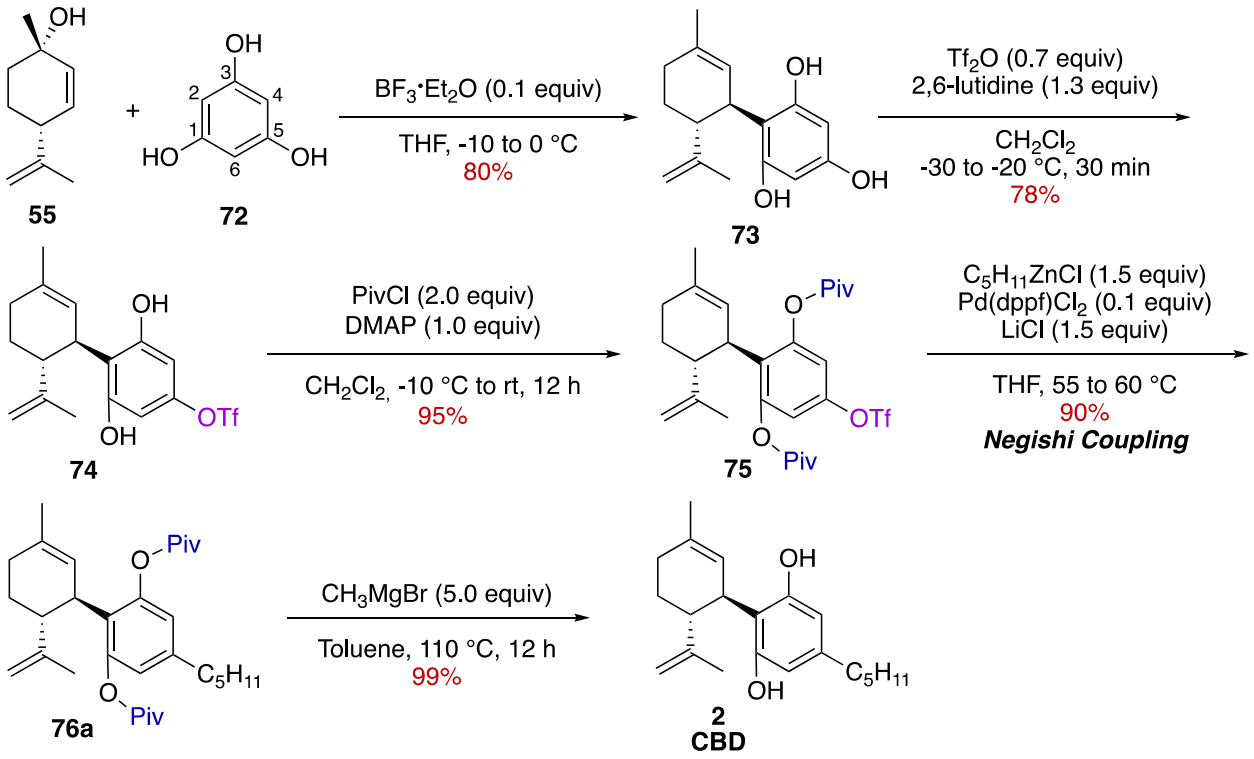

Scheme 12: Synthesis of (-)-CBD Derivatives via Late-Stage Functionalization, Gong *et al.*, 2020

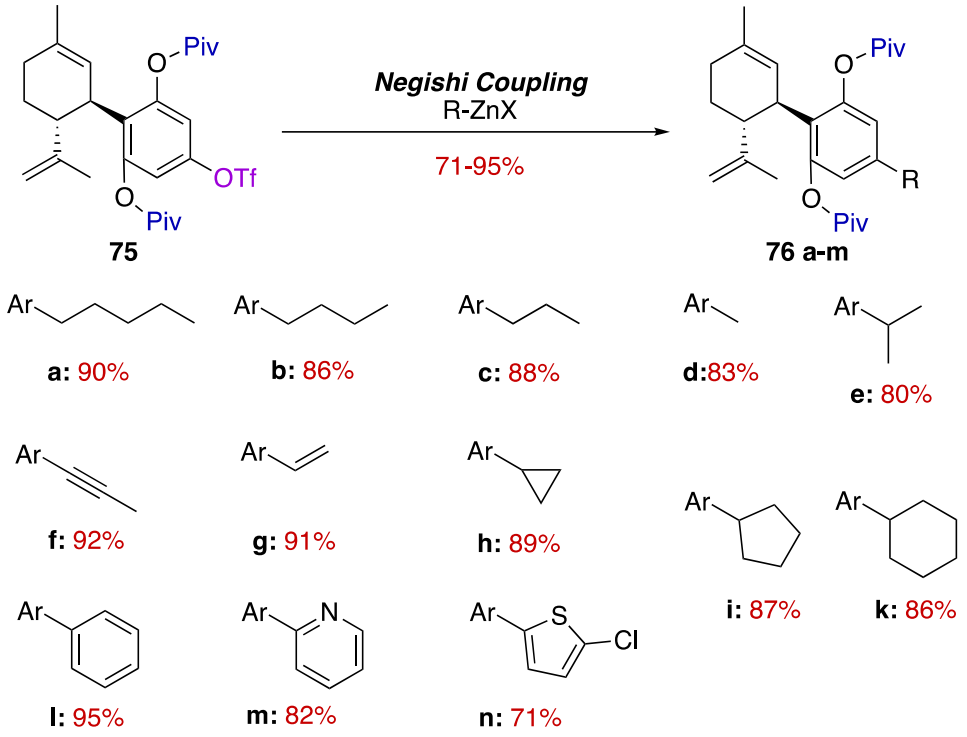

Scheme 13: CBD Derivatives Obtained via Negishi Coupling, Gong *et al.,* 2020

As Gong *et al.'s* method for the synthesis of CBD derivatives was published while we were working on our own project, we wanted to offer another approach to avoid the use of toxic and expensive metal catalyst while allowing to access a wide scope of functionalization and minimizing the overall cost by choosing a more affordable starting material.

1.5. *Objectives*

In light of the recent discoveries on the potential offered by the use of CBs in drug treatment as well as the relaxation of the legislation around medical marijuana the Charette group has decided to focus some research project on the synthesis of CBD destined to therapeutic uses. The possibility of accessing several CBD derivatives is essential as the research on different analogs is still limited and synthesizing different analogs expands the research on potential drugs. Furthermore, the need for CBD derivatives with an increased bioavailability is strong.

Our goal was to develop a reproducible, cost and time effective synthesis of the targeted compound, with a potential of being adapted to continuous flow chemistry. We focused on a synthesis that allows the production of various CBD analogs. We aimed to develop a synthetic

route permitting a late-stage functionalization utilizing an affordable starting material. Our approach combines the Diels-Alder strategy allowing to control the stereochemistry of the product with post-functionalization of the aromatic fragment. The use of the Diels-Alder approach potentially enables the functionalization of the terpene ring to access another variety of derivatives using different dienophiles.

2. Synthesis of Cannabidiol and Derivatives

2.1. *Retrosynthetic Analysis*

The synthetic routes proposed by Korte *et al.*[40] and Ballerini *et al.*[41] were chosen as the starting point for the synthesis of CBD analogs. As stated in the introduction, proposing new synthetic pathways enabling the production of several CBD derivatives has become highly relevant. The alternative recently proposed by Gong *et al.*[54] offers an elegant approach, though both of *p*-mentha-2,8-dien-1-ol **55** and phloroglucinol **72** are expensive compounds and those reaction conditions could be challenging to adapt to large scale production.

The goal was to establish an affordable route for the synthesis of various CBD derivatives. Choosing the synthetic pathway relying on the Diels-Alder reaction for the formation of the bicyclic adduct followed by an epimerization ensures the formation of the desired stereoisomer. The retrosynthetic analysis of the functionalizable CBD precursor led to the conclusion that the desired product could be obtained through the borylation or the halogenation of the appropriate CBD precursor.

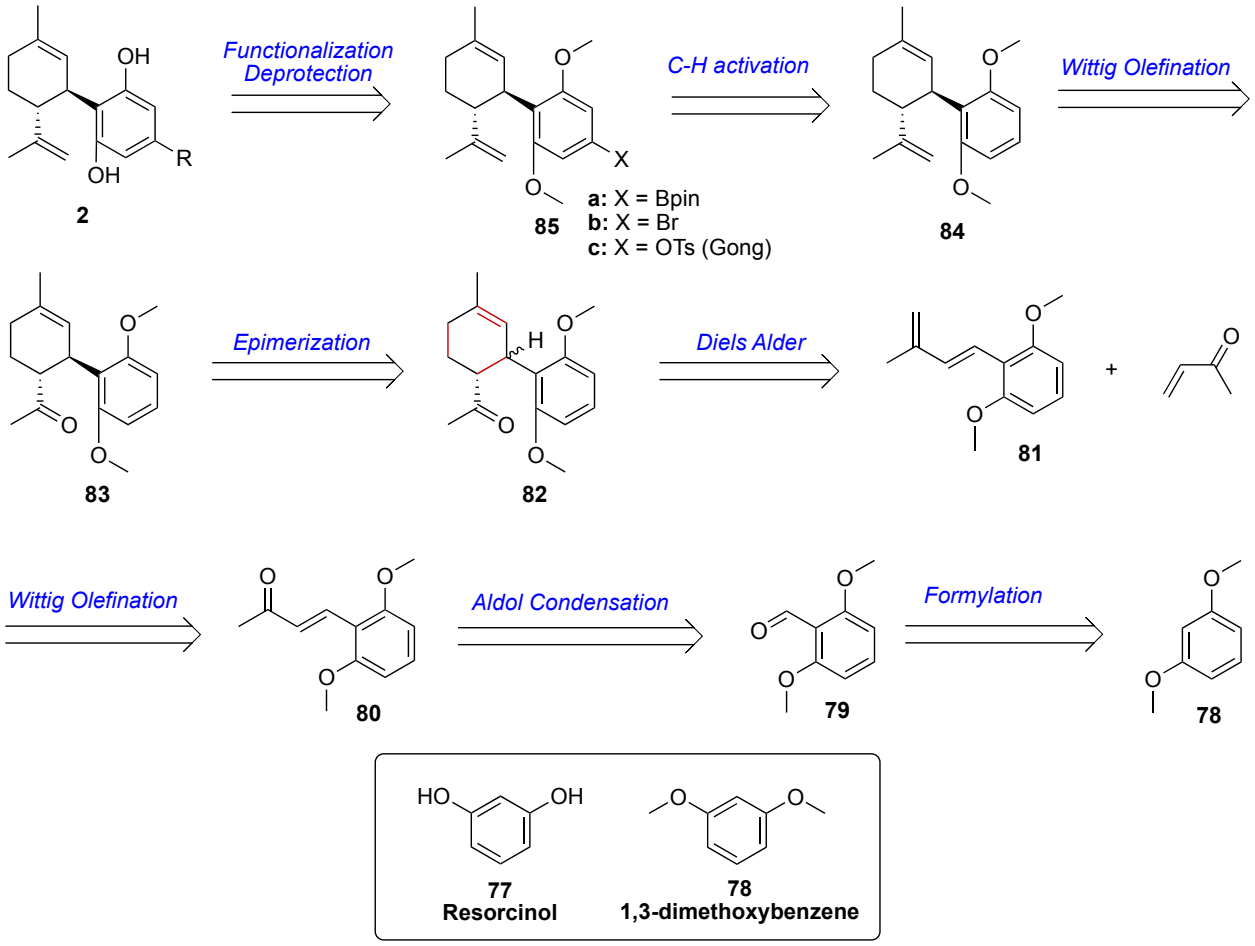

Scheme 14: Retrosynthetic Approach to the Late-Stage Functionalization of CBD

The Diels-Alder route was chosen as it enables the use of the affordable resorcinol derivative **78** as starting material (24 USD/mole). We proposed a synthetic route (see Scheme 14) using starting material **78** to generate the formylated product **79**. Aldol condensation of the aldehyde **79** followed with Wittig olefination of ketone **80** lead to the formation of the diene **81**. The diene **81** can then be used to generate adduct **82** as the product of the Diels-Alder reaction with 3-buten-2-one. The bicyclic ketone **82** can be subjected to an epimerization to cycloadduct **83**, followed by a second Wittig olefination to obtain the CBD precursor **84**. Substrate **84** can then be used for the C-H activation of the aromatic ring, leading to the late-stage functionalization via **85a** and deprotection to obtain CBD **2** and its derivatives.

2.2. *Synthesis of the Cannabidiol Precursor*

The synthesis started by with the formylation of substrate **78** (see Scheme 15), according to a procedure developed by Schultz *et al.*[55] The desired product was obtained through the initial reaction of **78** with *n*-butyllithium and tetramethylethylenediamine at -78 °C, leading to the lithiation of the aromatic ring. Then, the addition of dimethylformamide led to the synthesis of the desired formylated product 1,3-dimethoxybenzaldehyde **79** with a 73% yield.

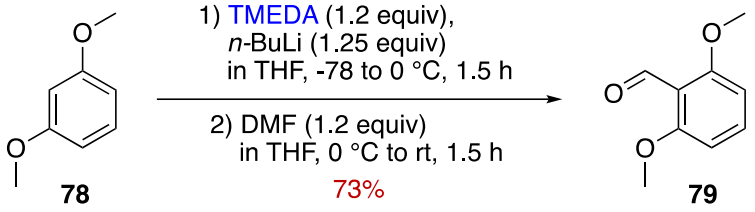

Scheme 15: Formylation of 1,3-Dimethoxybenzene

Metalation reactions do not generally require the addition of TMEDA to be effective. However, its addition allows to increase the rate of the reaction by breaking up the aggregates formed by *n*-butyllithium when they are found in solution and therefore increasing their basicity.[56a] Snieckus *et al.* confirmed their hypothesis through the observation of an increased deprotonation of benzene when using the metalating agent *n*-butyllithium-TMEDA complex compared to the use of *n*-butyllithium alone.[56a] The study of ortho metalation reactions revealed that the reaction proceeds through the lithiation of a site *ortho* to the directed metalation group (DMG).[56a] The resorcinol derivative substrate **78** used for the reaction bears two methoxy (OMe) groups, which are classified as moderate DMGs.[56a] Their presence on arene **78** ensures the stereoselectivity of the formylation reaction leading to the formation of the desired aldehyde **79**. According to Snieckus *et al.* the metalation proceeds through the initial formation of a complex with the alkyl lithium species (**i**), followed with the deprotonation of the aromatic ring to generate the corresponding ortho-lithiated intermediate (**ii**) (see Scheme 16).[56a] Finally, the addition of the electrophile leads to the formation of the desired product **79**.[56a]

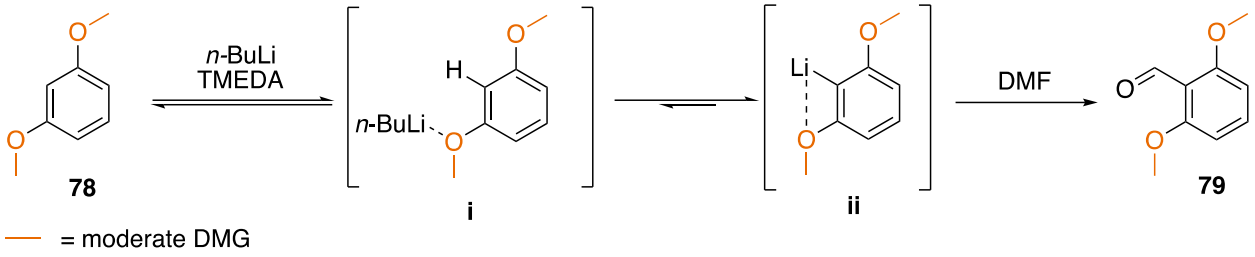

Scheme 16: Ortho Metalation Reaction Mechanism

The second step was the aldol condensation of aldehyde **79** (see Scheme 16)**.** The first approach taken was a catalyzed condensation reaction developed by List *et al.* using the morpholin-4-ium 2,2,2-trifluoroacetate (VI) catalyst **88**.[57] The catalyst **88** was synthesized with an 88% yield by treating morpholine **87** with trifluoroacetic acid (TFA).[57] Catalyst **88** was developed to avoid the oligomerization and self-aldol condensation that can occur when between the acetone and the aldol formed during the reaction.[57] However, List *et al.'s* method only generated the α,ß-unsaturated ketone **80** in a 64% yield and we were unable to reproduce the yields reported by List *et al.*[57] An alternative procedure using the stronger base NaOH in a 1:1 mixture of acetone to water enabled to yield 84% of **80** while decreasing the reaction time to 7 h and lowering the temperature to 50 °C.[58] The reaction proceeds via the formation of enolate through the deprotonation of aldehyde **79** by the base, followed with the aldol addition to the acetone present in the reaction environment and final loss of H_2O generating a,b-unsaturated ketone **80**.

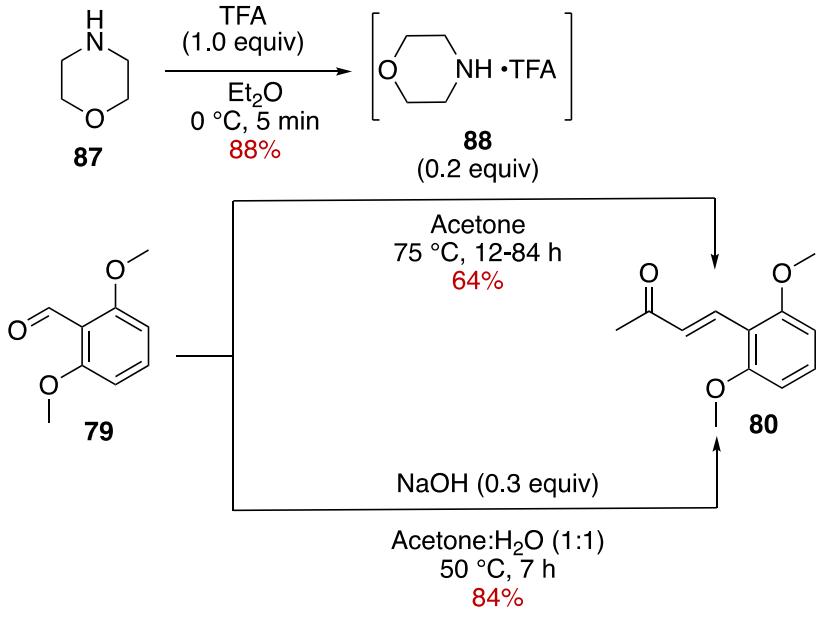

Scheme 17: Aldol Condensation of 1,3-Dimethoxybenzaldehyde

The aldol condensation of aldehyde **79** was followed with the methylenation of a,b-unsaturated ketone **80** to the corresponding diene **81** via a Wittig olefination (see Scheme 17).[40] The formation of diene **81** proceeds through the initial formation of an ylide when the Wittig reagent is treated with *n*-butyllithium at low temperature. Several reaction conditions were screened for the optimization of the Wittig reaction. Methyltriphenylphosphonium bromide ($MePh_3PBr$) was chosen as the Wittig reagent to generate diene **81**.[40] $MePh_3PBr$ yields a non-stabilized ylide bearing an electron donating group. Initially, $MePh_3PBr$ was allowed to react with *n*-butyllithium in for 3 h at room temperature allowing the formation of the ylide. Then, after the addition of a,b-unsaturated ketone **80** the reaction mixture was stirred for 15 h at room temperature. The attack of the ylide onto the ketone triggers the formation of a betaine. A nucleophilic attack of the oxygen onto phosphorus leads to the formation of the oxophosphetane. Finally, the formation of the desired product proceeds through a reverse [2+2] cycloaddition and the release of the phosphine oxide byproduct. When performed on a small scale, the reaction yielded 75% of diene **81** consistently. However, the result was not reproducible when scaling up the reaction. Several reaction conditions were screened, varying reagents equivalents, solvents, temperatures, and reaction times (see Table 1). Consistent satisfying results were obtained when using an excess of the Wittig reagent with *n*-butyllithium at -78 °C for 30 minutes and refluxing the reaction for 3 h upon addition of the substrate. The optimized reaction conditions allowed to generate diene **81** with an 84% yield. Non-stabilized ylides are less stable and react faster than stabilized ylides obtained from Wittig reagent bearing an electron withdrawing group. Therefore, a shorter reaction time for the olefination of the aldol led to better result. Due to the excess of Wittig reagent used in the reaction, an important amount of the undesired phosphine oxide was generated. The phosphine oxide byproduct can make the purification of the alkene complicated. However, the problem was avoided by rinsing the residue with cold hexanes causing the precipitation of phosphine oxide. The column chromatography purification can then be performed smoothly after filtering of the phosphine oxide residue.

Table 1: Reaction Conditions Screening for the Wittig Olefination of α,ß-Unsaturated Ketone **80**

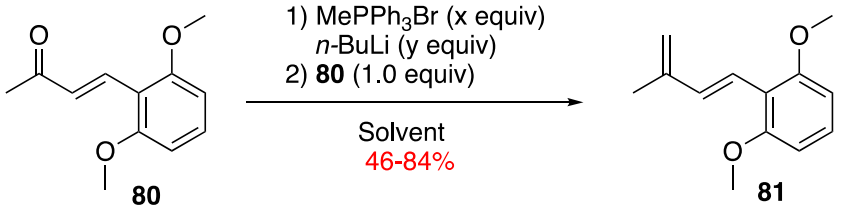

	Equiv		Solvent	Conditions	% Yield
Substrate	$MePPh_3Br$	*n*-BuLi			
1.45 mmol	1.50	1.50	THF	rt, 3 h then 15 h	75
12.9 mmol	1.50	1.50	THF	rt, 3 h then 15 h	46
1.75 mmol	1.50	1.50	THF	0°C, 3 h then rt, 15 h	75
13.2 mmol	2.00	2.00	THF	0°C, 3 h then rt, 15 h	74
1.45 mmol	1.50	1.50	DMF	0°C, 3 h then rt, 15 h	0
1.45 mmol	1.50	1.50	DMSO	0°C, 3 h then rt, 15 h	0
9.16 mmol	2.0	1.20	THF	0°C, 30 min then rt,3 h	68
14.5 mmol	**2.0**	**1.20**	**THF**	**-78 °C, 30 min then 60 °C, 3 h**	**84**

After olefination of the a,ß-unsaturated ketone**,** diene **81** was subjected to the Diels-Alder reaction with 3-buten-2-one (see Scheme 18).[41] The formation of bicyclic adduct **82** proceeds through the formation of two new C-C bonds between the diene **81** and the dienophile. The reaction generates both the *cis* and the *trans* products with a 77% yield in a racemic mixture of both isomers *cis*- and *trans*-**82**.[41,42] The purification using column chromatography on silica gel did not separate the two isomers, hence the presence of a doublet at 5.15-5.30 ppm (see Figure 10) that does not match the data provided by Ballerini *et al.* for the pure *cis* product.[41,42]

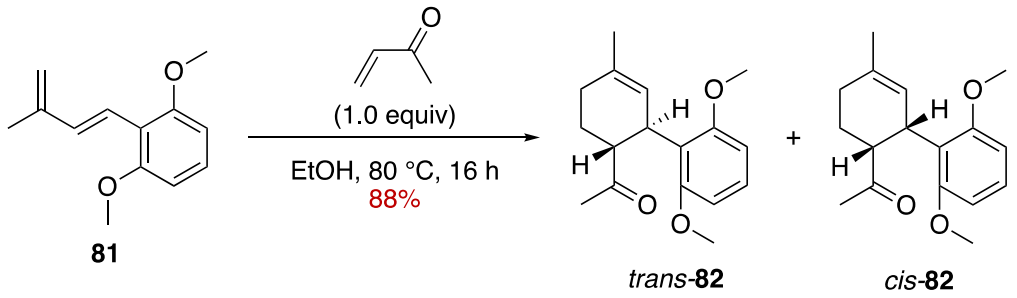

Scheme 18: Diels-Alder Reaction of Diene **81** with 3-Buten-2-one

Since the Diels-Alder reaction generates a racemic mixture of the *cis* and *trans* diastereoisomers, an epimerization reaction is necessary to obtain the stereochemically pure *trans* conformation of the product. The epimerization of the bicyclic ketone **82** is achieved through a reaction of the substrate with sodium methoxide (NaOMe) in methanol for 72 h at 50 °C[42] to yield 88% of the enantiomerically pure product **83** (see Table 2). The base catalyzed epimerization of the substrate allows a change of configuration of the chiral center to generate the desired diastereoisomers. By raising the temperature to 80 °C, the reaction time was reduced to 36 h while maintaining the same yield (see Table 2).[59] The formation of the desired product was confirmed by

NMR analysis (see Figure 9). The approach combining a Diels-Alder reaction with an epimerization reaction provides the control over the stereochemistry of the product.

Table 2: Reaction Condition Screening for the Epimerization to the *trans* Cycloadduct

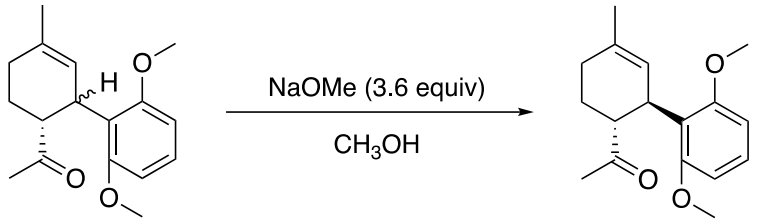

82 **83**

Conditions	% Yield
50 °C, 72 h	88
80 °C, 36 h	**89**

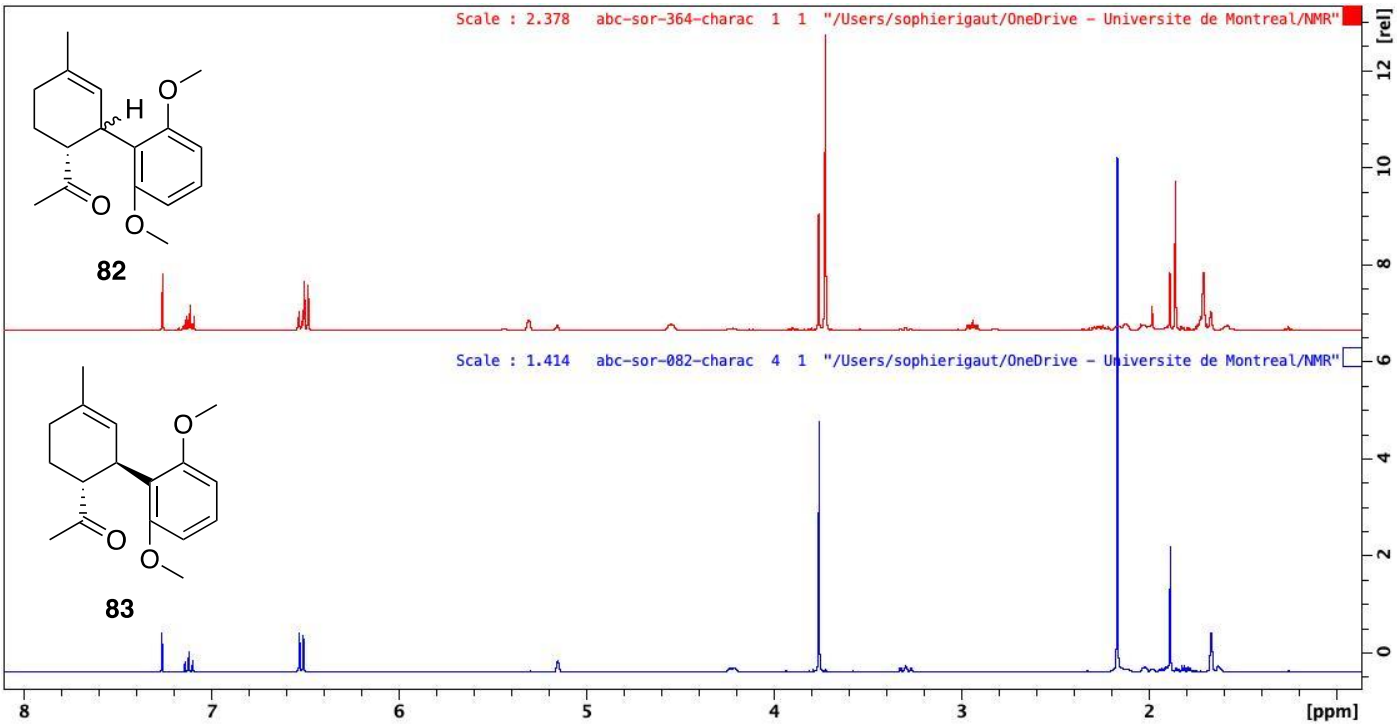

Figure 9: ^{1}H NMR Analysis of Diels-Alder Product **82** vs Epimerization Product **83**

The synthesis was pursued with a second Wittig olefination to obtain the methylenation of ketone **83**.[40] The second Wittig reaction revealed itself to be more challenging than the first Wittig reaction, due to the steric hindrance around the ketone. The olefination was obtained following the same procedure as the reduction of ketone **80** (see Table 3). The use of $MePh_3PBr$ as a Wittig

reagent ensured the formation of the allyl group characteristic of CBD derivatives.[40] Again the reproducibility of the reaction was inconsistent. On a small scale, we managed to obtain a 68% yield of the desired product **84** however, the result was not reproducible on larger scale. The equivalents of reagents, the temperature, and time of reaction were varied to optimize the reaction (see Table 3). The best results were achieved when the reaction of the Wittig reagent with *n*-butyllithium was done at -78 °C for 30 min followed by the addition of the substrate at low temperature and an additional 4 h of stirring at 60 °C. The conditions led to the formation of 74% yield of cycloadduct **84**. Reducing the reaction time led to an increase yield due to the use of a non-stabilized ylide. Again, the residue obtained was rinsed with cold hexanes to remove the phosphine oxide byproduct before purification.

Table 3: Optimization of the Reaction Conditions for the Wittig Olefination of Ketone **83**

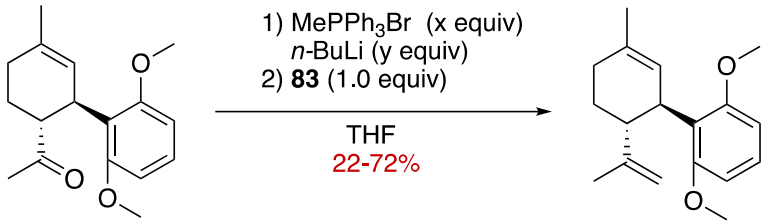

83 **84**

Equiv		Conditions	% Yield
$MePPh_3Br$	*n*-BuLi		
0.60	1.40	rt, 3 h then 25 h	22
0.60	1.40	rt, 3 h then 60 °C, 25 h	23
2.00	2.00	rt, 3 h then 60 °C, 25 h	68
2.00	1.22	0 °C, 3 h then rt, 3 h	55
2.00	2.00	0 °C, 3 h then rt, 25 h	54
2.00	1.22	-78 °C, 3 h then rt, 12 h	32
2.00	2.00	-78 °C, 3 h then rt, 12 h	63
2.00	**1.22**	**-78 °C, 3 h then 60 °C, 4 h**	**72**

These steps allowed us to generate a CBD precursor suitable for the exploration of late-stage functionalization options. Using the resorcinol derivative **78** we were able to optimize previous synthetic pathways towards the formation of CBD precursor **84** with an overall yield of 32%. The goal of the project is to use CBD precursor **84** to enable late-stage functionalization of the aromatic ring to gain access to several CBD derivatives. The various post-functionalization methods explored will be discussed in the following chapters.

2.3. *Post-Functionalization via Hartwig-Miyaura Borylation*

The last step necessary for a late functionalization of the precursor is the C-H activation of the aromatic ring. The C-H activation of the arene can be obtained through the substitution of a (pinacolato)boron (Bpin) substituent via a Hartwig-Miyaura borylation.[45] Goudreau, a former student of the group, performed a Hartwig-Miyaura borylation in his work on the synthesis and applications of trisubstituted cyclopropane derivatives (see Scheme 19).[60] A Hartwig-Miyaura borylation was performed on the aromatic compound **89** via an iridium catalyst followed by a Suzuki coupling leading to the formation of compound **91**. Goudreau's approach was applied to the formation of CBD derivatives.

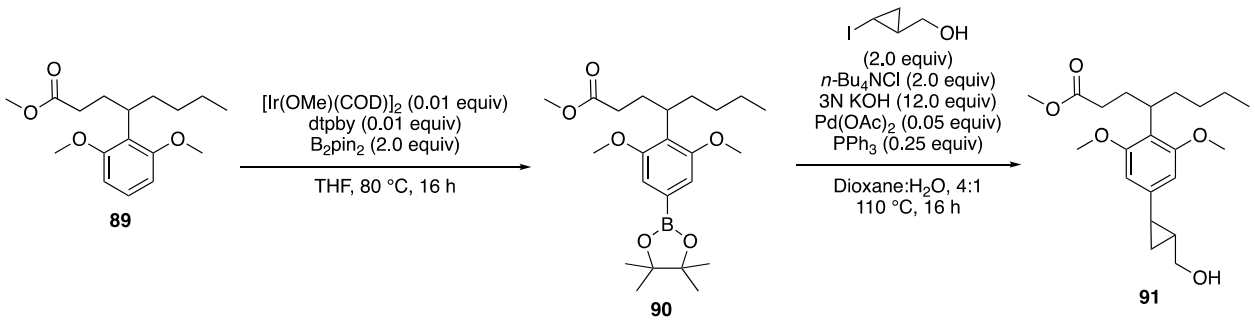

Scheme 19: Goudreau's Application of Hartwig-Miyaura Borylation

2.3.1. Optimization of the Borylation Reaction Conditions

Following the procedure proposed by Goudreau, 1,3-dimethoxybenzene **78** was treated with bispinacoldiboron (B_2pin_2) in combination with the (1,5-cyclooctadiene)(methoxy)iridium(I) dimer ($[Ir(OMe)(COD)]_2$) pre-catalyst and 4,4′-di-tert-butyl-2,2′-dipyridyl (dtbpy) as the ligand under inert conditions (see Table 4). [60] The procedure did not lead to the expected results and the formation of borylated product **92** was not observed. Different reaction conditions were explored using the commercially available and affordable starting material **78** (Table 4). Gaffhari *et al.* [61] conducted extensive screening for borylation on various aromatic substrates. They concluded that the order of addition of the reagents was critical to obtain a great conversion to the borylated compound.[61] In agreement with their observations, the best results were obtained when the order of addition was adding B_2pin_2 first, then the ligand, and the pre-catalyst after which the tube was sealed and removed from the glovebox. Finally, substrate **78** was added to the reaction in solution

under argon to ensure there was no contact to air. The reaction generated the desired product both under neat conditions and in anhydrous THF, yielding respectively 55% and 93% of borylated product **92**.

Table 4: Reaction Condition Screening for the Borylation of 1,3-Dimethoxybenzene

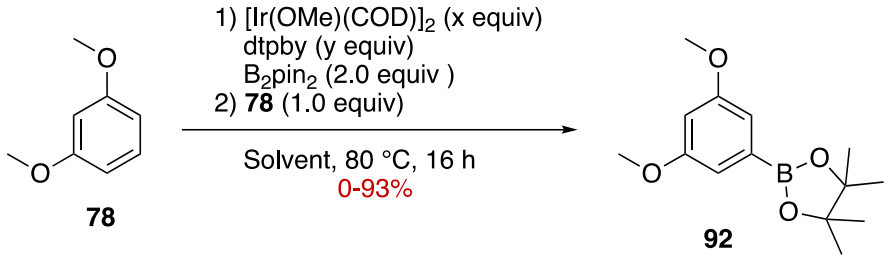

Equiv		Solvent	Order of Addition	% Yield
$[Ir(OMe)(COD)]_2$	dtbpy			
0.025	0.05	Hexanes	1) Substrate 2) Ligand & Pre-cat. 3) B_2pin_2	0
0.005	0.01	THF	1) Substrate 2) Ligand & Pre- cat. 3) B_2pin_2	0
0.005	0.01	neat	1) Substrate 2) Ligand & Pre- cat. 3) B_2pin_2	0
0.005	0.01	neat	1) B_2pin_2 2) Ligand & Pre- cat. 3) Substrate	55
0.005	**0.01**	**THF**	**1) B_2pin_2 2) Ligand & Pre- cat. 3) Substrate**	**93**

Once the ideal conditions were established, they were applied to cycloadduct **84** (see Table 5). To optimize the reaction further the equivalents of reagent were increased, and different solvent options were examined (see Table 5).

Table 5: Reaction Condition Screening for the Hartwig-Miyaura Borylation of Cycloadduct **84**

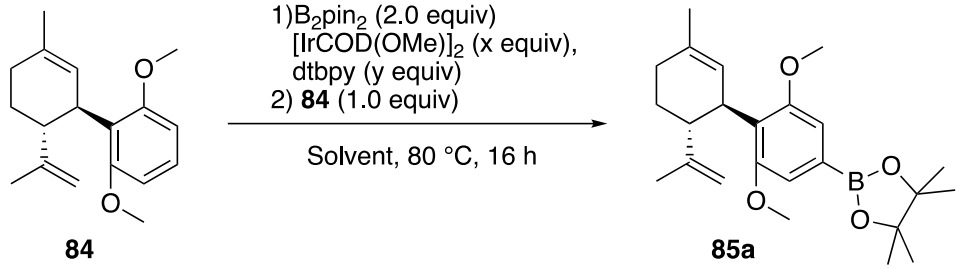

84 **85a**

Equiv		Solvent	% Yield
$[Ir(OMe)(COD)]_2$	dtbpy		
0.013	0.01	THF	0
0.025	0.05	Hexanes	0
0.005	0.01	neat	0
0.005	0.01	THF	0
0.005	0.01	DMF	0
0.005	0.01	Toluene	0
0.005	0.01	Hexanes	0
1.00	2.00	THF	Traces
0.10	**0.20**	**THF**	**Traces**

After an increase of the equivalents of pre-catalyst and ligand, the borylation reaction generated a mixture of products that included traces of CBD precursor **85a** however, other borylation products were found. NMR analysis of the crude product showed the presence of multiple byproducts or the potential borylation at several position of the substrate. Several purification methods were used to separate the product: Kugel Rohr distillation, flash chromatography, and finally preparative thin-layer chromatography (TLC prep). TLC prep enabled the isolation of traces of the final compound. Though substrate **84** presented some similarities to the substrate used by Goudreau, it also bears a terpene ring and a vinyl group, which can both undergo borylation (see Figure 11). NMR analysis of the product indicated that the peaks at 5.15 ppm are gone, indicating the borylation of the terpene ring, while the missing peak at 6.32 ppm indicates the borylation of the aromatic ring. The mechanism of the borylation reaction was investigated in order to understand the presence of the multiple undesired byproducts.

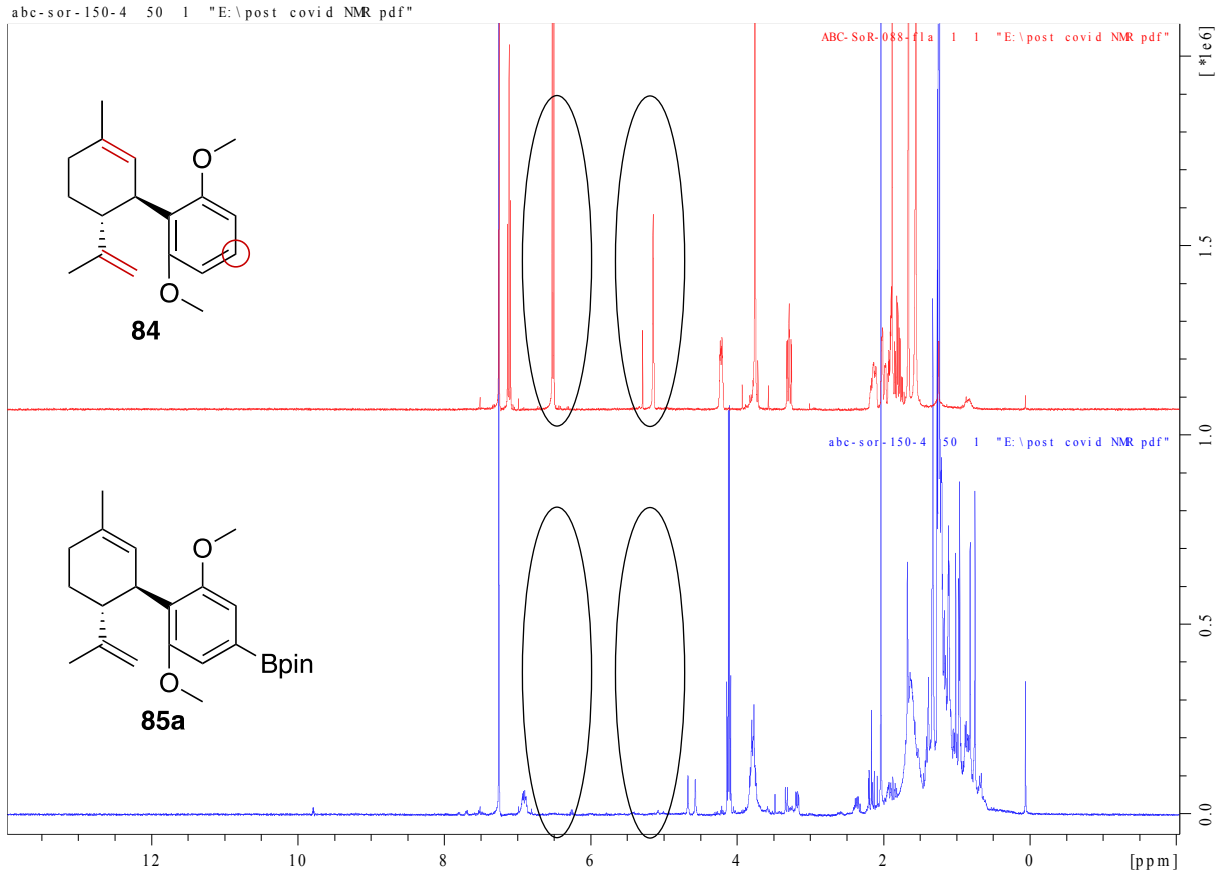

Figure 10: NMR Analysis of Compounds **84** and **85a**

2.3.2. Mechanistic Explanation of the Borylation

Using Hartwig *et al.*'s borylation for the functionalization of aromatic rings was successfully applied to 1,3-dimethoxybenzene **78**. However, we observed that applying the Hartwig-Miyaura borylation method to cycloadduct **84** was met with some limitations. After thorough analysis of the products obtained from the attempted borylation of cycloadduct **84**, it became clear that the substrate was borylated at multiple positions. The formation of several byproducts is due to the presence of multiple p bonds in the substrate. The mechanism for the borylation of vinylic and allylic carbons is similar to the one of the borylation of aromatic rings, explaining the formation of multiple borylated products.

The borylation of aromatic rings proceeds through the nucleophilic substitution of the C-H bond facilitated by the formation of a complex between the iridium pre-catalyst, the ligand dtbpy, and B_2pin_2 (see Scheme 20).[45] According to Miyaura *et al.*, the formation of a catalytic complex is

followed by the oxidative addition of the arene substrate onto the complex **93**.[45] Then, the release of an Ir(V) species **94** leading to the reductive elimination of the borylated arene and the formation of an Ir(III) hydride complex **95**.[45] The subsequent oxidative addition of B_2pin_2 to the complex results in the reductive elimination of an HBpin entity, triggering another cycle of the oxidative addition of the arene to the catalytic complex resulting in the hydrogen reductive elimination from an $18e^-$ Ir(V) intermediates **93** and **97**.[45] The borylation of the arene substituent is a two-step process with a fast C-H activation by B_2pin_2 and a slow C-H activation by HBpin.[45]

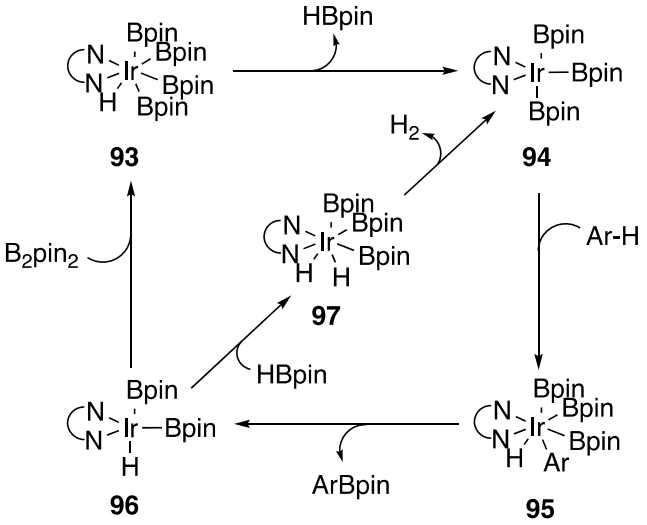

Scheme 20: Mechanism of the Ir-cat. C-H Activation

Hartwig *et al.*'s borylation method is not only reactive towards aryl halides but towards vinyl halides as well. Szabó *et al.*[62] studied the formation of allylic and vinylic boronates and concluded that the borylation of cyclic vinylic ethers (see Scheme 21) also proceeds through an Ir(V) mechanism, explaining the formation of the undesired byproduct for the activation of the CBD precursor. After extensive mechanistic studies, they concluded that the borylation of cyclic vinylic ethers may proceed through a different mechanism.[62] Their deuterium isotope effect experiments led to the conclusion that the reaction goes through a dehydrogenative borylation via ß-hydride elimination rather than through an oxidative addition.[62] The borylated product obtained then undergoes allylic rearrangement leading to the formation of an isomer.[64]

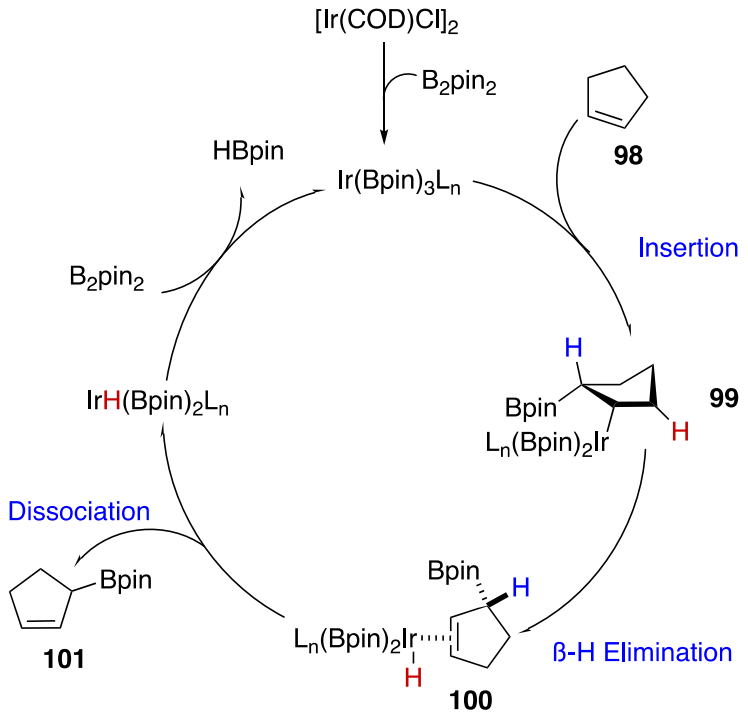

Scheme 21: Cyclic Vinylic Ether Borylation Mechanism, Szabò *et al.,* 2009

Though the exact mechanism of the borylation was not elucidated, substrate **84** was borylated at multiple positions with no control over chemoselectivity. Therefore, the use of the Hartwig-Miyaura borylation for the late-stage functionalization of the CBD precursor was abandoned. The use of a halogenated aromatic ring was explored.

2.4. *Post-Functionalization using a Halogenated Arene*

In our initial attempt, the CBD precursor **84** was generated via the Diels-Alder approach resulting in the formation of a bicyclic adduct. However, the C-H activation of cycloadduct **84** using the Hartwig-Miyaura borylation did not yield the desired product **85a**. Since the borylation was not applicable, we explored the possibility of using a halogenated starting material. 1-Bromo-3,5-dimethoxybenzene **60** was chosen as we hoped it would remain stable under the conditions leading to the late functionalization of the CBD precursor (see Scheme 22). Substrate **60** is commercially available; however, its synthesis was attempted through the bromination of the more affordable 1,3-dimethoxybenzene **78**.

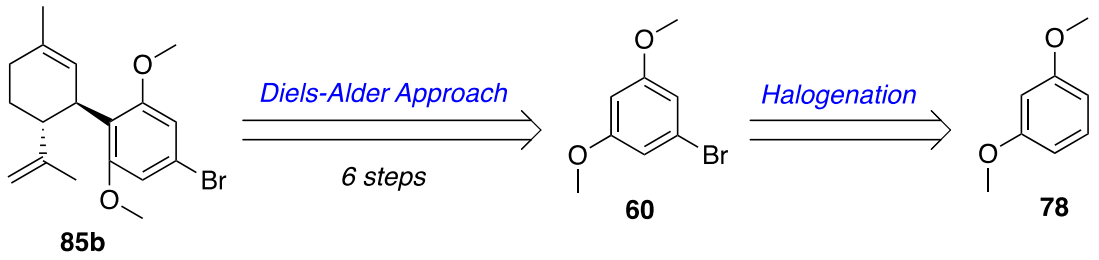

Scheme 22: Retrosynthetic Analysis of Post-Functionalization using a Halogenated Arene

2.4.1. Bromination using *N*-Bromosuccimide

The first bromination attempt was performed according to a procedure by Lee *et al.* developed to obtain the bromination of 2,6-dimethoxyphenol using *N*-bromosuccimide (NBS) and NaOH.[64] Lee *et al'*s method was applied to aldehyde **79** to brominate the aromatic ring at the C4 position (see Table 6). After screening different solvents (see Table 6), the reaction consistently resulted in the bromination of the aromatic ring at the C3 position rather than the C4 position. According to Vorländer's rules of aromatic substitution, the presence of a OMe group results *ortho* and *para* directing effects resulting in the halogenation of substrate **79** at the C3 position.[65] The presence of the aldehyde at the C1 position did not have a strong enough meta directing effect compared to the hydroxy group present on the aromatic ring in Lee *at al.*'s reaction.[64] The OMe groups have a strongly activating *meta* directing effect leading to the formation of 4-bromo-2,6-dimethoxyphenol **102b**.[65]

Table 6: Reaction Condition Screening for the NBS Bromination of 2,6-Dimethoxybenzaldehyde

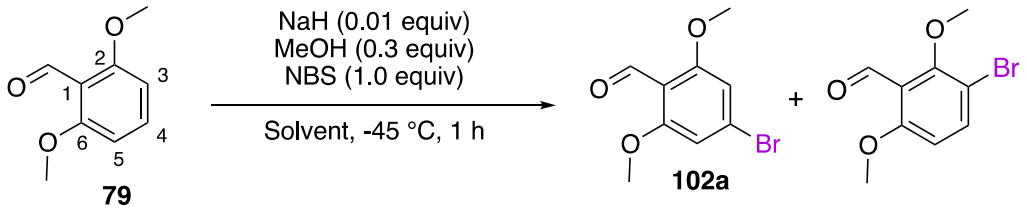

Solvent	% Yield
	102a
$CHCl_3$	0
CH_3CN	0
DMF	0

The bromination of aldehyde **79** was then attempted according to the procedure developed by Gromada *et al.* using the stronger bromination agent dibromide (Br_2).[65] The reaction presented the same issue as the previous one, namely the bromination of benzaldehyde **79** at the C3 position rather than the C4 position due to the inductive effects of the substituents.[63] The electron donating group present on the substrate used by Gromada *et al.* (see Scheme 23) allows for an activation of the desired position that is not observed on the substrate bearing an electron withdrawing aldehyde substituent.

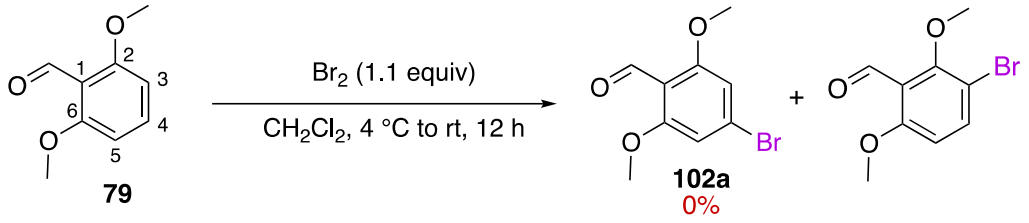

Scheme 23: Bromination of 2,6-Dimethoxybenzaldehyde using Br_2

The OMe groups present on substrate **79** results in an inductive effect due to the electronegativity difference between the oxygen atoms and the methyl group[63] leading to the polarization of the molecule where the oxygen bears a partial negative charge, and the alkyl groups bears a partial positive charge.[66] The inductive effects affect the reactivity of the molecule and dictate which positions of the aromatic ring are more likely to undergo substitution reactions. Here, the OMe groups are electron donating groups and *ortho/para* directing.[63] The strongly activating groups increase the rate of the reaction. Here, since C4 is the carbon at the *meta* position to the OMe groups, the formation of the desired product is not favored.[63] Therefore, an alternative bromination procedure using photochemistry was explored.

2.4.2. UV Light Bromination Attempt

The bromination of different resorcinol derivatives was attempted using NBS under blue LED. The use of photochemistry presents many advantages, such as shorter reaction time and a safer reaction environment. The process would easily be adaptable to continuous flow chemistry. Zhang *et al.*[67] claimed to be used to brominate 1,3-dimethoxybenzene **78** at the C4 position using visible light and bromoacetic acid to promote the reaction. The methodology was applied to four resorcinol derivatives **78** and **79**, 3-methoxyphenol **77a**, and 1,3-phenylene bis(2,2-

dimethylpropanoate) **77b** (see Scheme 24). For the first three substrates, bromination was observed at the C3 position instead of the C4 position, which was attributed to the strongly activating *para/ortho* directing OMe groups. Our results did not match the result reported by Zang *et al.,* however the reported bromination of resorcinol derivative **78** was not characterized in their paper. The bromination of Piv protected resorcinol **77b** was not observed and the starting material was recovered which was attributed to the bulkiness of the Piv PG inhibiting the reaction.

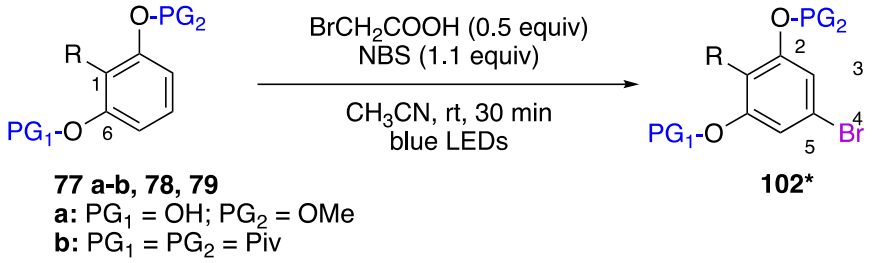

Scheme 24: Bromination of Resorcinol Derivatives using LEDs

2.4.3. Bromination via Iridium-Catalyzed Borylation

Finally, the bromination of resorcinol derivative **78** was attempted using a borylated intermediate as reported by Ijima *et al.*[68] As the borylation of resorcinol derivative **78** had previously been successful therefore, we wanted to explore the possibility of brominating substituent **92** to generate the desired compound **60**. Subjecting arene **92** to a halogenation reaction using copper bromide in an aqueous environment at 80 °C for 4 h led to the formation of the desired product **60** with a yield of 29% (see Scheme 25).

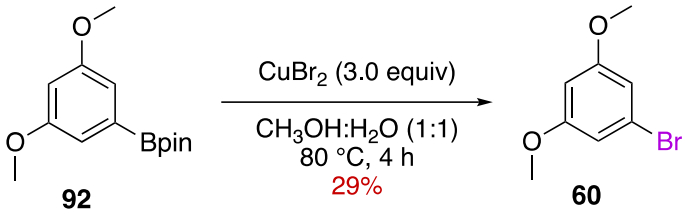

Scheme 25: Bromination of 1,3-Dimethoxybenzene via Borylated Intermediate

The method enabled the formation of the targeted compound with a low yield and presented reproducibility issues. In light of the obstacles encountered with the bromination of substrate **92** the synthesis of halogenated arene **60** was abandoned. However, compound **60** is commercially

available. Therefore, the late-stage functionalization of the CBD precursor was further explored using commercial 1-bromo-3,5-dimethoxybenzene **60**.

2.5. *Synthesis of 1-Bromo-3,5-dimethoxybenzene*

The limitations encountered with the halogenation of the starting material pushed us towards taking a different approach. We explored the possibility of formylating halogenated arene **60**. The formylation was attempted under the same conditions used for starting material **78** (Scheme 15).[55] The reaction yielded both 1,3-dimethoxybenzaldehyde **79** and aldehyde **102b** but not the desired product **102a**. The procedure was repeated using LDA (pKa = 35.7) instead of *n*-butyllithium (pKa = 50) (see Table 7). LDA was chosen because of its lower pKa to avoid the loss of the bromine substituent. However, LDA's pKa was too low to enable the deprotonation and subsequent lithiation of the substrate and the formylation did not take place. The reaction was also attempted in Et_2O instead of THF, following a procedure developed by Rempel *et al.*[69] reporting the successful formylation of substrate **60**, however we were unable to reproduce their results.

Table 7: Reaction Conditions Screening for the Formylation of 1-Bromo-3,5-dimethoxybenzene

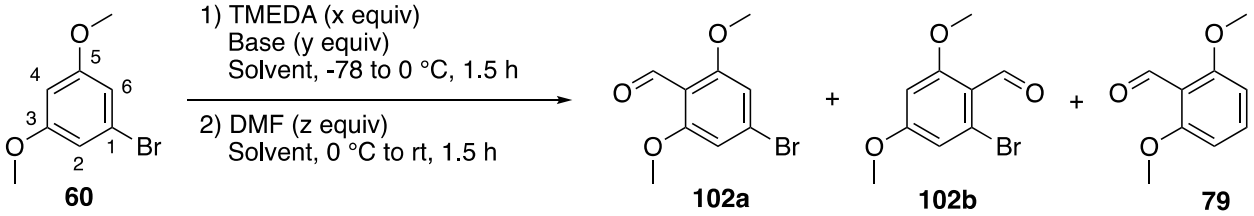

Base	Equiv			Solvent	% Yield	Byproducts	
	TMEDA	Base	DMF		a	b	c
n-BuLi	1.20	1.25	1.20	THF	0	Yes*	Yes*
n-BuLi	1.20	1.25	1.20	Et_2O, 0 °C, 6 h	0	No	Yes*
LDA	-	1.25	1.20	THF	0	No	No

*Byproducts not isolated

Due to the limitations encountered with this formylation method, several other formylation procedures were examined, namely the Vilsmeier-Haack reaction, the Rieche reaction, and the Duff Reaction.

2.5.1. Vilsmeier Haack Formylation of Halogenated Arene

The Vilsmeier-Haack reaction was developed to enable the formylation of electron rich aromatic compounds. The procedure relies on the use of phosphorus oxychloride and DMF to generate the Vilsmeier reagent. Ushijima *et al.* reported a procedure using a Vilsmeier-Haack formylation followed by a reaction with iodine in aqueous ammonia to access electron rich aromatic compounds.[70] Based on their work, we attempted the formylation of arene **60** (see Scheme 26), but the reaction resulted in the formation of undesired product **102b** which was attributed to the substituent effects induced by the strongly *ortho/para* directing electron donating protecting groups. [63]

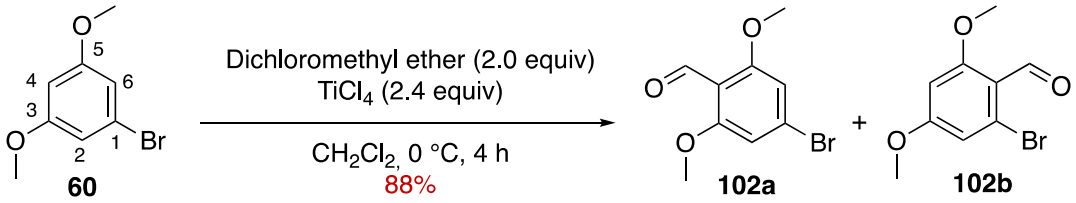

Scheme 26: Vilsmeier-Haack Formylation of 1-Bromo-3,5-dimethoxybenzene

2.5.2. Rieche Formylation of Halogenated Arene

The Rieche formylation is another procedure developed for the formylation of electron rich aromatic rings. Yang *et al.*[71] reported its use to obtain aldehyde **102a** (see Scheme 27). The reaction uses dichloromethyl methyl ether and titanium tetrachloride to generate the desired aldehyde substituent and reported the formation of a 15:85 ratio of products **102a** to **102b**.[71] When applied to 1-bromo-3,5-dimethoxybenzene **60**, these reaction conditions produced a mixture of formylated compounds **102a** and **102b** with a 69% yield. The NMR analysis indicated the presence of two products in the purified residue, but we were unable to isolate either. NMR analysis also showed that the undesired aldehyde **102b** was the major product. The regioselectivity of the reaction is again explained by the OMe substituents.[63] Our results were corroborated by the results of Ramos-Tomerillo *et al.* who worked on the formylation of various substrates using the Rieche Formylation procedure.[72]

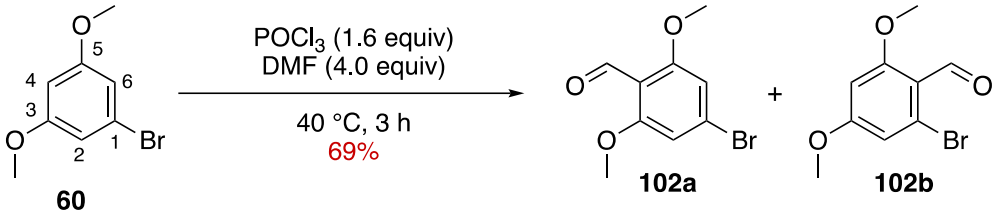

Scheme 27: Rieche Formylation of 1-Bromo-3,5-dimethoxybenzene

2.5.3. Duff Reaction on Halogenated Arene

The Duff reaction is an electrophilic aromatic substitution targeting the *ortho* position to electron donating groups on the aromatic ring. Since all other formylation methods were unsuccessful, the approach enabling the formylation *ortho* to the OMe groups seemed promising. It was applied to both substrate **60** and 3-bromo-5-methoxyphenol following a procedure developed by Lindoy *et al.*[73] The procedure was developed to obtain the mono- and bisformylation of aromatic phenols.[74] The substrate was treated with hexamethylenetetramine (HMTA) in TFA (see Scheme 28). TFA reportedly permits the selective formylation of the arene, however it was not observed here. We obtained a mixture of products for which NMR analysis showed that formylation of either substrate happened at several positions. It was attributed to the presence of two electron donating group on this arene, as opposed to the mono-substitued substrates use in Lindoy *et al.*'s research. We were not able to isolate the different products therefore, the Duff reaction route was abandoned.

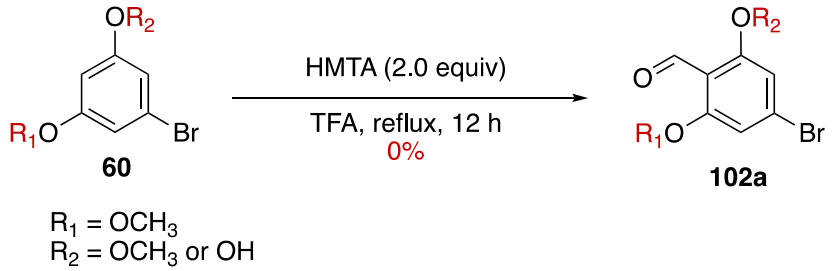

Scheme 28: Formylation Attempt via Duff Reaction

The inefficacy of the Hartwig-Miyaura C-H activation method and consistent limitations due to the OMe substituents present on aromatic substrates **60** and **78** forced us to fully reconsider the approach taken to the late-stage functionalization of CBD. Instead, we turned to the use of a

starting material bearing a carboxylic acid substituent at the position targeted for functionalization. The new approach will be discussed in the next chapter.

3. Post-Functionalization via Weinreb Amide Functionality

Considering the limitations encountered with the functionalization of the aromatic ring, the approach taken to for the late-stage functionalization of CBD was reexamined. As the OMe groups found on resorcinol derivative **78** have such strong substituent effects preventing a functionalization at the desired position, the possibility of using a starting material with a functionalizable substituent at the C1 position was explored. The use of the carboxylic acid **103** was retained as it gives access to Weinreb amides (WA). The synthetic pathway to CBDD **2c** remained the same besides the introduction of the WA functionality (see Scheme 14 and 29).

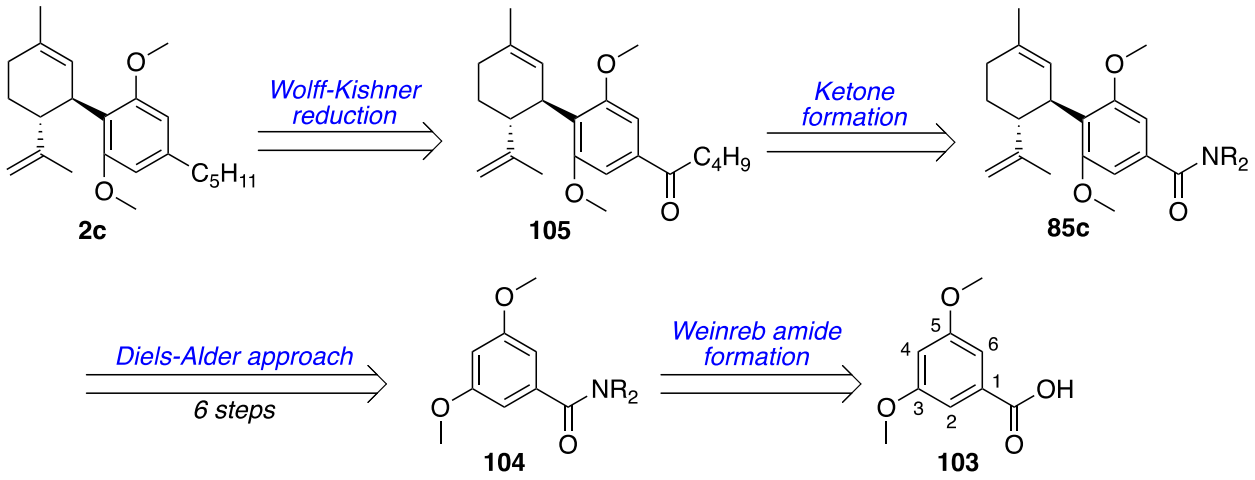

Scheme 29: Retrosynthetic Analysis of the Weinreb Amide Approach

3.1. *Development of the Weinreb Amide Method*

The use of WA was first developed by Weinreb *et al.* to provide a solution to issues typically encountered when synthesizing ketones or aldehydes (see Scheme 30).[74] The method using *N,O*-dimethylhydroxylamine (DMHA) allows for a straightforward procedure. The Weinreb approach does not require precise temperature control or meticulous addition of the organometallic reagent to avoid an over addition to the substrate leading to a tertiary alcohol product.[74] The procedure presents an efficient synthesis of ketones from carboxylic acids even when adding an excess of the

organometallic reagent.[74] The efficiency of the reaction is attributed to the stability of the five-membered ring chelate intermediate **107**.[75]

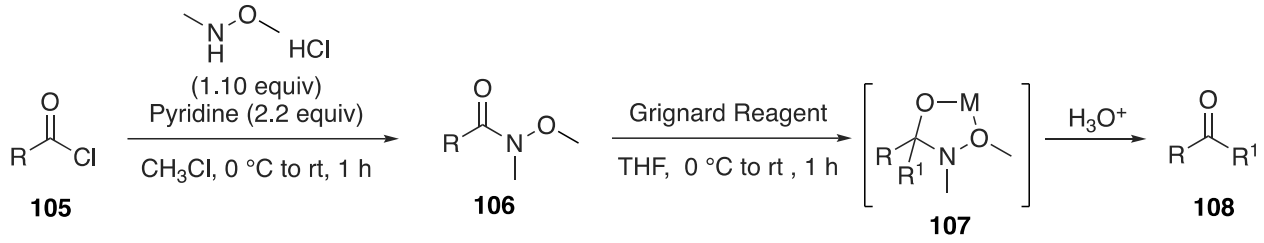

Scheme 30: Synthesis of Ketones using Weinreb Amides

The potential of the WA functionality has since been expanded to other amide derivatives.[76,77] DMHA is a nucleophilic amine allowing to generate the corresponding ketone effectively, but it is an expensive compound. The utility of WA has been proven through the synthesis of various pharmaceutical targets and will be discussed in the following section.

3.2. *Uses of the Weinreb Amide Functionality*

The utility of WA ranges from its applications in heterocyclic chemistry to the total synthesis of natural products and its adaptability to industrial scale production.[78] A few years back, Charette *et al.* developed a method for the chemoselective synthesis of ketones through the addition of organometallic reagents to secondary amides expanding the possibilities offered by Weinreb amides (see Scheme 31).[75] Their work describes a method allowing to generate ketones through a cyclohexylamine WA derivative as a response to the need for chemoselective approaches to the formation of new C-C bonds. Using a WA intermediate avoids a 1,2-addition of the organometallic reagent onto a carboxylic acid substrate which often requires excess reagent and strict control of the reaction conditions for low yields of the desired product.[75] WA **109** was obtained through the coupling of a carboxylic acid substituent with cyclohexylamine. Substrate **109** was subjected to a reaction with the activating agent trifluoromethanesulfonic anhydride combined with the use of a base buffer leading to the formation of an imidoyl triflate.[75] Finally the addition of the appropriate Grignard reagent resulted in the formation of the desired ketone **110**.

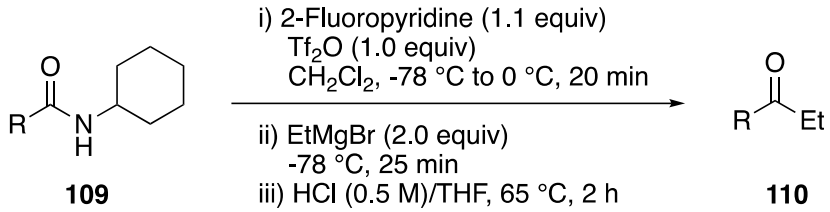

Scheme 31: Chemoselective Synthesis of Ketones, Charette *et al.*, 2012

Recent developments surrounding WA allowed for greater substituent tolerance as well as milder reaction environment giving the method a great advantage for a more sustainable access to functionalized products. According to Jammula *et al.* the WA functionality is a useful tool for the green synthesis of various compounds (see Scheme 32).[78] Here, WA **112** was obtained from the treatment of 2-furoic acid **111** with a propylphosphonic anhydride (T3P) solution and *N,O*-dimethylhydroxylamine hydrochloride (DMHA·HCl) in a basic reaction environment. The amide **112** was then treated with the appropriate Grignard reagent to obtain the desired ketone **113**. The use of T3P results in a less toxic and milder reaction, while also generating water soluble byproducts, making the isolation of the desired product less strenuous.[78]

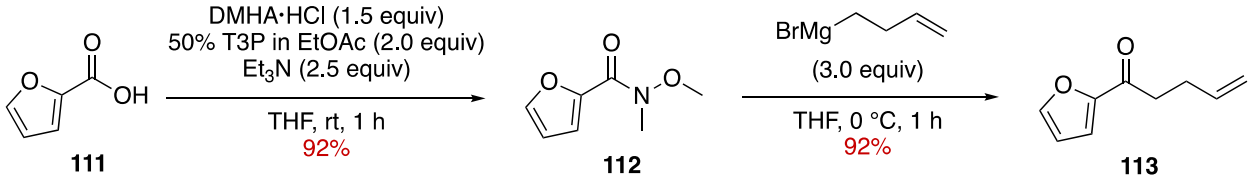

Scheme 32: Green synthesis of Ipomoeassin precursors via WA, Jammula *et al.,* 2016

The use of WA has also been applied to develop syntheses destined to the industrial scale production of several pharmaceutical targets. The synthetic pathway to FTY-720 developed by Aidhen *et al.* (see Scheme 33) targets an immunosuppressant derived from a natural product.[79] Their approach presents an alternative to the existing synthesis of ipomoeassin utilizing $Fe(acac)_3$ for the coupling reaction enabling the formation of the alkyl chain. They avoided the use of an iron coupling reagent by relying on a WA to obtain the formation of a new C-C bond.[79]

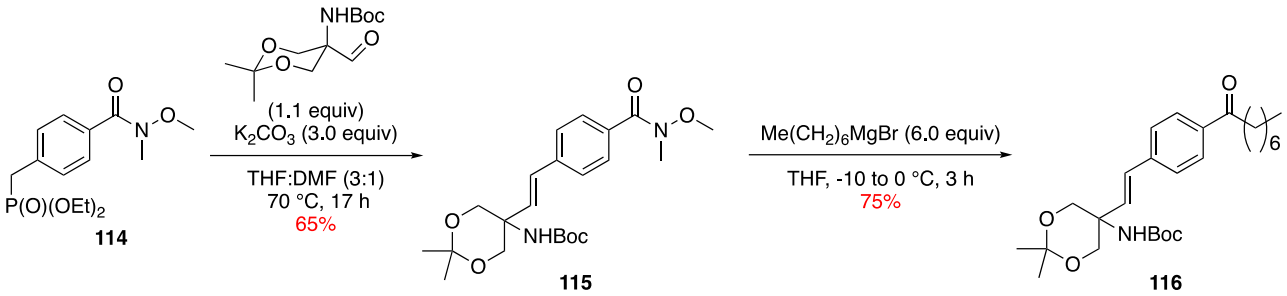

Scheme 33: Synthesis of FTY720 via Weinreb Amide, Aidhen *et al.*, 2007

The examples previously mentioned encouraged us to explore the potential of the Weinreb functionality for the late-stage functionalization of a CBD precursor. Those methods inspired a novel synthetic pathway to both olivetol and CBD using 3,5-Dimethoxybenzoicacid **103** as the starting material. We aimed to generate WA using different amines, followed by the formation of the CBD precursor using the Diels-Alder approach. We chose to generate different amides to examine different options for the synthesis of CBD derivatives.[77] Both cyclohexylamine and morpholine were retained for their commercial availability and affordability. The resulting precursor can then be functionalized to obtain CBD or other analogs. The WA can be used to synthesize the corresponding ketone. The ketone is then reduced to the corresponding alkyl chain via the well-known Wolff-Kishner reaction, and finally the substrate undergoes demethylation (see Scheme 29). Relying on the Weinreb approach also presents an interesting alternative to the existing syntheses of olivetol. The examples cited showcasing the use of Weinreb derivatives can be adapted to large scale production and exhibit potential for more sustainable synthetic pathways increase the appeal of this proposal

3.3. *Synthesis of Weinreb Amide and Derivatives*

The synthesis of WA was obtained according to a procedure described by Charette *et al.* (see Scheme 34).[75] All WA derivatives were successfully prepared using thionyl chloride and DMF for the initial formation of the acid halide from carboxylic acid **103** followed by treatment with a base and the desired secondary amine to obtain the corresponding WA. *N*-3,5-Trimethoxy-*N*-methylbenzamide **104a**, (3,5-dimethoxyphenyl)(morpholino)methanone **104b**, and *N*-cyclohexyl-3,5-dimethoxybenzamide **104c** were obtained with 63%, 96% and 76% yield respectively.

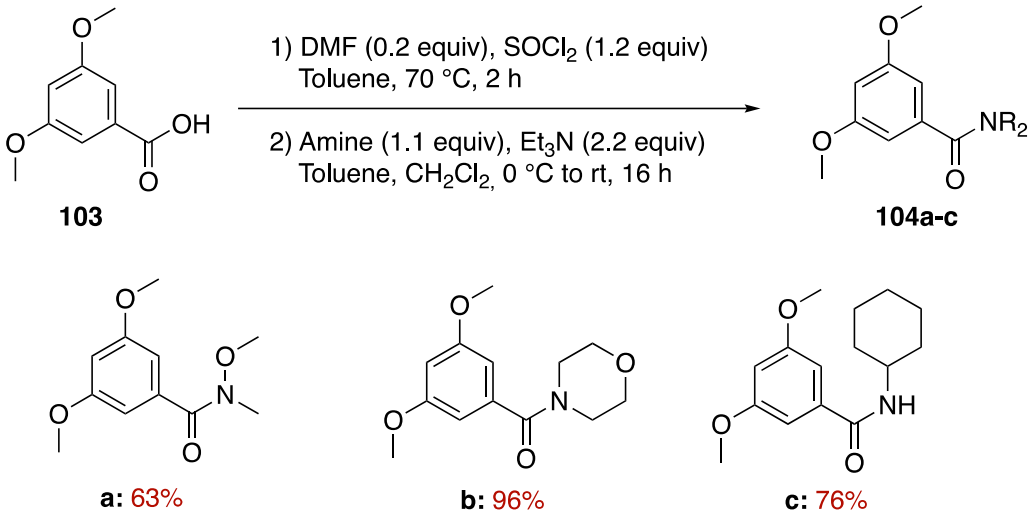

Scheme 34: Synthesis of Weinreb Amides **104a-c**

WA **104c** was retained to explore the possibility of generating a CBD precursor suitable for late-stage functionalization. The late-stage functionalization through the synthesis of ketones was explored using all three of these WA as different amide functionality yielded the best results for specific derivatives. The results will be discussed in the following sections.

3.4. *Formylation of Weinreb Amides*

3.4.1. Formylation of *N*-Cyclohexyl-4-formyl-3,5-dimethoxybenzamide

The possibility of using the WA functionality for the late-stage functionalization of CBD was explored using WA **104c**. Subjecting WA **104b** to formylation conditions containing *n*-butyllithium leads to the formation of the corresponding ketone at the C1 position. The reactivity of WA **104b** towards organolithium reagents is incompatible with the chosen formylation method as it triggers the synthesis of the ketone, defeating the purpose of using the WA functionality for late-stage functionalization.[55] Amide **104c** was chosen for the bulky structure of the WA as well as the commercial availability and affordability of cyclohexylamine. We expected that the steric hindrance introduced by the bulkiness of the hexyl substituent on **104c** to prevent the formylation of the aromatic ring at the C4 position (see Table 8).[55] The formylation conditions used for the formylation of arene **78** were applied to the amide **104c**. However, the desired product **119a** was only obtained with a 19% yield and presented reproducibility issues. Several formylation conditions were investigated (see Table 8). The best results were obtained when treating substrate

104c with a 1:2 ratio of TMEDA to *n*-butyllithium. Using a 1:1 ratio of TMEDA to *n*-butyllithium led to byproduct **119b** as the major product. As expected, treating the substrate with a 2:2 ratio of TMEDA to *n*-butyllithium led to the formation of byproduct **119c** with formylation at both the C2 and C4 position.

Table 8: Reaction Condition Screening for the Formylation of *N*-Cyclohexyl-3,5-dimethoxybenzamide

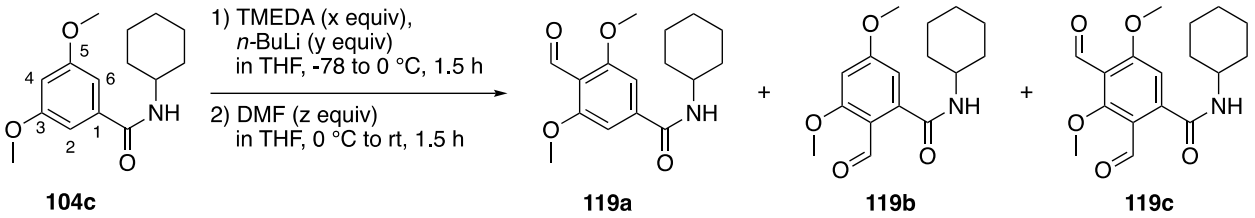

104c **119a** **119b** **119c**

Equiv			**% Yield**		
TMEDA	*n*-butyllithium	DMF	**119a**	**119b**	**119c**
1.2	**2.5**	**1.2**	**19**	**7**	**41**
1.2	1.2	1.2	Traces	Observed*	0
2.1	2.1	1.2	0	Observed*	Observed*

*Not isolated

The formation of byproducts **119b** and **119c** can be explained by the presence of a third DMG on substrate **104c**. According to Snieckus *et al.* the strength of a DMG is determined by both its inductive and substituent effects.[56a] The amide substituent found at the C1 position constitutes a stronger DMG than the OMe groups due to the stronger stability it provides.[56b] Therefore, the site *ortho* to the amide group, namely the C2 position, is more likely to undergo lithiation than the C4 position (see Table 8). The presence of two OMe groups on the aromatic compound **104c** leads to the formation of the desired product **119a**, however it cannot compete with the presence of a strong DMG with the amide substituent, hence the formation of several byproducts (see Scheme 35).

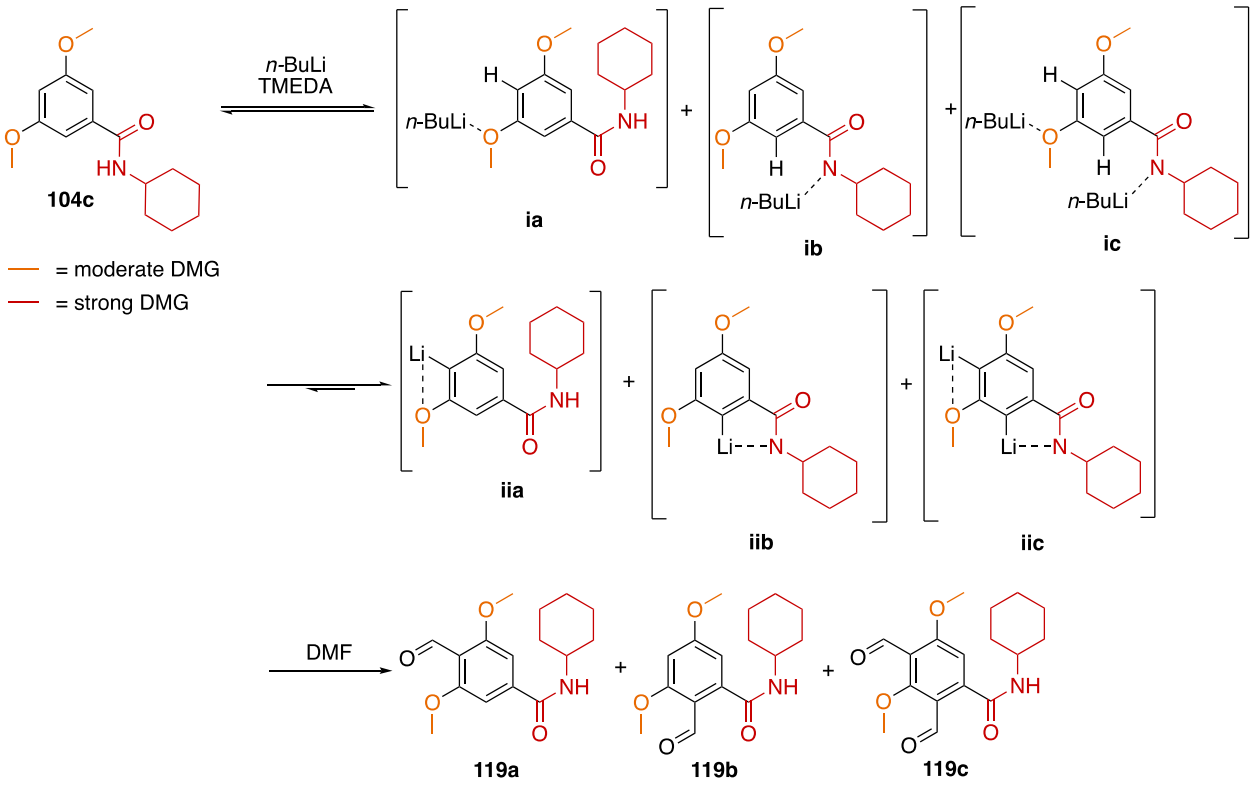

Scheme 35: Ortho Metalation Reaction Mechanism for the Formylation of Aromatic Amide **104c**

The formylation of WA **104c** was then attempted using Vilsmeier Haack's formylation following a procedure reported by Ushijima *et al.* (see Scheme 36) treating the substrate **104c** with phosphorus oxychloride and DMF at 40 °C.[70] The reaction did not yield the desired product **119a** which was explained by the presence of the Weinreb substituent. The electron withdrawing deactivating group diminishes the reactivity of the substrate and makes it a poor candidate for the further modification necessary for the formation of the desired CBD precursor.

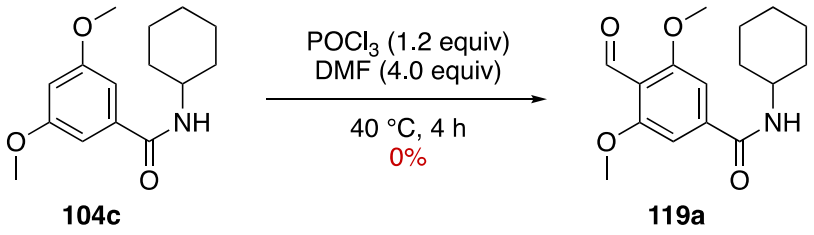

Scheme 36: Vilsmeier Haack's Formylation on *N*-Cyclohexyl-3,5-dimethoxybenzamide

3.4.2. Synthesis of a Boc Protected Weinreb Amide

Since no reproducible results were obtained for the formylation of WA **104c** to the desired aldehyde **119a**, we explored the option of increasing the steric hinderance at the C2 position of the arene through the introduction of an even larger substituent. The *tert*-butoxycarbonyl (Boc) PG was chosen to increase the bulkiness of the amide and block the access to the C2/C6 position due to its orientation in space. The Boc PG is compatible with the following steps of the synthesis as it is stable under basic conditions. The protection of the amide**104c** with a Boc group after the formation of the WA was attempted (see Table 9) under different reaction conditions.[80a,b,c] However, the desired product **124** was not observed (see Table 9).

Table 9: Reaction Condition Screening for Boc Protection of *N*-Cyclohexyl-3,5-dimethoxybenzamide

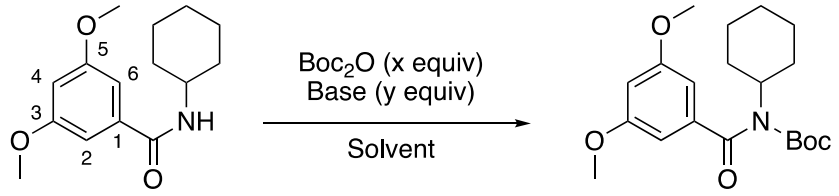

104c **120**

Equiv		Solvent	Conditions	% Yield
Boc_2O	Base			
1.3	DMAP – 0.1	CH_3CN	rt, 12 h	0
1.1	NaOH – 1.3	THF	0 °C, 12 h	0
1.3	DMAP – 0.1	CH_2Cl_2	rt, 12 h	0
10.0	DMAP – 0.1	CH_2Cl_2	rt, 12 h	0
10.0	DMAP – 0.5	CH_2Cl_2	rt, 12 h	0
10.0	DMAP – 0.8	CH_2Cl_2	rt, 12 h	0
10.0	DMAP – 1.0	CH_2Cl_2	rt, 12 h	0
2.0	NaH – 1.3	CH_2Cl_2	rt, 12 h	0
1.0	-	CH_3CN	rt, 20 min	0

The protection of the WA was then attempted following a procedure used by Takashi *et al.* [80] The procedure was applied to the Boc protection of **104c** (see Scheme 44). The addition of Et_3N meant to help the deprotonation of the amide to facilitate the Boc protection. Traces of **120** were observed however, we were unable to isolate it. NMR analysis of the product after purification

revealed the presence of both the desired product and an unidentified byproduct. The reaction resulted in the recovery of 83% of the starting material.

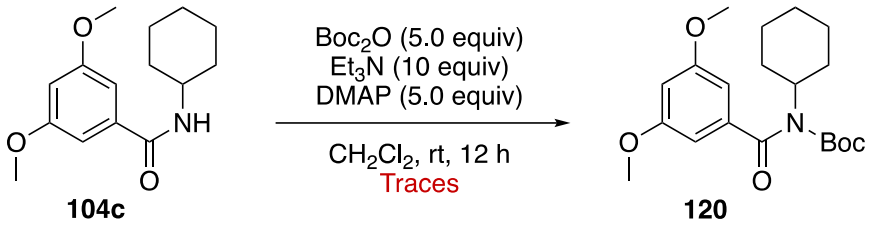

Scheme 37: Attempted Boc protection of *N*-Cyclohexyl-3,5-dimethoxybenzamide using Et_3N

Since the Boc protection of the WA did not lead to satisfying results, we examined the possibility of protecting cyclohexylamine with a Boc group to generate *tert*-butyl cyclohexylcarbamate **121** prior to the coupling of the amine and the carboxylic acid. Cyclohexylamine was protected with a Boc group following standard procedure and amine **121** was obtained with a 99% yield.[81] Several amide coupling procedures were attempted using amine **121**. First the coupling was attempted using the procedure by Charette *et al.* (see Table 10).[75] Different reaction conditions were explored (see Table 10) however, the formation of the WA **120** was unsuccessful due to the bulkiness and the deactivating nature of the electron withdrawing Boc group.[84]

Table 10: Reaction Condition Screening for the Formation of the Boc Protected Amide using *tert*-Butyl Cyclohexylcarbamate

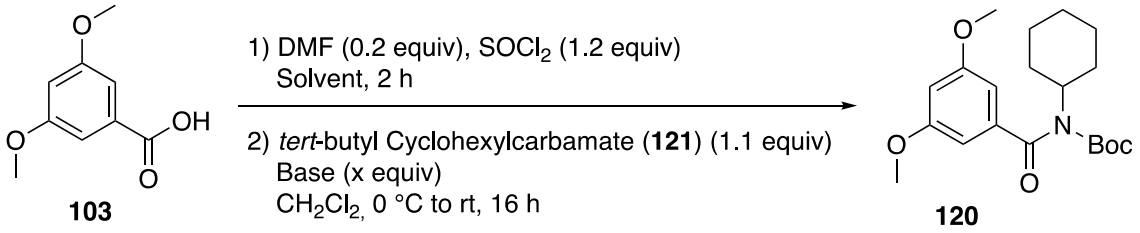

Base	Equiv	Solvent	% Yield
Et_3N	2.2	Toluene, 70 °C	0
KO*t*Bu	2.2	Toluene, 70 °C	0
KO*t*Bu	1.2	CH_2Cl_2, 35 °C	0

The coupling of carboxylic acid **103** and amide **121** was then attempted using different coupling reagents. The formation of amides using a coupling reagent proceeds through the activation of the carboxylic acid substrate followed by the activation of the amine to obtain the peptide bond of the

WA. Trost *et al.* published their work on the synthesis of several amide coupling reactions.[84] Ethyl-3-carbodiimide hydrochloride (EDC) is typically used for the coupling of primary amines but is suitable for the coupling of a secondary amine. Using EDC for amide coupling can be a convenient choice as it is conveniently removed during workup.[85] The reaction was applied to the coupling of carboxylic acid **103** and amide **121** (see Table 11). The reaction did not yield the expected product and other reaction conditions were screened (see Table 11). Both the equivalents of DMAP and EDC were increased, though the desired product was never observed.

Table 11: Reaction Condition Screening for the Amide Coupling Attempt using EDC

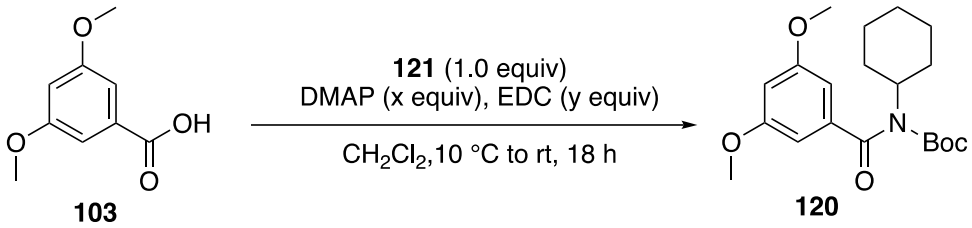

Equiv		% Yield
DMAP	EDC	
0.1	1.2	0
0.5	1.2	0
0.1	1.5	0

Since EDC did not yield the desired results, further coupling agents were considered. Isobutyl chloroformate (IBC) is commonly used for the formation of amide, and suitable for the secondary amines. It is a widely available and inexpensive reagent, less toxic than ethyl chloroformate, making it ideal for large-scale synthesis.[85] IBC was used by Trost *et al.* for the coupling of a second amide.[84] The use of IBC for the formation of an amide bearing a Boc protecting group encouraged us to apply this procedure to the formation of amide **120** (see Scheme 38). However, the procedure did not lead to the formation of the desired amide.

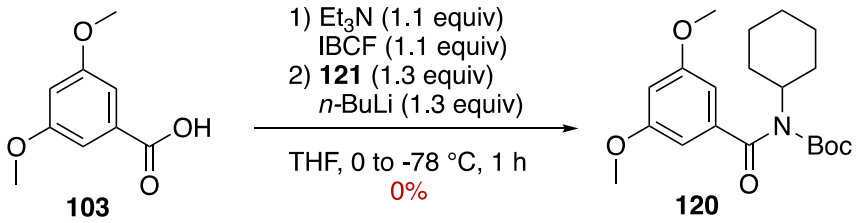

Scheme 38: Amide Coupling Attempt using IBC

The coupling of carboxylic acid **103** and amide **121** was attempted using hexafluorophosphate benzotriazole tetramethyl uranium (HBTU) according to a procedure developed by Charette *et al.* (see Scheme 39).[75] HBTU is known to be an efficient coupling reagent leading to the formation of the amide through the formation of the urea byproduct.[86] Considering the sterically hindered nature of the secondary amine used for this coupling, we hoped the use of HBTU would allow to generate the desired product. The HBTU amide coupling was applied to the coupling of carboxylic acid **103** and amide **121** but did not lead to the formation of the desired amide **120**.[75]

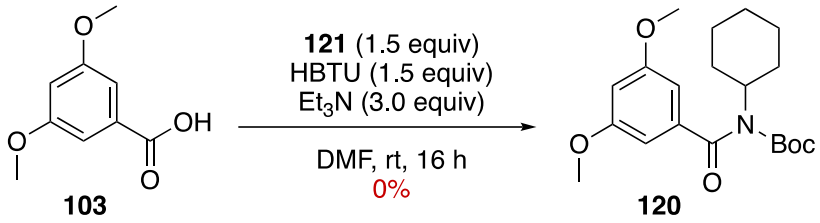

Scheme 39: Amide Coupling Attempt using HBTU

Finally, the amide coupling was attempted by treating carboxylic acid **103** with triethyl phosphite ($P(OEt)_3$), iodine (I_2), and Et_3N according to a procedure developed by Chen *et al.*[87a] The use of phosphorous compounds has become widespread for the synthesis of amides.[86] Triphenylphosphine (PPh_3) is often used due to its affordability, though it presents the disadvantage of generating a toxic phosphine oxide byproduct.[87a] Here, the use of $P(OEt)_3$ in combination with the halogen I_2 presents an alternative to the usual procedures requiring the activation of the carboxylic acid substrate through the formation of an acid chloride.[87a] The coupling of amides had been reported using various phosphorous compounds. Triphenyl phosphine is widely used due to its availability and affordability however, the formation of the toxic byproduct triphenylphosphine oxide is a limitation.[87a] The use of $P(OEt)_3$ for a cyclodehydration process by Huy *et al.* inspired Chen *el al.* to develop a similar process to obtain amidation through the combination of $P(OEt)_3$ and a halide source.[87a,b] When applied to the coupling of carboxylic acid **103** and amide **121**, the procedure did not yield WA **120** (see Scheme 40). Though Chen *et al.* successfully used $P(OEt)_3$ for the formation of tertiary amide, the presence of the Boc group on the amine leads to an increased steric hindrance while decreasing the reactivity of the secondary amine **121**.

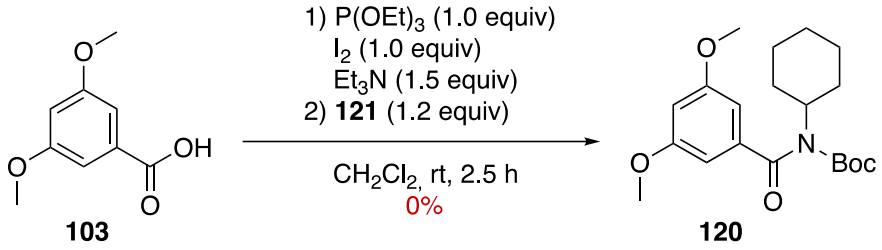

Scheme 40: Amide Coupling Attempt using $P(OEt)_3$ and I_2

The hypothesis of the Boc protecting group hindering the coupling due to its important steric hindrance and its deactivation of the amine was confirmed when amide **104c** was easily obtained using the activation of carboxylic acid **103** following Chen *et al.*'s procedure (see Scheme 41).[87a]

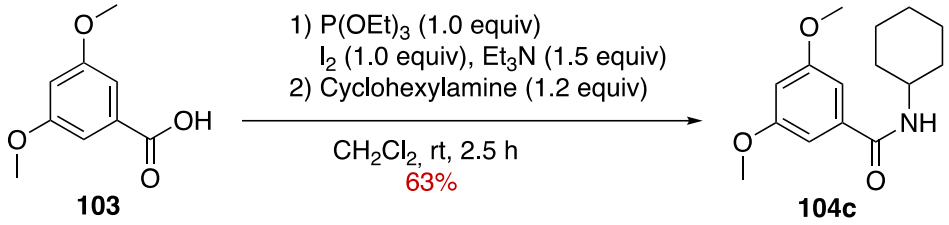

Scheme 41: Amide Coupling using Cyclohexylamine

Due to the obstacles encountered, the Weinreb approach for the late functionalization of CBD was abandoned in the interest of focusing on using the Weinreb approach to offer an alternative to the existing syntheses of olivetol. For the sake of time, the possibility of a late-stage functionalization of CBD via WA could not be explored, though the approach presents a potential alternative to the existing synthetic route to CBD. The observation of traces of formylated WA **119a** during the screening of formylation conditions for this substrate is encouraging (see Table 8). An optimization of the reaction could potentially lead to a solution for a synthesis of CBD allowing for late-stage functionalization.

4. Synthesis of Olivetol

Olivetol is essential to the synthesis of CBD proposed by many chemists. Recent advances in the large-scale synthesis of CBD rely on the coupling of the arene and the terpene fragments (see Scheme 3,4,8).[37,38,44] The synthesis of CBD derivatives via the coupling of an arene and a terpene has great potential for the future industrial production of CBD and other CBs, though the high cost of olivetol and terpenes can be a limitation. Efficient and affordable synthetic pathways to these compounds are necessary. As mentioned earlier, WAs enable the formation of various ketone and the use of the WA functionality has been reported on several occasions for the large-scale production of other pharmaceutical targets (see Chapter 3.2). Here, the use of the WA functionality was applied to offer a practical synthesis of olivetol and its derivatives.

4.1. *Previous Olivetol Syntheses*

The synthesis of olivetol **56** was recently studied by Sisa *et al.* (see Scheme 42).[88] Using the halogenated arene **60** they explored two routes for the synthesis of the desired compound. The Sonogoshira route relies on the coupling of 1-pentyne to the starting material, followed by a reduction of alkyne **122** to the corresponding alkane using Pd/C. The Suzuki route relies on a single step consisting of the coupling of the halogenated arene **60** with pentylboronic acid. The final step for both route is the demethylation of dimethyl ether **36** using boron tribromide, leading to the formation of olivetol **56** with an overall yield of 88% and 92% respectively.

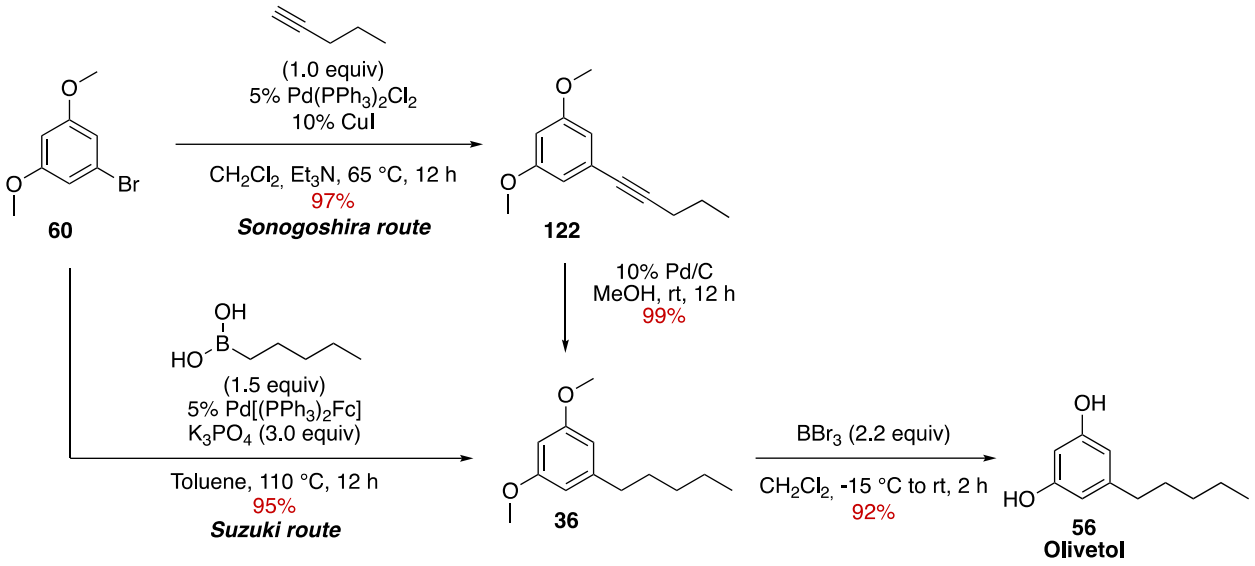

Scheme 42: Suzuki and Sonogoshira Routes for the Synthesis of Olivetol, Sisa *et al.*, 2017

The synthesis of olivetol using a Sonogoshira coupling was briefly explored while researching the possibility of using a halogenated aromatic ring for the late-stage functionalization of CBD. The Sonogoshira coupling of the halogenated arene **60** and 1-pentyne was obtained with high yields following a procedure developed by Morales *et al.*[89] The halogenated arene **60** was treated with copper iodide, triphenylphosphine, and a catalytic amount of tris(dibenzylideneacetone)dipalladium(0) before addition of 1-pentyne, yielding 90% of the corresponding alkyne **122** (see Scheme 43).[89] However, the hydrogenation of alkyne **122** was problematic as the reaction yielded the alkene instead of the desired alkane, therefore we explored other options for the synthesis of olivetol.

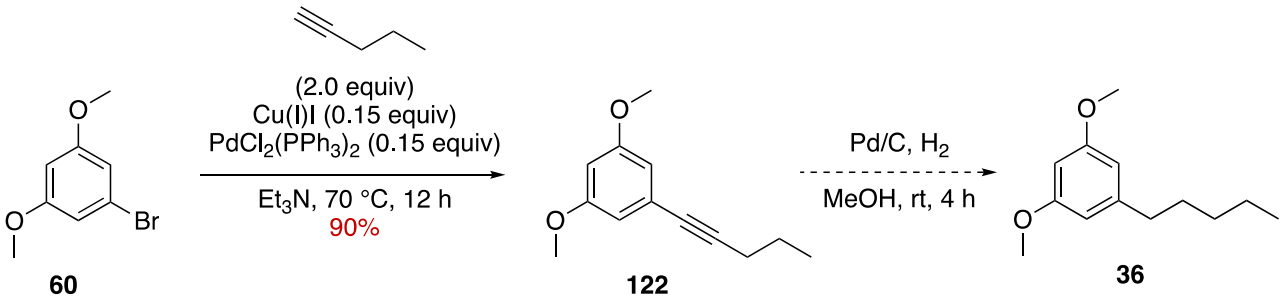

Scheme 43: Sonogoshira Coupling of 1-Bromo-3,5-dimethoxybenzene and 1-Pentyne

The development of an efficient and affordable synthesis of olivetol is of great interest to be able to obtain more affordable processes for the production of CBs. Using a WA intermediate

avoids the use of expensive metal catalysts. Furthermore, the WA approach enables the use of a cheaper starting material and utilizes more sustainable reagents.

Our proposal to use the WA functionality for the synthesis of olivetol enables a synthesis using 3,5-Dimethoxybenzoic acid **103** (382 USD/mole) as starting material rather than 1-Bromo-3,5-dimethoxybenzene **60** (753 USD/mole). The steps necessary for the formation of olivetol using the Weinreb functionality are adaptable to a large-scale synthesis and do not require toxic reagent, making it a good candidate for the potential large-scale production of olivetol.

4.2. *Formation of the Weinreb Ketone*

The use of the WA functionality enables a straightforward synthesis of a range of ketones. Different WA derivatives led to the synthesis of olivetol and its derivatives through the addition of the appropriate organometallic reagent. The synthesis the WA derivatives will be discussed in the following chapter. All the Grignard reagents needed for the formation of ketones were prepared by according to standard procedure found in literature.[90]

As mentioned previously, the Weinreb approach relies on amide derivatives obtained from the coupling of a carboxylic acid with DMHA. However, more affordable amines exhibit the same properties. Therefore, the synthesis of the desired ketones was also explored with amides **104b** and **104c** to provide an affordable alternative. Different organometallic reagents were used for the transformation of WA **104b** to the corresponding ketone (see Table 12). The best results were obtained when WA **104b** was treated with *n*-butyllithium in anhydrous THF at 0 °C for one hour (see Table 12).[91] The electronegativity in the C-Li bond explains why the organolithium reagent was more reactive than the Grignard reagent for the formation of the ketone. The formation of 1-(3,5-Dimethoxyphenyl)pentan-1-one **123a** proceeds through the reaction of the organolithium reagent with the substrate forming a stable chelate and resulting in the desired ketone upon aqueous work up. The reaction yielded up to 79% of the desired product **123a**.

Table 12: Reaction Condition Screening for the Formation of 1-(3,5-Dimethoxyphenyl)pentan-1-one

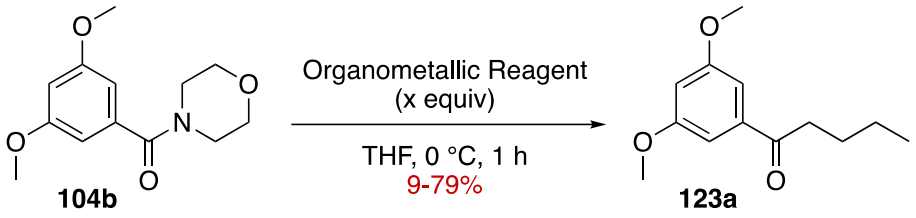

n	Organometallic Reagent	Equiv	% Yield
2.79 mmol	BuMgBr	3.0	9
199 µmol	*n*-BuLi	1.2	46
398 µmol	*n*-BuLi	2.0	63
21.5 mmol	***n*-BuLi**	**2.0**	**79**

When using WA **104c**, the transformation to the ketone requires the chemoselective activation of the substrate by triflic anhydride (Tf_2O) due to the low Lewis basicity of the substrate.[75] 2-Fluoropyridine was added to ensure the stability of the imidoyl triflate.[75] The ketone **123a** was obtained after addition of the Grignard reagent **124** followed by hydrolysis. The reaction allowed to obtain up to 63% of the desired product (see Scheme 44).

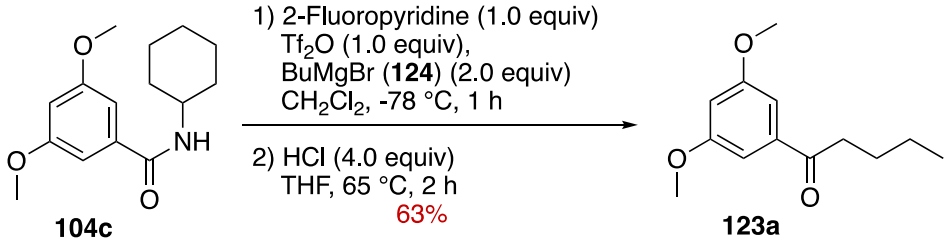

Scheme 44: Ketone Synthesis using *N*-Cyclohexyl-3,5-dimethoxybenzamide

Finally, ketone **123a** was also generated using WA **104a**. When treating WA **104a** with the Grignard reagent **124** in THF at 0 °C for 30 min the desired ketone **123a** was obtained with 59% yield (see Scheme 45).[78]

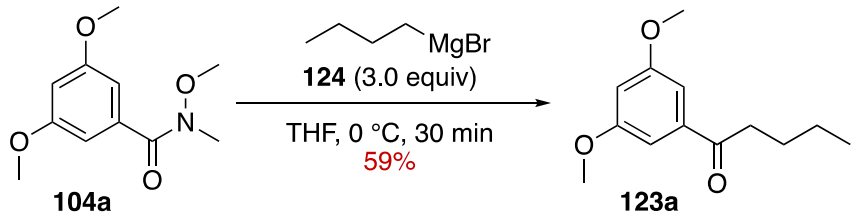

Scheme 45: Ketone Synthesis using *N*-3,5-Trimethoxy-N-methylbenzamide

Due to the straightforward and mild reaction conditions, and scalability (see Table 12), of this last procedure, WA **104a** was retained to generate additional ketones that result in the synthesis of olivetol derivatives.[78] Treating the WA **104a** with the appropriate homemade Grignard reagents led to the successful synthesis of the following ketones (see Scheme 46).

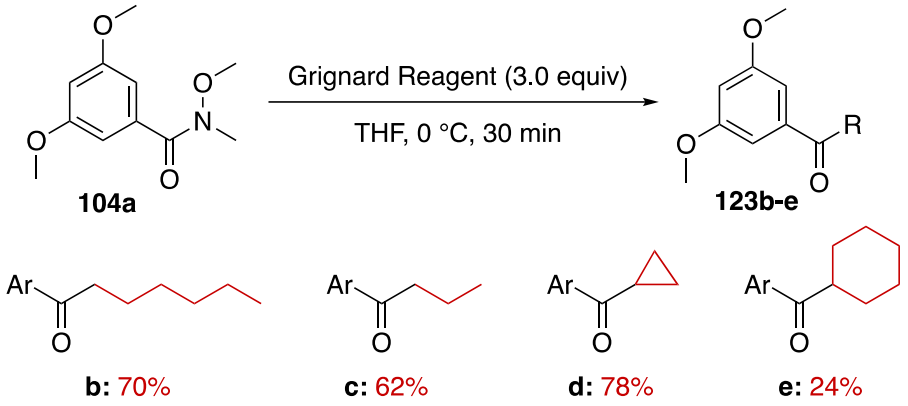

Scheme 46: Synthesis of Ketones **123b-e** using Grignard Reagents

For comparative purposes, the formation of ketone **123a** was attempted by treating the carboxylic acid **103** with both the Grignard reagent **124**[92] and *n*-butyllithium[93] (see Table 13). Using the Grignard reagent **124** yielded only 23% of the corresponding ketone **123a**. The reaction using an organolithium reagent demanded strict control of the reaction environment by maintaining the reaction temperature at -20 °C and yielded 47% of the desired ketone **123a**. These results confirmed the advantages presented by the use of a WA functionality.

Table 13: Reaction Conditions Screening for the Ketone Synthesis using 3,5-Dimethoxybenzoic acid

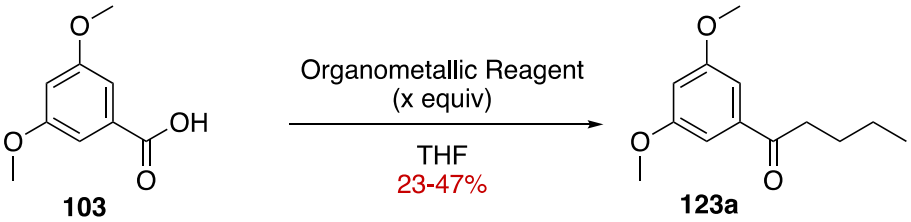

Organometallic Reagent	Equiv	Conditions	% Yield
124	8.0	rt, 24 h	23
***n*-BuLi**	**2.0**	**-20 °C, 1 h**	**47**

4.3. *Wolff-Kishner Reduction*

Following the formation of the ketone, compounds **123a-e** were subjected to a Wolff-Kishner reduction to obtain the corresponding alkane substituent **125a-e** (see Scheme 47).[94] The substrate was first treated with NaOH and hydrazine hydrate in diethylene glycol for 1 hour at 100 °C, then 4 hours at 170 °C. The reduction of the ketone proceeds in two steps. While the mixture is heated to 100 °C, the hydrazine adds onto the carbonyl of the substrate leading to the formation of a hydrazone. When the reaction mixture is then heated to 170 °C, a diimide anion is formed through the action of the base which will subsequently lead to the loss of nitrogen gas.[94] The water generated during the reaction can conveniently be removed from the reaction by equipping the reaction flask with a distillation apparatus. The desired product **125a** was obtained with a 75% yield.

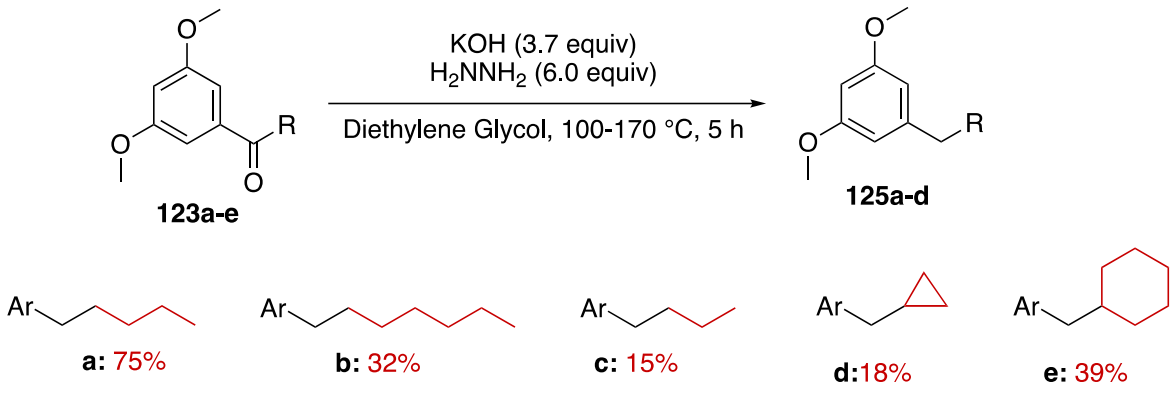

Scheme 47: Wolff-Kishner Reduction of Ketones **125-e**

4.4. *Deprotection to Olivetol and Potential Cannabidiol Derivatives*

The final step necessary to the formation of olivetol is the demethylation reaction. The crucial deprotection of the substrate has often been problematic in previous syntheses of CBD. The demethylation has been reported using various methods. The most efficient method requires boron tribromide (BBr_3) as reported by Sisa *et al*. in their proposal for the synthesis of olivetol (see Scheme 51).[88] The procedure was also reported for the successful demethylation of CBDD on a

large scale with a 92% yield.[95] Despite its efficiency, the highly pyrophoric nature of BBr_3 led us to explore alternative procedures for the demethylation of potential CBD analogs.

The demethylation of the CBD derivative **126** has been obtained by treating the dimethyl ether substrate with the Grignard reagent methyl magnesium iodide in Et_2O at high temperature, with a reported 40% yield of the desired product **127** (see Scheme 48).[96] The procedure generated the desired product though the harsh reaction conditions and low yield make this reaction unsuitable for large scale production.

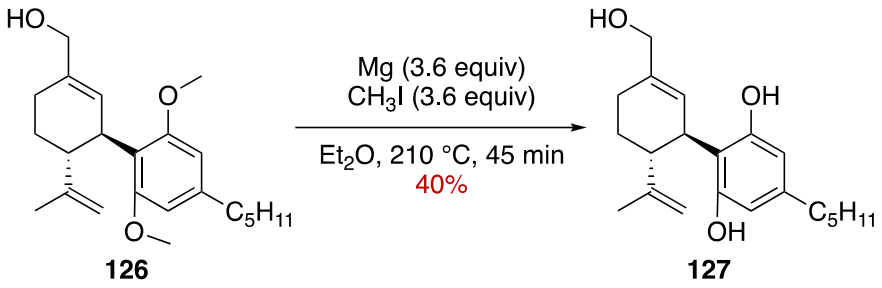

Scheme 48: Demethylation using Grignard Reagent, Hanuš *et al.*, 2005

A few years later, Ballerini *et al.* proposed a synthesis of THC derivatives relying on the demethylation of their precursor using a thiol reagent (see Scheme 49).[42] Their synthesis describes the mono-demethylation of substrate **128** followed by the formation of the pyran leading to CBD precursor **130**, and finally the demethylation of the second methyl ether substituent using an excess amount of the thiol reagent yielded Δ^8-THC **4***. Though it is suitable for the synthesis of THC derivatives, using a thiol for the demethylation of disubstituted substrates presents limitations for the synthesis of CBD which will be later discussed.

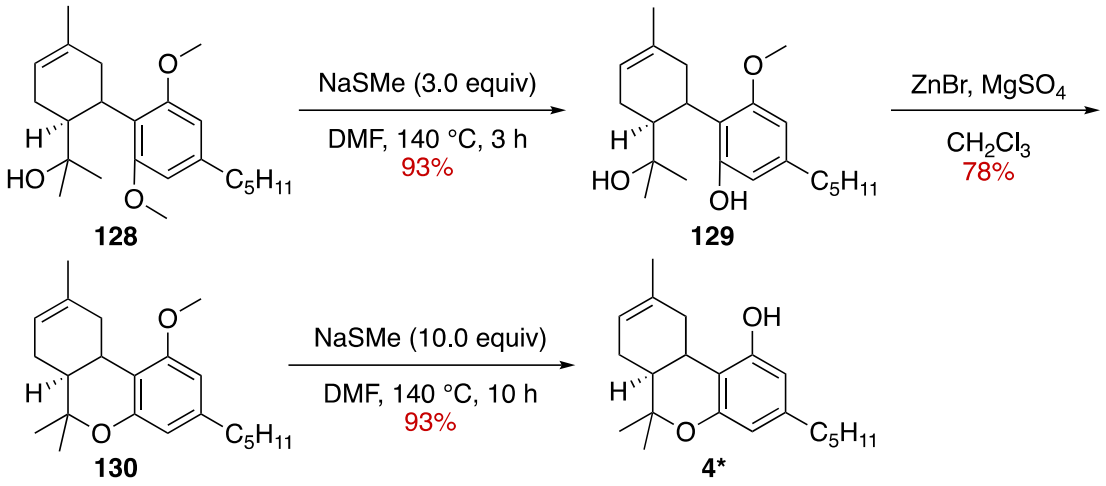

Scheme 49: Demethylation of THC Derivative, Ballerini *et al.*, 2010

4.4.1. Boron Tribromide Demethylation

As reported by Sisa *et al.* the demethylation of the substrate can be obtained by treating olivetol dimethyl ether **125a** with BBr_3 in CH_2Cl_2 at -15°C for 1.5 h (see Scheme 50).[88] The cleavage of the ether proceeds through an S_N2 type reaction with the formation of a Lewis-base adduct followed by the loss of bromide. The release of bromide leads to the attack of the methyl group leading to the cleavage of that C-O bond and the formation of methylbromide. The resulting aryloxydibromoborane finally undergoes hydrolysis during the workup, leading to the formation of olivetol **56**.[97] The BBr_3 demethylation enabled the formation of olivetol with a yield of 97% on a gram scale reaction.

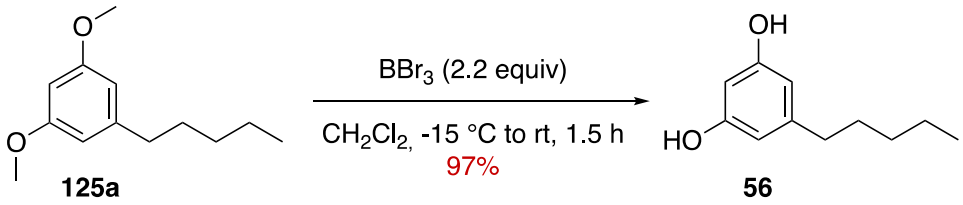

Scheme 50: BBr_3 Demethylation of Olivetol Dimethyl Ether

The method has proven to be efficient however, the use of a highly pyrophoric reagent such as boron tribromide is not suitable for the adaptation to large-scale production or potentially to continuous flow chemistry. As such, we explored alternative demethylation procedures.

4.4.2. Acidic Conditions

The demethylation under acidic conditions was briefly explored via a Zeisel-Prey ether cleavage process using hydrochloric acid in water at high temperature. Bomon *et al.* reported the successful demethylation of a substrate similar to ours.[98] However, we were not able to reproduce their results and the several attempts to adapt the procedure to resorcinol dimethyl ether **78** were not successful (see Scheme 51).

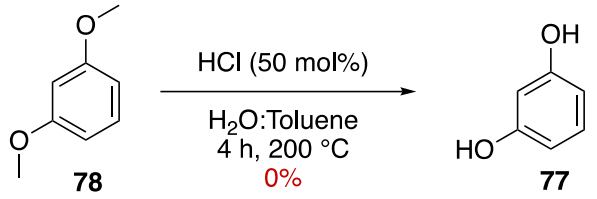

Scheme 51: Demethylation Attempt under Acidic Conditions

4.4.3. Demethylation using an Odorless Thiol Reagent

The demethylation of resorcinol dimethyl ether **78** and olivetol dimethyl ether **36** was then attempted via a procedure developed by Chae *et al.* for the demethylation of aryl methyl ethers using an odorless thiol reagent (see Table 15).[99] Their work reported a demethylation procedure using a thiolate generated from 1-dodecanethiol and NaOH. The *in situ* formation of the thiolate enables the use of the weaker base NaOH, instead of a stronger bases like sodium hydride otherwise used for demethylation reactions as they can be dangerous for industrial scale processes.[99]

Several reaction conditions were screened (see Table 15) however, all were met with the formation of the mono-deprotected product **131a-b**. Doubling the equivalents of reagents did not lead to the formation of olivetol **56**, but rather the mono-deprotected product. We attempted to use excess of both reagents in an order to push the reaction to obtain the desired product, though the desired result was not observed. Finally, the ratio of thiol to base was modified in another effort force the formation of the fully deprotected product. We hoped that by doing so the alcohol would be formed by gaining a hydrogen from thiol excess found in the reaction environment after the first attack of the thiolate onto one of the protecting groups however, it was not the case.

Table 14: Reaction Condition Screening for the Demethylation of Aryl Methyl Ethers using Thiolate

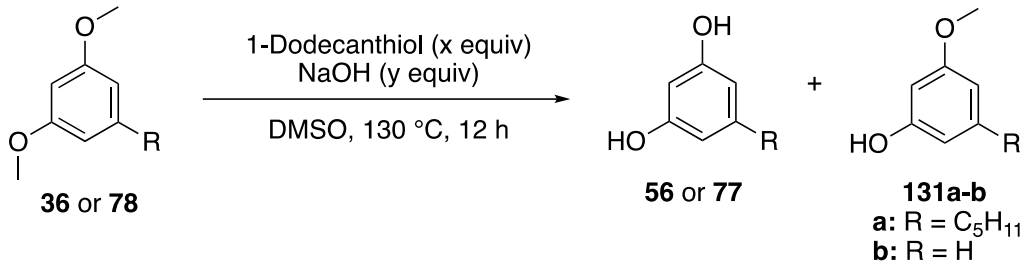

Substrate	Equiv		% Yield	Byproduct (137a-b)
R	Thiol	NaOH		
127	1.0	3.0	0	56%
127	3.0	6.0	0	73%
127	10.0	10.0	0	Yes*
127	10.0	20.0	0	Yes*
95	6.0	2.0	0	Yes*
95	6.0	1.0	0	Yes*

*Byproduct was not isolated

The difficulties encountered while trying to obtain the complete demethylation of the product were reported by Feutrill *et al.* as they encountered the same limitations when researching the deprotection of dimethoxy substituted compounds using thiols.[100] Indeed, for disubstituted substrates only the mono-deprotection was reported.[100] The thiol-mediated demethylation proceeds through the formation of a thiolate ion followed by an S_N2 reaction of the nucleophile onto the partially positively charged C atom of dimethyl ether **78** (see Scheme 52) resulting in the loss of the methyl group (**78**) and formation of the corresponding phenol group (**131b**).[101] The inability to obtain the demethylation of both OMe substituents was attributed to the highly nucleophilic nature of the oxygen anion formed after the loss of the methyl group. The second S_N2 substitution necessary for the formation of the desired product was then impeded, leading to the formation of the mono-deprotected product **131b**.[101]

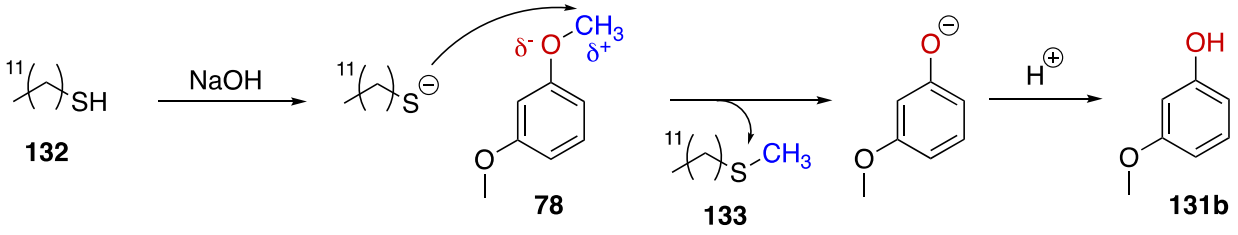

Scheme 52: Mechanism of the Thiol-Mediated Demethylation

The issue was avoided when synthesizing THC analogues, as one of the methyl ether substituents can be demethylated using a thiolate, followed with the formation of the pyran characteristic of THC derivatives. Once the pyran is formed, the second methyl ether can be demethylated via the same method as it was described by Ballerini *et al.* (see Scheme 49).[41,42] Despite our best efforts, the alternative attempts for demethylation of olivetol were inconclusive.

4.5. *Synthesis of Olivetol Derivatives*

The synthesis of additional olivetol derivatives was explored through the introduction of modifications to the alkyl chain. The challenge of the low bioavailability of those compounds can be tackled by introducing various functionalities on the substituted aromatic. Besides the formation of different ketones, other methods can be used to improve bioavailability. The introduction of cyclopropanes on natural compounds is of particular interest as it unlocks potential for therapeutic applications as they present antiviral, antitumorigenic, and antibiotic properties.[102] They can also be used as building blocks for further synthetic modifications. The modification of the alkyl chain is also necessary for the synthesis of analogues such as a nabilone precursor. Both options will be discussed in the following section.

4.5.1. Cyclopropanation

The ketone **123a** was used to generate a derivative of olivetol bearing a butyl cyclopropyl substituent. The introduction of the cyclopropanated substituent increases the drug potency of the molecule.[102,103] The cyclopropanated product was generated from ketone **123a** through two steps. First, ketone **123a** was reduced via a Wittig olefination (see Scheme 65).[40] The reaction allowed to obtain 1-(hex-1-en-2-yl)-3,5-dimethoxybenzene **134** with an 82% yield.

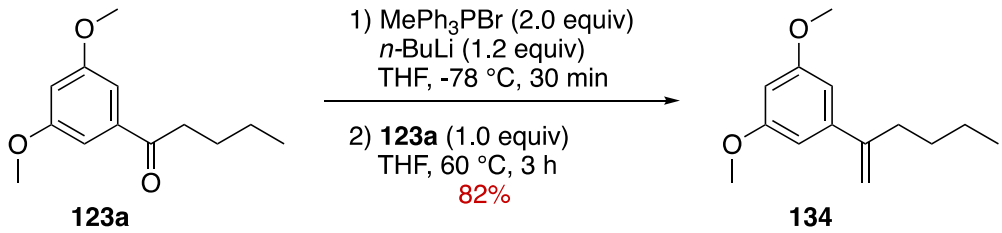

Scheme 53: Wittig Olefination of 1-(3,5-Dimethoxyphenyl)heptan-1-one

Arene **134** was then used to obtain the cyclopropanated product. The desired product was obtained via a Simmons-Smith reaction.[104] The arene **134** was added to a solution of zinc copper couple (Zn(Cu)), I_2 and iodomethane (CH_2I_2) in Et_2O at 35 °C for 16 h (see Scheme 54). The formation of the cyclopropane proceeds through an a-iodomethylmetal intermediate such as ICH_2ZnI.[105] It requires the formation of a complex between the reactive species prior to the addition of the substrate, which is followed by the simultaneous formation of both new C-C bonds. The nucleophilic nature of the alkene leads to the loss of the iodine and the formation of the 2nd C-C bond. The cyclopropanated product **136** was not purified due to the small scale of the reaction, however NMR of the crude product indicated a 9:1 ratio of starting material **135** to desired product **136**. When applied to a-methylstyrene, NMR analysis of the product indicated that the reaction allowed for full conversion to the cyclopropanated products. Unfortunately, the optimization of the cyclopropanation procedure or exploration of alternative procedures using diethyl zinc were not attempted due to a lack of time, though preliminary results indicate great potential for substrate **135**.

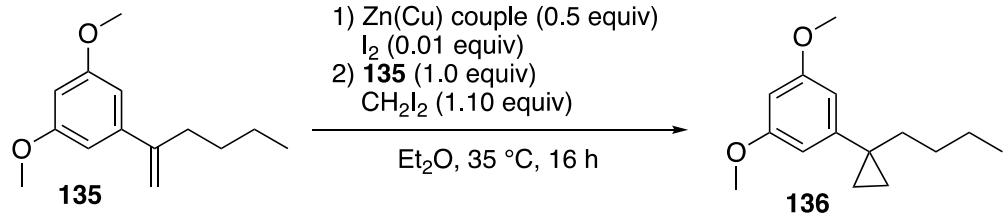

Scheme 54: Simmons-Smith Cyclopropanation on 1-(Hex-1-en-2-yl)-3,5-dimethoxybenzene

4.5.2. Synthesis of Nabilone Aromatic Fragment

Nabilone **14** is a THC derivative bearing a dimethylheptyl alkyl chain substituent. It is also found in appetite stimulant drug treatments designed for cancer patients suffering of anorexia and weight loss. It has a much higher bioavailability than dronabinol **13** due to the variation in the aromatic substituent.[106]

The WA approach was applied to the synthesis of a nabilone precursor following a method proposed by Bourne *et al.* in 2007 for the synthesis of anandamide derivatives (see Figure 3).[108] In their work, they proposed an efficient synthesis of derivatives for the purpose of testing them for their CB_1 and CB_2 receptors affinity (see Scheme 55).[107]

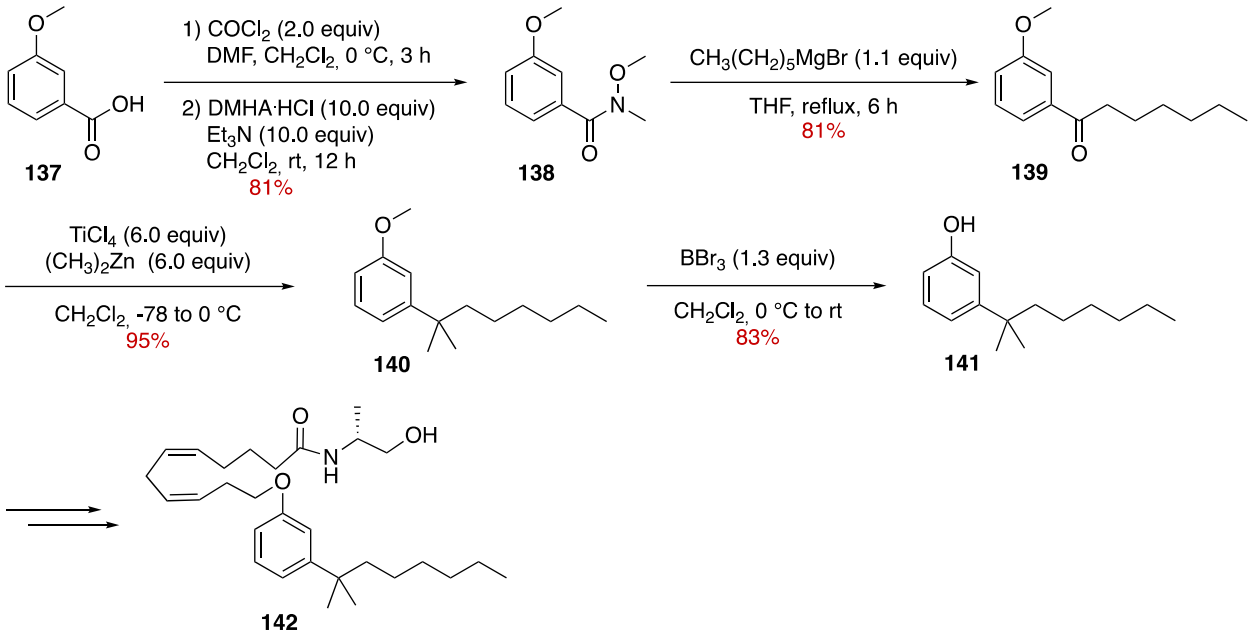

Scheme 55: Synthesis of Anandamide Derivatives, Bourne *et al,* 2007

Bourne *et al*.'s approach was applied to the synthesis of the substituted aromatic fragment of nabilone.[107] Using ketone **123b** the dimethylation of the substrate results in the formation of the nabilone precursor. Unfortunately, due to a lack of time the reaction was not attempted. According to Selwood *et al.* the dimethylation can be obtained be treating the ketone **143** with $TiCl_4$ and trimethylaluminium, yielding 85% of the desired product **144** (see Scheme 56).[108] However, it has been reported that the use of $AlMe_3$ can lead to the formation of undesired byproducts due to rearrangements, elimination, and enolization.[108]

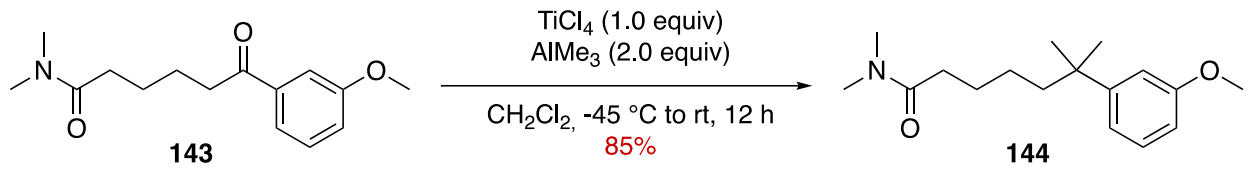

Scheme 56: Ketone Dimethylation, Selwood *et al.*, 2008

Instead of using $AlMe_3$, the desired product can also be obtained from treating the ketone **145** with a combination of $TiCl_4$ and dimethylzinc at very low temperatures leading to the formation of 98% of **146** (see Scheme 57).[109] The 98% yield of the reaction is ensured through the presence of an excess of the methyl groups in the organometallic reagent.[110]

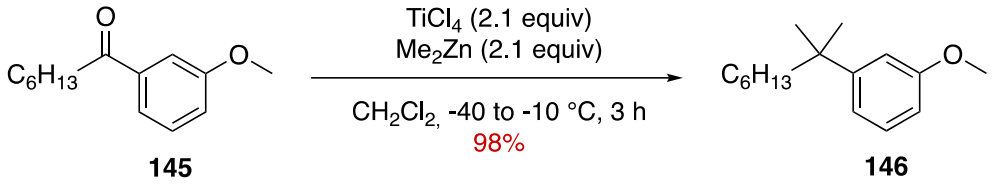

145 **146**

Scheme 57: Ketone Dimethylation, Cheng *et al.,* 2012

The introduction of the WA functionality enables the variation of the alkyl chain found on olivetol. Though the late-stage functionalization of CBD was met with many limitations, the proposal to use WA for an easy access to olivetol derivatives could also facilitate the synthesis of CBD derivatives. The olivetol molecule obtained using the WA approach was used for the synthesis of CBDD following the Diels-Alder approach.

4.6. *Synthesis of Cannabidiol Dimethyl Ether*

Once an efficient synthesis of the olivetol precursor **125a** was developed, it was used to obtain CBDD **2c** applying the synthetic steps mentioned in Chapter 2.1 (see Scheme 58). Due to the presence of the alkyl chain on the aromatic ring, the reaction conditions for some of the steps needed optimization. The formylation of the substrate proceeded smoothly, yielding 78% of the corresponding aldehyde **146.**[55] The reaction conditions of the aldol condensation needed to be optimized;[58] stirring the reaction solution at 60 °C or 8 h yielded 75% of the unsaturated ketone **44**. Similarly, the reaction time of the Wittig olefination was increased to 8 h at 60 °C instead of 3 h to ensure maximal conversion to the desired product **45** with a 56% yield.[40] The reaction conditions for the Diels-Alder reaction and the epimerization reaction were not optimized, yielding 59% and 97% of the respective desired product **46** and **147**.[41,42] Finally, the second Wittig olefination was performed following the usual procedure, yielding 68% of the final product **2c**.[40] The demethylation of CBDD was not attempted due to the limited timeline.

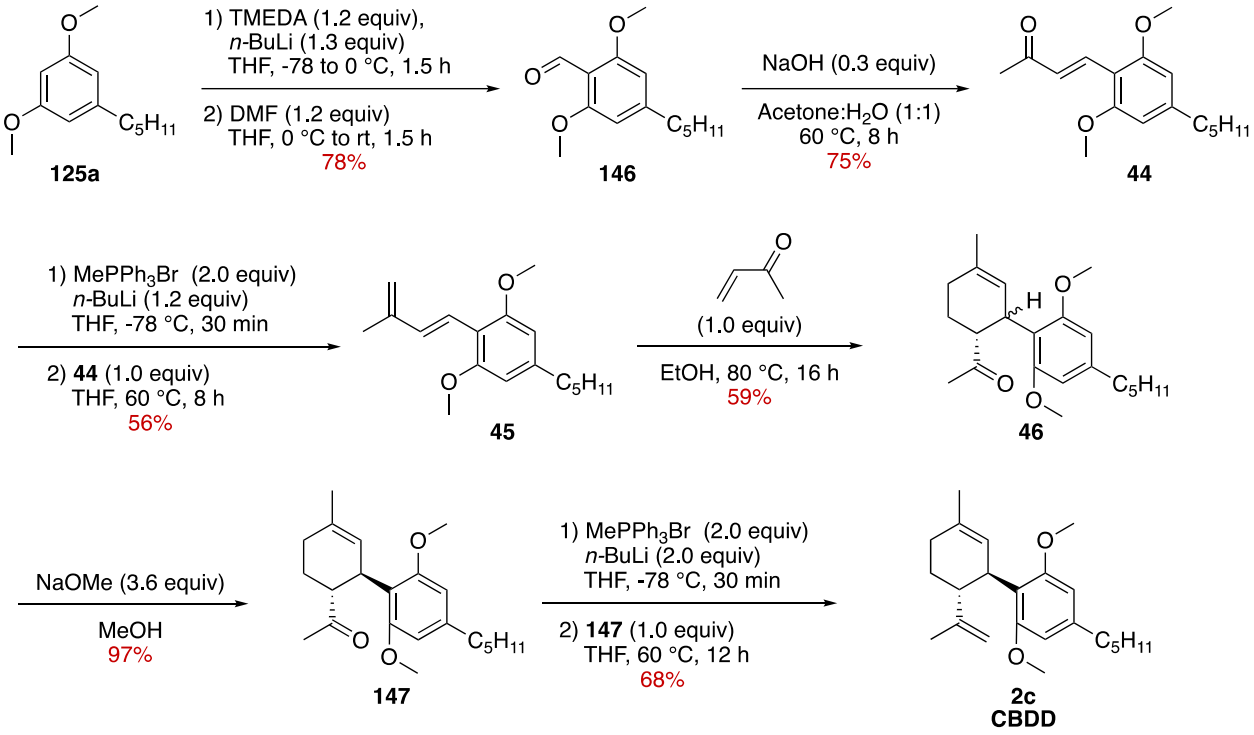

Scheme 58: Synthesis of CBD Dimethyl Ether

5. Future Work

5.1. *Scope of Functionalization*

The use of the Weinreb amide functionality opens the possibilities for the synthesis of olivetol and CBD derivatives The WA **104a** was successfully used to generate derivatives **123a-e** upon treatment with the desired Grignard reagent (see Scheme 59). The synthesis of ketones could be applied to the synthesis of derivatives **123f-i** with potential increased bioavailability.

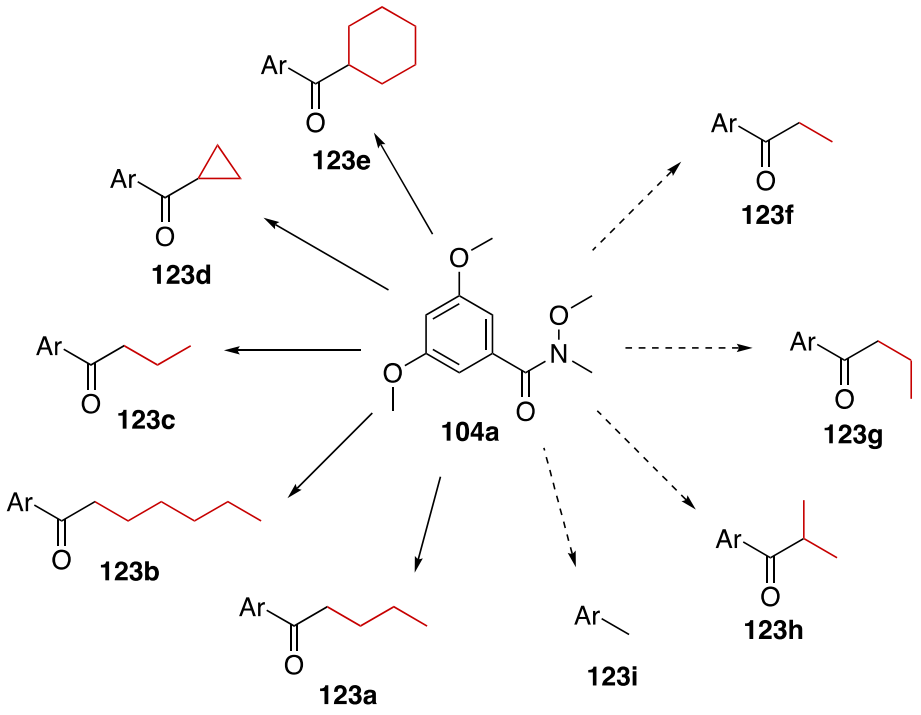

Scheme 59: Potential Olivetol Derivatives

For the synthesis of a methylated aromatic ring, the WA functionality can be exploited following a catalytic methylation procedure proposed by Feng *et al* (see Scheme 60).[111] The methylation of amide **104** was obtained by treating the amide using trimethylboroxine (TMB) as the methylating agent, in combination with a pre-catalyst allylpalladium chloride dimer ($[Pd(allyl)Cl]_2$), a ligand 1,4-bis(diphenylphosphino)butane (dppb), and cesium fluoride in dioxane at 160 °C for 24 h. Applying this method to the appropriate WA could lead to the synthesis of the aromatic precursor of CBD-C1 (see Figure 5).

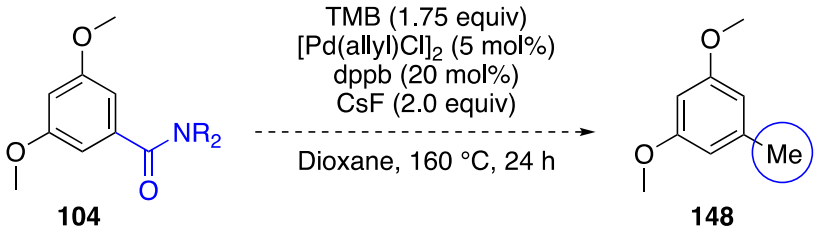

Scheme 60: Potential methylation of WA

5.2. *Optimization of the Olefination reactions*

Finding an alternative to the Wittig olefinations necessary for the methylenation of the ketones **80** and **83** would be essential to propose a more sustainable and efficient synthesis of the CBD and olivetol precursor. The Wittig reactions reported used in the work generate a toxic and insoluble phosphine oxide. Besides presenting a sustainability issue, the phosphine oxide byproduct is also a limitation for the potential application of the Wittig reaction to continuous flow chemistry. The reduction of the ketones **80** and **83** could be obtained from an olefination relying on a Tebbe reagent rather than a Wittig reagent. The Tebbe reagent is an organometallic reagent containing titanium which has been proven to be or more efficient than the Wittig reagent for the carbonyl methylenation of various substrates (see Table 15).[112] The use of the Tebbe reagent presents many advantages as the reaction takes place in non-basic conditions, therefore preventing racemization, and leads to the formation of the desired product in much shorter reaction time.

Table 15: Substrate Screening for the Comparison of Tebbe and Wittig Reagents

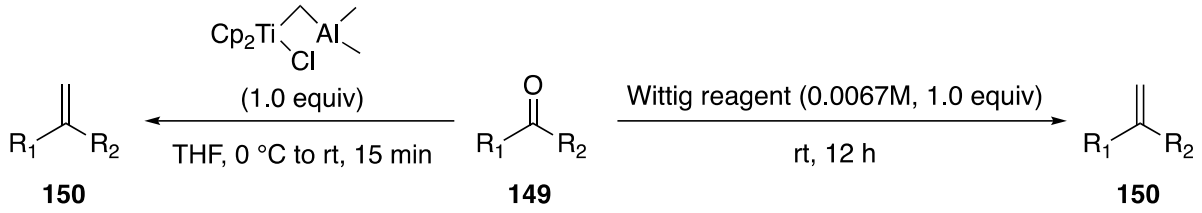

Substrate	Product	% Yield	
		Tebbe	Wittig
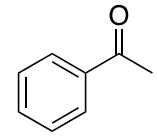	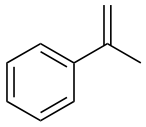	98	88
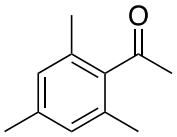	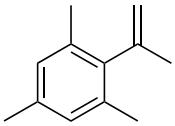	77	4

Applying the Tebbe olefination conditions to the methylenation of ketones **80** and **83** could be a solution to avoid the use of the unsustainable Wittig reaction (see Scheme 61). The Tebbe reaction would allow to significantly reduce reaction times while also simplifying the purification of the products and avoiding the formation of the toxic phosphine oxide byproduct generated by the Wittig olefination reaction.

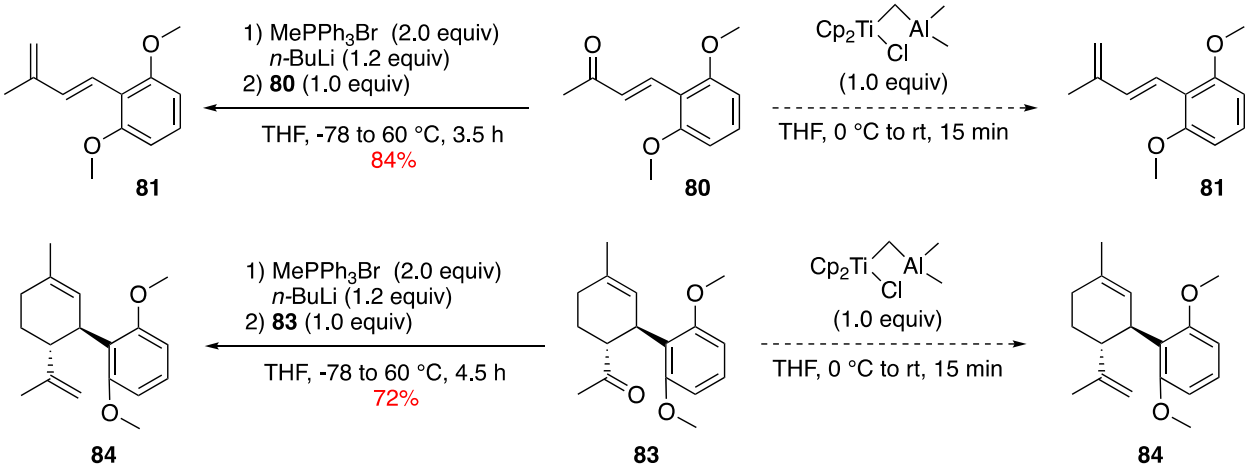

Scheme 61: Alternative Olefination Procedure for Ketones **80** and **83**

If the olefination of the ketones **80** and **83** can be performed smoothly using the Tebbe reagent, the reaction could be further optimized using the Petasis reagent dimethyltitanocene (Cp_2TiMe_2), which has the potential to enable the olefination under continuous flow conditions. The Petasis reagent comes from the same class of reagents and was applied by Koch *et al.* for the olefination of esters to enol ethers.[113] Cp_2TiMe_2 can be easily generated by reacting methyl magnesium chloride or methyllithium with titanocene chloride.[114] It is easily stored as it is both air and water stable. The oxo-bridged titanocene dimer byproduct formed during the olefination reaction can be recycled after treatment with hydrochloric acid.[114] The process was efficiently applied to the large-scale olefination of esters. Koch *et al.*'s work show that the Petasis olefination can be successfully adapted to continuous flow conditions (see Scheme 62).[113] The successful adaptation of an olefination reaction to continuous flow chemistry could be of great interest for the synthesis of CBD precursors.

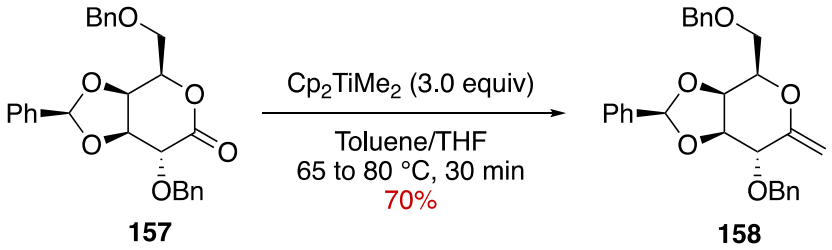

Scheme 62: Olefination of Sugar Lactones by Koch *et al.,* 2011

6. Conclusion

The thesis focuses on the development of an efficient synthetic access to CBD derivatives. The proposed approach utilizes the affordable 1,3-Dimethoxybenzene as starting material and relies on a Diels-Alder reaction with a late-stage functionalization. The synthesis of the desired CBD precursor was achieved following procedures previously established by Korte *et al.*[40] and Ballerini *et al.*[41,41] The post functionalization of the bicyclic precursor was attempted using various techniques. The initial proposal was to rely on the C-H activation of the aromatic ring via a Hartwig-Miyaura borylation, however it led to the borylation of the substrate at several positions. As an alternative, the use of a halogenated aromatic ring was explored. Due to the inductive effect exhibited by 1-bromo-3,5-dimethoxybenzene, the use of 1-bromo-3,5-dimethoxybenzene did not enable the synthesis of the diene needed for the Diels-Alder reaction. In light of the encountered limitations, we turned to the use of a Weinreb amide functionality to obtain the functionalization of the aromatic ring. Subjecting the generated WA derivative to the synthetic steps necessary to the formation of CBD was met with the same constraints due to the inductive effect of the substituents. Though the WA approach was not viable for the chosen pathway for the synthesis of CBD derivatives, the possibilities offered by the WA functionality were explored to obtain the synthesis of olivetol derivatives.

For the synthesis of olivetol derivatives, various WA were generated using 3,5-dimethoxybenzoic acid. Olivetol was obtained after the treatment of (3,5-dimethoxyphenyl)(morpholino)methanone with an organolithium reagent leading to the formation of the ketone, followed by a Wolff- Kishner reduction and a deprotection. 3,5-Dimethoxybenzoic acid was used to generate several WA derivatives. *N*-3,5-Trimethoxy-*N*-methylbenzamide was chosen to generate a range of ketones leading to the synthesis of several olivetol derivatives after treatment with the appropriate Grignard reagent. The introduction of a cyclopropanated substituent as well as the synthesis of the aromatic fragment of nabilone were explored as well. Using the Weinreb functionality offers the possibility of a greener synthetic pathway to cannabinoid precursors and could potentially be extrapolated to a kilogram scale production.

7. Experimental Section

All reactions were performed under argon atmosphere with flame dried glassware. The solvents (toluene, Et_2O, DMF, MeCN) were dried by GlassContour solvent filtration system consisting of two columns of zeolite under argon pressure. The solvents (THF, DCM, acetone, pyridine, Et_3N) were dried by distillation over Na or CaH_2. Thin-layer chromatography (TLC) were done using a sheet of glass covered with silica gel. After elution, the products were revealed using UV light and the following stains: iodine/SiO_2, $KMnO_4$ aqueous solution, and *p*-anisaldehyde. Flash chromatography purification was performed using silica gel following standard procedure. Infrared spectra were obtained using an FTIR apparatus and are reported in cm^{-1}. Melting points were measured using EZ-Melt Automated Melting Point System and are uncorrected. Nuclear magnetic resonance spectra (^1H, ^{13}C, ^{11}B) were recorded on a Bruker Ascend 400 MHz NMR spectrometer. Chemical shifts for the ^1H spectra are expressed in ppm in relation to the internal reference of the residual non-deuterated solvent chloroform (δ 7.26 ppm). The analysis of spectra is presented reporting the chemical shift, followed by multiplicity, the integration, and the coupling constant in Hz. Chemical shifts for the ^{13}C spectra are expressed in ppm in relation to the internal reference of the residual non-deuterated solvent chloroform (δ 77.0 ppm). ^{13}C spectra were obtained using complete decoupling of protons. HRMS data was provided by the Mass Spectrometry Center of the Université de Montreal.

TMEDA, cyclohexylamine, 1-bromopropane, 1-bromobutane, 1-bromocyclopropane, 1-bromocyclohexane were distilled before utilization[115] while all other purchased chemicals were used without further purification. 1,3-Dimethoxybenzene, 1-bromo-3,5-dimethoxybenzene, and 3,5-dimethoxybenzoic acid are commercially available starting materials. Grignard reagents were synthesized following procedures found in the literature and stored under argon.[94]

8. Bibliography

1. Sussman, S. *Addiction*, **1998**, *93*, 934.
2. Pisanti, S.; Bifulco, M. *J. Cell. Physiol*., **2019**, *234*, 8342-8351.
3. Li, H. L. *In Rubin, V. (Ed.), Cannabis and Culture*, **1975**, 51-62.
4. Smith, F. P. *Shanghai: American Presbyterian Mission Press*., **1911**, 90–91.
5. Chopra, I. C.; Chopra, R. N. *Bulletin on Narcotics*, **1957**, *9*, 4-29.
6. Mechoulam, R.; Parker, L. A. *Annual review of psychology*, **2013**, *64*, 21-47.
7. Russo, E. B. *Chemistry & Biodiversity,* **2007**,*4*, 614-648
8. Pain, S. *New Scientist*. **2007**.
9. Lozano, I. *In E. B. Russo, & F. Grotenherman (Eds.),* **2006**, *5-12*.
10. Forster, E. *Journal of the International Hemp Association,* **1996**, *3*, 72.
11. Arata, L. *Janus Head,* **2004**, *7*, 34-49.
12. Fankhauser, M. *New York: The Haworth Integrative Healing Press*, **2002**, *37-49.*
13. Booth, M. *Macmillan,* **2005**.
14. Kynett, H. H.; Butler, S. W.; Brinton, D. G. *Medical and Surgical Reporter,* **1863***, 10*.
15. a) Adams, R. *U.S. Patent 2304669*, **1942**.
    b) Adams, R.; Pease, D. C.; Clark, J. H. *J. Am. Chem. Soc.*, **1940**, *62*, 2194-2196.
16. Mechoulam, R.; Gaoni, Y. *J. Am. Chem. Soc.*, **1964**, *86*, 1646-1647.
17. Mechoulam, R.; Gaoni, Y. *J. Am. Chem. Soc.*, **1965,** *87*, 3273-3275.
18. Di Marzo, V.; Bifulco, M.; De Petrocellis, L. *Nat. Rev. Drug Discov.*, **2004**, *3*, 771-784.
19. Freitas, H.R.; Isaac, A.R.; Malcher-Lopes, R.; Diaz, B.L.; Trevenzoli, I.H.; de Melo Reis, R.A. *Nutr. Neurosci.*, **2018**, *21*, 695-714.
20. Pertwee, R.G. *Br. J. Clin. Pharmacol.* **2008**, *153*, 199-215.
21. Reggio, P.H. *Curr. Med. Chem.*, **2010**, *17,* 1468-1486.
22. Pisanti, S.; Bifulco, M. *Pharmacol. Res.*, **2009**, *60*, 107-116.
23. Massi, P.; Solinas, M.; Cinquina, V.; Parolaro, D. *Br. J. Clin. Pharmacol.* **2013**, *75*, 303-312.
24. Sharma, P.; Murthy, P.; Bharath, M.S. *Iran. J. Psychiatry*, **2012**, *7*,149.
25. Patheon Softgels Inc., Marinol (Dronabinol), [package insert]. U.S. Food and Drug Administration website. https://www.accessdata.fda.gov/drugsatfda_docs/label/2017/018651s029lbl.pdf. Revised August **2017**. Accessed June **2021**.
26. Valeant Pharmaceutical International, Cesamet (Nabilone), [package insert]. U.S. Food and Drug Administration website. https://www.accessdata.fda.gov/drugsatfda_docs/label/2006/018677s011lbl.pdf. Revised May **2006**. Accessed June **2021**.
27. Greenwich Biosciences, Inc., Epidiolex (Cannabidiol) oral solution, [package insert]. U.S. Food and Drug Administration website. https://www.accessdata.fda.gov/drugsatfda_docs/label/2018/210365lbl.pdf. Revised June **2018**. Accessed June **2021**.
28. US Food and Drug Administration Website. https://www.fda.gov/news-events/press-announcements/fda-approves-first-drug-comprised-active-ingredient-derived-marijuana-treat-rare-severe-forms. Published June **2018**, Accessed June **2021**.
29. Stott, C. G.; White, L.; Wright, S.; Wilbraham, D.; Guy, G. W. *Eur. J. Clin. Pharmacol.*, **2013**, *69*, 825-834.
30. Cherniakov, I.; Izgelov, D.; Domb, A. J.; Hoffman, A. *Eur. J. Pharm. Sci.*, **2017**, *109*, 21-30.

31. Morales, P.; Reggio, P. H.; Jagerovic, N. *Frontiers in Pharmacology*, **2017**, *8*, 422.
32. Salaün, J.; Bairtr, M. *Curr. Med. Chem*, **1995**, *2*, 511-542.
33. Appendino, G.; Taglialatela-Scafati, O. *Nat. Prod. Res.*, **2013**, *3415-3435*.
34. Tahir, M. N.; Shahbazi, F.; Rondeau-Gagné, S.; Trant, J. F. *J. Cann. Res.*, **2021**, *3*, 1-12.
35. Ramirez, C. L.; Fanovich, M. A.; Churio, M. S. *Elsevier*, **2019**, *61,* 143-173.
36. Pirrung, M. C. *J. Med. Chem.*, **2020**, *63*, 12131-12136.
37. Vaillancourt, V.; Albizati, K. F. *J. Org. Chem.,* **1992**, *57*, 3627-3631.
38. Kobayashi, Y.; Takeuchi, A.; Wang, Y.G. *Org. Lett.*, **2006**, *8*, 2699-2702.
39. Lago-Fernandez, A.; Redondo, V.; Hernandez-Folgado, L.; Figuerola-Asencio, L.; Jagerovic, N. *Methods in Enzymology*, **2017**, *593*, 237-257.
40. Korte F.; Dlugosch E.; Claussen U. *Liebigs. Ann. Chem*., **1966**, *693*, 165-170.
41. Ballerini, E.; Minuti, L.; Piermatti, O.; Pizzo, F. *J. Org. Chem*., **2009**, *74*, 4311–4317.
42. Minuti, L.; Ballerini, E. *J. Org. Chem*. **2011**, *76*, 5392-5403.
43. Baumann, M.; Baxendale, I. R. *Beilstein J. Org. Chem.*, **2015**, *11*, 1194-1219.
44. Bloemendal, V. R.; Spierenburg, B.; Boltje, T. J.; van Hest, J. C.; Rutjes, F. P. *J. Flow Chem.*, **2021**, *11*, 99-105.
45. Ishiyama, T.; Miyaura, N. *Pure Appl. Chem.*, **2006**, *78*, 1369-1375.
46. Robbins, D. W.; Hartwig, J. F. *Angew. Chem.*, **2013**, *125*, 967-971.
47. Shinokubo, H. *Proc. Jpn. Acad*., **2014**, *90*, 1-11.
48. Dethe, D. H.; Erande, R. D.; Mahapatra, S.; Das, S.; Kumar, B. V. *Chem. Commun.*, **2015**, *51*, 2871-2873.
49. Wang, Q.; Huang, Q.; Chen, B.; Lu, J.; Wang, H.; She, X.; Pan, X. *Angew. Chem. Int. Ed.*, **2006**, *45*, 3651-3653.
50. Czaplik, W.M.; Mayer, M.; von Wangelin, J. A. *Angew. Chem. Int. Ed.,* **2009**, *48*, 607-610.
51. Miyaura, N.; Yamada, K.; Suzuki, A. *Tet. Lett*., **1979**, *20*, 3437–3440.
52. Sonogashira, K. *J. Organomet. Chem.,* **2002**, *653*, 46–49.
53. Tamao, K.; Sumitani, K.; Kumada, M. *J. Am. Chem. Soc.,* **1972**, *94*, 4374–4376.
54. Gong, X.; Sun, C.; Abame, M. A.; Shi, W.; Xie, Y.; Xu, W.; Zhu, F.; Zhang, Y.; Shen, J.; Aisa, H. A. *J. Org. Chem.* **2019**, *85*, 2704–2715.
55. Shultz, Z. P.; Lawrence, G. A.; Jacobson, J. M.; Cruz, E. J.; Leahy, J. W. *Org. Lett*., **2018**, *20*, 381-384.
56. a)Snieckus, V. *Chemical Reviews*, **1990**, *90*, 879-933.
    b) Schlosser, M. *Angew. Chem. Int. Ed*., **2005**, *44*, 376-393.
57. Zumbansen, K.; Doehring, A.; List, B. *Adv. Synth. Catal*., **2010**, *352*, 1135-1138.
58. Cheng, Y. F.; Dong, X. Y.; Gu, Q. S.; Yu, Z. L.; Liu, X. Y. *Angew. Chem. Int. Ed*., **2017**, *56*, 8883-8886.
59. Roy, J. *Elsevier*. **2011**.
60. Goudreau, R. S. *[Doctoral Dissertation, Université de Montréal], Papyrus,* **2010**.
61. Preshlock, S. M.; Ghaffari, B.; Maligres, P.E.; Krska, S. W.; Maleczka Jr, R. E.; Smith III, M. R. *J. Am. Chem. Soc.*, **2013**, *135*, 7572-7582.
62. Olsson, V. J.; Szabo, K. J. *J. Org. Chem.*, **2009**, *74*, 7715-7723.
63. Mann, F. G., Saunders, B. C. *Orient Blackswan*, **1975**.
64. Lee, H.; Kim, D.; Lee, H. K.; Qiu, W.; Oh, N. K.; Zin, W. C.; Kim, K. *Tet. Lett.*, **2004**, *45,* 1019-1022.
65. Kyratsous, C.; Nitolli, T.; Zumsteg, A.; Gromada, J.; Gusarova, V.; Han, A.; Olson, W.; Sleeman, M. *WO2019/217591*, **2019**, A, 0881.
66. Murray, P. R. *Heinemann*, **1977**.

67. Zhang, K.; Ma, R.; Wang, Y.; Shi, Z.; Lu, T.; Feng, J. *ACS Sustainable Chem. Eng.*, **2019**, *7*, 18542-18546.
68. Iijima, T.; Makabe, H. *Biosci. Biotechnol. Biochem*., **2009**, *73*, 2547-2548.
69. Rempel, V.; Volz, N.; Hinz, S.; Karcz, T.; Meliciani, I.; Nieger, M.; Müller, C. E. *J. Med. Chem.*, **2012**, *55*, 7967-7977.
70. Ushijima, S.; Togo, H. *Synlett*, **2010**, *7*, 1067-1070.
71. Yang, W. R.; Choi, Y. S.; Jeong, J. H. *Org. Biomol. Chem.*, **2017**, *15*, 3074-3083.
72. Ramos-Tomillero, I.; Paradís-Bas, M.; De Pinho Ribeiro Moreira, I.; Bofill, J.M.; Nicolás, E.; Albericio, F. *Molecules*, **2015**, *20*, 5409-5422.
73. Lindoy, L.F.; Meehan, G.V.; Svenstrup, N. *Synthesis*, **1998**, *7*, 1029-1032.
74. Nahm, S.; Weinreb, S. M. *Tet. Lett*., **1981**, *22*, 3815-3818.
75. Bechara, W. S.; Pelletier, G.; Charette, A. B. *Nature Chemistry*, **2012**, *4*, 228-234.
76. Graham, S. L.; Scholz, T. H. *Tet. Lett.*, **1990**, *31*, 6269-6272.
77. Balasubramaniam, S.; Aidhen, I. S. *Synthesis*, **2008**, *23*, 3707-3738.
78. Jammula, S. R. *Tet. Lett*., **2016**, *57*, 3924-3928.
79. Balasubramaniam, S.; Annamalai, S.; Aidhen, I. S. *Synlett*, **2007**, *18*, 2841-2846.
80. a) Englund, E. A., Gopi, H. N., Appella, D. H. *Org. Lett*., **2004**, *6*, 213-215.
    b) Kainosho, M., Terauchi, T. *WO2002JP13303/20021219*, **2003**, A1, 17.
    c) Basel, Y.; Hassner, A. *J. Org. Chem.*, **2000**, *65*, 6368-6380.
81. Takahashi, M.; Maehara, T.; Sengoku, T.; Fujita, N.; Takabe, K.; Yoda, H. *Tetrahedron*, **2008**, *64*, 5254-5261.
82. George, N.; Ofori, S.; Parkin, S.; Awuah, S. G. *RSC Adv.*, **2020**, *10*, 24017-24026.
83. Ragnarsson, U., Grehn, L. *RSC advances*, **2013**, *3*, 18691-18697.
84. Trost, B. M.; McDougall, P. J. *Org. Lett*., **2009**, *11*, 3782-3785.
85. Albericio, F.; El-Faham, A. *Org. Process Res. Dev.,* **2018**, *22*, 760-772.
86. Dunetz, J. R.; Magano, J.; Weisenburger, G. A. *Org. Process Res. Dev.,* **2016**, *20*, 140−177
87. a) Chen, P. J.; Wang, H. Y.; Peng, A. Y. *RSC advances*, **2015**, *5*, 94328-94331.
    b) Huy P. H.; Westphal J. C.; Koskinen A. M. P. *Beilstein J. Org. Chem*., **2014**, *10*, 369–383
88. Sisa, M.; Dvorakova, M.; Vanek, T. *Tetrahedron*, **2017**, *73*, 5297-5301.
89. Morales, P.; Azofra Mesa, L. M.; Cumella, J.; Hernandez-Folgado, L.; Roldán, M.; Alkorta, I.; Jagerovic, N. *Arkivoc*. **2014**.
90. Charette, A. B.; Lebel, H. *Org. Synth.*, **1999**, *76*, 86-100.
91. Jackson, M. M.; Leverett, C.; Toczko, J. F.; Roberts, J. C. *J. Org. Chem.*, **2002**, *67*, 5032-5035.
92. Fiandanese, V.; Marchese, G.; Ronzini, L. *Tet. Lett.*, **1983**, *24*, 3677-3680.
93. Bures, E.; Nieman, J. A.; Yu, S.; Spinazzé, P. G.; Bontront, J. L. J.; Hunt, I. R.; Keay, B. A. *J. Org. Chem.*, **1997**, *62*, 8750-8759.
94. Szmant, H. H.; Harmuth, C. M. *J. Am. Chem. Soc.*, **1964**, *86*, 2909-2914.
95. Changcheng, Z.; Liang, X.; Zili, Y.; Yi, J.; Rong, L.; Zhiheng, L.; Changmin, G.; Jinfang, Y.; Fulan, X. *CN111848365*, **2020**, A.
96. Hanuš, L. O.; Tchilibon, S.; Ponde, D. E.; Breuer, A.; Fride, E.; Mechoulam, R. *Org. Biomol. Chem.* **2005**, *3*, 1116-1123.
97. Kosak, T. M.; Conrad, H. A.; Korich, A. L.; Lord, R. L. *Eur. J. Org. Chem*., **2015**, *34*, 7460–7467.
98. Bomon, J.; Van Den Broeck, E.; Bal, M.; Liao, Y.; Sergeyev, S.; Van Speybroeck, V.; Maes, B. U. *Angew. Chem.*, **2020**, *132*, 3087-3092.
99. Chae, J. *Arch. Pharm. Res.*, **2008**, *31*, 305-309.

100. Feutrill, G. I.; Mirrington, R. N. *Tet. Lett.*, **1970**, *11*, 1327-1328.
101. Hu, L.; Pan, H.; Zhou, Y.; Hse, C. Y.; Liu, C.; Zhang, B.; Xu, B. *J. Wood Chem. Technol.*, **2014**, *34*, 122-134.
102. Salaün J. *In: de Meijere A. (eds) Small Ring Compounds in Organic Synthesis VI,* **2000**, *207*.
103. Wu, W.; Lin, Z.; Jiang, H. *Org. Biomol. Chem.*, **2018**, *16*, 7315-7329.
104. Smith, R. D.; Simmons, H. E. *Org. Synth.*, **2003**, *41*, 72-72.
105. Helquist, P. *Elsevier,* **1991**, *951-997*.
106. Turcott, J. G.; Núñez, M. D. R. G.; Flores-Estrada, D.; Oñate-Ocaña, L. F.; Zatarain-Barrón, Z. L.; Barrón, F.; Arrieta, O. *Supportive Care in Cancer*, **2018**, *26*, 3029-3038.
107. Bourne, C. *Bioorg. Med. Chem*., **2007**, *15*, 7850-7864.
108. Selwood, D.; Visintin, C.; Baker, D.; Pryce, G.; Okuyama M. *US2008/262011*, **2008**, A1, 19, 14.
109. Cheng, L. J.; Xie, J. H.; Wang, L. X.; Zhou, Q. L. *Adv. Synth. Catal.*, **2012**, *354*, 1105-1113.
110. Reetz, M. T.; Westermann, J.; Steinbach, R. *J. Chem. Soc., Chem. Commun.*, **1981**, *5*, 237-239.
111. Feng, B.; Yang, Y.; You, J. *Chem. Sci.*, **2020**, *11*, 6031-6035.
112. Pine, S. H.; Shen, G. S., Hoang, H. *Synthesis*, **1991**, *2*, 165-167.
113. Koch, S.; Löwe, H.; Kunz, H. *Synlett*, **2011**,*14*, 1978.
114. Payack, J. F.; Huffman, M. A.; Cai, D.; Hughes, D. L.; Collins, P. C.; Johnson, B. K.; Tuma, L. D. *Org. Process Res. Dev.,* **2004**, *8*, 256-259.
115. Armarego, W. L.; Chai, C. L. L. *Elsevier Inc.*, *ISBN: 978-1-85617-567-8*, **2009**.

Annex: Experimental Section and Characterization

Synthesis of the Cannabidiol Precursor

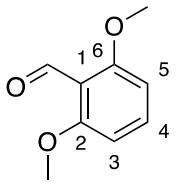

(79) 2,6-Dimethoxybenzaldehyde. In a flame dried round bottom flask was prepared a solution of 1,3-dimethoxybenzene (948 µL, 7.24 mmol, 1.0 equiv) and TMEDA (1.29 mL, 8.69 mmol, 1.20 equiv) in THF (29 mL). This solution was cooled down to -78 °C. *n*-Butyllithium (3.62 mL, 9.05 mmol, 1.25 equiv) was added over 5 minutes and the reaction mixture was stirred for 30 min at -78 °C. The solution was then allowed to warm up to 0 °C. After 1 hour, the solution of DMF (673 µL, 8.69 mmol 1.20 equiv) in THF (1.51mL) was added. The resulting mixture was stirred for an additional 30 min at 0 °C, and then allowed to warm to room temperature for another hour. The reaction was quenched with 5mL of each sat. NH_4Cl and DI water. The aqueous layers were extracted twice with EtOAc (25 mL), and the combined organic layers were washed with brine, dried over Na_2SO_4, and concentrated under vacuum. Flash chromatography (3:2 hexanes:EtOAc) afforded the desired compound as a powdery white solid with a 73% yield (0.884 g, 5.33 mmol). **R_f** = 0.31; **mp** = 95-97 °C. **FTIR** (cm^{-1}) (neat) 2955, 2845, 2797, 1671, 1578, 1459, 1437, 1418; **^{1}H NMR** (400 MHz, $CDCl_3$) δ 10.50 (s, 1H), 7.44 (t, *J* = 8.5 Hz, 1H), 6.57 (d, *J* = 8.3 Hz, 2H), 3.88 (s, 6H); **^{13}C NMR** (100 MHz, $CDCl_3$) δ 189.4, 162.2, 135.9, 114.4, 103.9, 56.1. HRMS (m/z): Calculated for $C_9H_{10}O_3$ (M+H) 167.07103, found (M+H) 167.07027. The data is in accordance with the literature.

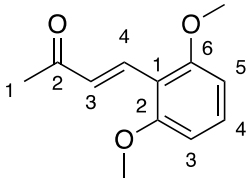

(80) (*E*)-4-(2,6-Dimethoxyphenyl)but-3-en-2-one. 2.5M NaOH (2.09mL, 2.54 mmol, 0.30 equiv) was added dropwise to a solution of **96** (2.90g, 17.5 mmol, 1.0 equiv) in 1:1 Acetone:H_2O mixture (10.3 mL each). The solution was stirred at room temperature for 14 h. The reaction was quenched with 5 mL EtOAc, which precipitated the product. The organic layer was extracted twice using

EtOAc (25 mL). The combined organic layers were washed with brine, dried over Na_2SO_4, and concentrated under vacuum. Flash chromatography over silica gel (4:1 hexanes:EtOAc) afforded the desired compound as a powdery white solid with an 84% yield (0.984 g, 4.76 mmol). $\mathbf{R_f}$ = 0.28; **mp** = 86-88 °C. **FTIR** (cm $^{-1}$) (neat) 2938, 2838, 2673,1575, 1470, 1428; **^{1}H NMR** (400 MHz, $CDCl_3$) δ 7.98 (d, *J* = 16.6 Hz, 1H), 7.28 (t, J = 8.4 Hz, 1H), 7.17 (d, *J* = 16.6 Hz, 1H), 6.57 (d, *J* = 8.4 Hz, 2H), 3.89 (s, 6H), 2.37 (s, 3H); **^{13}C NMR** (100 MHz, $CDCl_3$) δ 200.8, 160.8, 134.8, 131.5, 130.4, 112.4, 103.7, 55.8, 27.0. **HRMS** (m/z): Calculated for $C_{12}H_{14}O_3$ (M+H) 207.10239, found (M+H) 207.10157. The data is in accordance with the literature.

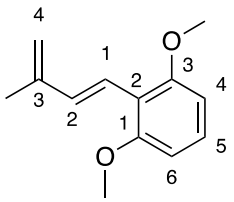

(81) (*E*)-1,3-Dimethoxy-2-(3-methylbuta-1,3-dien-1-yl)benzene. In a flame dried round bottom flask, *n*-butyllithium (2.33 mL, 5.82 mmol) was slowly added to a solution of methyltriphenylphosphonium bromide, 98% (1.91 g, 9.54 mmol) in THF (17.7 mL) and the solution was cooled down to 0 °C. After 30 min, the solution was allowed to warm up to room temperature, and a solution of **97** (0.984 g, 4.77 mmol) in THF (17.7 mL) was added to the reaction mixture. After 3 hours, the reaction was quenched with ice cold DI water. The organic layer was extracted twice with hexanes (15 mL). The combined organic layers were washed with brine, dried over Na_2SO_4, filtered, and concentrated under vacuum. The residue was rinsed with hexanes to precipitate the phosphine oxides that was removed by filtration before flash chromatography. Flash chromatography over silica gel (10% EtOAC in hexanes) afforded the desired compound as a waxy white solid with an 84% yield (0.984 g, 4.76 mmol). $\mathbf{R_f}$ = 0.47; **mp** = 40-42 °C; **FTIR** (cm $^{-1}$) (neat) 2940, 2836, 1581, 1470, 1432; **^{1}H NMR** (400 MHz, $CDCl_3$) δ 7.32 (d, *J* = 16.6 Hz,1H), 7.14 (t, *J* = 8.3 Hz, 1H), 6.85 (d, *J* = 16.6 Hz, 1H), 6.56 (d, *J* = 8.3 Hz 2H), 5.05 (d, *J* = 15.1 Hz, 2H), 3.86 (s, 6H), 2.00 (s, 3H): **^{13}C NMR** (100 MHz, $CDCl_3$) δ 158.5, 143.7, 135.6, 127.9, 119.8, 116.3, 114.9, 104.0, 55.8, 18.4. **HRMS** (m/z): Calculated for $C_{13}H_{16}O_3$ (M+H) 205.12223, found (M+H) 205.12231. The data is in accordance with the literature.

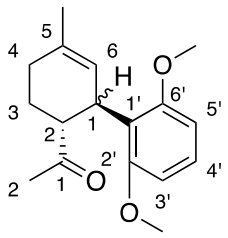

(82) 1-(2',6'-Dimethoxy-5-methyl-1,2,3,4-tetrahydro-[1,1'-biphenyl]-2-yl)ethan-1-one, (racemic mixture). In a flame dried round bottomed, a solution of **98** (675 mg, 3.30 mmol, 1.0 equiv) in EtOH (5.49 mL) was prepared, followed by the addition of 3-Buten-2-one, 99% (356 µL, 3.30 mmol, 1.0 equiv) and Hydroquinone (3.64 mg, 33.0 µmol, 0.01 equiv). The reaction was stirred at 80 °C for 16 h, at which time the reaction was cooled down, then poured onto saturated brine (5 mL) and extracted twice with Et_2O (15 mL). The combined organic layers were dried over Na_2SO_4, filtered, and concentrated under vacuum. Flash chromatography over silica gel (20% EtOAC in hexanes) afforded the desired compound as an oil with an 88% yield (841 mg, 2.89 mmol). $\mathbf{R_f}$ = 0.35; **FTIR** (cm $^{-1}$) (neat) 2926, 2835, 1706, 1590, 1471, 1435; **^{1}H NMR** (400 MHz, $CDCl_3$) δ 7.17-7.09 (m, 1H), 6.53-6.48 (m, 2H), 5.31-5.15 (m, 1H), 4.55-4.20 (m, 1H), 3.74 (d, *J* = 14.6 Hz, 6H), 3.33-2.90 (m, 1H), 2.32-2.22 (m, 1H), 2.19-2.11 (m, 1H), 2.04-1.98 (m, 1H), 1.87 (d, *J* = 12.12 Hz, 3H), 1.74-1.69 (m, 1H), 1.69 (d, *J* = 15.4 Hz, 3H); **^{13}C NMR** (100 MHz, $CDCl_3$) δ 211.0, 158.8,132.5, 131.3, 127.9, 127.7, 124.6, 122.6, 120.1, 118.4, 118.0, 104.7, 104.5, 104.2, 56.0, 55.9, 55.1, 51.4, 51.0, 34.8, 33.1, 32.1 30.8, 30.4, 29.6, 29.1, 28.6, 28.3, 26.6, 23.8, 23.3, 21.8. **HRMS** (m/z): Calculated for $C_{17}H_{22}O_3$ (M+H) 275.16404, found (M+H) 275.16417. The data is in accordance with the literature

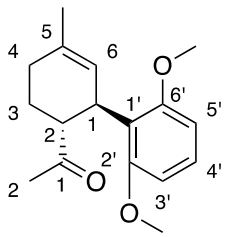

(83) 1-((1*R*,2*R*)-2',6'-Dimethoxy-5-methyl-1,2,3,4-tetrahydro-[1,1'-biphenyl]-2-yl)ethan-1-one. In a flame dried round bottomed flask, a solution of **99** (471 mg, 1.72 mmol, 1.0 equiv) and NaOMe (331 mg, 6.13 mmol, 3.6 equiv) in MeOH (3.07 mL) was prepared. The reaction mixture was stirred at 80 °C for 36 h. The reaction was quenched by addition of 1N HCl (10 mL), followed by Et_2O extraction (15 mL). The combined organic layers were washed with brine, dried over

Na_2SO_4, filtered, and concentrated under vacuum. Flash chromatography over silica gel (10% EtOAc in hexanes) afforded the desired compound as a white solid with an 84% yield (397 mg, 1.45 mmol). **R_f** = 0.46; **mp** = 42-44 °C. **FTIR** (cm^{-1}) (neat) 3004, 2962, 2920, 2854, 2834, 1699, 1590, 1472, 1461, 1430**; ^{1}H NMR** (400 MHz, $CDCl_3$) δ 7.12 (t, *J* = 8.2 Hz, 1H), 6.52 (d, *J* = 8.2 Hz, 2H), 5.15 (br s, 1H), 4.25-4.19 (m, 1H) 3.76 (s, 6H), 3.32-3.26 (m, 1H), 2.14-2.09 (m, 1H), 2.04-1.97 (m, 2H), 1.94-1.92 (m, 1H), 1.88 (s, 3H) 1.85-1.78 (m, 1H), 1.66 (m, 3H); **^{13}C NMR** (100 MHz, $CDCl_3$) δ 213.4, 158.8, 131.3, 127.7, 124.5, 120.1, 104.7, 55.9, 51.0, 34.8, 30.9, 29.6, 28.6 26.6, 23.3. **HRMS** (m/z): Calculated for $C_{17}H_{22}O_3$ (M+Na) 297.14510, found (M+Na) 297.14612.

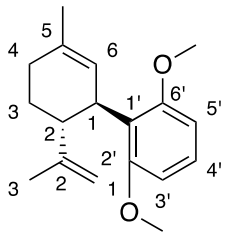

(84) (1*R*,2*R*)-2',6'-Dimethoxy-5-methyl-2-(prop-1-en-2-yl)-1,2,3,4-tetrahydro-1,1'-biphenyl. In a flame dried round bottomed flask, a solution of methyltriphenylphosphonium bromide, 98% (1.91 g, 5.36 mmol, 2.0 equiv) in THF (9.92 mL) was prepared, then cooled down to -78 °C before slowly adding *n*-butyllithium (2.14 mL, 5.36 mmol, 2.0 equiv). After 30 min, a solution of **100** (0.735 g, 2.68 mmol, 1.0 equiv) in THF (9.92 mL) was added. The reaction mixture was stirred while allowing the reaction to warm up to room temperature. After 7 h, the solution was poured onto ice cold DI water, extracted twice with hexanes (15 mL). The combined organic layers were washed with brine, dried over Na_2SO_4, filtered, and concentrated under vacuum. The resulting residue was rinsed with hexanes to precipitate the phosphine oxides that was then removed by filtration before flash chromatography. Flash chromatography over silica gel (5% EtOAC in Hexanes) afforded the desired compound as a waxy white solid with an 72% yield (0.25 g, 1.93 mmol). **R_f** = 0.63; **mp** = 49-51 °C. **FTIR** (cm^{-1}) (neat) 3008, 2958, 2918, 2854, 2834, 1629, 1591, 1471, 1434; **^{1}H NMR** (400 MHz, $CDCl_3$) δ 7.09 (t, *J* = 8.1 Hz, 1 H), 6.51 (d, *J* = 8.1 Hz, 2H), 5.21 (br s, 1H), 4.41 (d, *J* = 9.4 Hz), 4.06-4.02 (m, 1H), 3.74 (s, 6H), 2.94-2.88 (m, 1H), 2.22-2.16 (m, 1H), 2.00-1.97 (m, 1H), 1.79-1.73 (m, 2H), 1.67 (s, 3H), 1.60 (s, 3H); **^{13}C NMR** (100 MHz, $CDCl_3$) δ 149.4, 133.8, 133.6, 131.3, 128.7, 128.5, 128.5, 126.8, 125.6, 121.8, 109.7, 55.9, 45.2, 36.2,

30.8, 29.6, 23.4, 18.9. **HRMS** (m/z): Calculated for $C_{18}H_{24}O_2$ (M+H) 273.18527, found (M+H) 273.18491. The data is in accordance with the literature

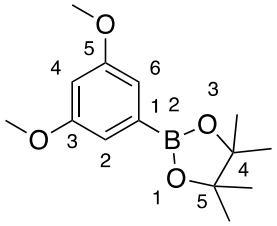

(98) 2-(3,5-Dimethoxyphenyl)-4,4,5,5-tetramethyl-1,3,2-dioxaborolane. In a glovebox under argon (after 2 purges), Bis(pinacolato)diboron (3.68 g, 14.5 mmol), Methoxyiridium(I) dimer (24.5 mg, 36.9 µmol), and dtbpy (19.4 mg, 72.4 µmol) were added to a vial. The flask was sealed with a microwave cap and removed from the glovebox before addition of 1,3-Dimethoxybenzene (948 µL, 7.24 mmol) in THF (5.33 mL). The vial was placed in an oil bath at 65 °C. After 16 h, the reaction was allowed to cool down before being poured into ice cold DI water and extracted twice with Benzene (25 mL). The combined organic layers were washed with NaOH, dried over Na_2SO_4, filtered, and concentrated under vacuum. Flash chromatography over silica gel (20% EtOAC in hexanes) afforded the desired compound as a white solid with an 87% yield (1.67 g, 6.33 mmol). $\mathbf{R_f}$ = 0.62; **mp** = 90-91 °C. **FTIR** (cm $^{-1}$) (neat) 2975, 1587, 1448, 1418; **^{1}H NMR** (400 MHz, $CDCl_3$) δ 6.94 (d, *J* = 2.4 Hz, 2H), 6.56 (t, *J* = 2.4 Hz, 1H), 3.80 (s, 6H), 1.33 (s, 12H); **^{13}C NMR** (100 MHz, $CDCl_3$) δ 160.4, 111.6, 104.5, 83.9, 55.4, 24.9; **^{11}B NMR** (128 MHz, $CDCl_3$) δ 30.5. **HRMS** (m/z): Calculated for $C_{14}H_{21}BO_4$ (M+H) 265.16, found (M+H) 265.16. The data is in accordance with the literature

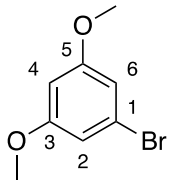

(60) 1-Bromo-3,5-dimethoxybenzene. In a flame dried round bottom flask a solution of **98** (75.0 mg, 284 µmol, 1.0 equiv) in CH_3OH (3.55 mL) was prepared. To this solution was added a solution of copper (II) bromide (190 mg, 852 µmol, 3.0 equiv) in H_2O (3.55 mL). The reaction mixture was stirred at 80 °C for 4 h. The solution was cooled down before being extracted twice with Et_2O (10 mL). The organic layers were combined, washed with H_2O (10mL) and brine (10mL), dried over Na_2SO_4, filtered, and concentrated under vacuum. The residue was purified using flash

chromatography over silica gel (15% EtOAC in hexanes) affording the desired compound as a white solid with an 29% yield (17.4 mg, 80.2 µmol). **R_f** = 0.61; **mp** = 63-65 °C °C. **FTIR** (cm $^{-1}$) (neat) 3079, 3004, 2929, 2838, 1708, 1575, 1470, 1453, 1426; **^{1}H NMR** (400 MHz, $CDCl_3$) δ 6.66 (d, *J* = 2.3 Hz, 2H), 6.37 (t, *J* = 2.3 Hz, 1H), 3.76 (s, 6H); **^{13}C NMR** (100 MHz, $CDCl_3$) δ 161.2, 109.9, 99.8, 55.5; **HRMS** (m/z): Calculated for $C_8H_9BrO_2$ (M+H) 216.98537, found (M+H) 216.98587. The data is in accordance with the literature

Weinreb Amide Approach

A. General procedure for the synthesis of a Weinreb amide: In a flame dried round bottom flask, a solution of 3,5-dimethoxybenzoic acid (300 mg, 1.65 mmol, 1.0 equiv) and DMF (25.5 µL, 329 µmol, 0.20 equiv) in toluene (5.50 mL) was prepared. The solution was cooled down to 0 °C before addition of thionyl chloride, 97% (148 µL, 1.98 mmol, 1.20 equiv). The resulting solution was stirred at 70 °C for 2 h. The solution was then cooled down to 0 °C before dilution with CH_2Cl_2 (5.50 mL). Then, Et_3N (505 µL, 3.62 mmol, 2.20 equiv) and the desired amine (1.10 equiv) were added to the reaction flask. The reaction mixture was allowed to warm up to room temperature and stirred for an additional 16 h. The reaction was then quenched by addition of sat. Na_2CO_3 until pH 10 was attained. The biphasic solution was diluted and extracted with CH_2Cl_2 (15 mL). The combined organic layers were washed with 1N HCl (10 mL) and brine (10 mL), dried over Na_2SO_4, filtered, and concentrated under vacuum. The residue was purified using flash chromatography over silica gel using 20% EtOAc, affording the desired product with a 63% yield (243 mg, 1.65 mmol).

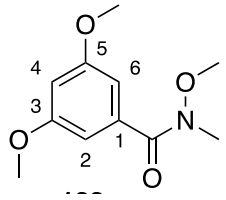

(104a) *N*-3,5-Trimethoxy-*N*-methylbenzamide. Prepared according to procedure A using 3,5-dimethoxybenzoic acid (300 mg, 1.65 mmol, 1.0 equiv) and N,O-dimethyl hydroxylamine hydrochloride, 98% (180 mg, 1.81 mmol, 1.10 equiv). Yield: 63% (234 mg) as a pale-yellow oil. **R_f** = 0.12. **FTIR** (cm $^{-1}$) (neat) 2937, 2839, 1646, 1588, 1455, 1424; **^{1}H NMR** (400 MHz, $CDCl_3$)

δ 6.78 (d, *J* = 2.2 Hz, 1H**)**, 6.53 (t, *J* = 2.3 Hz, 2H), 3.80 (s, 6H), 3.59 (s, 3H), 3.33 (s, 3H); **^{13}C NMR** (100 MHz, $CDCl_3$) δ 169.6, 160.4, 136.0, 106.0, 102.8, 61.2, 55.5, 34.0. **HRMS** (m/z): Calculated for $C_{11}H_{15}NO_4$ (M+H) 226.10824, found (M+H) 226.10738. The data is in accordance with the literature.

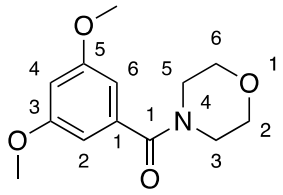

(104b) (3,5-Dimethoxyphenyl)(morpholino)methanone.. Prepared according to procedure A using 3,5-dimethoxybenzoic acid (3.0 g, 16.5 mmol, 1.0 equiv) and morpholine (1.58 mL, 18.1 mmol, 1.10 equiv), flash chromatography over silica gel with 1:1 EtOAc:hexanes. Yield: 96% (4.16 g) as a colorless solid. **R_f** = 0.15, **mp** = 70-72 °C. **FTIR** (cm $^{-1}$) (neat) 2970, 2843, 1626, 1590, 1449, 1420; **^{1}H NMR** (400 MHz, $CDCl_3$) δ 6.51 (d, *J* = 2.3 Hz, 1H**)**, 6.49 (t, *J* = 2.2 Hz), 3.80 (s, 6H), 3.77-3.45 (m, 8H); **^{13}C NMR** (100 MHz, $CDCl_3$) δ 170.1, 160.9, 137.2, 104.9, 101.7, 66.9, 55.5, 48.3, 44.7; **HRMS** (m/z): Calculated for $C_{13}H_{17}NO_4$ (M+H) 252.12427, found (M+H) 252.12303. The data is in accordance with the literature.

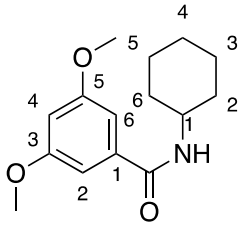

(104c) *N*-Cyclohexyl-3,5-dimethoxybenzamide Prepared according to procedure A using 3,5-dimethoxybenzoic acid (2.0 g, 11.0 mmol, 1.0 equiv) and cyclohexylamine (1.20 mL, 12.1 mmol, 1.10 equiv). Flash chromatography over silica gel with 30% EtOAc in hexanes. Yield: 76% (2.20 g) as a white solid. **R_f** = 0.25; **mp** = 129-131 °C. **FTIR** (cm $^{-1}$) (neat) 3280, 2934, 2852, 1631,1589, 1533, 1454, 1421;**^{1}H NMR** (400 MHz, $CDCl_3$) δ 6.85 (d, *J* = 2.3 Hz, 1H), 6.54 (t, , *J* = 2.2 Hz, 2H), 5.96 (br s, 1H), 3.97-3.86 (m, 1H), 3.80 (s, 6H), 2.01-1.98 (m, 2H), 1.76-1.71 (m, 2H), 1.65-1.62 (m, 1H), 1.47-1.36 (m, 2H), 1.26-1.16 (m, 3H); **^{13}C NMR** (100 MHz, $CDCl_3$) δ 166.4, 160.8, 137.4, 104.8, 103.2, 55.8, 48.7, 33.2, 25.6, 24.8. **HRMS** (m/z): Calculated for $C_{15}H_{21}NO_3$ (M+H) 264.15962, found (M+H) 264.15942. The data is in accordance with the literature.

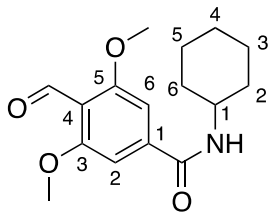

(119a) *N*-Cyclohexyl-4-formyl-3,5-dimethoxybenzamide. In a flame dried round bottom flask a solution of **104c** (100 mg, 380 µmol, 1.0 equiv) and TMEDA (67.8 µmL, 456 µmol, 1.20 equiv) in THF (1.52 mL) was prepared and cooled down to -78 °C. *n*-Butyllithium (413 µL, 949 µmol, 2.50 equiv) was added over 5 minutes and the reaction mixture was stirred for 30 min at -78 °C. The solution was then allowed to warm up to 0 °C. After 1 hour, the solution of DMF (35.3 µmL, 456 µmol 1.20 equiv) in THF (1.51mL) was added. The resulting mixture was stirred for an additional 30 min at 0 °C, and then allowed to warm to room temperature for another hour. The reaction was quenched with 5mL of each sat. NH_4Cl and DI water. The aqueous layers were extracted twice with EtOAc (10 mL), and the combined organic layers were washed with brine (10 mL), dried over Na_2SO_4, and concentrated under vacuum. Flash chromatography (3:2 hexanes:EtOAc) afforded the desired compound as a powdery white solid with a 19% yield (21 mg, 72 µmol). $\mathbf{R_f}$ = 0.09; **mp** = 169-171 °C. **FTIR** (cm $^{-1}$) (neat) 3275, 2934, 2853, 1689, 1629, 1567, 1532, 1454; **^{1}H NMR** (400 MHz, $CDCl_3$) δ 10.48 (s, 1H), 6.87 (s, 2H), 5.96 (br s, 1H), 3.99-3.91 (m, 1H), 3.94 (s, 6H), 2.09-2.04 (m, 2H), 1.80-1.75 (m, 2H), 1.70-1.65 (m, 1H), 1.48-1.38 (m, 2H), 1.31-1.18 (m, 3H); **^{13}C NMR** (100 MHz, $CDCl_3$) δ 189.1, 165.8, 162.1, 137.0, 115.8, 102.5, 56.4, 49.2, 33.2, 25.5, 24.9. **HRMS** (m/z): Calculated for $C_{16}H_{21}NO_4$ (M+H) 292.15502, found (M+H) 292.15433.

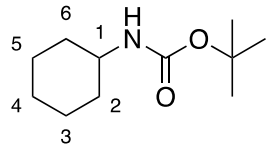

(121) *tert*-Butyl cyclohexylcarbamate. In a round bottom flask, a solution of cyclohexylamine (2 mL, 17.4 mmol, 1.0 equiv) and Et_3N (7.29 mL, 52.3 mmol, 3.0 equiv) in a 2:1 water: THF (104 mL, 52 mL) mixture was prepared. This solution was allowed to stir at room temperature for 5 min. The reaction solution was then cooled down to 0 °C before addition of Boc_2O (5.71 g, 26.2 mmol, 1.50 equiv). The reaction was stirred at 0 °C for 2 h, then allowed to warm up to room temperature and stirred for an additional 4 h. THF was then removed from the reaction flask under vacuum.

The resulting aqueous solution was extracted twice with CH_2Cl_2 (15 mL). The combined organic layers were washed with water (25 mL) and brine (25 mL), dried over Na_2SO_4, filtered, and concentrated under vacuum. The resulting product was recrystallized from hexanes affording the desired product with a 99% yield (3.44 g, 17.2 mmol) as a colorless solid. $\mathbf{R_f}$ = 0.45 (15% EtOAc in hexanes); **mp** = 79-81 °C. **FTIR** (cm^{-1}) (neat) 3329, 2981, 2930, 2853, 1809, 1677, 1519, 1450; **^{1}H NMR** (400 MHz, $CDCl_3$) δ 4.40 (br s, 1H), 3.40 (br s, 1H), 1.93-1.89 (m, 2H), 1.71-1.66 (m, 2H), 1.59-1.54 (m, 2H), 1.43 (1, 9H), 1.37-1.26 (m, 2H), 1.18-1.03 (m, 2H); **^{13}C NMR** (100 MHz, $CDCl_3$) δ 153.7, 78.9, 49.6, 33.6, 28.5, 25.6, 24.9; **HRMS** (m/z): Calculated for $C_{11}H_{21}NO_2$ (M+Na) 222.14681, found (M+Na) 222.14645. The data is in accordance with the literature.

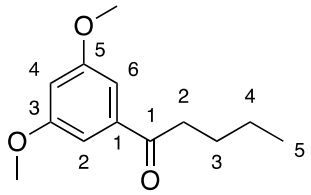

(123a) 1-(3,5-Dimethoxyphenyl)pentan-1-one.

Using (3,5-Dimethoxyphenyl)(morpholino)methanone 104b: In a flame dried round bottom flask, a solution of **122b** (5.39 g, 21.5 mmol, 1.0 equiv) in dry THF (28.0 mL) was prepared. The solution was cooled down to 0 °C before addition of *n*-butyllithium (18.7 mL, 42.9 mmol, 2.0 equiv). The solution was stirred at 0 °C for 2 h, before it was quenched by addition of a solution of H_2O:acetone (1:2, 23mL:45 mL). The reaction solution was stirred for an additional 10 min at room temperature before being extracted twice with H_2O (25 mL). The organic layers were combined, washed with brine (20 mL), dried over Na_2SO_4, filtered, and concentrated under vacuum. The resulting residue was purified using flash chromatography over silica gel using 20% EtOAc in hexanes, affording the desired product with a 79% yield (3.78 g, 21.5 mmol) as a white solid.

Using *N*-Cyclohexyl-3,5-dimethoxybenzamide 104c: In a flame dried round bottom flask a solution of **122c** (100 mg, 380 µmol, 1.0 equiv) in CH_2Cl_2 (8.45 mL) was prepared, followed by addition of 2-fluoropyridine (36 µL, 418 µmol, 1.10 equiv). The solution was cooled down to -78 °C and stirred for 5 min. Then, trifluormethanesulfonic anhydride (63.9 µL, 380 µmol, 1.0 equiv) was added dropwise and the solution was stirred at -78 °C for an additional 10 min. The reaction mixture was then allowed to warm up to 0 °C and stirred at 0°C for 10 min. The solution was cooled down to -78 °C before addition of butylmagnesium bromide (330 µL, 759 µmol, 2.0 equiv). The resulting solution was stirred for 25 min at -78 °C. The reaction was quenched by addition of

HCl (0.5M, 3 mL) and THF (3 mL). The biphasic mixture was stirred at 65 °C for 2 h. The organic layers were combined, dried over Na_2SO_4, filtered, and concentrated under vacuum. The resulting residue was purified using flash chromatography over silica gel using 20% EtOAc in hexanes, affording the desired product with 63% yield (53.2 mg, 440 µmol) as a white solid.

B. General procedure for the formation of ketones using 104a and Grignard reagent: In a flame dried round bottom flask, the appropriate Grignard reagent (1.7 M, 3.0 equiv) was added. The solution was cooled down to 0 °C before addition of a solution of **104a** (100 mg, 444 µmol, 1.0 equiv) in THF (673 µL). The resulting mixture was stirred at 0 °C for 30 min. The reaction solution was quenched by addition of sat. NH_4Cl (10 mL). The solution was then diluted with H_2O (5 mL) before being extracted twice with EtOAc (10 mL). The combined organic layers were washed with brine (10 mL), dried over Na_2SO_4, filtered, and concentrated under vacuum. The resulting residue was purified using flash chromatography over silica gel using 10% EtOAc in hexanes.

R_f = 0.38; **mp** = 38-40 °C. **FTIR** (cm $^{-1}$) (neat) 2961, 2938, 2870, 2840, 1681, 1586, 1454, 1426; **^{1}H NMR** (400 MHz, $CDCl_3$) δ 7.09 (d, *J* = 2.3 Hz, 2H**)**, 6.64 (t, *J* = 2.2 Hz, 1H), 3.84 (s, 6H), 2.92 (t, *J* = 7.3 Hz, 2H), 1.73-1.69 (m, 2H), 1.43-1.37 (m, 2H), 0.95 (t, *J* = 7.3 Hz, 3H); **^{13}C NMR** (100 MHz, $CDCl_3$) δ 200.3, 160.9, 139.1, 105.9, 105.1, 55.6, 38.5, 26.6, 22.5, 13.9. **HRMS** (m/z): Calculated for $C_{13}H_{18}O_3$ (M+H) 223.13379, found (M+H) 223.13287. The data is in accordance with the literature.

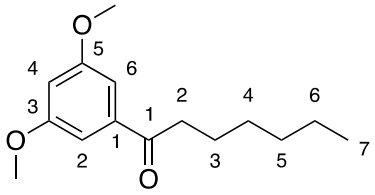

(123b) 1-(3,5-Dimethoxyphenyl)heptan-1-one. Prepared according to procedure B using the Grignard reagent hexylmagnesium bromide (1.7 M, 3.0 equiv). The desired compound was obtained with a 70% yield (77.5 mg, 310 µmol) as an oil. **R_f** = 0.38 (10% EtOAc in hexanes). **FTIR** (cm $^{-1}$) (neat) 2930, 2859, 1684, 1591, 1456, 1425. **^{1}H NMR** (400 MHz, $CDCl_3$) δ 7.09 (d, *J* = 2.3 Hz, 2H), 6.64 (t, *J* = 2.3 Hz, 1H), 3.84 (s, 6H), 2.91 (t, *J* = 7.3 Hz, 2H), 1.73-1.70 (m, 2H), 1.39-1.29 (m, 6H), 0.89 (t, *J* = 7.0 Hz, 3H); **^{13}C NMR** (100 MHz, $CDCl_3$) δ 200.3, 160.9, 139.1, 105.9, 105.1, 55.6, 38.8, 31.7, 29.0, 24.5, 22.5, 14.1; **HRMS** (m/z): Calculated for $C_{15}H_{22}NO_3$ (M+H) 251.16442, found (M+H) 251.16417. The data is in accordance with the literature.

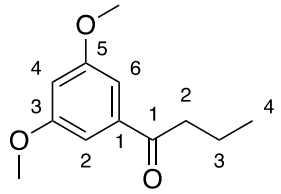

(123c) 1-(3,5-Dimethoxyphenyl)butan-1-one. Prepared according to procedure B using the Grignard reagent propylmagnesium bromide (1.7 M, 3.0 equiv). The desired compound was obtained with a 62% yield (57.3 mg, 275 μmol) as an oil. $\mathbf{R_f}$ = 0.52 (15% EtOAc in hexanes). **FTIR** (cm $^{-1}$) (neat) 2961, 2839, 1683, 1591, 1456, 1425. **^{1}H NMR** (400 MHz, $CDCl_3$) d 7.09 (d, *J* = 2.3 Hz, 2H), 6.64 (t, *J* = 2.2 Hz, 1H), 3.83 (s, 6H), 2.90 (t, *J* = 7.3 Hz, 2H), 1.78-1.73 (m, 2H), 0.99 (t, *J* = 7.3 Hz, 3H); **^{13}C NMR** (100 MHz, $CDCl_3$) d 200.1, 160.9, 139.1, 105.9, 105.1, 55.6, 40.6, 17.9, 13.9; **HRMS** (m/z): Calculated for $C_{12}H_{16}O_3$ (M+H) 209.11722, found (M+H) 209.11722. The data is in accordance with the literature.

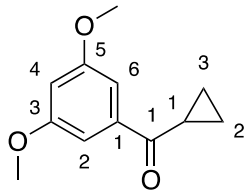

(123d) Cyclopropyl(3,5-dimethoxyphenyl)methanone. Prepared according to procedure B using the Grignard reagent cyclopropylmagnesium bromide (1.7 M, 3.0 equiv). The desired compound was obtained with a 78% yield (71.8 mg, 348 μmol) as an oil. $\mathbf{R_f}$ = 0.61 (30% EtOAc in hexanes). **FTIR** (cm $^{-1}$) (neat) 3006, 2939, 2839, 1668, 1589, 1455, 1425. **^{1}H NMR** (400 MHz, $CDCl_3$) δ 7.15 (d, *J* = 2.3 Hz, 2H), 6.65 (t, *J* = 2.3 Hz, 1H), 3.84 (s, 6H), 2.65-2.58 (m, 1H), 1.25-1.21 (m, 2H), 1.06-1.01 (m, 2H); **^{13}C NMR** (100 MHz, $CDCl_3$) δ 200.3, 160.8, 140.0, 105.9, 105.0, 55.6, 17.3, 11.8; **HRMS** (m/z): Calculated for $C_{12}H_{14}O_3$ (M+H) 207.10129, found (M+H) 207.10157.

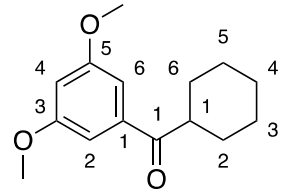

(123e) Cyclohexyl(3,5-dimethoxyphenyl)methanone Prepared according to procedure B using the Grignard reagent cyclohexylmagnesium bromide(1.7 M, 3.0 equiv). The desired compound was obtained with a 24% yield (26.9 mg, 108 μmol) as an oil. $\mathbf{R_f}$ = 0.56 (30% EtOAc in hexanes). **FTIR** (cm $^{-1}$) (neat) 2929, 2853, 1679, 1589, 1452, 1424. **^{1}H NMR** (400 MHz, $CDCl_3$) δ 7.07 (d,

J = 2.3 Hz, 2H), 6.63 (t, J = 2.3 Hz, 1H), 3.83 (s, 6H), 3.21-3.14 (t, J = 11.2 Hz, 1H), 1.89-1.80 (m, 4H), 1.74-1.71 (m, 1H), 1.55-1.355 (m, 5H); **^{13}C NMR** (100 MHz, $CDCl_3$) δ 203.6, 160.9, 138.4, 106.2, 104.7, 55.6, 45.8, 29.5, 25.9, 25.8; **HRMS** (m/z): Calculated for $C_{15}H_{20}O_3$ (M+H) 249.14894, found (M+H) 249.14852. The data is in accordance with the literature.

C. General procedure for the Wolff-Kishner reduction of ketones: In a flame dried round bottom flask, a solution of the desired ketone (1.0 equiv) and KOH (3.65 equiv) in Diethylene glycol (8.10 mL) was prepared. Then, Hydrazine monohydrate, 98% (6.20 equiv) was added to the solution. The flask was equipped with a distillation apparatus and stirred at 100 °C for 1 h. The reaction mixture was then slowly heated to 170 °C and stirred for an additional 4.5 h, removing the water from the reaction. The solution was then allowed to cool down to room temperature before washing the solution with H_2O (25 mL) followed by EtOAc extraction (25 mL). The organic layers were combined, washed with brine (25 mL), dried over Na_2SO_4, filtered, and concentrated under vacuum. The resulting residue was purified using flash chromatography over silica gel using 10% EtOAc in Hexanes.

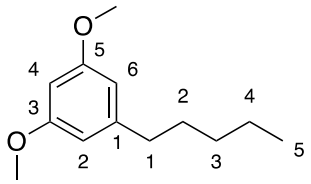

(125a) 1,3-Dimethoxy-5-pentylbenzene. Prepared according to procedure C using **129a** (3.78g, 17.0 mmol, 1.0 equiv). Yield: 75% yield (2.67 g, 17.0 mmol) as a clear oil. **R_f** = 0.55. **FTIR** (cm $^{-1}$) (neat) 2929, 1593, 1459, 1427; **^{1}H NMR** (400 MHz, $CDCl_3$) δ 6.34 (d, J = 2.3 Hz, 2H), 6.30 (t, J = 2.3 Hz, 1H), 3.78 (s, 6H), 2.54 (t, J = 7.3 Hz, 2H), 1.63-1.59 (m, 2H), 1.34-1.31 (m, 4H), 0.89 (t, J = 6.9 Hz, 3H); **^{13}C NMR** (100 MHz, $CDCl_3$) δ 160.7, 145.4, 106.5, 97.5, 55.2, 36.3, 31.5, 31.0, 22.6, 14.0. **HRMS** (m/z): Calculated for $C_{13}H_{20}O_2$ (M+H) 209.15441, found (M+H) 209.15361. The data is in accordance with the literature.

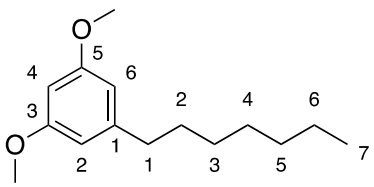

(125b) 1-Heptyl-3,5-dimethoxybenzene. Prepared according to procedure B using **129b** (35.0 mg, 140 µmol, 1.0 equiv). Yield: 32% (10.6 mg, 45µmol) as a clear oil. $\mathbf{R_f}$ = 0.72 (5% EtOAc in hexanes). **FTIR** (cm $^{-1}$) (neat) 2925, 2854, 1594, 1459, 1427; **^{1}H NMR** (400 MHz, $CDCl_3$) δ 6.34 (d, *J* = 2.2 Hz, 2H), 6.29 (t, *J* = 2.2 Hz,1H), 3.78 (s, 6H), 2.54 (t, *J* = 7.8 Hz, 2H), 1.62-1.58 (m, 2H), 1.33-1.26 (m, 6H), 0.88 (t, *J* = 6.7 Hz, 3H); **^{13}C NMR** (100 MHz, $CDCl_3$) δ 160.7, 145.4, 106.5, 97.6, 55.2, 36.3, 31.8, 31.3, 29.3, 29.2, 22.7, 14.1. **HRMS** (m/z): Calculated for $C_{15}H_{24}O_2$ (M+H) 237.18534, found (M+H) 237.18491. The data is in accordance with the literature.

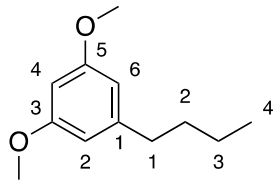

(125c) 1-Butyl-3,5-dimethoxybenzene. Prepared according to the Wolff-Kishner reaction procedure using **129c** (15 mg, 72 µmol, 1.0 equiv). Yield: 20% (2.8 mg, 14 µmol,) as a clear oil. $\mathbf{R_f}$ = 0.63 (10% EtOAc in hexanes). **FTIR** (cm $^{-1}$) (neat) 2925, 2854, 1594, 1459, 1427; **^{1}H NMR** (400 MHz, $CDCl_3$) δ 6.34 (d, *J* = 2.2 Hz,2H), 6.29 (t, *J* = 2.1 Hz,1H), 3.78 (s, 6H), 2.55 (t, *J* = 7.7 Hz, 2H), 1.61-1.55 (m, 2H), 1.38-1.30 (m, 2H), 0.92 (t, *J* = 6.7 Hz, 3H); **^{13}C NMR** (100 MHz, $CDCl_3$) δ 160.7, 145.4, 106.5, 97.6, 55.2, 36.0, 33.4, 22.7, 14.1. **HRMS** (m/z): Calculated for $C_{12}H_{18}O_2$ (M+H) 195.13795, found (M+H) 195.13796. The data is in accordance with the literature.

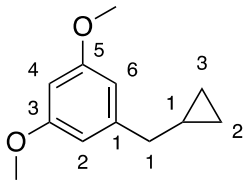

(125d) 1-(Cyclopropylmethyl)-3,5-dimethoxybenzene. Prepared according to the Wolff-Kishner reaction procedure using **129d** (20.0 mg, 97 µmol, 1.0 equiv). Yield: 18 % (3.4 mg, 18 µmol) as a clear oil. $\mathbf{R_f}$ = 0.56 (10% EtOAc in hexanes). **FTIR** (cm $^{-1}$) (neat) 3076, 3001, 2927, 2855, 1712, 1504, 1457, 1429; **^{1}H NMR** (400 MHz, $CDCl_3$) δ 6.44 (d, *J* = 2.3 Hz,2H), 6.32 (t, *J* = 2.2 Hz,1H), 3.79 (s, 6H), 2.49 (d, *J* = 6.9 Hz, 2H), 1.02-0.94 (m, 1H), 0.55-0.51 (m, 2H), 0.22-0.18 (m, 2H); **^{13}C NMR** (100 MHz, $CDCl_3$) δ 160.7, 144.7, 106.5, 97.7, 55.3, 40.6, 11.6, 4.7. **HRMS** (m/z): Calculated for $C_{12}H_{16}O_2$ (M+H) 193.12175, found (M+H) 193.12231.

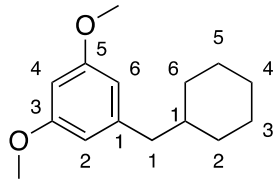

(125e) 1-(Cyclohexylmethyl)-3,5-dimethoxybenzene. Prepared according to the Wolff-Kishner reaction procedure using **129e** (20.0 mg, 81 μmol, 1.0 equiv). Yield: 39% (7.3 mg, 31 μmol) as a clear oil. $\mathbf{R_f}$ = 0.56 (10% EtOAc in hexanes). **FTIR** (cm $^{-1}$) (neat) 2960, 2922, 2851, 1595, 1469, 1427; **^{1}H NMR** (400 MHz, $CDCl_3$) δ 6.30 (s, 3H**)**, 3.77 (s, 6H), 2.41 (d, *J* = 7.1 Hz, 2H), 1.70-1.65 (m, 5H), 1.54-1.46 (m, 1H), 1.22-1.15 (m, 3H), 0.97-0.88 (m, 2H); **^{13}C NMR** (100 MHz, $CDCl_3$) δ 160.5, 143.8, 107.3, 97.5, 55.2, 44.5, 39.6, 33.2, 26.6, 26.3. **HRMS** (m/z): Calculated for $C_{15}H_{22}O_2$ (M+H) 235.16895, found (M+H) 235.16926. The data is in accordance with the literature.

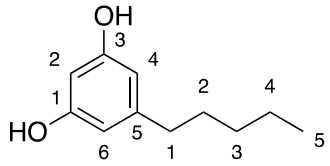

(56) 5-Pentylbenzene-1,3-diol (Olivetol). In a flame dried round bottom flask, prepare a solution of boron tribromide (183 μL, 1.06 mmol, 2.20 equiv) in CH_2Cl_2 (2.68 mL). The solution was cooled down to -15 °C before a solution of **131a** (100 mg, 480 μmol, 1.0 equiv) in CH_2Cl_2 (100 μL) was added to the reaction flask. The reaction solution was then stirred and allowed to warm up to room temp. After 1.5 h, the reaction was quenched by addition of sat. $NaHCO_3$ and extracted twice with CH_2Cl_2 (10 mL). The organic layers were combined, dried over Na_2SO_4, filtered, and concentrated under vacuum. The resulting residue was purified using flash chromatography over silica gel using 1:2 EtOAc:hexanes, affording the desired product with a 71% yield (61.8 g, 480 μmol) as white solid. $\mathbf{R_f}$ = 0.44; **mp** = 46-48 °C. **FTIR** (cm $^{-1}$) (neat) 3307, 2928, 2857, 1595, 1466; **^{1}H NMR** (400 MHz, $CDCl_3$) δ 6.24 (d, *J* = 2.2 Hz, 2H**)**, 6.17 (t, *J* = 2.2 Hz, 1H), 4.65 (br s, 2H), 2.48 (t, *J* = 7.8 Hz, 2H), 1.61-1.53 (m, 2H), 1.36-1.27 (m, 4H), 0.88 (t, *J* = 6.7 Hz, 3H); **^{13}C NMR** (100 MHz, $CDCl_3$) δ 156.5, 146.3, 108.2, 100.2, 35.8, 31.5, 30.7, 22.5, 14.0. **HRMS** (m/z): Calculated for $C_{11}H_{16}O_2$ (M+H) 181.12208, found (M+H) 181.12231. The data is in accordance with the literature.

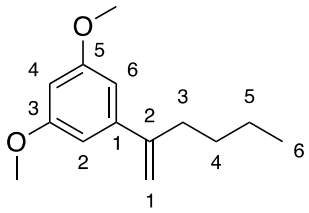

(134) 1-(Hex-1-en-2-yl)-3,5-dimethoxybenzene. Prepared according to the procedure of the first Wittig reaction using **129a** (390 mg, 1.75 mmol, 1.0 equiv). Yield: 82% (318 mg, 1.44 mmol) as a clear oil. $\mathbf{R_f}$ = 0.28 (10% EtOAc in hexanes). **FTIR** (cm $^{-1}$) (neat) 2931, 2871, 1588, 1454, 1420; **^{1}H NMR** (400 MHz, $CDCl_3$) δ 6.55 (d, *J* = 2.3 Hz, 2H**)**, 6.39 (t, *J* = 2.2 Hz, 1H), 5.25 (d, *J* = 1.5 Hz, 1H), 5.04-5.03 (m, 1H), 3.80 (s, 6H), 2.45 (t, *J* = 7.2 Hz, 2H), 1.45-1.39 (m, 2H), 1.36-1.31 (m, 2H), 0.89 (t, *J* = 7.2 Hz, 3H); **^{13}C NMR** (100 MHz, $CDCl_3$) δ 160.6, 148.9, 143.9, 112.3, 104.6, 99.1, 55.3, 35.2, 30.5, 22.4, 13.9. **HRMS** (m/z): Calculated for $C_{14}H_{20}O_2$ (M+H) 221.15447 found (M+H) 221.15361.

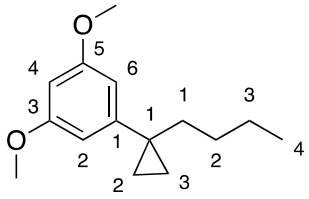

(135) 1-(1-Butylcyclopropyl)-3,5-dimethoxybenzene. In the glovebox, zinc copper couple (29.3 mg, 227 µmol, 0.50 equiv) was added to a vial. The vial was then removed from the glovebox and placed under argon. Et_2O (175 µL) was added to the flask, followed by iodine (1.15 mg, 4.54 µmol, 0.01 equiv). This solution was stirred at room temp until the brown color disappeared. A solution of **142** (100 mg, 454 µmol, 1.0 equiv) and diiodomethane, 99% (40.7 µL, 499 µmol, 1.10 equiv) was then added to the reaction flask. The reaction flask was stirred at 35 °C for 45 min. The reaction mixture was then taken out of the oil bath and left to stir at room temperature for 30 min. The reaction flask was then put back in an oil bath at 35 °C for 15 h. The solution was then washed with Et_2O. The organic layers were combined and washed with sat. NH_4Cl (10 mL), sat. $NaHCO_3$ (10 mL), and water (10 mL). The combined organic layers were then dried over Na_2SO_4, filtered, and concentrated under vacuum. – not isolated- $\mathbf{R_f}$ = 0.57. (10% EtOAc in hexanes) **FTIR** (cm $^{-1}$) (neat) 2930, 2859, 1454, 1420. **^{1}H NMR** (400 MHz, $CDCl_3$) δ 6.45 (d, *J* = 2.3 Hz, 2H**)**, 6.29 (t, *J* = 2.2 Hz, 1H), 3.78 (s, 6H), 2.45 (t, *J* = 7.2 Hz, 2H), 1.47-1.39 (m, 2H), 1.36-1.31 (m, 2H), 0.89 (t, *J* = 7.2 Hz, 3H), 0.77-0.74 (m, 2H), 0.63-0.60 (m, 2H) ; **^{13}C NMR** (100 MHz $CDCl_3$) δ 160.4,

148.9, 107.1, 99.1, 55.3, 35.3, 30.5, 22.4, 13.9, 13.3. **HRMS** (m/z): Calculated for $C_{15}H_{22}O_2$ (M+H) 235.16902 found (M+H) 235.16926.

Synthesis of Cannabidiol Dimethyl Ether

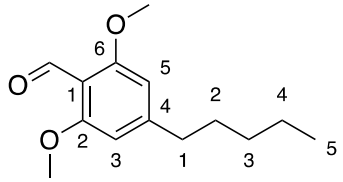

(146) 2,6-Dimethoxy-4-pentylbenzaldehyde. Prepared according to formylation reaction procedure previously described using 1,3-dimethoxy-5-pentylbenzene (300 mg, 1.44 mmol, 1.0 equiv). Yield: 78% (265 mg, 1.12 mmol) as a clear oil. $\mathbf{R_f}$ = 0.42 (30% EtOAc in hexanes). **FTIR** (cm $^{-1}$) (neat) 2930, 2856, 1682, 1604, 1568, 1457, 1406; **^{1}H NMR** (400 MHz, $CDCl_3$) δ 10.45 (s, 1H), 6.38 (s, 2H), 3.88 (s, 6H), 2.60 (t, *J* = 7.6 Hz, 2H), 1.65-1.63 (m, 2H), 1.36-1.33 (m, 4H), 0.91 (t, *J* = 6.7 Hz, 3H); **^{13}C NMR** (100 MHz, $CDCl_3$) δ 189.0, 162.3, 152.6, 112.3, 104.0, 56.0, 37.2, 31.5, 30.6, 22.5, 14.0. **HRMS** (m/z): Calculated for $C_{14}H_{20}O_3$ (M+H) 237.24880, found (M+H) 237.24887. The data is in accordance with the literature.

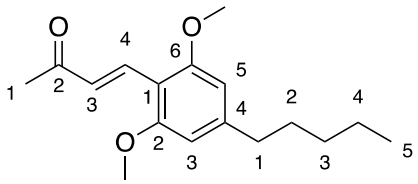

(*E*)-5-(2,6-Dimethoxy-4-pentylphenyl)pent-4-en-2-one. Prepared according to aldol condensation reaction procedure previously described using **157** (403 mg, 1.71 mmol, 1.0 equiv), the reaction was stirred at 60 °C for 8 h. Yield: 75% (352 mg, 1.28 mmol) as a light-yellow oil. $\mathbf{R_f}$ = 0.54 (30% EtOAc in hexanes). **FTIR** (cm $^{-1}$) (neat) 2929, 2856, 1682, 1658, 1604, 1564, 1457, 1418; **^{1}H NMR** (400 MHz, $CDCl_3$) δ 7.96 (d, *J* = 16.6 Hz), d 7.12 (d, *J* = 16.7 Hz, 1 H), 6.38 (s, 2H), 3.87 (s, 6H), 2.58 (t, *J* = 7.7 Hz, 2H), 2.35 (s, 3H), 1.63-1.61 (m, 2H), 1.35-1.32 (m, 4H), 0.90 (t, *J* = 6.7 Hz, 3H); **^{13}C NMR** (100 MHz, $CDCl_3$) δ 200.6, 160.0, 147.7, 135.1, 129.4, 109.8, 104.0, 55.7, 36.9, 31.6, 30.9, 26.9, 22.5, 14.0. **HRMS** (m/z): Calculated for $C_{17}H_{24}O_3$ (M+H) 277.18030, found (M+H) 277.17982. The data is in accordance with the literature.

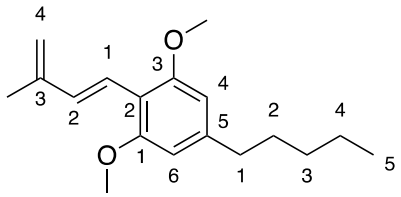

(44) (*E*)-1,3-Dimethoxy-2-(4-methylpenta-1,4-dien-1-yl)-5-pentylbenzene. Prepared according to the first Wittig reaction procedure previously described using **158** (352 mg, 1.27 mmol, 1.0 equiv), the reaction stirred at -78 °C for 30 min, then 60 °C for 8 h. Yield: 56% (196 mg, 713 µmol) as a light-yellow oil. $\mathbf{R_f}$ = 0.78 (10% EtOAc in hexanes). **FTIR** (cm^{-1}) (neat) 2929, 2856, 1600, 1568,1454, 1417; **^{1}H NMR** (400 MHz, $CDCl_3$) δ 7.28 (d, *J* = 16.2 Hz, 1 H), 6.83 (d, *J* = 16.5 Hz, 1 H), 6.39 (s, 2H), 5.02 (d, *J* = 17.6 Hz, 2H), 3.86 (s, 6H), 2.57 (t, *J* = 7.7 Hz, 2H), 1.99 (s, 3H), 1.65-1.61 (m, 2H), 1.36-1.33 (m, 4H), 0.90 (t, *J* = 7.0 Hz, 3H); **^{13}C NMR** (100 MHz, $CDCl_3$) δ 158.3, 143.9, 143.4, 134.6, 120.0, 115.7, 112.4, 104.2, 55.7, 36.7, 31.6, 31.0, 22.6,18.4, 14.1. **HRMS** (m/z): Calculated for $C_{18}H_{26}O_2$ (M+H) 275.20153, found (M+H) 275.20056. The data is in accordance with the literature.

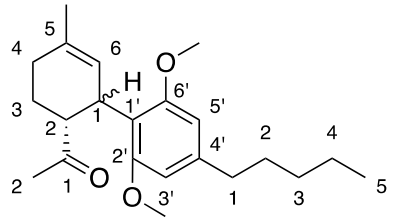

(46) 1-((2*R*)-2',6'-Dimethoxy-5-methyl-4'-pentyl-1,2,3,4-tetrahydro-[1,1'-biphenyl]-2-yl)ethan-1-one. (racemic) Prepared according to the Diels-Alder reaction procedure using **159** (100 mg, 364 µmol, 1.0 equiv). Yield: 59% (78 mg, 225 µmol) as a clear oil. $\mathbf{R_f}$ = 0.42 (30% EtOAc in hexanes). **FTIR** (cm^{-1}) (neat) 2957, 2929, 2856, 1709, 1608, 1579,1455, 1420; **^{1}H NMR** (400 MHz, $CDCl_3$) δ 6.34-6.31 (d, *J* = 11.5 Hz, 2 H), 5.30-5.15 (t, *J* = 49.8, 59.0 Hz, 1 H), 4.50-4.15 (m, 1H), 3.73 (d, *J* = 14.4 Hz, 6H), 3.30-2.89 (m, 1H), 2.57-2.49 (m, 2H), 2.31-2.21 (m, 1H), 2.14-2.11 (m, 1H), 2.04-1.98 (m, 1H), 1.87 (d, *J* = 13.1 Hz, 3H), 1.73-1.67 (m, 1H), 1.70 (s, 3H), 1.62-1.55 (m, 2H), 1.37-1.27 (m, 4H), 0.89 (t, *J* = 6.7 Hz, 3H); **^{13}C NMR** (100 MHz, $CDCl_3$) δ 211.2, 158.6, 143.1, 132.3, 131.2, 124.9, 122.8, 115.5, 104.7, 55.9, 55.6, 51.6, 51.4, 36.4, 34.7, 32.0, 31.7, 31.0, 29.6, 29.1, 28.7, 26.7, 23.8, 23.3, 22.6, 21.8, 14.1. **HRMS** (m/z): Calculated for $C_{22}H_{32}O_3$ (M+H) 345.24362, found (M+H) 345.24242.

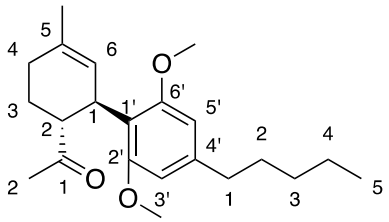

1-((1*R*,2*R*)-2',6'-Dimethoxy-5-methyl-4'-pentyl-1,2,3,4-tetrahydro-[1,1'-biphenyl]-2-yl)ethan-1-one. Prepared according to the epimerization reaction procedure using **160** (78 mg, 225 µmol, 1.0 equiv). Yield: 97% (75 mg, 218 µmol) as a clear oil. $\mathbf{R_f}$=0.38 (10% EtOAc in hexanes). **FTIR** (cm $^{-1}$) (neat) 2957, 2929, 2856, 1708, 1608, 1579,1454, 1420; **^{1}H NMR** (400 MHz, $CDCl_3$) d 6.34 (s, 2H), 5.15 (m, 1H), 4.18-4.14 (m, 1H), 3.74 (s, 6H), 3.30-3.24 (m, 1H), 2.53 (t, *J* = 7.6, 8.2 Hz, 2H), 2.19-2.08 (m, 1H), 2.03-1.95 (m, 1H), 1.93-1.89 (m, 1H), 1.88 (s, 3H), 1.84-1.77 (m, 1H), 1.66 (s, 3H), 1.62-1.55 (m, 2H), 1.37-1.29 (m, 4H), 0.89 (t, *J* = 6.6 Hz, 3H); **^{13}C NMR** (100 MHz, $CDCl_3$) δ 213.6, 158.5, 142.8, 131.1, 124.9, 117.22, 104.9, 55.9, 51.1, 36.5, 34.7, 31.7, 31.0, 29.6, 28.6, 26.6, 23.3, 22.6, 14.1. **HRMS** (m/z): Calculated for $C_{22}H_{32}O_3$ (M+Na) 367.22573, found (M+Na) 367.72437. The data is in accordance with the literature.

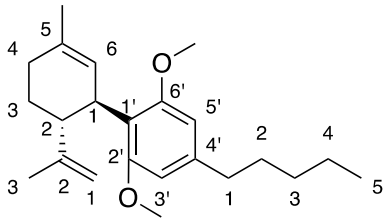

(1*R*,2*R*)-2',6'-Dimethoxy-5-methyl-4'-pentyl-2-(prop-1-en-2-yl)-1,2,3,4-tetrahydro-1,1'-biphenyl. Prepared according to the second Wittig reaction procedure using **161** (30.5 mg, 85.3 µmol, 1.0 equiv). Yield: 68% (10.0 mg, 29.2 µmol). The compound was a clear oil. $\mathbf{R_f}$= 0.77 (10% EtOAc in hexanes). **FTIR** (cm $^{-1}$) (neat) 2925, 2855, 1716, 1643, 1608, 1580,1454, 1419; **^{1}H NMR** (400 MHz, $CDCl_3$) δ 6.33 (s, 2H), 5.20 (s, 1H), 4.44-4.42 (m, 2H), 4.0-3.96 (m, 1H), 3.73 (s, 6H), 2.93-2.86 (ddd, *J* = 4.0, 4.3, 4.2, 1H), 2.53 (t, *J* = 7.9 Hz, 2H), 2.24-2.13 (m, 1H), 2.02-1.94 (m, 1H), 1.78-1.72(m, 1H), 1.71-1.57 (m, 1H), 1.66 (s, 3H), 1,62-1.58 (m, 1H), 1.60 (s, 3H), 1.54 (m, 2H), 1.37-1.30 (m, 4H), 0.90 (t, *J* = 6.9 Hz, 3H); **^{13}C NMR** (100 MHz, $CDCl_3$) δ 149.6, 141.9, 131.2, 125.9, 119.0, 109.6, 56.0, 45.2, 36.4, 36.1, 31.7, 31.0, 30.8, 29.7, 23.5, 22.6, 19.1, 14.1,

1.03. **HRMS** (m/z): Calculated for $C_{23}H_{34}O_2$ (M+H) 343.26339, found (M+H) 343.26316. The data is in accordance with the literature.

^{1}H NMR and ^{13}C NMR respectively

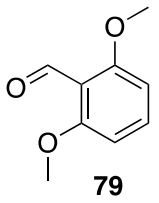

79

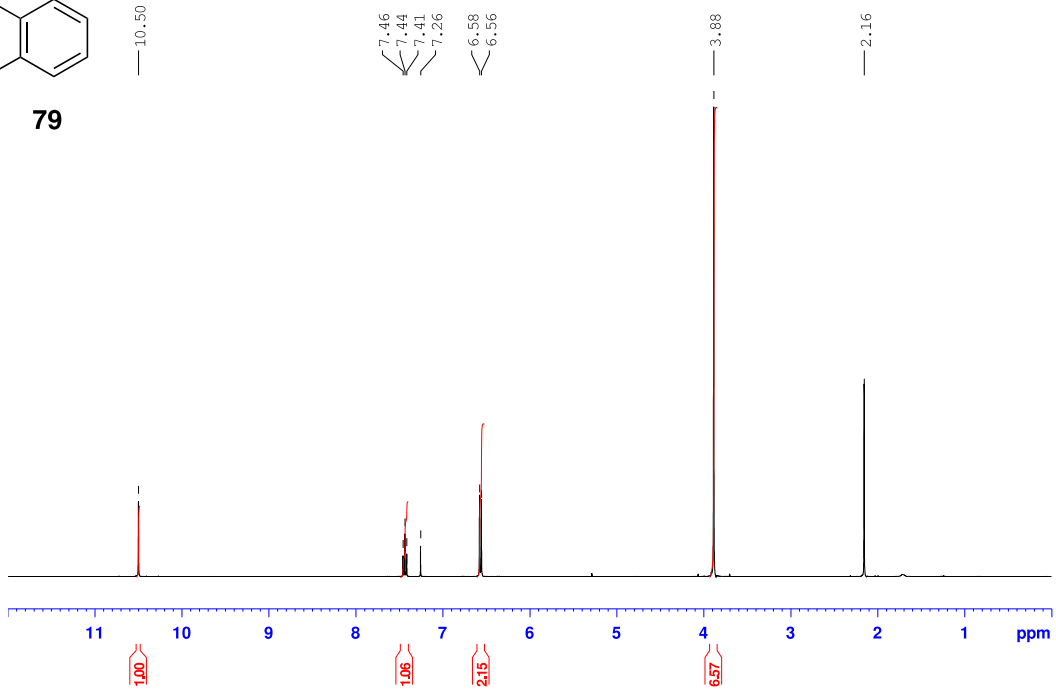

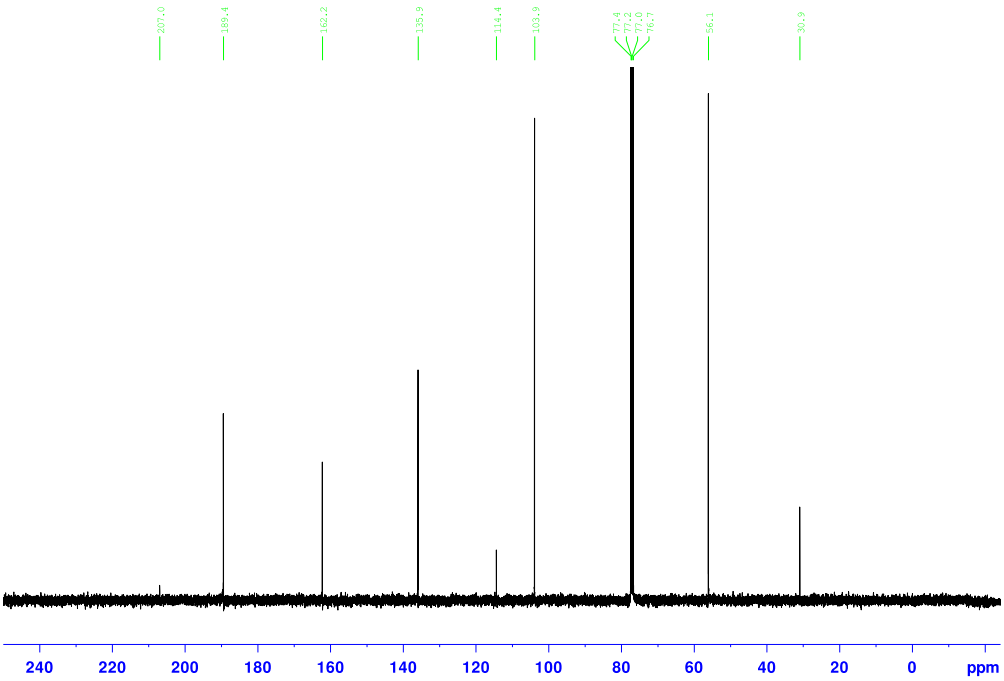

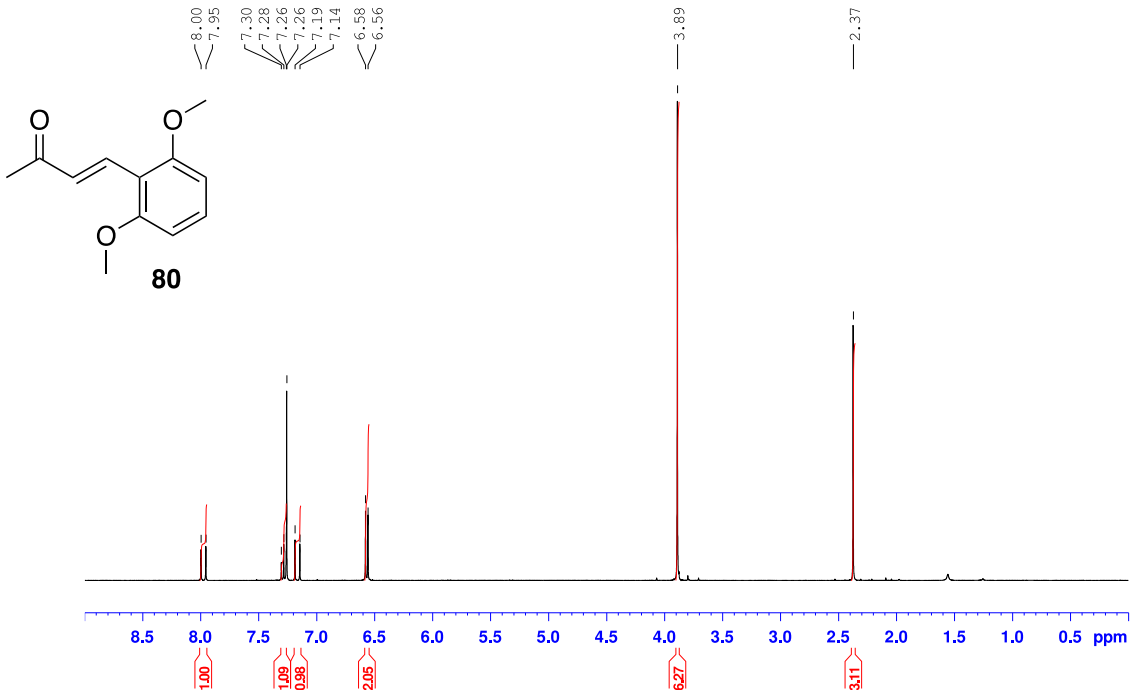
8.00
7.95
7.30
7.28
7.26
7.26
7.19
7.14
6.58
6.56
3.89
2.37
O
O
O
80
8.5
8.0
7.5
7.0
6.5
6.0
5.5
5.0
4.5
4.0
3.5
3.0
2.5
2.0
1.5
1.0
0.5
ppm
1.00
1.09
0.98
2.05
6.27
3.11

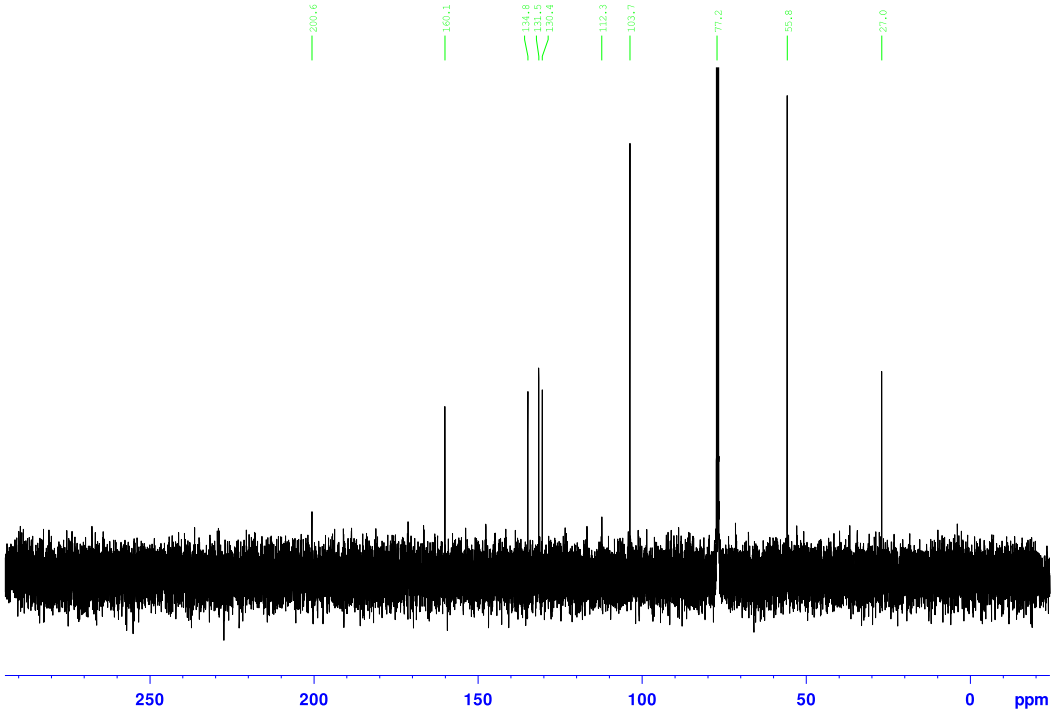
200.6
160.1
134.8
131.5
130.4
112.3
103.7
77.2
55.8
27.0
250
200
150
100
50
0
ppm

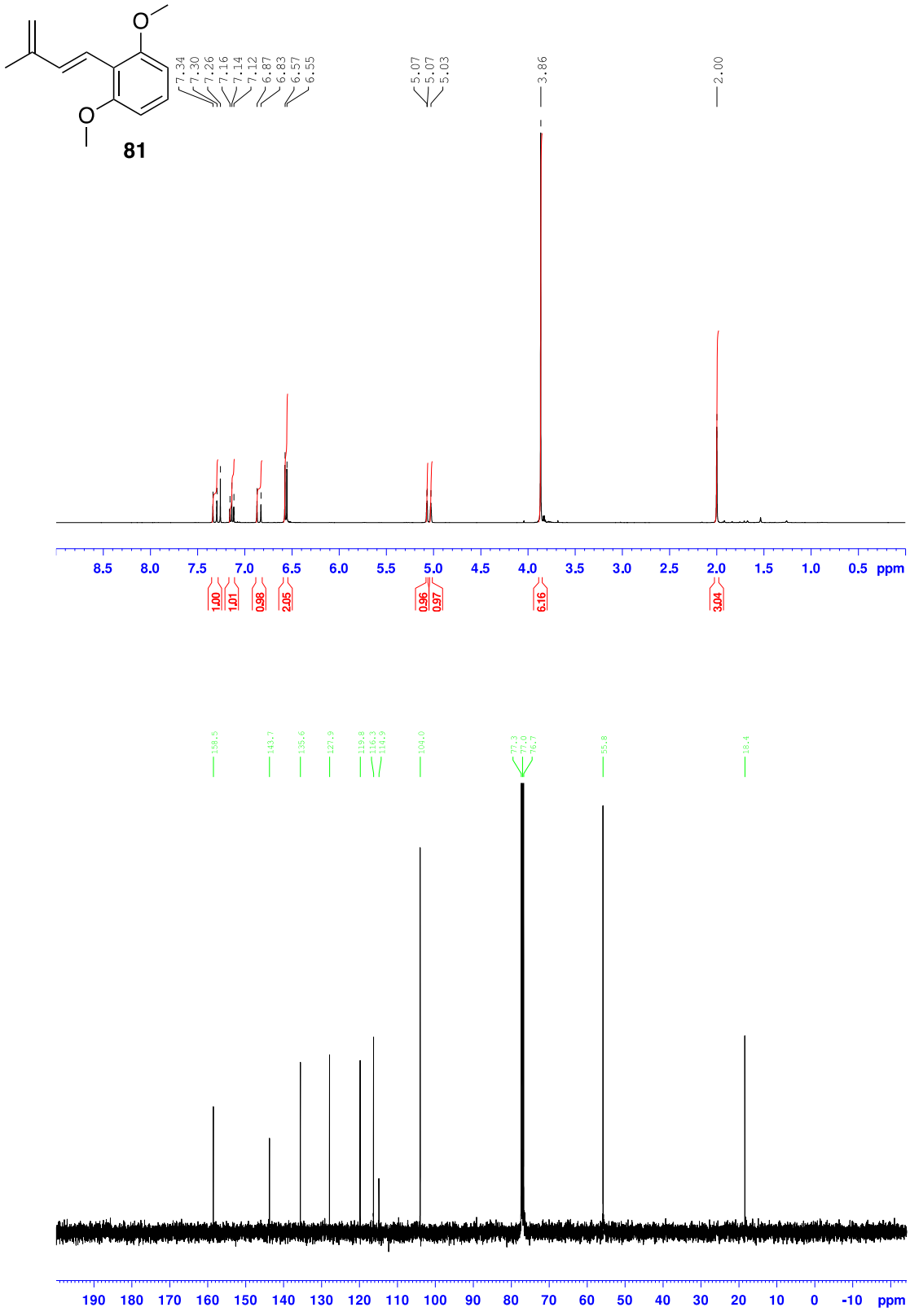
81
7.34
7.30
7.26
7.16
7.14
7.12
6.87
6.83
6.57
6.55
5.07
5.07
5.03
3.86
2.00
8.5 8.0 7.5 7.0 6.5 6.0 5.5 5.0 4.5 4.0 3.5 3.0 2.5 2.0 1.5 1.0 0.5 ppm
1.00
1.01
0.98
2.05
0.96
0.97
6.16
3.04
158.5
143.7
135.6
127.9
119.8
116.3
114.9
104.0
77.3
77.0
76.7
55.8
18.4
190 180 170 160 150 140 130 120 110 100 90 80 70 60 50 40 30 20 10 0 -10 ppm

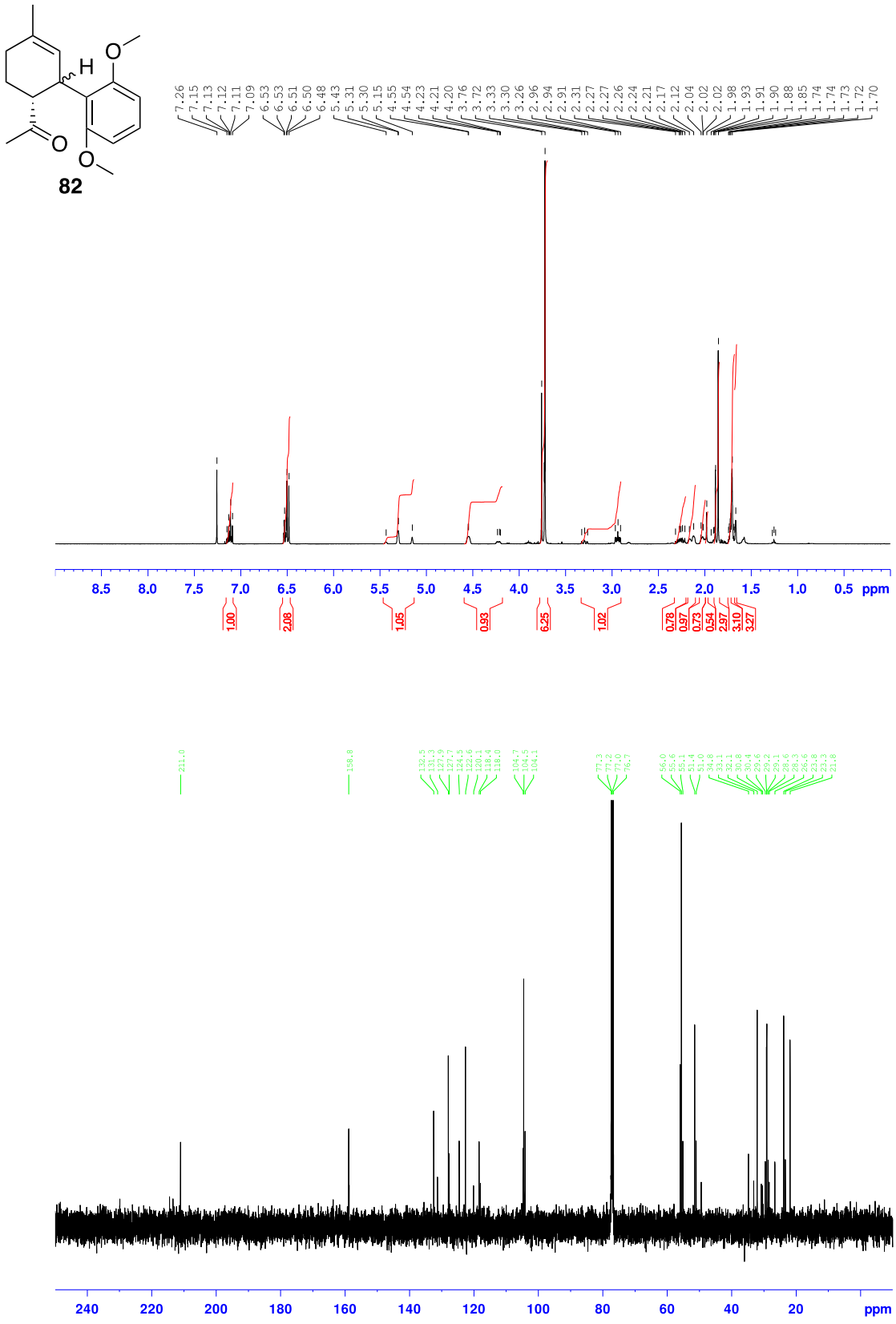
82
7.26 7.15 7.13 7.12 7.11 7.09 6.53 6.51 6.50 6.48 5.43 5.31 5.30 5.15 4.55 4.54 4.23 4.21 4.20 3.76 3.72 3.33 3.30 3.26 2.96 2.94 2.91 2.31 2.27 2.26 2.24 2.21 2.17 2.12 2.04 2.02 2.02 1.98 1.93 1.91 1.90 1.88 1.85 1.74 1.74 1.73 1.72 1.70
8.5 8.0 7.5 7.0 6.5 6.0 5.5 5.0 4.5 4.0 3.5 3.0 2.5 2.0 1.5 1.0 0.5 ppm
1.00 2.08 1.05 0.93 6.25 1.02 0.78 0.97 0.73 0.54 2.97 3.10 3.27
211.0 158.8 132.5 131.3 127.9 127.7 124.5 122.6 120.1 118.4 118.0 104.7 104.5 104.1 77.3 77.2 77.0 76.7 56.0 55.6 55.1 51.4 34.0 33.1 32.1 30.8 30.4 29.6 29.2 29.1 28.6 28.3 26.6 23.8 23.8 21.8
240 220 200 180 160 140 120 100 80 60 40 20 ppm

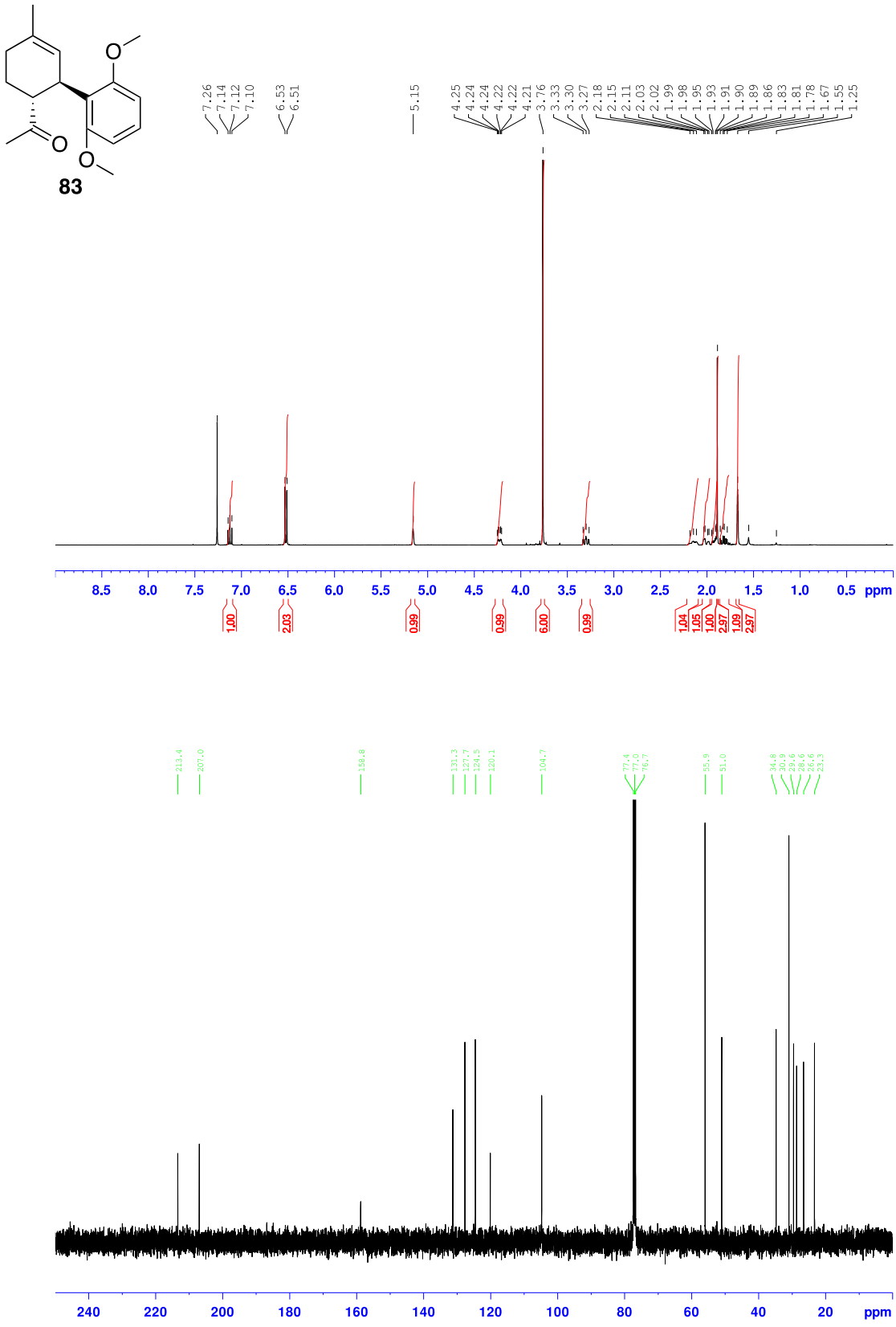
83
7.26
7.14
7.12
7.10
6.53
6.51
5.15
4.25
4.24
4.24
4.22
4.22
4.21
3.76
3.33
3.30
3.27
2.18
2.15
2.11
2.03
2.02
1.99
1.98
1.95
1.93
1.91
1.90
1.89
1.86
1.83
1.81
1.78
1.67
1.55
1.25
8.5 8.0 7.5 7.0 6.5 6.0 5.5 5.0 4.5 4.0 3.5 3.0 2.5 2.0 1.5 1.0 0.5 ppm
1.00 2.03 0.99 0.99 6.00 0.99 1.04 1.05 1.00 2.97 1.09 2.97
213.4
207.0
158.8
131.3
127.7
124.5
120.1
104.7
77.4
77.0
76.7
55.9
51.0
34.8
30.9
28.6
28.1
26.6
23.3
240 220 200 180 160 140 120 100 80 60 40 20 ppm

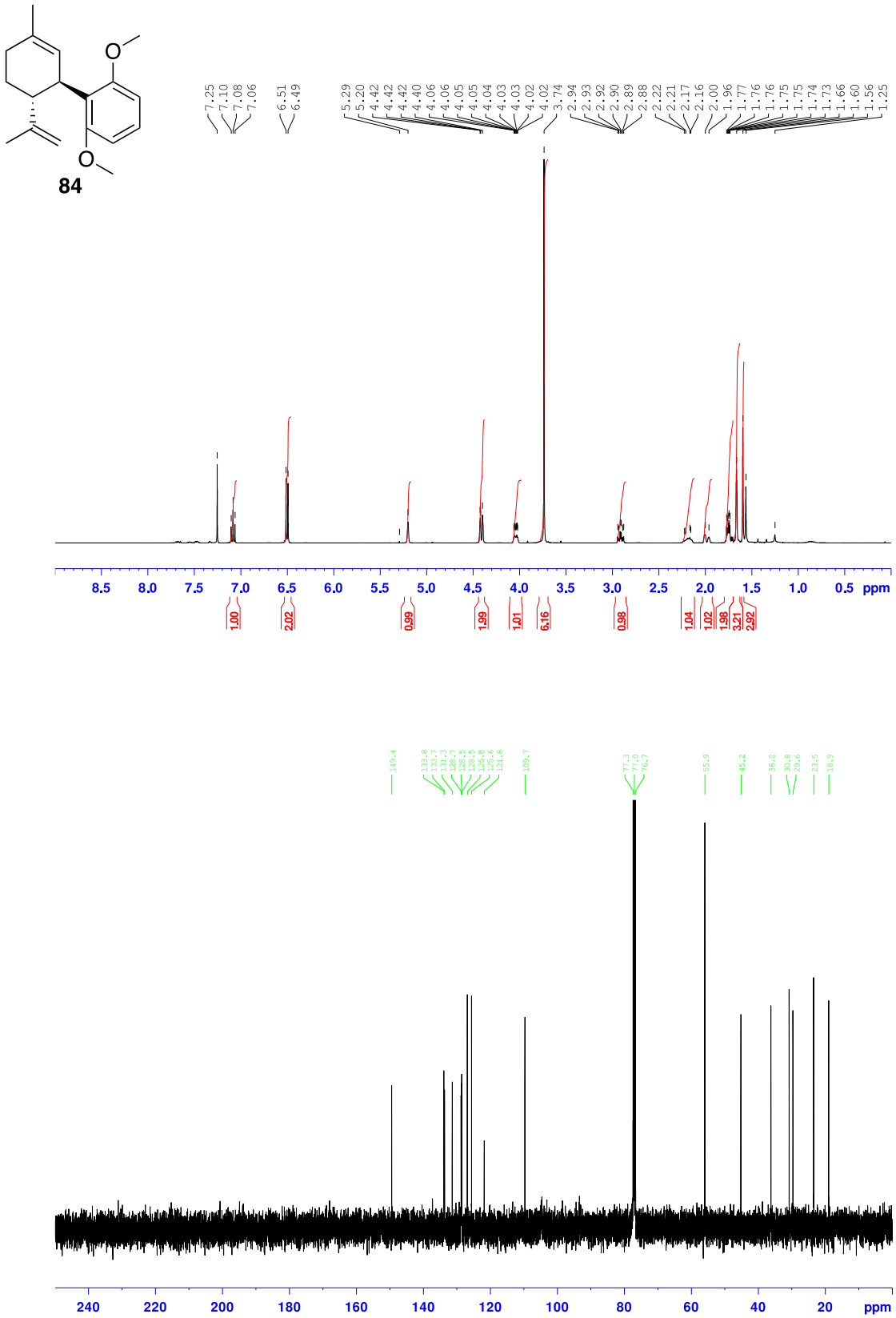
84
7.25
7.10
7.08
7.06
6.51
6.49
5.29
5.20
4.42
4.42
4.42
4.40
4.06
4.06
4.05
4.05
4.04
4.03
4.03
4.02
4.02
3.74
2.94
2.93
2.92
2.90
2.89
2.88
2.22
2.21
2.17
2.16
2.00
1.96
1.77
1.76
1.76
1.75
1.75
1.74
1.73
1.66
1.60
1.56
1.25
8.5 8.0 7.5 7.0 6.5 6.0 5.5 5.0 4.5 4.0 3.5 3.0 2.5 2.0 1.5 1.0 0.5 ppm
1.00
2.02
0.99
1.99
1.01
6.16
0.98
1.04
1.02
1.98
3.21
2.92
149.4
133.8
133.7
131.3
128.7
128.5
128.5
126.8
125.6
121.8
109.7
77.3
77.0
76.7
56.9
45.2
36.2
30.8
29.6
23.5
18.9
240 220 200 180 160 140 120 100 80 60 40 20 ppm

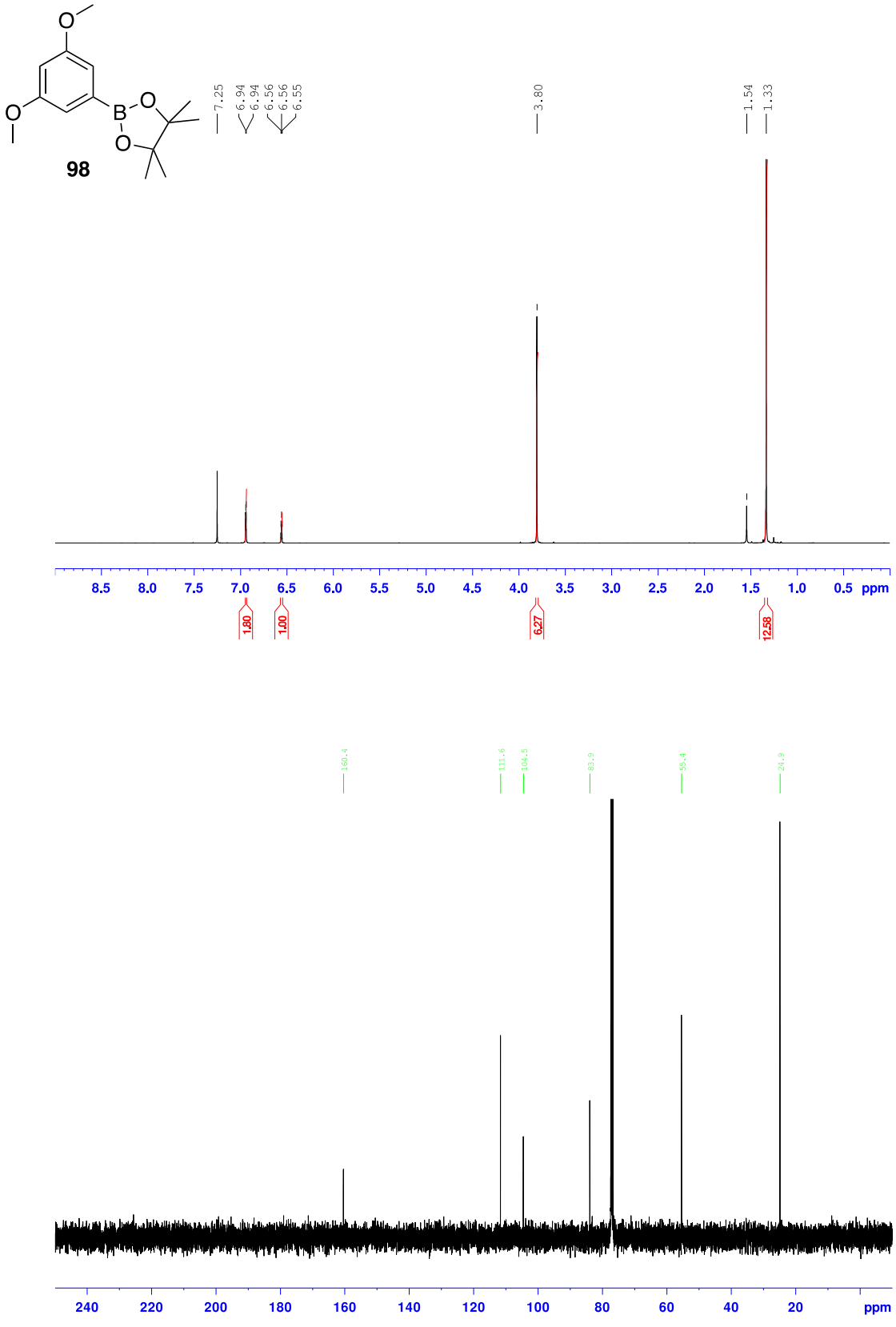
98
7.25
6.94
6.94
6.56
6.56
6.55
3.80
1.54
1.33
8.5 8.0 7.5 7.0 6.5 6.0 5.5 5.0 4.5 4.0 3.5 3.0 2.5 2.0 1.5 1.0 0.5 ppm
1.80
1.00
6.27
12.58
160.4
111.6
104.5
83.9
55.4
24.9
240 220 200 180 160 140 120 100 80 60 40 20 ppm

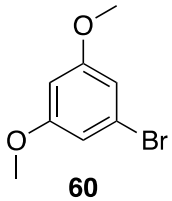
O
O
Br

60

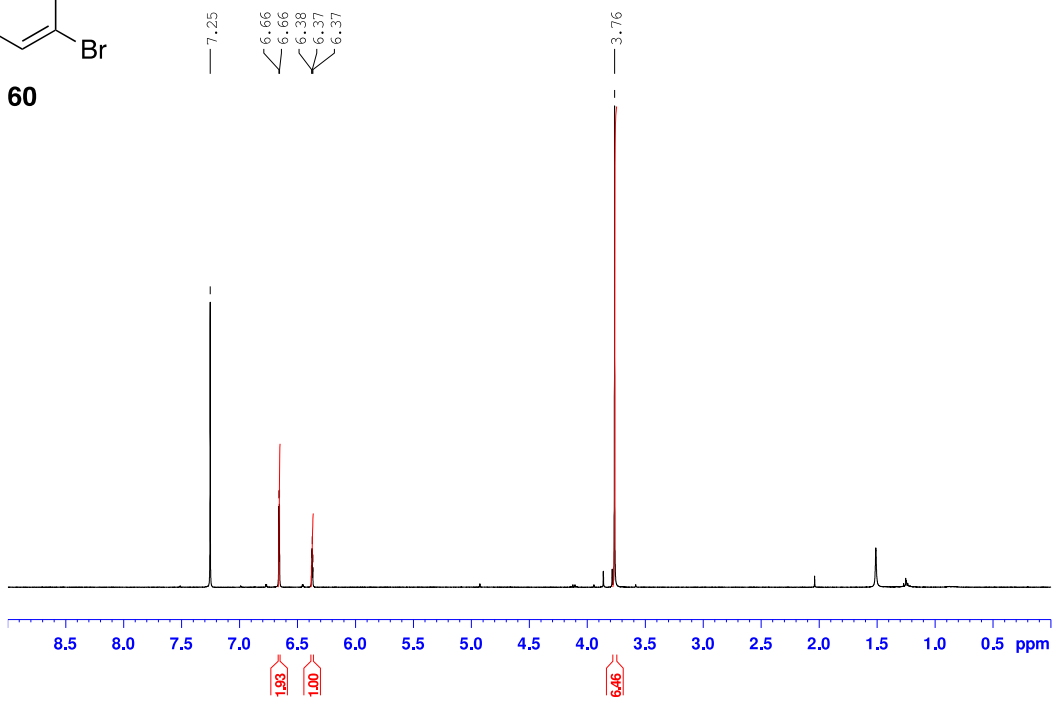
7.25
6.66
6.66
6.38
6.37
6.37
3.76
8.5
8.0
7.5
7.0
6.5
6.0
5.5
5.0
4.5
4.0
3.5
3.0
2.5
2.0
1.5
1.0
0.5
ppm
1.93
1.00
6.46

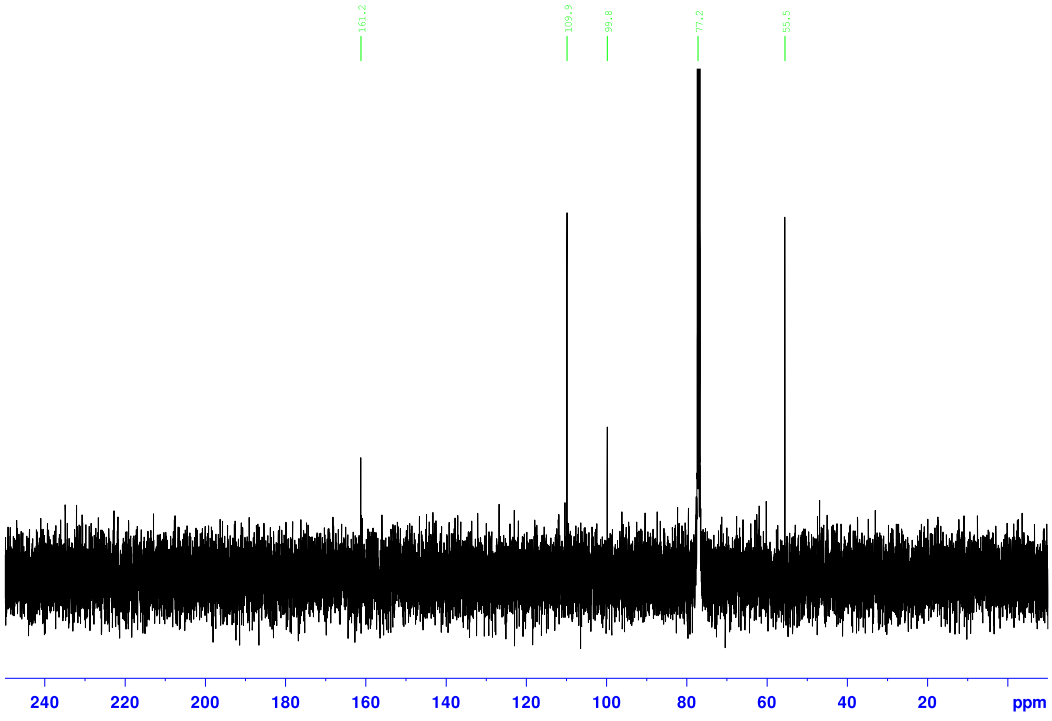
161.2
109.9
99.8
77.2
55.5
240
220
200
180
160
140
120
100
80
60
40
20
ppm

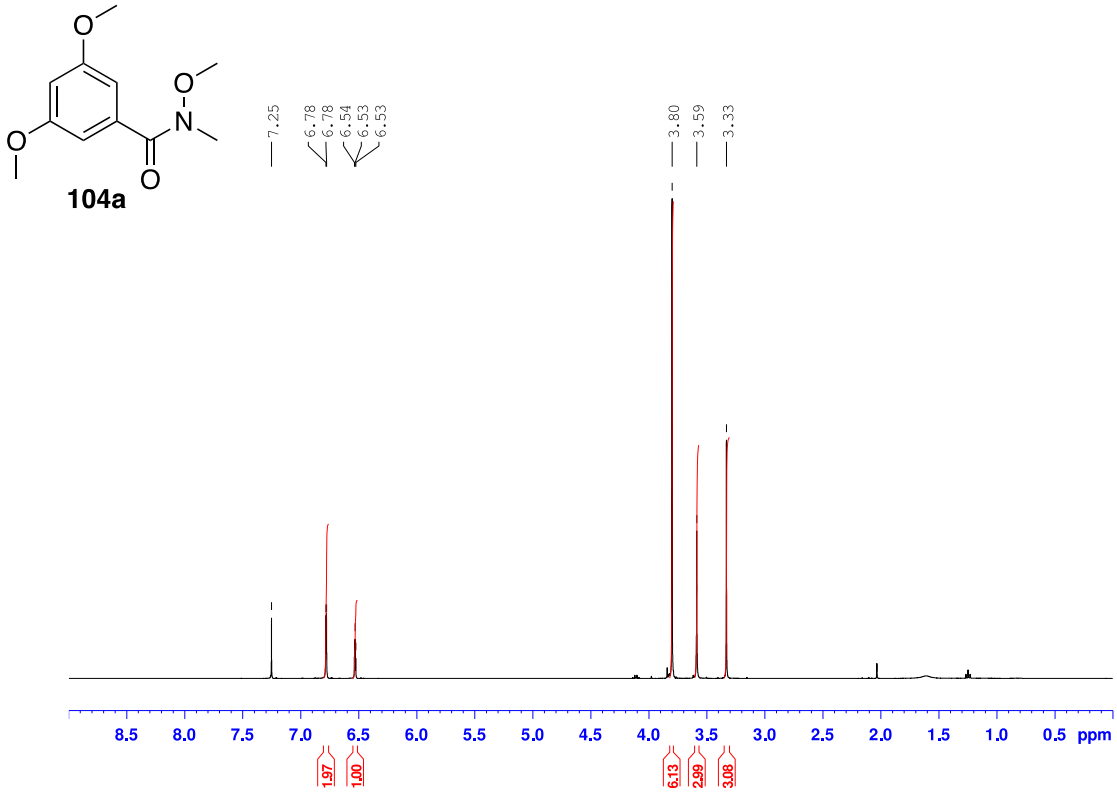
104a
7.25
6.78
6.78
6.54
6.53
6.53
3.80
3.59
3.33
8.5 8.0 7.5 7.0 6.5 6.0 5.5 5.0 4.5 4.0 3.5 3.0 2.5 2.0 1.5 1.0 0.5 ppm
1.97
1.00
6.13
2.99
3.08

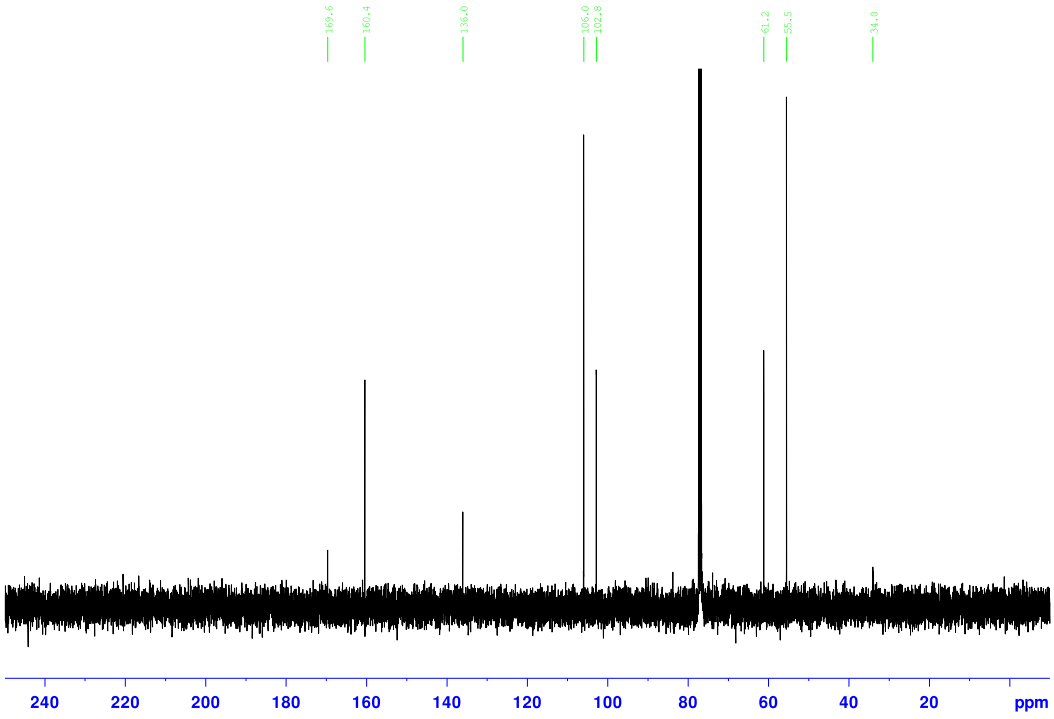
169.6
160.4
136.0
106.0
102.8
61.2
55.5
34.0
240 220 200 180 160 140 120 100 80 60 40 20 ppm

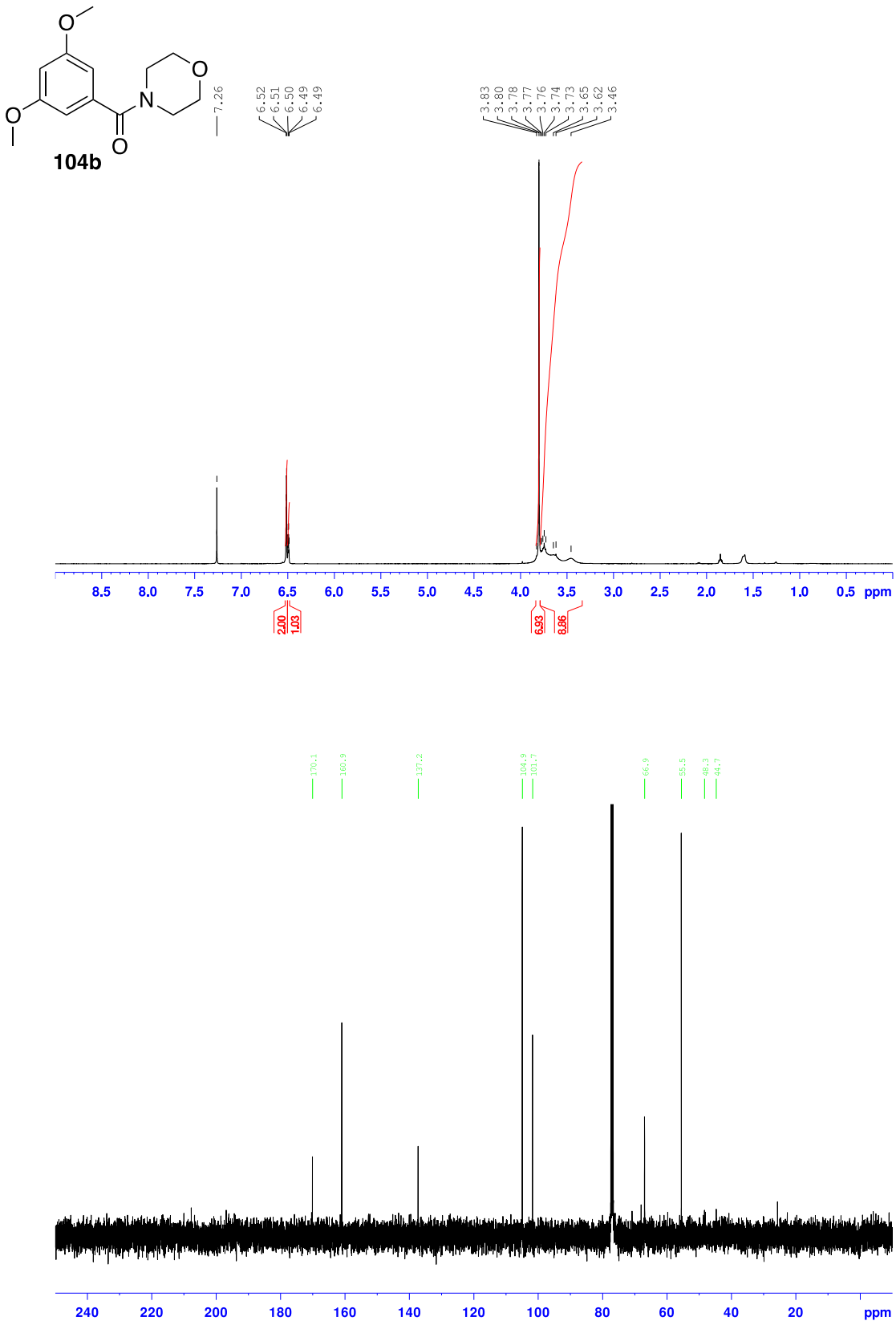
104b
7.26
6.52
6.51
6.50
6.49
6.49
3.83
3.80
3.78
3.77
3.76
3.74
3.73
3.65
3.62
3.46
8.5 8.0 7.5 7.0 6.5 6.0 5.5 5.0 4.5 4.0 3.5 3.0 2.5 2.0 1.5 1.0 0.5 ppm
2.00
1.03
6.93
8.86
170.1
160.9
137.2
104.9
101.7
66.9
55.5
48.3
44.7
240 220 200 180 160 140 120 100 80 60 40 20 ppm

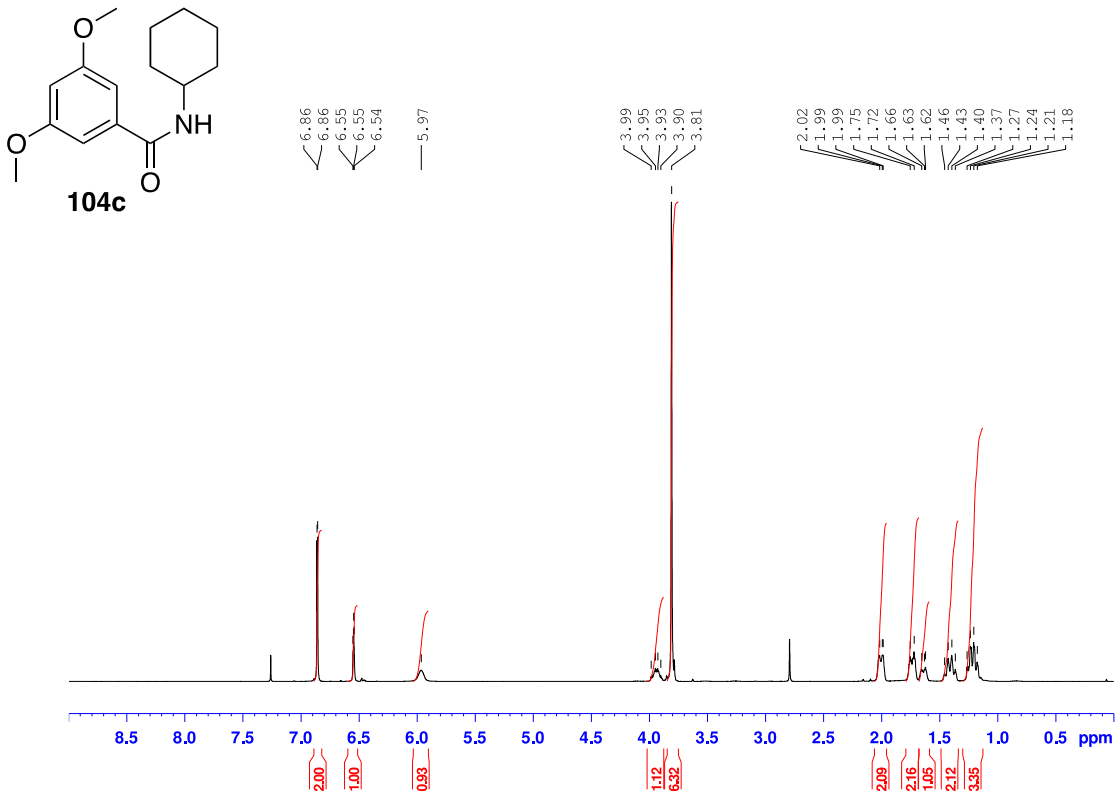
O
NH
O
O
104c
6.86
6.86
6.55
6.55
6.54
5.97
3.99
3.95
3.93
3.90
3.81
2.02
1.99
1.99
1.75
1.72
1.66
1.63
1.62
1.46
1.43
1.40
1.37
1.27
1.24
1.21
1.18
8.5
8.0
7.5
7.0
6.5
6.0
5.5
5.0
4.5
4.0
3.5
3.0
2.5
2.0
1.5
1.0
0.5
ppm
2.00
1.00
0.93
1.12
6.32
2.09
2.16
1.05
2.12
3.35

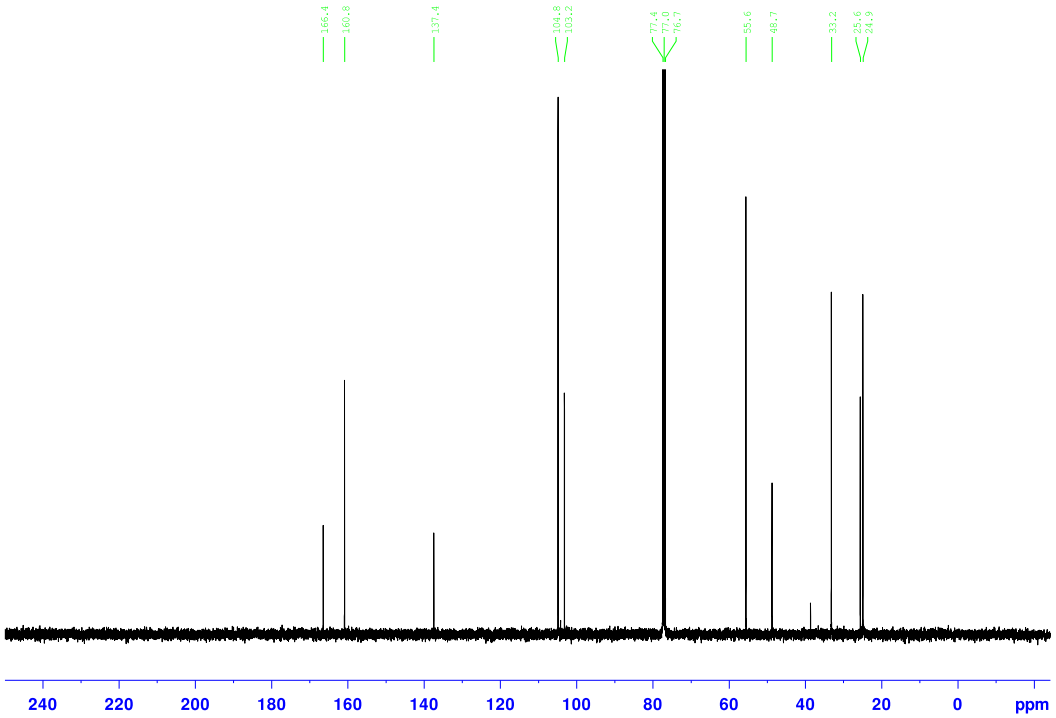
166.4
160.8
137.4
104.8
103.2
77.4
77.0
76.7
55.6
48.7
33.2
25.6
24.9
240
220
200
180
160
140
120
100
80
60
40
20
0
ppm

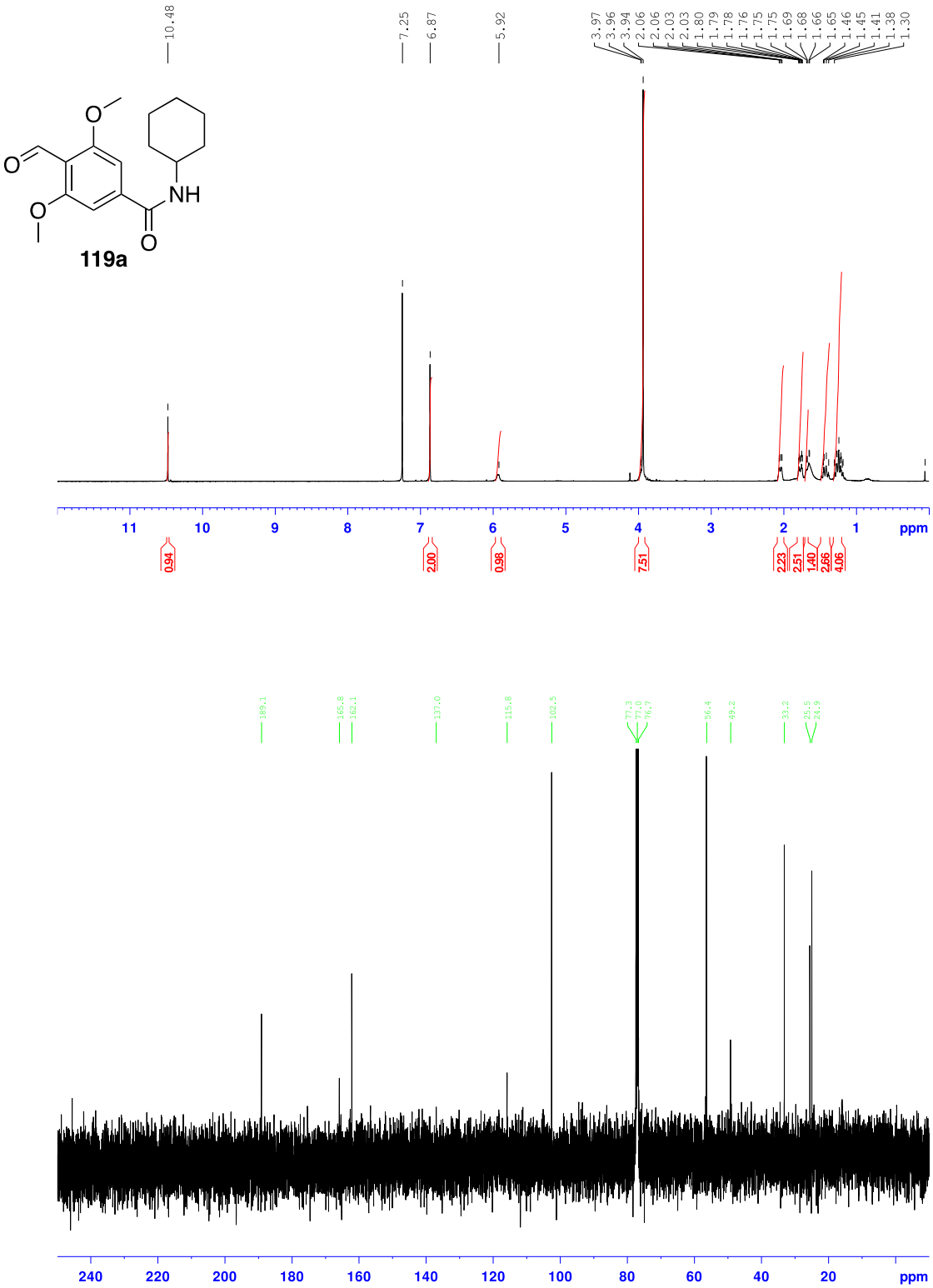
10.48
7.25
6.87
5.92
3.97
3.96
3.94
2.06
2.06
2.03
2.03
1.80
1.79
1.78
1.76
1.75
1.75
1.69
1.68
1.66
1.65
1.46
1.45
1.41
1.38
1.30
O
O
NH
O
O
119a
11
10
9
8
7
6
5
4
3
2
1
ppm
0.94
2.00
0.98
7.51
2.23
2.51
1.40
2.66
4.06
189.1
165.8
162.1
137.0
115.8
102.5
77.3
77.0
76.7
56.4
49.2
33.2
25.5
24.9
240
220
200
180
160
140
120
100
80
60
40
20
ppm

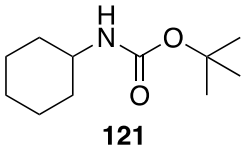
H
N
O
O

121

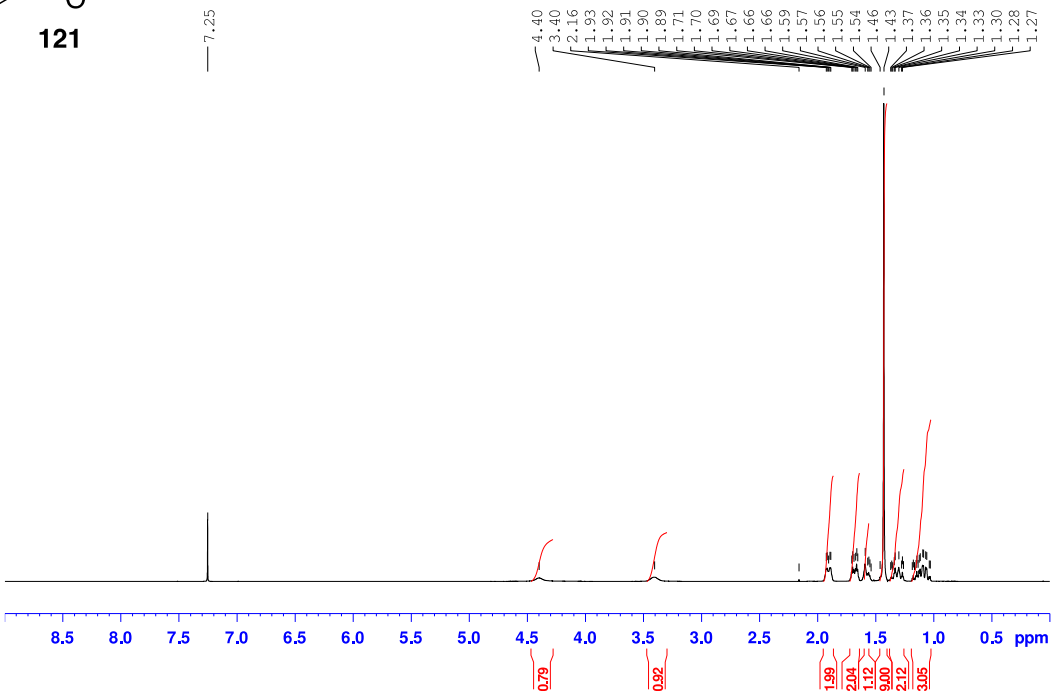
7.25
4.40
3.40
2.16
1.93
1.92
1.91
1.90
1.89
1.71
1.70
1.69
1.67
1.66
1.66
1.59
1.57
1.56
1.55
1.54
1.46
1.43
1.37
1.36
1.35
1.34
1.33
1.30
1.28
1.27
8.5
8.0
7.5
7.0
6.5
6.0
5.5
5.0
4.5
4.0
3.5
3.0
2.5
2.0
1.5
1.0
0.5
ppm
0.79
0.92
1.99
2.04
1.12
9.00
2.12
3.05

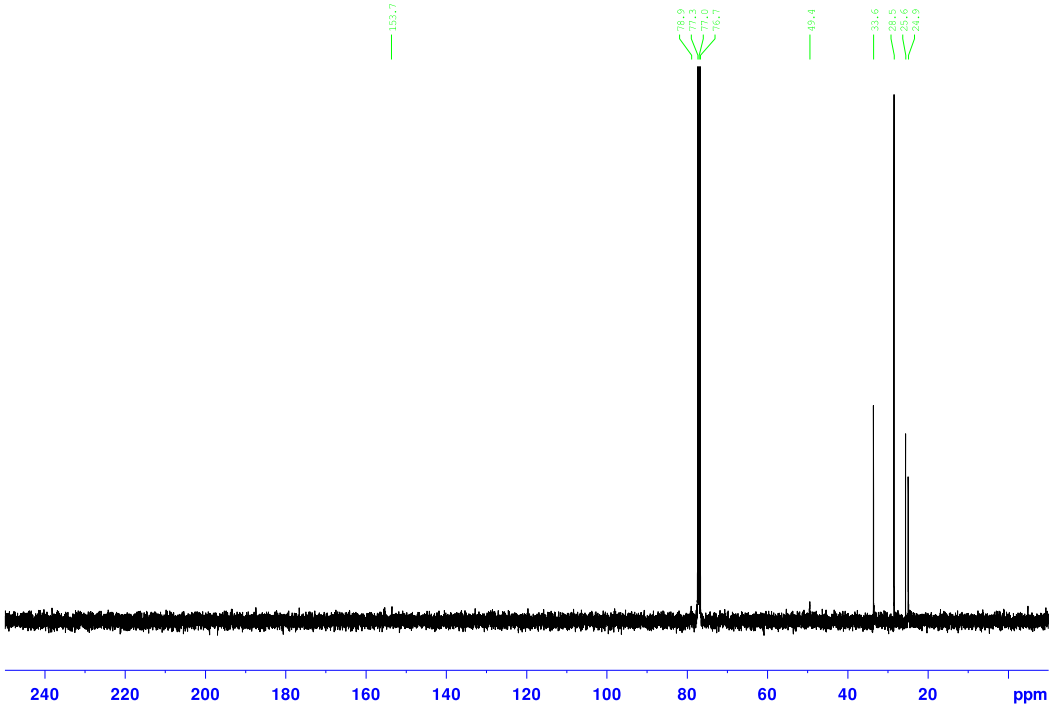
153.7
78.9
77.3
77.0
76.7
49.4
33.6
28.5
25.6
24.9
240
220
200
180
160
140
120
100
80
60
40
20
ppm

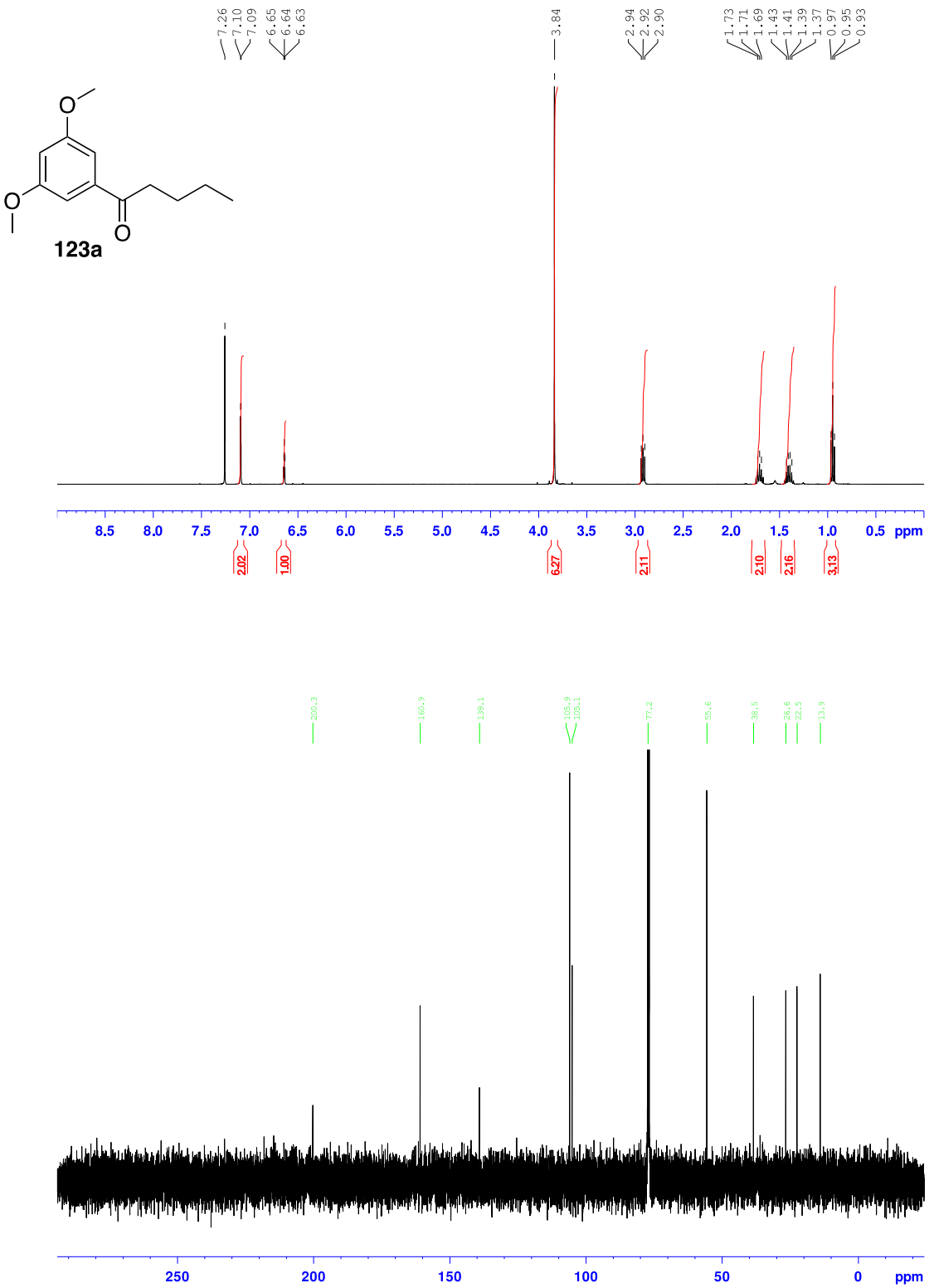
7.26
7.10
7.09
6.65
6.64
6.63
3.84
2.94
2.92
2.90
1.73
1.71
1.69
1.43
1.41
1.39
1.37
0.97
0.95
0.93
O
O
O
123a
8.5 8.0 7.5 7.0 6.5 6.0 5.5 5.0 4.5 4.0 3.5 3.0 2.5 2.0 1.5 1.0 0.5 ppm
2.02
1.00
6.27
2.11
2.10
2.16
3.13
200.3
160.9
139.1
105.9
105.1
77.2
55.6
38.5
26.6
22.5
13.9
250 200 150 100 50 0 ppm

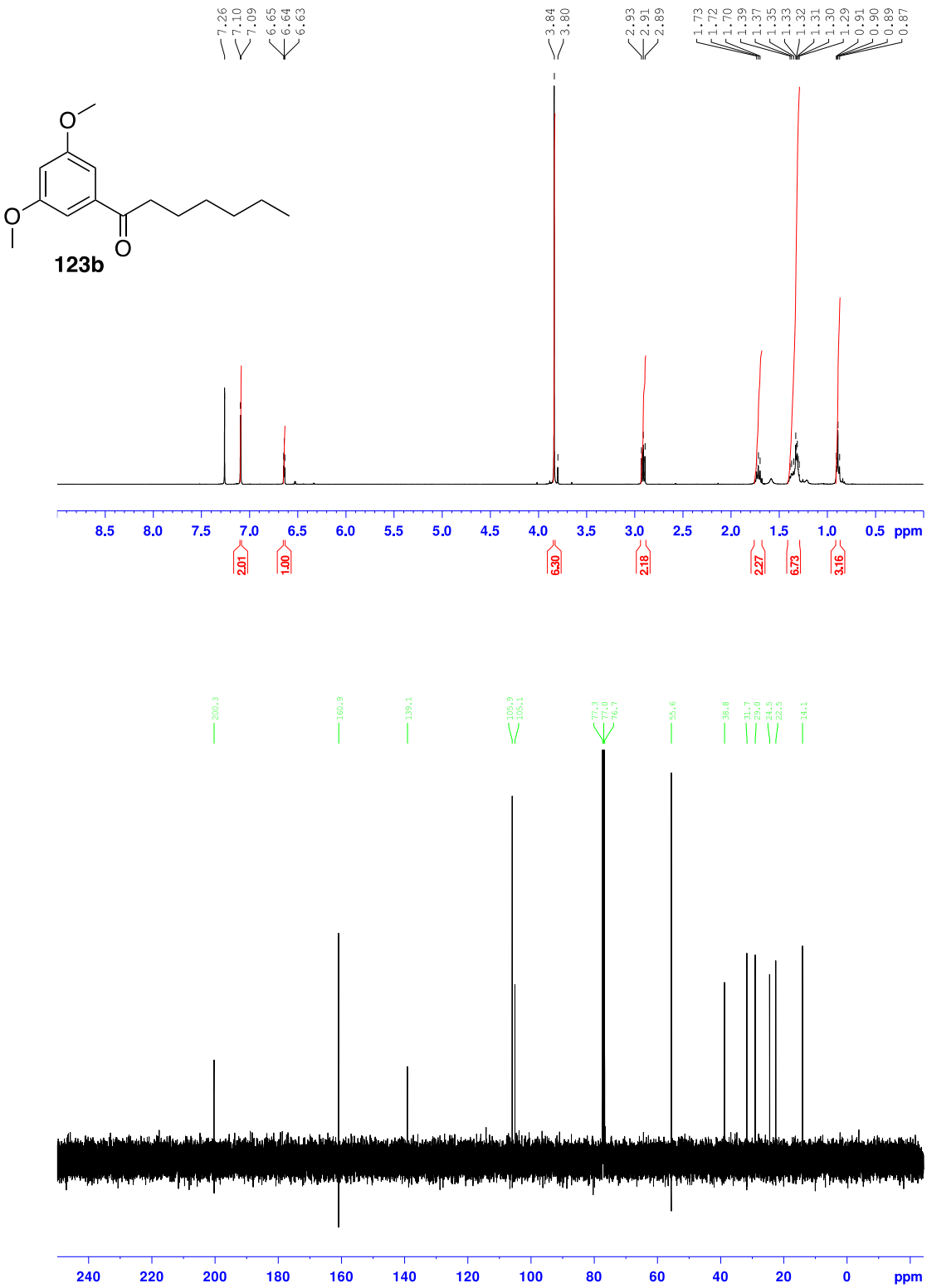
123b
7.26
7.10
7.09
6.65
6.64
6.63
3.84
3.80
2.93
2.91
2.89
1.73
1.72
1.70
1.39
1.37
1.35
1.33
1.32
1.31
1.30
1.29
0.91
0.90
0.89
0.87
8.5 8.0 7.5 7.0 6.5 6.0 5.5 5.0 4.5 4.0 3.5 3.0 2.5 2.0 1.5 1.0 0.5 ppm
2.01
1.00
6.30
2.18
2.27
6.73
3.16
200.3
160.9
139.1
105.9
105.1
77.3
77.0
76.7
55.6
38.8
31.7
29.0
24.5
22.5
14.1
240 220 200 180 160 140 120 100 80 60 40 20 0 ppm

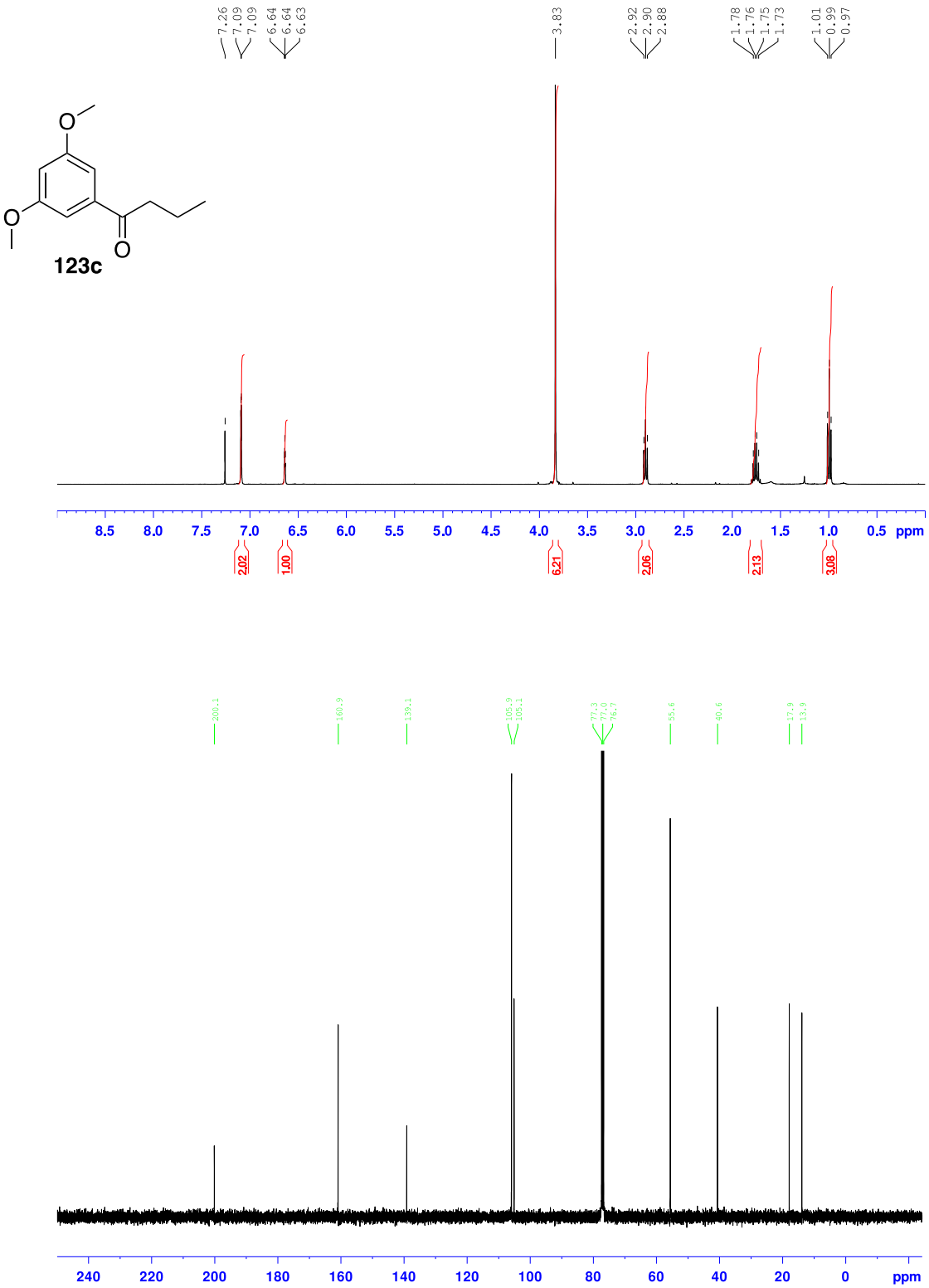
123c
7.26
7.09
7.09
6.64
6.64
6.63
3.83
2.92
2.90
2.88
1.78
1.76
1.75
1.73
1.01
0.99
0.97
8.5
8.0
7.5
7.0
6.5
6.0
5.5
5.0
4.5
4.0
3.5
3.0
2.5
2.0
1.5
1.0
0.5
ppm
2.02
1.00
6.21
2.06
2.13
3.08
200.1
160.9
139.1
105.9
105.1
77.3
77.0
76.7
55.6
40.6
17.9
13.9
240
220
200
180
160
140
120
100
80
60
40
20
0
ppm

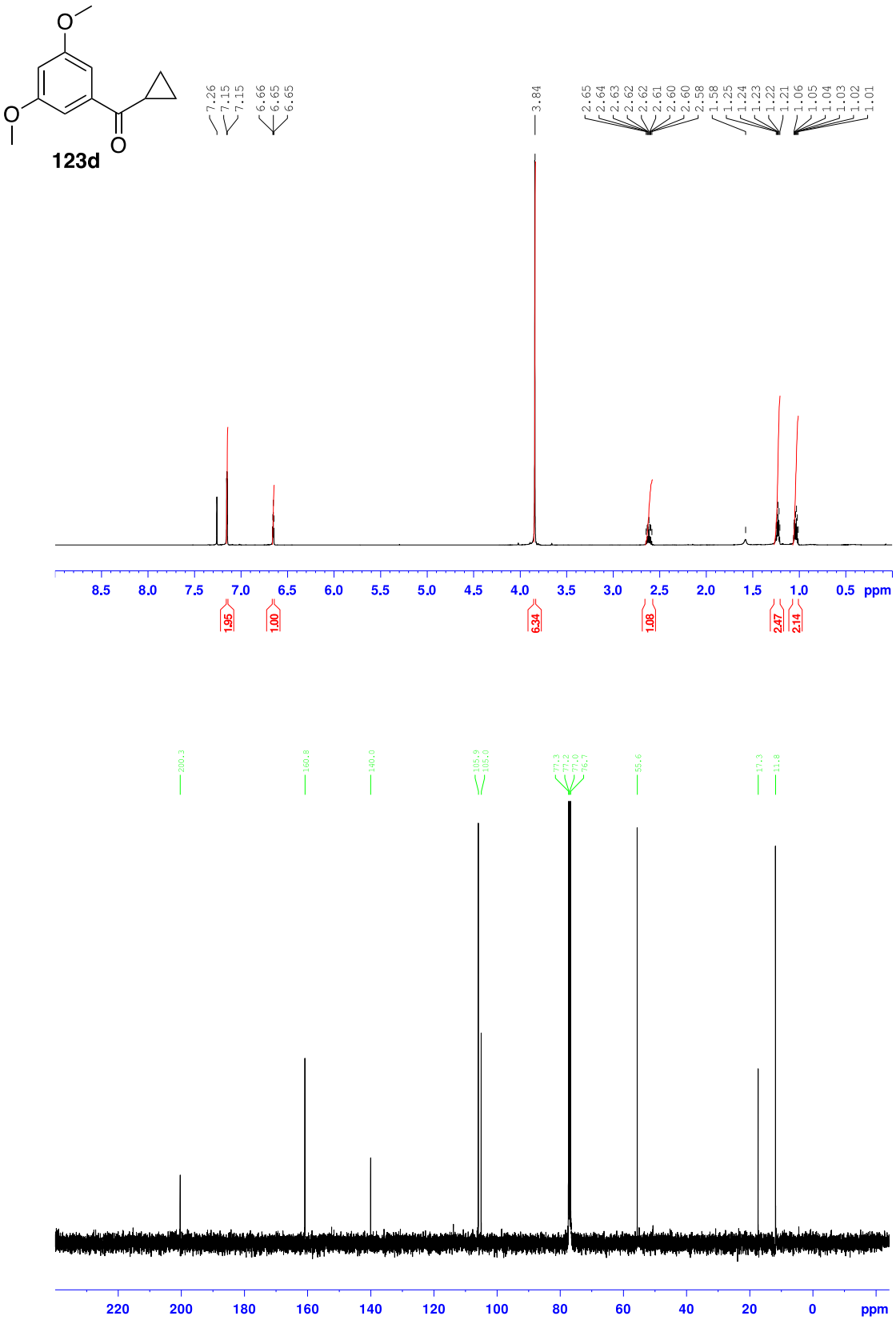
123d
7.26
7.15
7.15
6.66
6.65
6.65
3.84
2.65
2.64
2.63
2.62
2.62
2.61
2.60
2.60
2.58
1.58
1.25
1.24
1.23
1.22
1.21
1.06
1.05
1.04
1.03
1.02
1.01
8.5 8.0 7.5 7.0 6.5 6.0 5.5 5.0 4.5 4.0 3.5 3.0 2.5 2.0 1.5 1.0 0.5 ppm
1.95
1.00
6.34
1.08
2.47
2.14
200.3
160.8
140.0
105.9
105.0
77.3
77.2
77.0
76.7
55.6
17.3
11.8
220 200 180 160 140 120 100 80 60 40 20 0 ppm

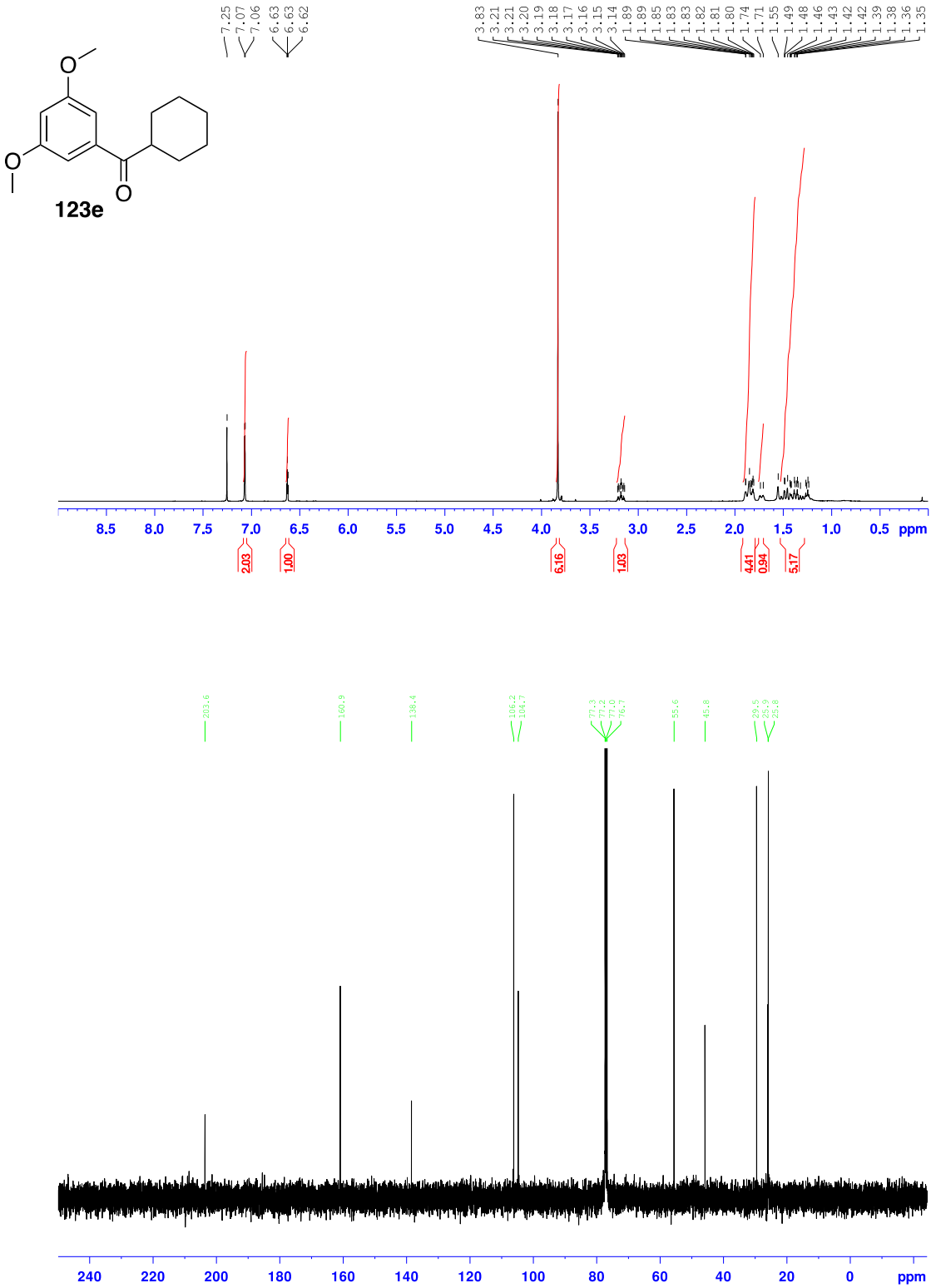
123e
7.25
7.07
7.06
6.63
6.63
6.62
3.83
3.21
3.21
3.20
3.19
3.18
3.17
3.16
3.15
3.14
1.89
1.89
1.85
1.83
1.83
1.82
1.81
1.80
1.74
1.71
1.55
1.49
1.48
1.46
1.43
1.42
1.42
1.39
1.38
1.36
1.35
8.5
8.0
7.5
7.0
6.5
6.0
5.5
5.0
4.5
4.0
3.5
3.0
2.5
2.0
1.5
1.0
0.5
ppm
2.03
1.00
6.16
1.03
4.41
0.94
5.17
203.6
160.9
138.4
106.2
104.7
77.3
77.2
77.0
76.7
55.6
45.8
29.5
25.9
25.8
240
220
200
180
160
140
120
100
80
60
40
20
0
ppm

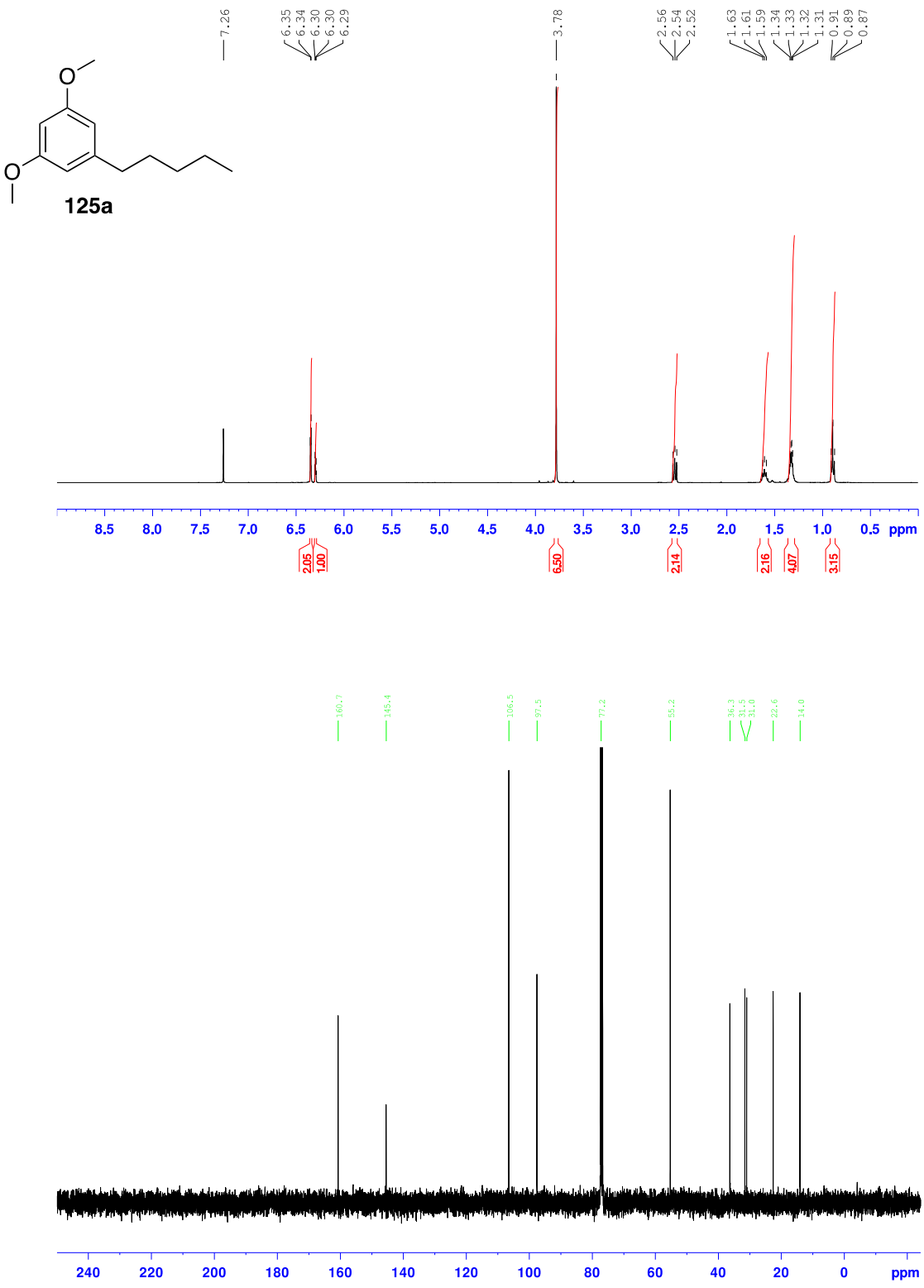
125a
7.26
6.35
6.34
6.30
6.30
6.29
3.78
2.56
2.54
2.52
1.63
1.61
1.59
1.34
1.33
1.32
1.31
0.91
0.89
0.87
8.5 8.0 7.5 7.0 6.5 6.0 5.5 5.0 4.5 4.0 3.5 3.0 2.5 2.0 1.5 1.0 0.5 ppm
2.05
1.00
6.50
2.14
2.16
4.07
3.15
160.7
145.4
106.5
97.5
77.2
55.2
36.3
31.5
31.0
22.6
14.0
240 220 200 180 160 140 120 100 80 60 40 20 0 ppm

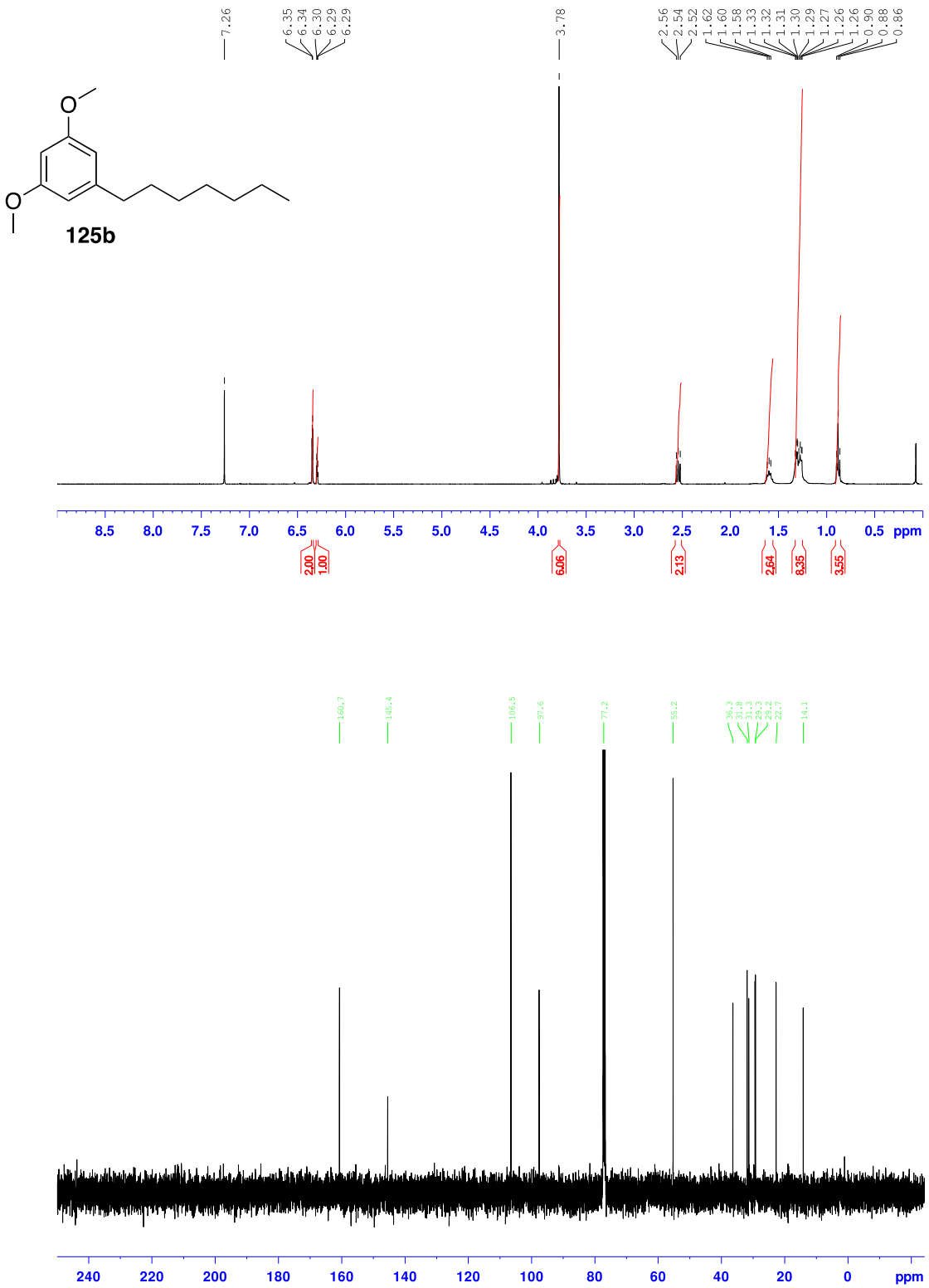
7.26
6.35
6.34
6.30
6.29
6.29
3.78
2.56
2.54
2.52
1.62
1.60
1.58
1.33
1.32
1.31
1.30
1.29
1.27
1.26
1.26
0.90
0.88
0.86
125b
8.5 8.0 7.5 7.0 6.5 6.0 5.5 5.0 4.5 4.0 3.5 3.0 2.5 2.0 1.5 1.0 0.5 ppm
2.00
1.00
6.06
2.13
2.64
6.35
3.55
160.7
145.4
106.5
97.6
77.2
55.2
36.3
31.8
31.3
29.3
29.2
22.7
14.1
240 220 200 180 160 140 120 100 80 60 40 20 0 ppm

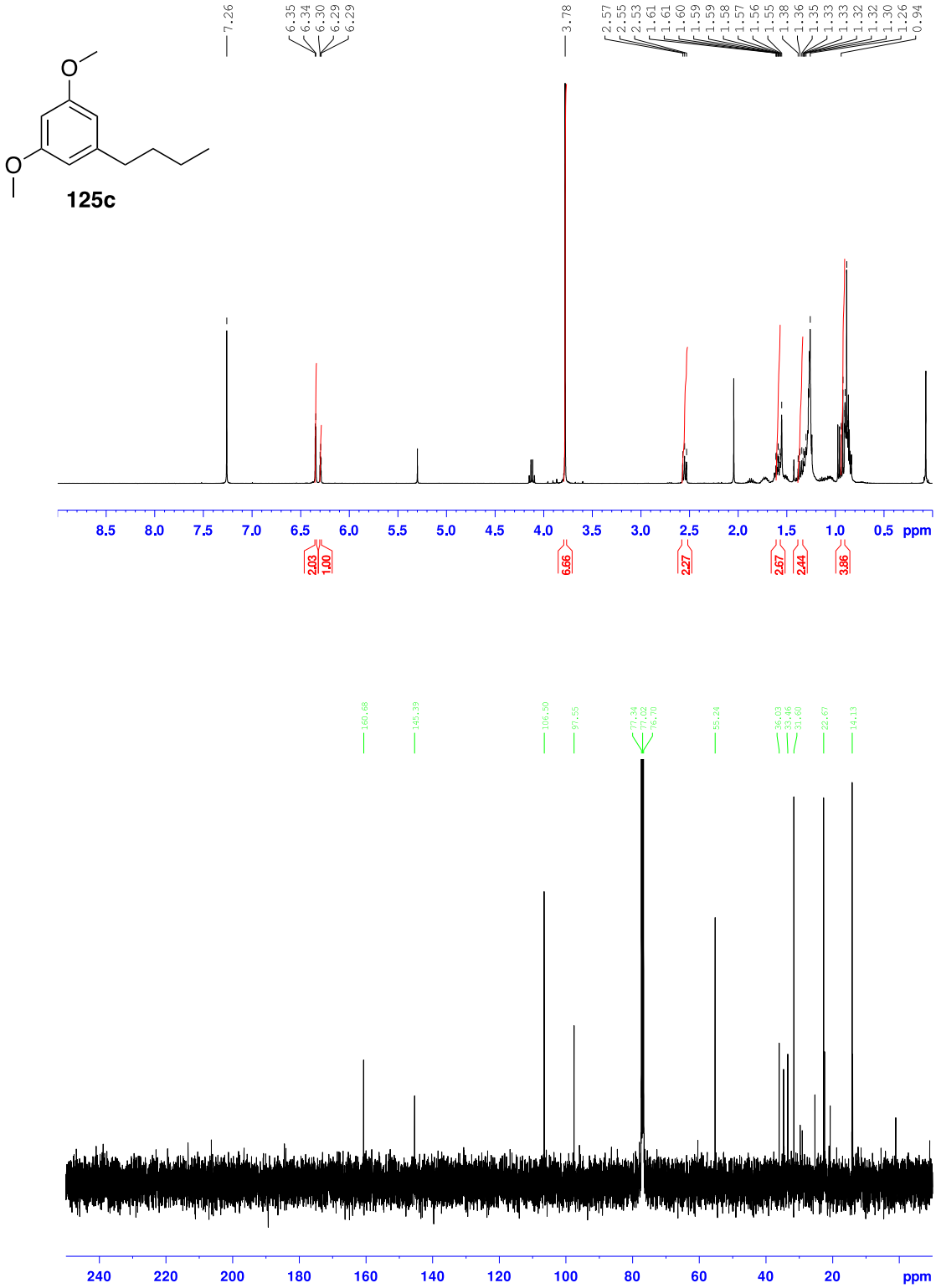
125c
7.26
6.35
6.34
6.30
6.29
6.29
3.78
2.57
2.55
2.53
1.61
1.61
1.60
1.59
1.59
1.58
1.57
1.56
1.55
1.38
1.36
1.35
1.33
1.33
1.32
1.32
1.30
1.26
0.94
8.5 8.0 7.5 7.0 6.5 6.0 5.5 5.0 4.5 4.0 3.5 3.0 2.5 2.0 1.5 1.0 0.5 ppm
2.03
1.00
6.66
2.27
2.67
2.44
3.86
160.68
145.39
106.50
97.55
77.34
77.02
76.70
55.24
36.03
33.46
31.60
22.67
14.13
240 220 200 180 160 140 120 100 80 60 40 20 ppm

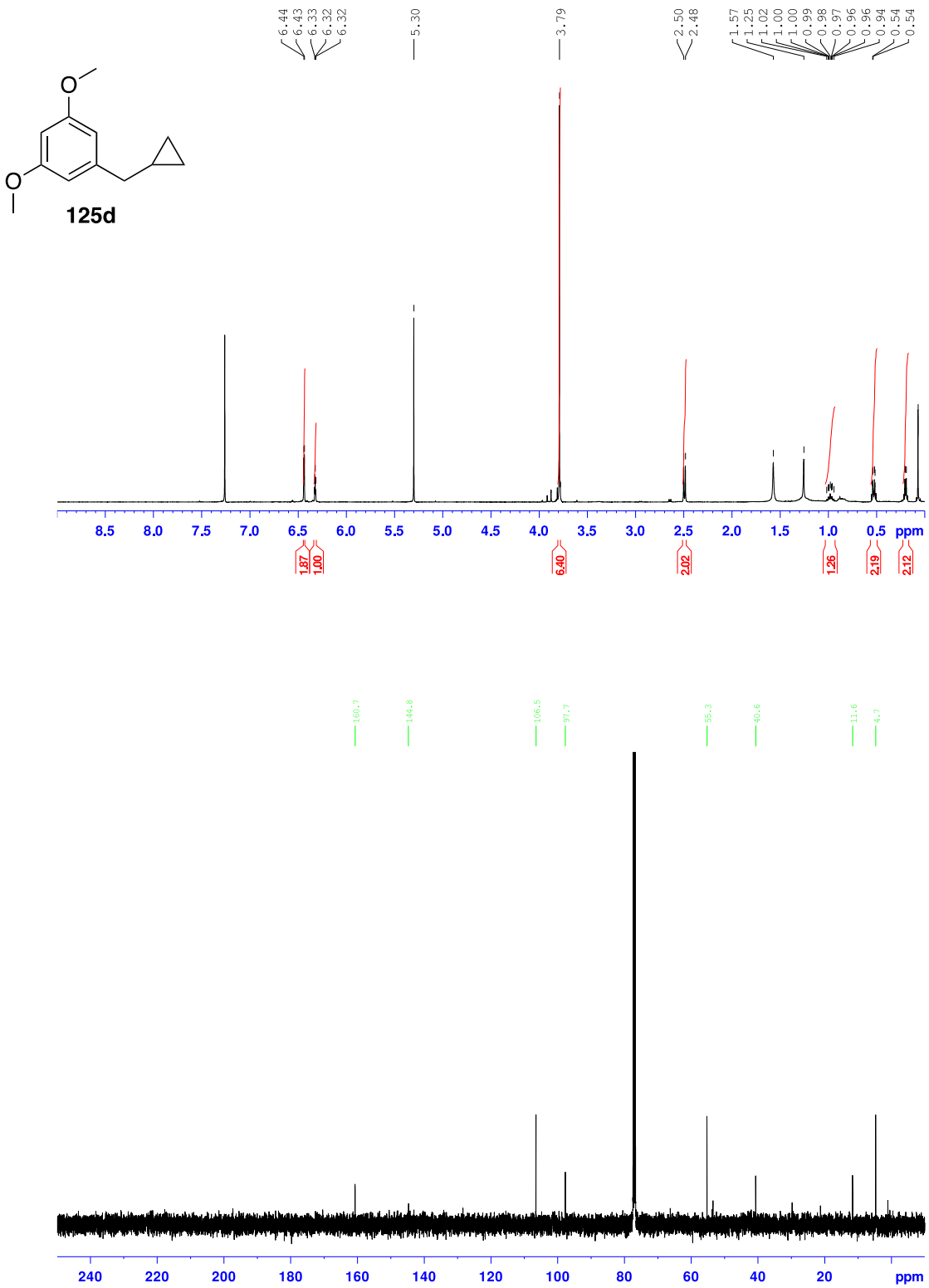
125d
6.44
6.43
6.33
6.32
6.32
5.30
3.79
2.50
2.48
1.57
1.25
1.02
1.00
1.00
0.99
0.98
0.97
0.96
0.96
0.94
0.54
0.54
8.5
8.0
7.5
7.0
6.5
6.0
5.5
5.0
4.5
4.0
3.5
3.0
2.5
2.0
1.5
1.0
0.5
ppm
1.87
1.00
6.40
2.02
1.26
2.19
2.12
160.7
144.8
106.5
97.7
55.3
40.6
11.6
4.7
240
220
200
180
160
140
120
100
80
60
40
20
ppm

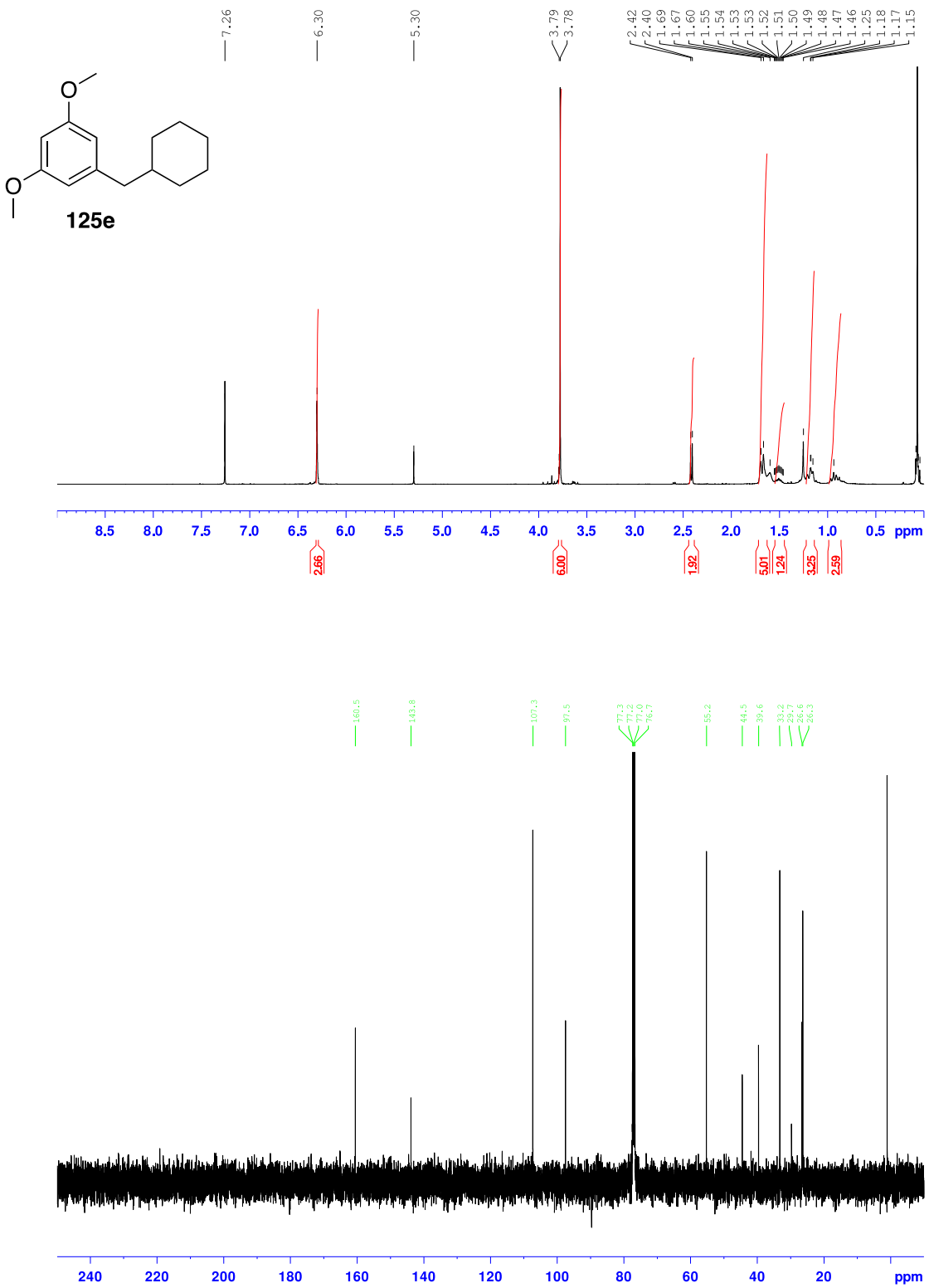
125e
7.26
6.30
5.30
3.79
3.78
2.42
2.40
1.69
1.67
1.60
1.55
1.54
1.53
1.53
1.52
1.51
1.50
1.49
1.48
1.47
1.46
1.25
1.18
1.17
1.15
8.5 8.0 7.5 7.0 6.5 6.0 5.5 5.0 4.5 4.0 3.5 3.0 2.5 2.0 1.5 1.0 0.5 ppm
2.66
6.00
1.92
5.01
1.24
3.25
2.59
160.5
143.8
107.3
97.5
77.3
77.2
77.0
76.7
55.2
44.5
39.6
33.2
29.7
26.6
26.3
240 220 200 180 160 140 120 100 80 60 40 20 ppm

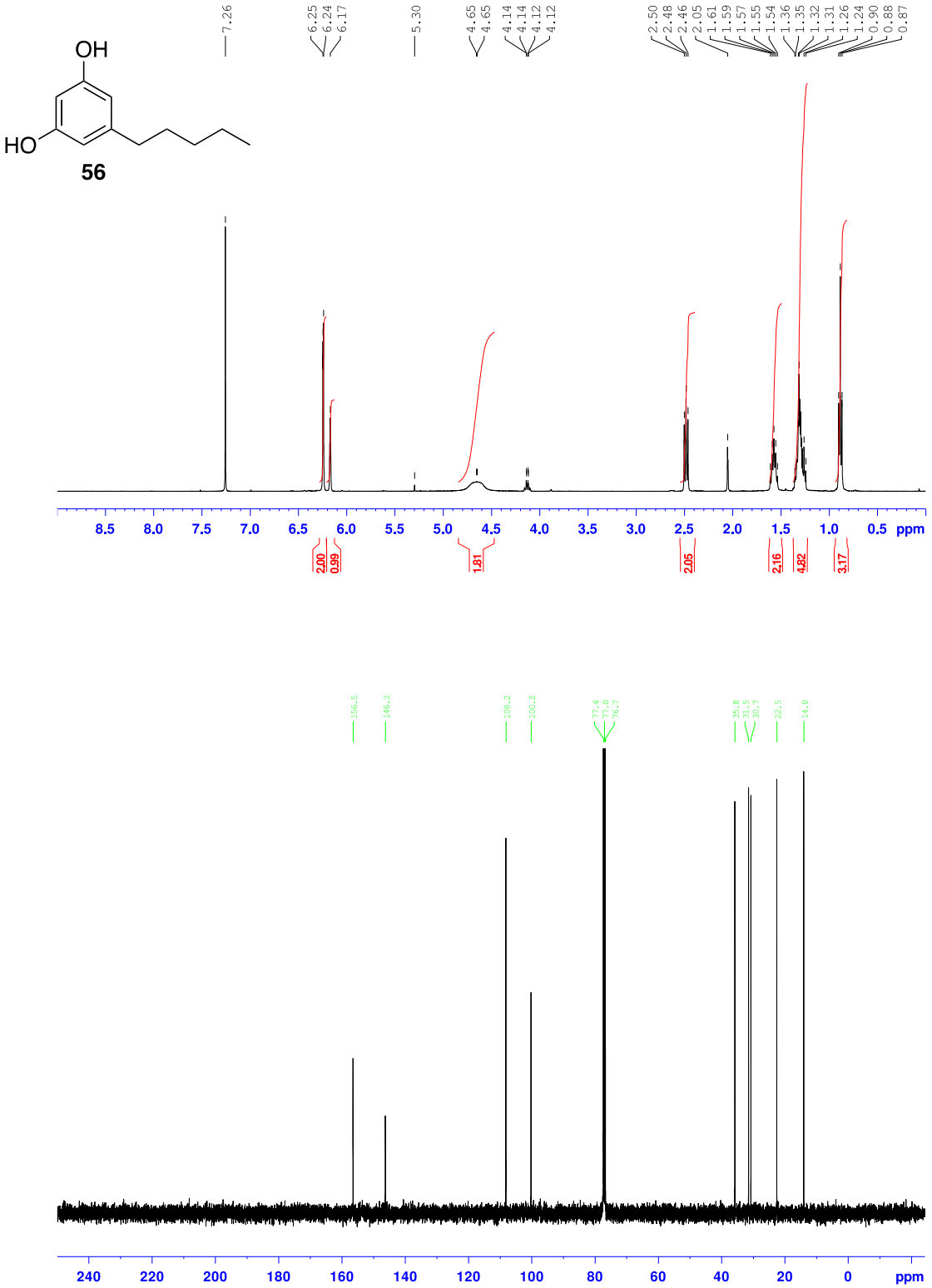
OH
HO
56
7.26
6.25
6.24
6.17
5.30
4.65
4.65
4.14
4.14
4.12
4.12
2.50
2.48
2.46
2.05
1.61
1.59
1.57
1.55
1.54
1.36
1.35
1.32
1.31
1.26
1.24
0.90
0.88
0.87
8.5
8.0
7.5
7.0
6.5
6.0
5.5
5.0
4.5
4.0
3.5
3.0
2.5
2.0
1.5
1.0
0.5
ppm
2.00
0.99
1.81
2.05
2.16
4.82
3.17
156.5
146.3
108.2
100.2
77.4
77.0
76.7
35.8
31.5
30.7
22.5
14.0
240
220
200
180
160
140
120
100
80
60
40
20
0
ppm

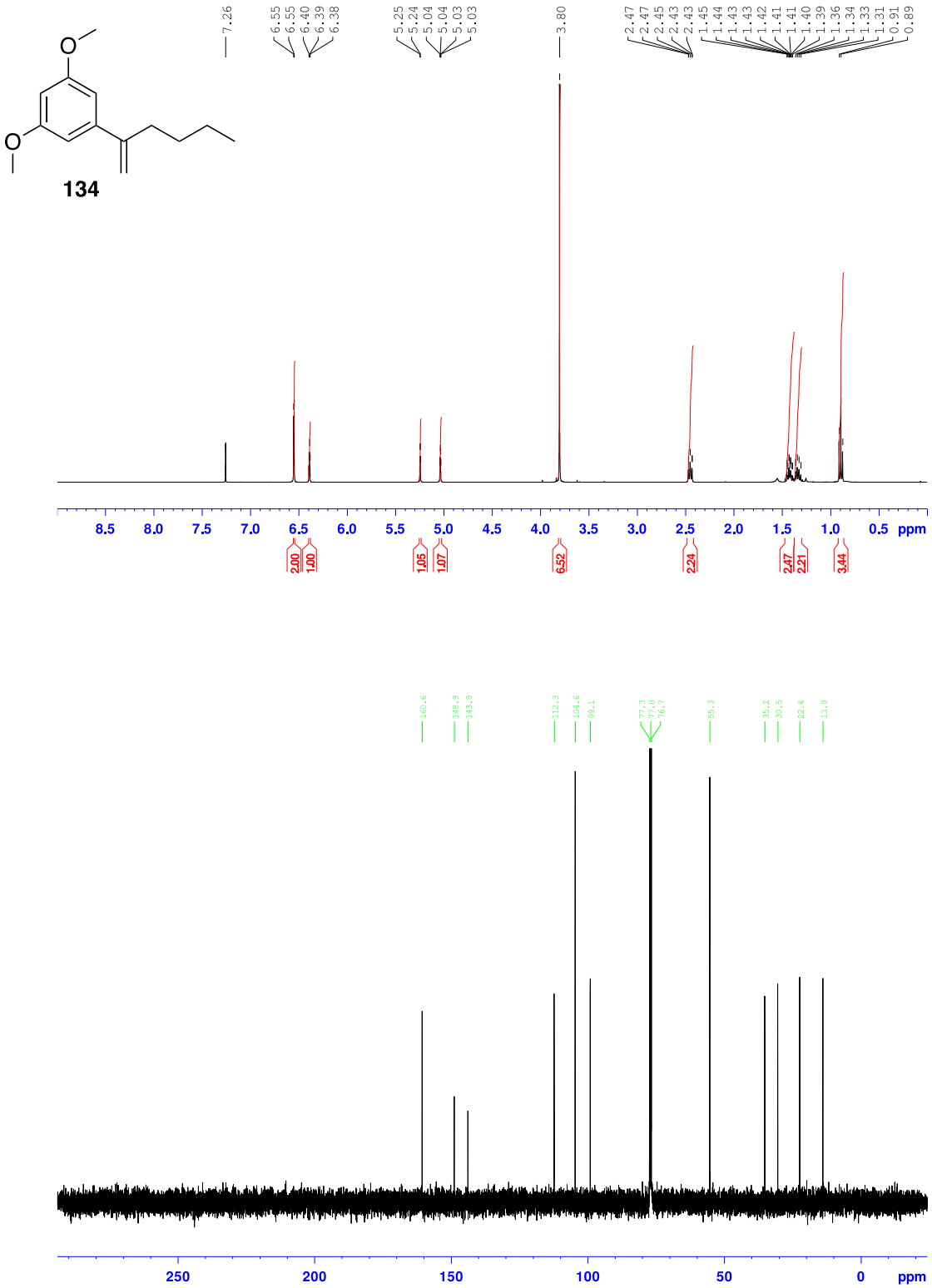
134
7.26
6.55
6.55
6.40
6.39
6.38
5.25
5.24
5.04
5.04
5.03
5.03
3.80
2.47
2.47
2.45
2.43
2.43
1.45
1.44
1.43
1.43
1.42
1.41
1.41
1.40
1.39
1.36
1.34
1.33
1.31
0.91
0.89
8.5
8.0
7.5
7.0
6.5
6.0
5.5
5.0
4.5
4.0
3.5
3.0
2.5
2.0
1.5
1.0
0.5
ppm
2.00
1.00
1.05
1.07
6.52
2.24
2.47
2.21
3.44
160.6
148.9
143.9
112.3
104.6
99.1
77.3
77.0
76.7
55.3
35.2
30.5
22.4
13.9
250
200
150
100
50
0
ppm

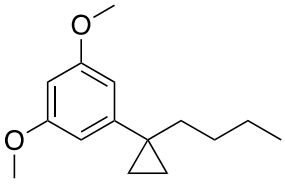

135

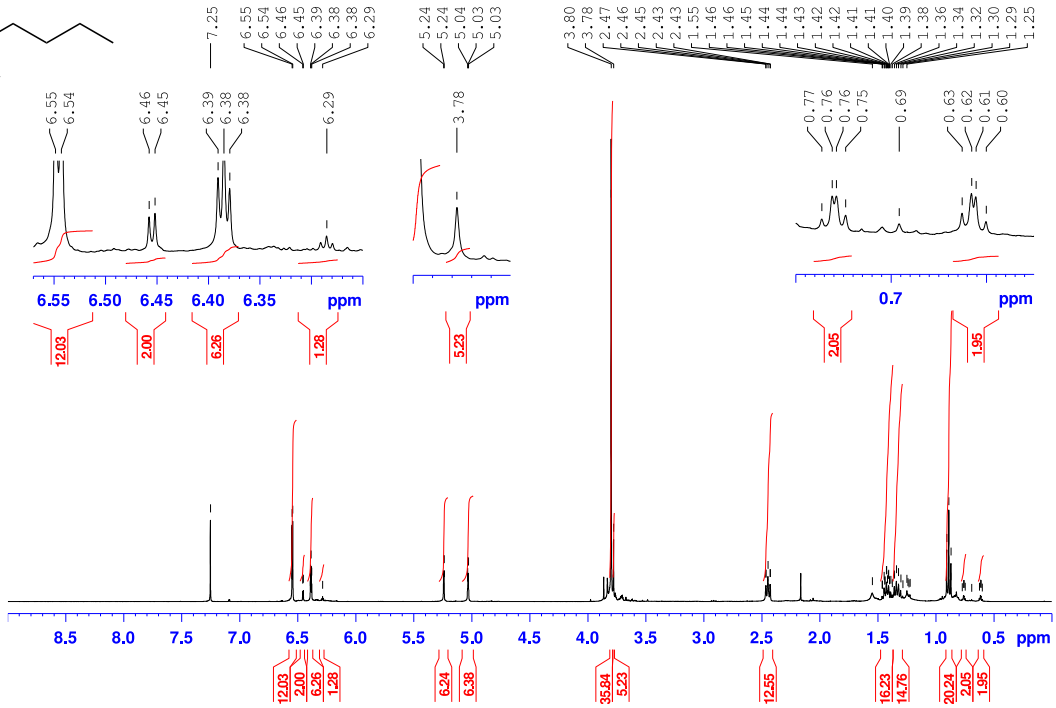

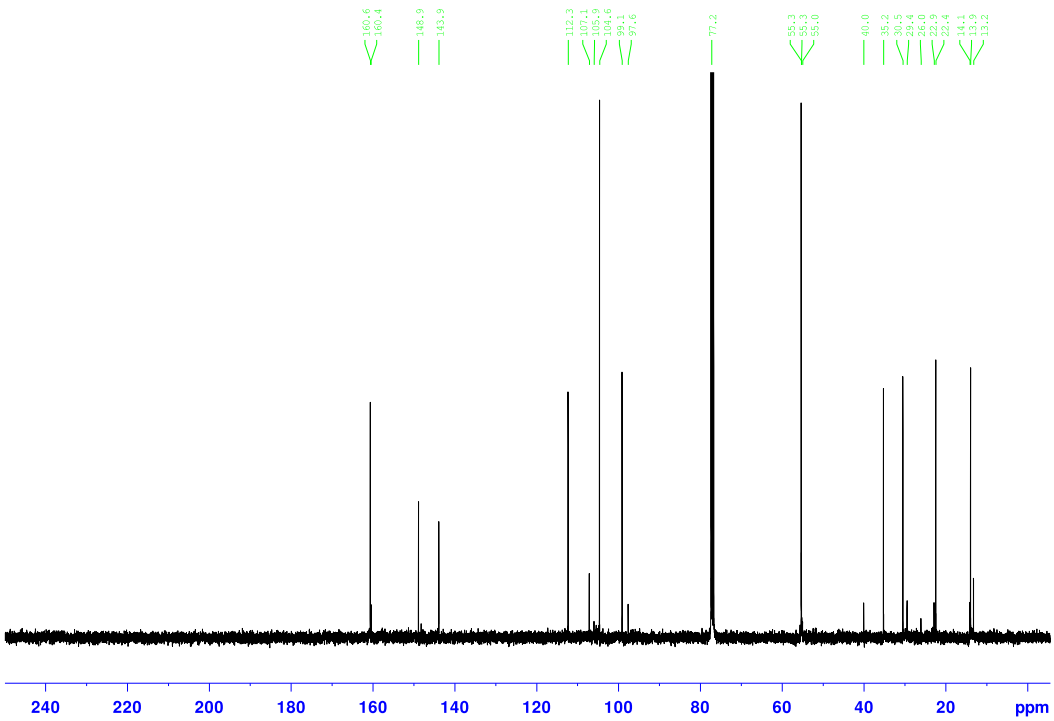

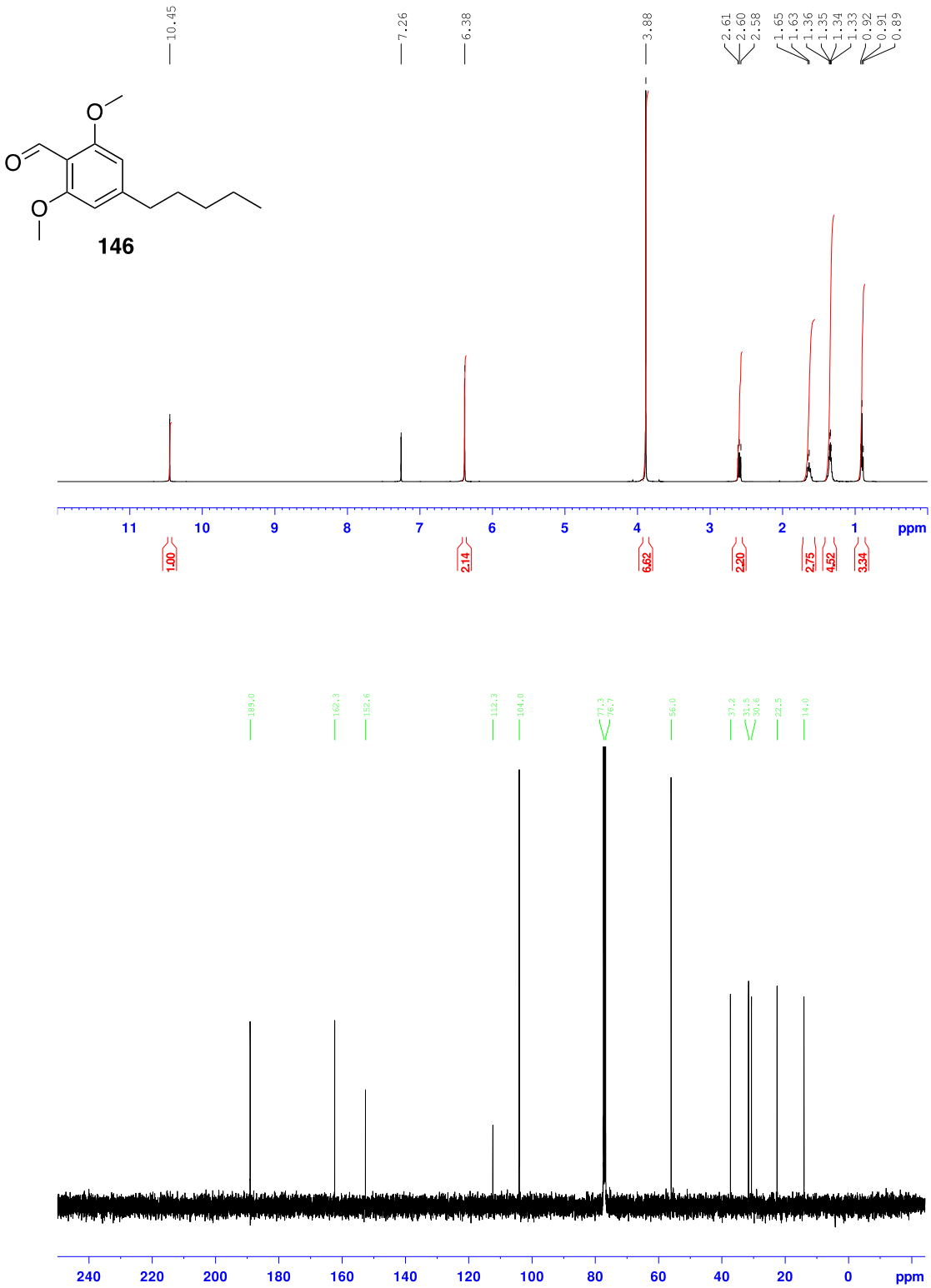
10.45
7.26
6.38
3.88
2.61
2.60
2.58
1.65
1.63
1.36
1.35
1.34
1.33
0.92
0.91
0.89
O
O
O
146
11
10
9
8
7
6
5
4
3
2
1
ppm
1.00
2.14
6.62
2.20
2.75
4.52
3.34
189.0
162.3
152.6
112.3
104.0
77.3
76.7
56.0
37.2
31.5
30.6
22.5
14.0
240
220
200
180
160
140
120
100
80
60
40
20
0
ppm

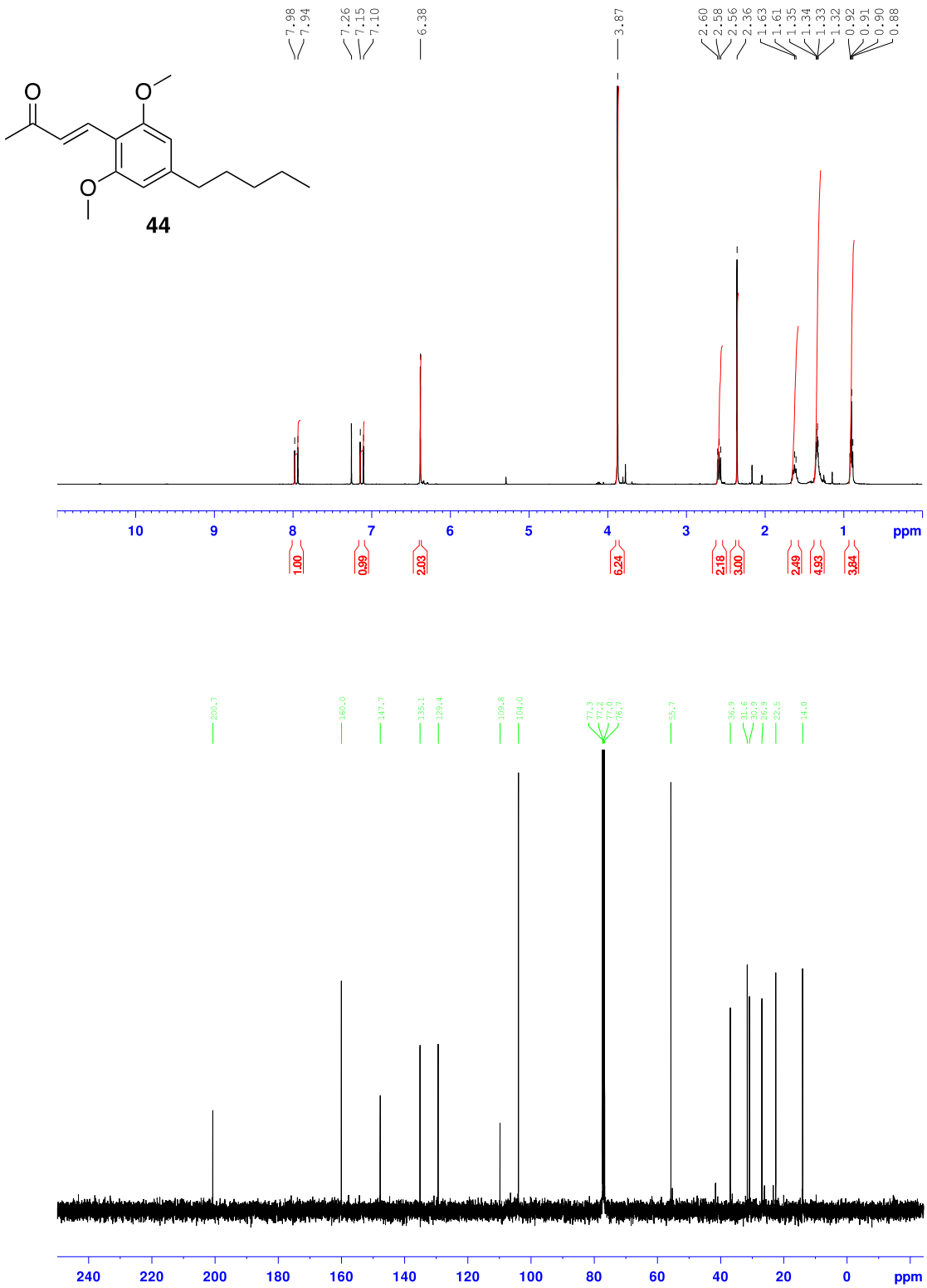
44
7.98
7.94
7.26
7.15
7.10
6.38
3.87
2.60
2.58
2.56
2.36
1.63
1.61
1.35
1.34
1.33
1.32
0.92
0.91
0.90
0.88
ppm
1.00
0.99
2.03
6.24
2.18
3.00
2.49
4.93
3.84
200.7
160.0
147.7
135.1
129.4
109.8
104.0
77.3
77.2
77.0
76.7
55.7
36.9
31.6
30.9
26.9
22.5
14.0
ppm

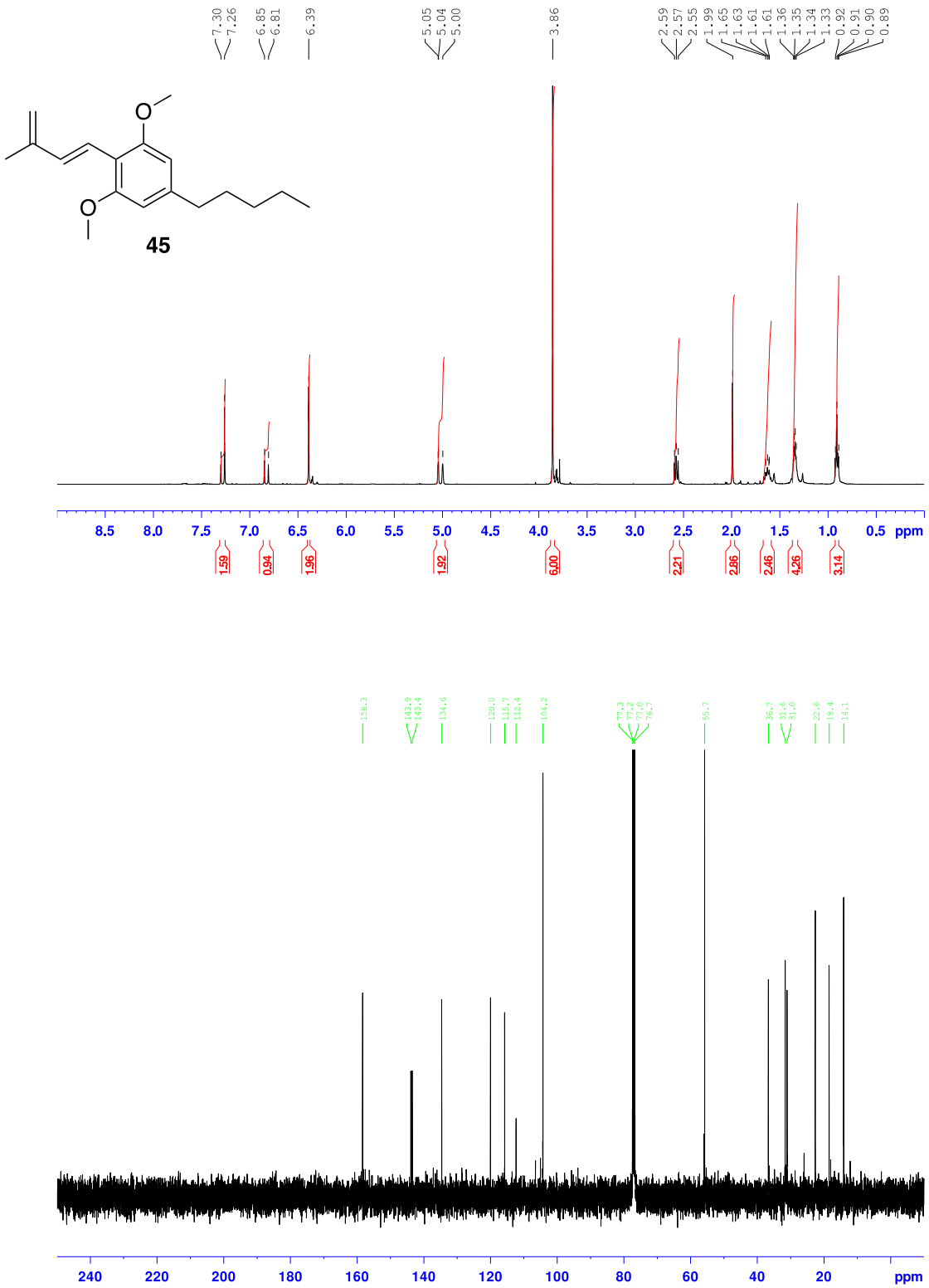
7.30
7.26
6.85
6.81
6.39
5.05
5.04
5.00
3.86
2.59
2.57
2.55
1.99
1.65
1.63
1.61
1.61
1.36
1.35
1.34
1.33
0.92
0.91
0.90
0.89
O
O
45
8.5
8.0
7.5
7.0
6.5
6.0
5.5
5.0
4.5
4.0
3.5
3.0
2.5
2.0
1.5
1.0
0.5
ppm
1.59
0.94
1.96
1.92
6.00
2.21
2.86
2.46
4.26
3.14
158.3
143.9
143.4
134.6
120.0
115.7
112.4
104.2
77.3
77.2
77.0
76.7
55.7
36.7
31.6
31.0
22.6
18.4
14.1
240
220
200
180
160
140
120
100
80
60
40
20
ppm

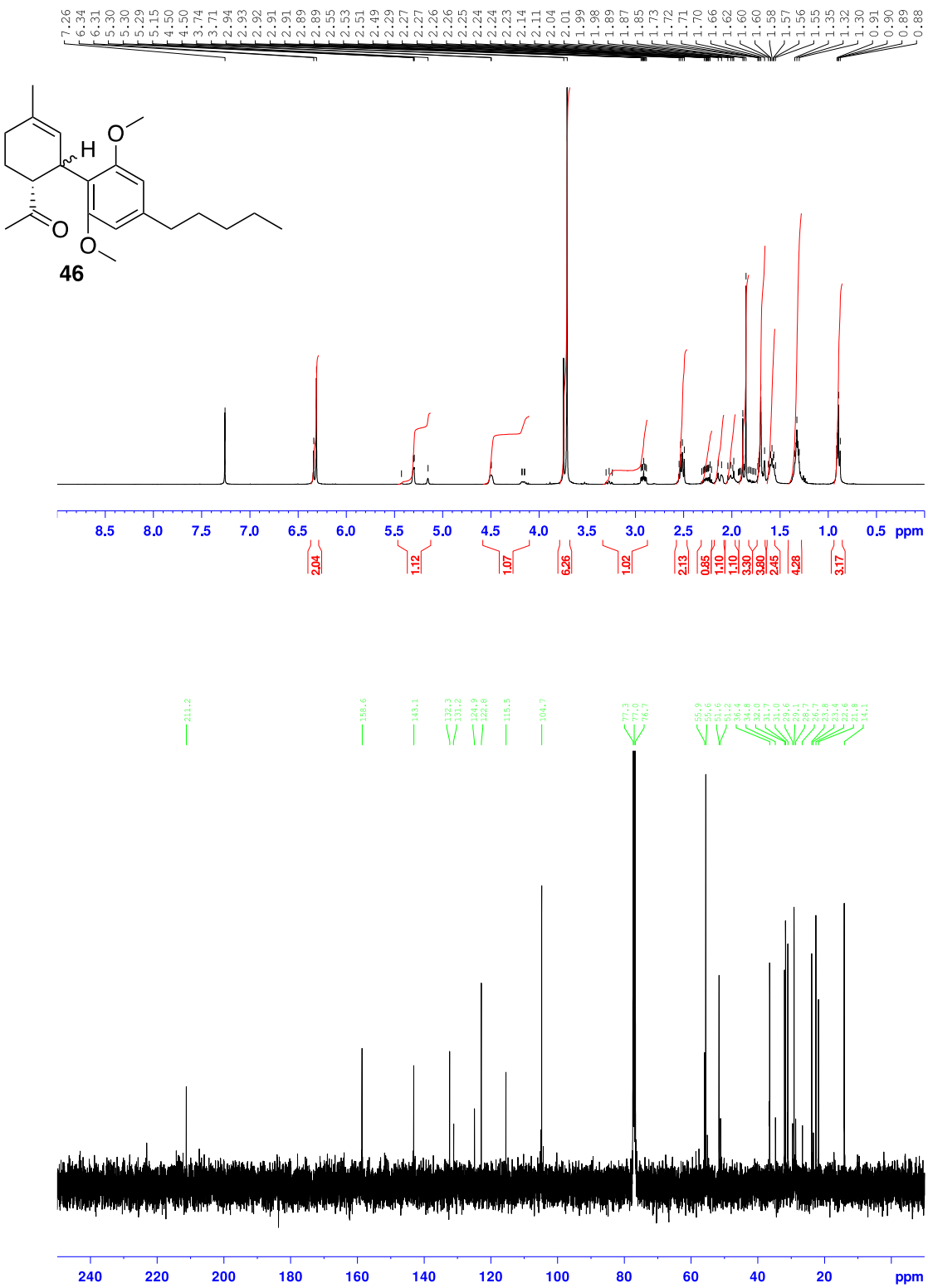
7.26 6.34 6.31 5.30 5.30 5.29 5.15 4.50 4.50 3.74 3.71 2.94 2.93 2.92 2.91 2.91 2.89 2.89 2.55 2.53 2.51 2.49 2.29 2.27 2.27 2.26 2.26 2.25 2.24 2.24 2.23 2.14 2.11 2.04 2.01 1.99 1.98 1.89 1.87 1.85 1.73 1.72 1.71 1.70 1.66 1.62 1.60 1.60 1.58 1.57 1.56 1.55 1.35 1.32 1.30 0.91 0.90 0.89 0.88
H
O
O
O
46
8.5 8.0 7.5 7.0 6.5 6.0 5.5 5.0 4.5 4.0 3.5 3.0 2.5 2.0 1.5 1.0 0.5 ppm
2.04 1.12 1.07 6.26 1.02 2.13 0.85 1.10 3.30 3.80 2.45 4.28 3.17
211.2 158.6 143.1 132.3 131.2 124.9 122.8 115.5 104.7 77.3 77.0 76.7 55.9 55.6 51.6 51.2 44.4 34.8 32.0 31.7 31.0 29.6 29.1 28.7 26.7 23.8 23.4 22.6 21.8 14.1
240 220 200 180 160 140 120 100 80 60 40 20 ppm

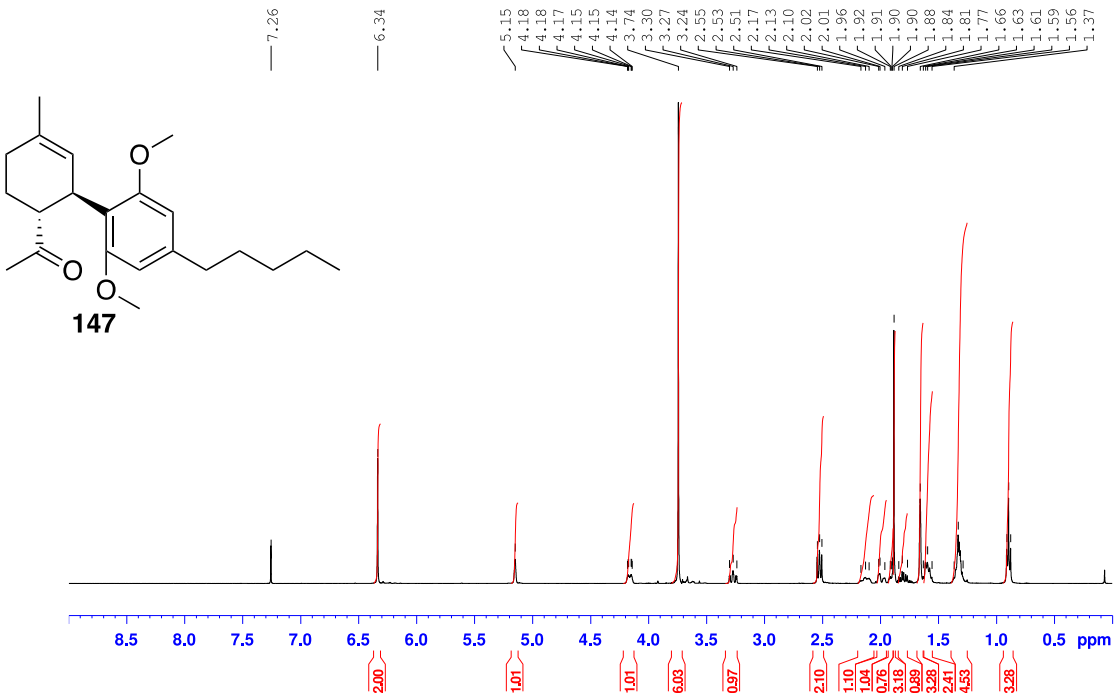
147
7.26
6.34
5.15
4.18
4.17
4.15
4.14
3.74
3.30
3.27
3.24
2.55
2.53
2.51
2.17
2.13
2.10
2.02
2.01
1.96
1.92
1.91
1.90
1.90
1.88
1.84
1.81
1.77
1.66
1.63
1.61
1.59
1.56
1.37
8.5
8.0
7.5
7.0
6.5
6.0
5.5
5.0
4.5
4.0
3.5
3.0
2.5
2.0
1.5
1.0
0.5
ppm
2.00
1.01
1.01
6.03
0.97
2.10
1.10
1.04
0.76
3.18
0.89
3.28
2.41
4.53
3.28

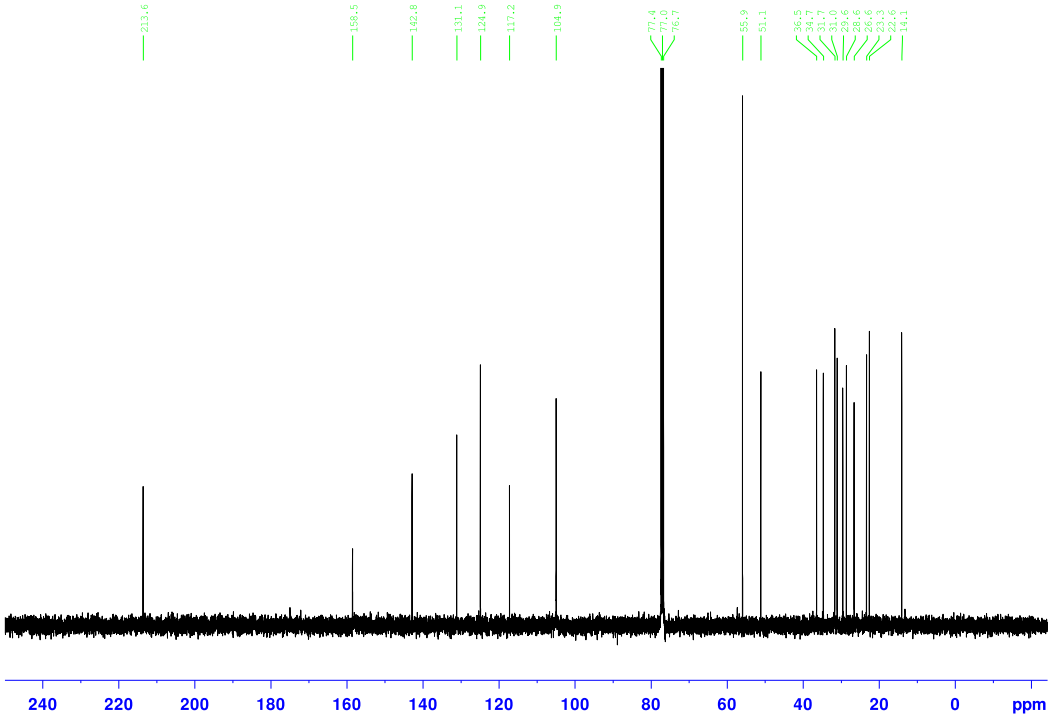
233.6
158.5
142.8
131.1
124.9
117.2
104.9
77.4
77.0
76.7
55.9
51.1
36.5
34.7
33.7
31.0
29.6
28.6
26.6
23.3
22.6
14.1
240
220
200
180
160
140
120
100
80
60
40
20
0
ppm

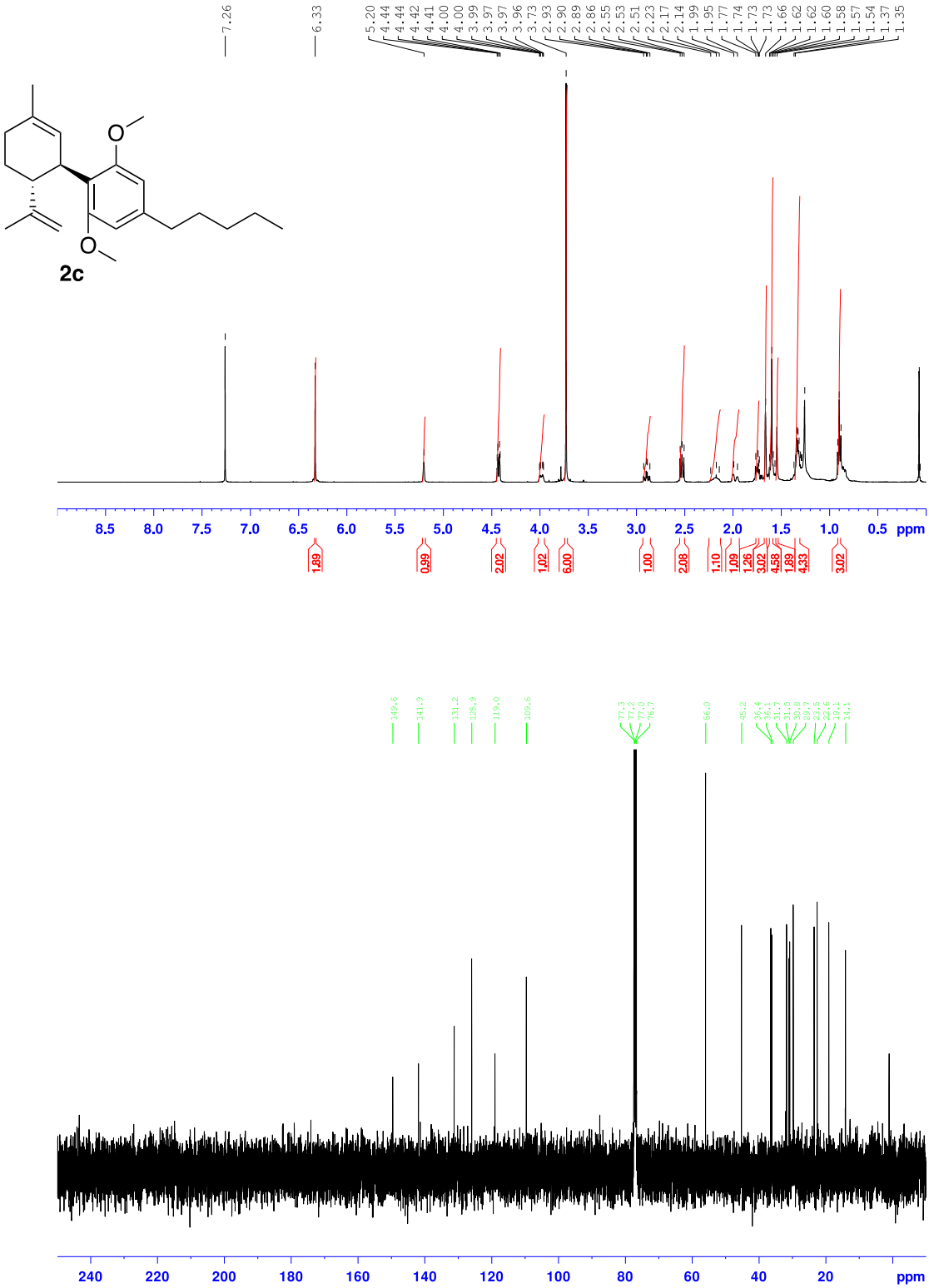
7.26
6.33
5.20
4.44
4.44
4.42
4.41
4.00
4.00
3.99
3.97
3.97
3.96
3.73
2.93
2.90
2.89
2.86
2.55
2.53
2.51
2.23
2.17
2.14
1.99
1.95
1.77
1.74
1.73
1.73
1.66
1.62
1.62
1.60
1.58
1.57
1.54
1.37
1.35
O
O
2c
8.5 8.0 7.5 7.0 6.5 6.0 5.5 5.0 4.5 4.0 3.5 3.0 2.5 2.0 1.5 1.0 0.5 ppm
1.89 0.99 2.02 1.02 6.00 1.00 2.08 1.10 1.09 1.26 3.02 4.58 1.89 4.33 3.02
149.6
141.9
131.2
125.9
119.0
109.6
77.3
77.2
77.0
76.7
56.0
45.2
36.4
36.1
31.7
31.0
30.9
29.7
23.5
22.6
19.1
14.1
240 220 200 180 160 140 120 100 80 60 40 20 ppm